VOLUME 28 (1961) No. 2

NUCLEAR PHYSICS

JOURNAL DEVOTED TO THE EXPERIMENTAL AND THEORETICAL STUDY OF THE FUNDAMENTAL CONSTITUENTS OF MATTER AND THEIR INTERACTIONS

EDITOR: L. ROSENFELD · COPENHAGEN

D. F. ZARETSKI and V. M. NOVIKOV, Theory of nuclear excitations by muons in heavy mesic atoms 177

V. N. GUMAN, Yu. I. KHARITONOV, L. A. SLIV and G. A. SOGOMONOVA, Pairing forces and pair correlations in Pb^{206}, Pb^{210} and Po^{210} 192

Yu. I. KHARITONOV, L. A. SLIV and G. A. SOGOMONOVA, Pairing forces and pair correlation in Tl^{206} and Bi^{210} 210

J. RAYNAL, Diffusion de protons polarisés par une cible de protons polarisés 220

I. S. SHAPIRO, On the dispersion theory of direct nuclear reactions 244

J. HÖGAASEN-FELDMAN, A study of some approximations of the pairing force 258

JERZY SAWICKI and TOSHIO SODA, Theory of collective excitations of spherical nuclei with particular application to the giant dipole state 270

X. DE BOUARD, H. LANGEVIN-JOLIOT, N. MARTY et B. TATISCHEFF, Excitation du niveau de 15.1 MeV de C^{12} par diffusion inélastique des protons de 150 MeV 293

P. MÖBIUS, Different modes of motion in special translationally invariant many-body systems 304

M. EL NADI and H. SHERIF, Stripping of heavy projectiles 331

V. M. STRUTINSKI, Angular correlations in statistical nuclear reactions 342

December 1961

NORTH-HOLLAND PUBLISHING COMPANY - AMSTERDAM

EDITORIAL BOARD

AUSTRALIA & NEW ZEALAND:	H. Messel (Sydney), M. L. Oliphant (Canberra)
AUSTRIA:	B. Karlik (Vienna), H. Thirring (Vienna)
BELGIUM:	M. de Hemptinne (Louvain), J. Verhaeghe (Ghent)
CANADA:	G. Volkoff (Vancouver)
DENMARK:	C. Møller (Copenhagen), S. Rozental (Copenhagen), G. E. Brown (Copenhagen)
EGYPT & ARAB COUNTRIES:	F. El Bedewi (Cairo), M. G. Nooh (Cairo)
FINLAND:	L. Simons (Helsinki)
FRANCE:	A. Berthelot (Saclay), S. Gorodetzky (Strasbourg)
GERMANY (DEM. REP.):	G. Hertz (Leipzig)
GERMANY (FED. REP.):	W. Gentner (Freiburg i. B.), J. H. D. Jensen (Heidelberg)
GREAT BRITAIN:	W. E. Burcham (Birmingham), R. J. Blin-Stoyle (Oxford)
HUNGARY:	L. Janossy (Budapest)
INDIA:	H. Bhabha (Bombay), R. Ramanna (Trombay)
IRISH REPUBLIC:	J. McConnell (Maynooth)
ISRAEL:	G. Racah (Jerusalem)
ITALY:	E. Amaldi (Rome)
JAPAN:	S. Kikuchi (Tokay), S. Tomonaga (Tokyo)
MEXICO:	M. Moshinsky (Mexico)
NETHERLANDS:	H. Brinkman (Groningen), S. R. de Groot (Leiden)
NORWAY:	E. Hylleraas (Oslo), A. Lundby (Oslo), H. Wergeland (Trondheim)
POLAND:	L. Infeld (Warsaw), J. Werle (Warsaw)
PORTUGAL:	J. M. Araújo (Porto), J. R. de Almeida Santos (Coimbra)
SOUTH AMERICA:	G. Beck (Rio de Janeiro), J. Leite Lopes (Rio de Janeiro)
SOUTH-EAST ASIA:	T. H. R. Skyrme (Kuala Lumpur)
SPAIN:	J. M. Otero (Madrid), C. Sanchez del Rio (Madrid)
SWEDEN:	O. Klein (Stockholm), K. Siegbahn (Uppsala), I. Waller (Uppsala)
SWITZERLAND:	P. Huber (Basel), P. Scherrer (Zürich)
U.S.A.:	H. H. Barschall (Madison, Wisconsin), S. Devons (New York), G. C. Wick (Brookhaven), D. Inglis (Argonne)
U.S.S.R.:	M. A. Markov (Moscow), I. S. Shapiro (Moscow), D. V. Skobeltzyn (Moscow)
YUGOSLAVIA:	I. Supek (Zagreb)

Contributors are requested to prepare the manuscripts of their papers according to the rules and conventions described in the *Instructions to Contributors* (see Nuclear Physics 26 (1961) 697). Special copies are available on request from the publisher or the Editor.

CONTRIBUTIONS may be sent to the Editor, Professor L. Rosenfeld, NORDITA, Blegdamsvej 17, Copenhagen Ø, either directly, or preferably through the intermediary of one of the members of the Editorial Board of the country or region in which the author is working. They may be written in English, French or German.

NUCLEAR PHYSICS is published in fortnightly issues. The subscription price per volume of 700 pages is fl 57.00; 114s; $ 15.00. Post-free.

SUBSCRIPTIONS should be sent to the publishers, NORTH-HOLLAND PUBLISHING COMPANY P.O. Box 103, Amsterdam or to any subscription-agent.

BOOKS FOR REVIEW should be sent to Professor Rosenfeld.

No part of this issue may be reproduced in any form, by print, photoprint, microfilm or any other means without permission from the publisher.

Printed in the Netherlands

NUCLEAR PHYSICS 1962

Personal subscription scheme

Only to be used for new personal subscriptions, not for renewals

When Nuclear Physics was started at the end of 1955, the intention was to publish one or two volumes a year of 700 pages each. Neither the publisher nor the editor could envisage that the influx of papers would make it necessary to publish eight such volumes a year, as were in 1961.

Although since 1955 the guilder has been revaluated with 4 %, the production costs of mathematical composition have risen by approximately 25% and the number of words per page has been increased by 20% since the first volume, the subscription price per volume has been maintained at $ 15.00 (108s.).

Moreover Nuclear Physics does not impose any page charge, in order to make it easier for scientists from countries with a weak currency to contribute to the journal.

It is difficult to compare subscription prices, but per page Nuclear Physics is undoubtedly one of the less expensive journals in the field of physics.

However, we realize that a total subscription price per year of $ 120.00 for eight volumes is prohibitive for a private subscriber and the suggestion has been made that Nuclear Physics could fix a special price for personal subscriptions.

Indeed, there are a number of scientific journals which give a certain discount to private subscribers. In the case of Nuclear Physics a discount of 30% or even 50% would not be sufficient to attract private subscriptions.

Now it is known that for technical publications the composition of the type is the most expensive part of the production and that as soon as the break-even point is reached, the run-on costs are comparatively low.

Accordingly, we decided early 1961 to make Nuclear Physics available to personal subscribers at the run-on costs. This meant that starting with 1961 individual physicists could subscribe for their own use to the eight volumes (approx. 5600 pages) of Nuclear Physics scheduled for 1961 at a total price of $ 20.00 or the equivalent in other currency (postage included).

Should you want to join this personal subscription scheme for 1962, please return the order-form.

It has to be understood that the publisher has the right to refuse a personal subscription or its renewal. In case of refusal, the publisher will return the cheque.

We were glad to see that this new arrangement appealed to many nuclear physicists and that it did not lead to any misunderstanding about the extremely complicated way of fixing subscription prices for learned journals.

THE EDITOR
L. Rosenfeld

THE PUBLISHER
M. D. Frank

How to act: Write a letter to the Subscription Department of North-Holland Publishing Company, P.O. Box 103, Amsterdam, Netherlands, asking for a personal subscription.

This letter should contain:

- **a cheque or banknotes for $ 20.00**
  (£ 7.4.0-; DM 80; N.Frs. 100)
- **a statement running as follows:**

"This subscription is for personal use only and will not replace an existing library subscription, nor will it be put at the disposal of any library now or in the future.

My position is: _____"

(Mention should be made of the institution to which you are attached.)

Any enquiry or communication concerning the personal subscription scheme should be addressed to the publisher, North-Holland Publishing Company, P.O. Box 103, Amsterdam, Netherlands.

Only to be used for NEW personal subscriptions, not for renewals

SUBSCRIPTION FORM

NORTH-HOLLAND PUBLISHING COMPANY
P.O. BOX 103
AMSTERDAM - NETHERLANDS

Date _____

Please enter my personal subscription to

NUCLEAR PHYSICS 1962

(VOLUMES 29–36)

at the **total** subscription price of $ 20.00

(£ 7.4.0.; DM. 80; N. Frs. 100)

I declare that this subscription is for my personal use only and that it will not replace an existing library subscription, nor will it be put at the disposal of any library now or in the future.

I enclose ☐ banknotes

☐ cheque

My position is _____

(mention should be made of the institution to which you are attached)

Name (please print) _____

_____

Address _____

_____

City, Zone, State _____

Signature

_____

(tear off here)

2.H:2.J

Nuclear Physics **28** (1961) 177—191; © *North-Holland Publishing Co., Amsterdam*

Not to be reproduced by photoprint or microfilm without written permission from the publisher

THEORY OF NUCLEAR EXCITATIONS BY MUONS IN HEAVY MESIC ATOMS

D. F. ZARETSKI and V. M. NOVIKOV

I. V. Kurchatov Atomic Energy Institute, Academy of Sciences, Moscow, USSR

Received 3 March 1961

Abstract: The paper is concerned with the electromagnetic nuclear excitation by muons in heavy mesic atoms (radiationless excitation). An expression for the probability of this process is obtained. The change of the nuclear fission barrier due to a muon in the K-shell is calculated. The theory is compared with experiment.

1. Introduction

In ref. [1]) it was shown that the transition of a muon from the 2p into the 1s state in heavy mesic atoms of the type of mesic uranium may occur through the transfer of all transition energy directly to the nucleus (radiationless excitation). It is of interest to consider this effect in two limiting cases: 1) $\rho\Gamma_n \gg 1$ and 2) $\rho\Gamma_n \ll 1$, where ρ is the nuclear level density at an excitation energy equal to that of the muon transition energy, Γ_n is the average width of the nuclear levels at the same excitation energy. In the first limiting case (of overlapping nuclear levels) the process of radiationless nuclear excitation can be interpreted as the inverse of internal conversion. This case was considered in ref. [1]). The second case (that of non-overlapping nuclear levels) differs from the first in that the excited nucleus, apart from decaying through one of the nuclear channels, can also transfer the excitation energy back to the muon. It is evident that in the first case the probability of the nucleus-muon transfer energy can be neglected. The second limiting case was considered in ref. [2]) under the assumption that $\Gamma_{r.l.} \gg \Gamma_\gamma$, where $\Gamma_{r.l.}$ is the width of nuclear radiationless excitation and Γ_γ is the width for the emission of a γ-quantum by a muon. Yet a more realistic case is $\Gamma_{r.l.} \approx \Gamma_\gamma$, as is shown in the present paper.

It is of interest to consider the effect of a muon on nuclear decay processes. Grechukhin [3]) suggested that the fission channel of the nucleus may be forbidden when the muon is in the K-shell and the nucleus is excited. The prohibition of the fission channel may occur as a result of an increasing fission barrier owing to the presence of a muon.

In sect. 2 of the present paper the ratio $\Gamma_{r.l.}/\Gamma_\gamma$ is calculated, and in sects. 3 and 4, the probability W_γ of emission of a γ-quantum by a muon, is calculated,

as well as the probability W_n of the decay of the muon-nucleus system, in terms of the parameters $\Gamma_{r.l.}/\Gamma_\gamma$ and $\rho\Gamma_n$; the ratio $\Gamma_{r.l.}/\Gamma_\gamma$ may be arbitrary and $\rho\Gamma_n \ll 1$. In the case of non-overlapping levels the effect in question is substantial only if the energy width of the mesic level is much larger than the distance between the nuclear levels. The calculation is therefore performed under the assumption

$$\rho\Gamma_{r.l.} \gg 1. \tag{1}$$

In heavy mesic atoms of the type of thorium or uranium, $\Gamma_{r.l.} \approx 1$ keV and $1/\rho$ is of the order of several eV. Therefore, the condition (1) basic to the calculation is fulfilled with good accuracy.

In sect. 5 the increase of the barrier is obtained for the fission of different nuclei when the muon is in the 1s-state. In sect. 6 the theory is compared with experimental data on radiationless nuclear excitation by muons.

2. Calculation of the Ratio $\Gamma_{r.l.}/\Gamma_\gamma$

Since the energy of the transition of a muon from the 2p into the 1s state is about 6 MeV in heavy mesic atoms of the type of uranium the calculation can be performed in non-relativistic approximation.

The operator of muon-nucleus dipole interaction leading to radiationless muon transition and nuclear excitation is of the form

$$V = -\tfrac{4}{3}\pi e^2 \sum_{i=1}^{Z} \sum_{m'} Y_{1m'}(i) Y^*_{1m'}(\mu) \times \begin{cases} \dfrac{r_i}{r_\mu^2} & \text{when} \quad r_\mu \geqq r_i, \\ \dfrac{r_\mu}{r_i^2} & \text{when} \quad r_\mu \leqq r_i. \end{cases} \tag{2}$$

where $\mathbf{r}_i$ snd $\mathbf{r}_\mu$ are the radius vector of a proton and a muon, respectively. The summation is performed for all protons of the nucleus and Ze is the nuclear charge.

Let us assume that the muon is in the 2p state initially, while the nucleus has zero spin in the ground state. Then the wave function of the muon-nucleus system is

$$\Psi_i = \psi_0 R_{2p} Y_{1m}(\mu), \tag{3}$$

where ψ_0 is the wave function of the nucleus in the ground state and $R_{2p} Y_{1m}(\mu)$ is the wave function of the muon in the 2p state. The wave function of the final state is

$$\Psi_f = \psi_{1M} \frac{1}{\sqrt{4\pi}} R_{1s}, \tag{4}$$

where ψ_{1M} is the wave function of the excited state of the nucleon with spin 1

and spin projection M and $(1/\sqrt{4\pi})R_{1s}$ is the wave function of the muon in the 1s state. The square of the matrix element of the operator (2) for the transformation from the state (3) into (4) is

$$|\langle\Psi_f|V|\Psi_1\rangle|^2 = \tfrac{4}{9}\pi e^4|\langle\psi_1|\sum_i r_i Y_1(i) f(r_i)|\psi_0\rangle|^2\delta_{mM}, \tag{5}$$

where

$$f(r_i) = \frac{1}{r_i^3}\int_0^{r_i} r^3 R_{1s}R_{2p}\,dr + \int_{r_i}^{\infty} R_{1s}R_{2p}\,dr. \tag{6}$$

The matrix element (5) does not depend on the magnetic quantum numbers. The width of the radiationless transition equals

$$\Gamma_{\text{r.l.}} = 2\pi\overline{|\langle\Psi_f|V|\Psi_1\rangle|^2}\rho. \tag{7}$$

The averaging sign in (7) denotes summing over the final and averaging over the initial states of the system as well as averaging the square of the nuclear matrix element over the nuclear levels lying close to the transition energy over the interval.

Substituting (5) into (7) and introducing $q_i = r_i Y_1(i)$ for the sake of brevity, we obtain

$$\Gamma_{\text{r.l.}} = \tfrac{8}{9}\pi^2 e^4|\langle\psi_1|\sum_i q_i f(r_i)|\psi_0\rangle|^2_{\text{Av}}\rho. \tag{8}$$

The width of the radiative transition of a muon from the 2p into 1s state equals

$$\Gamma_\gamma = \frac{4}{9}\frac{e^2\omega^3}{c^3}\left|\int_0^{\infty} r^3 R_{1s}R_{2p}\,dr\right|^2. \tag{9}$$

It is convenient to transform the integral in (9) in the following manner. Let us write the equation of motion of a muon in the matrix form

$$m_\mu\langle|\ddot{\mathbf{r}}|\rangle = -\langle|\nabla u|\rangle, \tag{10}$$

where m_μ is the muon mass and u is the muon potential in the nuclear field

$$u = -Ze^2\begin{cases} \dfrac{1}{r_\mu} & \text{for } r_\mu \geqq R \\ \dfrac{1}{2R}\left[3-\left(\dfrac{r_\mu}{R}\right)^2\right] & \text{for } r_\mu \leqq R, \end{cases} \tag{11}$$

where R is the nuclear radius.

Using (10) and (11) we obtain

$$\int_0^{\infty} r^3 R_{1s}R_{2p}\,dr = \frac{Ze^2}{m_\mu\omega^2}\left[\frac{1}{R^3}\int_0^R r^3 R_{1s}R_{2p}\,dr + \int_R^{\infty} R_{1s}R_{2p}\,dr\right] = \frac{Ze^2}{m_\mu\omega^2} f(R), \tag{12}$$

where $f(x)$ in (12) is the same as in (6).

Therefore the ratio $\Gamma_{\text{r.l.}}/\Gamma_\gamma$ of interest to us is

$$\frac{\Gamma_{\text{r.l.}}}{\Gamma_\gamma} = 2\pi^2 \frac{m_\mu{}^2 \omega c^3}{Z^2 e^2} \left| \langle \psi_1 \left| \sum_i q_i \frac{f(r_i)}{f(R)} \right| \psi_0 \rangle \right|^2_{\text{Av}} \rho. \tag{13}$$

The cross section of dipole photo-excitation is (see for example, ref. [4]))

$$\sigma = \tfrac{8}{3}\pi^3 \frac{\omega}{c} [|\langle Q_{1,1}| \rangle|^2_{\text{Av}} + |\langle |Q_{1,-1}| \rangle|^2_{\text{Av}}]. \tag{14}$$

Let us consider the nuclear photo-excitation cross section in the transition $\psi_0 \to \psi_1$. Isolating the dependence of the matrix elements on the magnetic quantum numbers in (14) and taking account of the notations introduced above, we obtain

$$\sigma = \tfrac{16}{3}\pi^3 \frac{\omega}{c} e^2 |\langle \psi_1| \sum_i q_i |\psi_0\rangle|^2_{\text{Av}} \rho. \tag{15}$$

Substituting (15) into (13) and introducing the notation

$$B = \frac{|\langle \psi_1| \sum_i q_i f(r_i) |\psi_0\rangle|^2_{\text{Av}}}{|\langle \psi_1| \sum_i q_i f(R) |\psi_0\rangle|^2_{\text{Av}}}, \tag{16}$$

we arrive at

$$\frac{\Gamma_{\text{r.l.}}}{\Gamma_\gamma} = \frac{3}{8\pi} \left(\frac{m_\mu c^2}{Ze^2} \right)^2 \sigma B. \tag{17}$$

In the case of an arbitrary initial nuclear spin I_0 and an arbitrary muon transition, the ratio $\Gamma_{\text{r.l.}}/\Gamma_\gamma$ for this transition is still given by an expression of the form (17), as is shown in ref. [5]), but the form factor B appears as

$$B = \frac{\sum_{I_f} (2I_f+1) |\langle \psi_{I_f}| \sum_i q_i f(r_i) |\psi_{I_0}\rangle|^2_{\text{Av}} \rho_{I_f}}{\sum_{I_f} (2I_f+1) |\langle \psi_{I_f}| \sum_i q_i f(R) |\psi_{I_0}\rangle|^2_{\text{Av}} \rho_{I_f}}. \tag{18}$$

The summation in (18) is performed for all possible finite values of the nuclear spin I_f and ρ_{I_f} is the nuclear level density for the spin I_f.

It is noteworthy that (17) depends on the transition energy mainly through the photo-excitation cross-section taken for the given muon transition energy, and the energy dependence of the form-factor B is rather weak.

The form-factor B takes account of the influence of the nuclear finite dimensions on the magnitude $\Gamma_{\text{r.l.}}/\Gamma_\gamma$. For heavy mesic atoms of the type of uranium, B is of the order of several units. For a point nucleus $B = 1$ and the ratio (17) does not depend at all on the muon matrix elements. This is understood if we take into account the fact that the effect of nuclear radiationless excitation can be interpreted as an inverse internal conversion effect and

the magnitude (17) as an inverse internal conversion coefficient. Since the latter contains no dependence on nuclear matrix elements for the point nucleus, in (17) there is naturally no dependence on muon matrix elements either.

The magnitude of the form-factor B can be estimated in the following manner. The matrix element in (16) can be written in the form

$$\langle k|\sum_i q_i f(r_i)|0\rangle = \sum_{k'}\langle k'|\sum_i q_i|0\rangle\langle k|f(r_i)|k'\rangle. \tag{19}$$

In squaring (19) we neglect the cross terms. This procedure is justified if the phases of the terms summed in k' (each term of the sum being a product of essentially different matrix elements of dipole and monopole transitions) are random.

For the transition to U^{238} under consideration, we obtain for $f(r)$, using the numerical wave functions of the muon given in ref. [6])

$$f(r) = 1-0.71\left(\frac{r}{R}\right)^2+0.3\left(\frac{r}{R}\right)^{\frac{7}{2}}-0.06\left(\frac{r}{R}\right)^5. \tag{20}$$

From (20) it is clear that $f(r)$ is a rather smooth function of r.

The state k belongs to the highly excited states of the nucleus ($E_k \approx 6.3$ MeV) and therefore $|\langle k|f(r)|k'\rangle|^2$ has a sharp maximum at $k' = k$, and is quasi-classically small for $k' \neq k$. On the other hand, the quantity $|\langle k'|\sum_i q_i|0\rangle|^2$ is proportional to the photo-excitation cross section and is a smooth function of k'. Therefore it can be placed before the summation sign:

$$|\langle k|\sum_i q_i f(r_i)|0\rangle|^2 \approx |\langle k|\sum_i q_i|0\rangle|^2\sum_{k'}|\langle k|f(r)|k'\rangle|^2$$
$$= |\langle k|\sum_i q_i|0\rangle|^2\langle k|f^2(r)|k\rangle. \tag{21}$$

Substituting (21) into (16) we obtain, under the assumption of uniform charged distribution in the nuclear excited state,

$$B \approx \frac{3}{f^2(1)}\int_0^1 x^2 f^2(x)\mathrm{d}x, \tag{22}$$

where $x = r/R$. Substituting (20) into (22) we obtain $B \approx 1.8$. The photo-fission cross section of U^{238} at the energy mentioned above is ≈ 12 mb (ref. [7])) and the ratio of the fission width to the sum of fission and neutron widths $\approx \frac{1}{4}$ (ref. [8])). Assuming that the photo-excitation cross section is due to the absorption of an electric dipole quantum we therefore obtain $\sigma \approx 50$ mb, which gives

$$\frac{\Gamma_{\mathrm{r.l.}}}{\Gamma_\gamma} \approx 0.7. \tag{23}$$

For Th we obtain the same ratio since the photo-excitation cross sections of Th and U^{238} are the same [8]).

The result (23) can be interpreted qualitatively in the following terms. The emission of a γ-quantum by a muon is a process of the first order and its probability $\approx e^2/\hbar c$, while the non-radiative nuclear excitation is a process of the second order and its probability $\approx (e^2/\hbar c)\ (Ze^2/\hbar c)$. Therefore, the ratio of the widths of interest to us is of the order $Ze^2/\hbar c$. It should be noted, however, that numerically the ratio of the above widths can differ strongly from $Ze^2/\hbar c$ in either direction depending on the magnitude of the nuclear matrix element for a specific nucleus and a given muon transition.

3. Coupled Muon-Nucleus System

The Hamiltonian H of the muon-nucleus system is written in the form $H = H_1+V$, where V is the operator of the dipole muon-nucleus interaction, the explicit form of which is given by eq. (2), and

$$H_1 = H_0+T_\mu-\langle\psi_0|\sum_{i=1}^{Z}\frac{e^2}{|\mathbf{r}_i-\mathbf{r}_\mu|}|\psi_0\rangle, \tag{24}$$

where H_0 is the Hamiltonian of the nucleus, T_μ is the operator of the muon kinetic energy, and the third term is the muon potential in the nuclear field averaged over the ground state of the nucleus; ψ_0 is the wave function of the ground nuclear state.

The eigenfunctions of H_1 are obviously all possible products of the wave functions of the nucleus ψ_c and the muon φ_k. Let us expand the wave functions of the total Hamiltonian H in the wave functions of H_1

$$\Psi_\gamma = \sum_{c,k} C_{\lambda;ck}\psi_c\varphi_k, \tag{25}$$

where $C_{\lambda;ck}$ are the expansion coefficients.

Since $\Gamma_{\text{r.l.}}$ is much less than the distance between the muon levels but much larger that that between the nuclear levels corresponding to the nuclear energy in the 2p—1s transition, the sum (25) for all E_λ in an interval $\approx \Gamma_{\text{r.l.}}$ around E_{2p-1s} can be written in the form

$$\Psi_\lambda = C_{\lambda,02p}\psi_0\varphi_{2p}+\sum_c C_{\lambda,c\,1s}\psi_c\varphi_{1s}. \tag{26}$$

The other terms are negligibly small. Hereafter we shal write $C_{\lambda,p}$, $C_{\lambda c}$; φ_p, φ_s and E_p instead of $C_{\lambda;02p}$, $C_{\lambda;c1s}$, φ_{2p}, φ_{1s} and E_{2p-1s}, respectively. Substituting (26) into the Schroedinger equation and taking account of the normalization of Ψ_λ, we obtain the following equations for the expansion coefficients and the eigenvalues of H:

$$C_{\lambda p}V_c = (E_\lambda-E_c)C_{\lambda c}, \tag{27}$$

$$\sum_c C_{\lambda c}V_c^* = (E_\lambda-E_p)C_{\lambda p}, \tag{28}$$

$$|C_{\lambda p}|^2+\sum_e |C_{\lambda e}|^2 = 1, \tag{29}$$

where $V_e = \langle \psi_e \varphi_s | V | \psi_0 \varphi_p \rangle$ and E_e is the energy of the excited level of the nucleus.

Substituting (27) into (29) we obtain

$$|C_{\lambda p}|^2 = \left[1+\sum_e \frac{|V_e|^2}{(E_\lambda - E_e)^2}\right]^{-1}. \tag{30}$$

Similarly, from (27) and (28) we find the equation for the eigenvalues

$$E_\lambda - E_p = \sum_e \frac{|V_e|^2}{E_\lambda - E_e}. \tag{31}$$

The characteristic interval for the sums in C is $|E_e - E_\lambda| \lesssim \Gamma_{r.l.}$, as is clear from (30). It can be assumed that the quantity $|V_e|^2$, proportional to the photo-excitation cross-section, is constant in this interval and that the nuclear levels are spaced equidistantly with a density equal to $\rho = 1/\mathscr{D}$, where $\overline{\mathscr{D}}$ is the average distance between the nuclear levels at $E_e \approx E_p$.

Bearing this in mind we find

$$\sum_e \frac{|V_e|^2}{E_\lambda - E_e} = \pi \overline{|V_e|^2} \rho \operatorname{ctg} \pi\rho\Delta, \tag{32}$$

where Δ is the distance from E_λ to the closest level E_e. Similarly, we obtain

$$\sum_e \frac{|V_e|^2}{(E_\lambda - E_e)^2} = \pi^2 \overline{|V_e|^2} \rho^2 \frac{1}{\sin^2 \pi\rho\Delta}. \tag{33}$$

A detailed method of computing the sums (32) and (33) is set down in ref. [2]). Eliminating Δ from (32) and (33) we find a relation between the sums in C of (30) and (31):

$$\sum_e \frac{|V_e|^2}{(E_\lambda - E_e)^2} = \frac{1}{\overline{|V_e|^2}} \left[\pi^2 \overline{|V_e|^4} \rho^2 + \left(\sum_e \frac{|V_e|^2}{E_\lambda - E_e}\right)^2\right]. \tag{34}$$

Combining (30) (31) and (34), we find

$$|C_{\lambda p}|^2 = \frac{\overline{|V_e|^2}}{(E_\lambda - E_p)^2 + \pi^2 \overline{|V_e|^4} \rho^2 + \overline{|V_e|^2}}. \tag{35}$$

Since in our case $q\Gamma_{r.l.} \gg 1$ the last term in the denominator of (35) can be neglected. Finally we obtain

$$|C_{\lambda p}|^2 = \frac{\Gamma_{r.l.}}{2\pi\rho} \frac{1}{(E_\lambda - E_p)^2 + (\frac{1}{2}\Gamma_{r.l.})^2}. \tag{36}$$

In the following we shall need the calculation of different sums over the levels of the coupled muon-nucleus system E_λ. The levels E_λ themselves are obtained from (31). The condition (1) leads to the levels E_λ being spaced almost equidistantly with the same density ρ as the nuclear levels E_c. The distance between the two neighbouring levels E_λ and $E_{\lambda'}$ is in fact

$$E_\lambda - E_{\lambda'} = \frac{1}{\rho}\left\{1+\frac{\pi}{2\rho\Gamma_{\text{r.l.}}}\left[1+\left(2\frac{E_\lambda-E_p}{\Gamma_{\text{r.l.}}}\right)^2\right]^{-1}\right\} \approx \frac{1}{\rho}. \tag{37}$$

4. Estimating the Attenuation of the Muon-Nucleus System

Let us assume for the sake of simplicity that the transition of a muon from a more excited state into the 2p state is not accompanied by a radiationless excitation effect. This means that we neglect the dipole muon-nucleus interaction in more excited states of the mesic atom. Therefore, the wave function of the system is $\psi_0\varphi_{ex}$, where φ_{ex} ia an excited state of the mesic atom higher than 2p. This assumption appears plausible since the transitions between higher states have lower energy and consequently lower probability of radiationless excitation. On the other hand, this assumption does not prevent the calculation from being easily generalized to the case of radiationless excitation in an arbitrary transition.

But to return to our scheme. The muon-nucleus system passes from the state $\psi_0\varphi_{ex}$ into states described by the eigenfunctions of Ψ_λ. The probability ω_λ of the excitation of the λ level is obviously proportional to the square of the matrix element of the transition

$$\omega_\lambda \approx |\langle\Psi_\lambda|H_\gamma|\psi_0\varphi_{ex}\rangle|^2 = |C_{\lambda p}|^2|\langle\varphi_p|H_\gamma|\varphi_{ex}\rangle^2,$$

where H_γ is the muon-electromagnetic field interaction leading to this transition. Taking account of the normalization condition $\sum_\lambda \omega_\lambda = 1$ we obtain

$$\omega_\lambda = |C_{\lambda p}|^2. \tag{38}$$

Without loss of generality we consider in the following that $C_{\lambda p}$ is a real quantity.

Since the probability of the system being in the state λ is equal to $C_{\lambda p}^2$ after the muon transition from a higher state into 2p, the total wave function of the system at $t = 0$ should be assigned the form

$$\Psi|_{t=0} = \sum_\lambda C_{\lambda p}\Psi_\lambda = \sum_\lambda C_{\lambda p}^2\psi_0\varphi_p + \sum_{\lambda c} C_{\lambda p}C_{\lambda c}\psi_c\varphi_s = \psi_0\varphi_p. \tag{39}$$

The second sum in (39) vanishes on account of the condition of orthogonality of the coefficients C_λ.

Let us consider the transitions from the states accompanied by the emission of a γ-quantum by a muon (muon-electromagnetic field interaction H_γ) and the

decay of the system through different nuclear channels (neutrons, nuclear quanta and fission). Let us denote the operators responsible for the decay through the nuclear channels by H_n. The explicit form of H_n is unknown, yet the final result incorporates only the square of the matrix element of the operator, proportional to the nuclear width.

For the sake of simplicity we assume that only one nuclear channel is open. If the decay of the excited nucleus occurs through different channels independently the partial nuclear width must be replaced by the total width in the final result. Let Φ_ν designate the wave function of the system when the nucleus and meson are in the ground state, and the muon-emitted γ-quantum has an energy E_ν; Φ_k designates the wave function of the system when the meson is in the ground state and the decayed nucleus and nuclear decay products have an energy E_k. The Hamiltonian of the decaying muon-nucleus system equals $\mathscr{H} = H_1+V+H_\gamma+H_n$. The wave function which is a solution of the nonstationary Schroedinger equation with the Hamiltonian $\mathscr{H}$ and satisfying the initial condition (39) can be written in the form

$$\Psi = \sum_\lambda b_\lambda(t)\Psi_\lambda e^{-i\frac{E_\lambda t}{\hbar}} + \sum_\nu b_\nu(t)\Phi_\nu e^{-i\frac{E_\nu t}{\hbar}} + \sum_k b_k(t)\Phi_k e^{-i\frac{E_k t}{\hbar}} \tag{40}$$

where

$$b_\lambda(0) = C_{\lambda p}, \qquad b_\nu(0) = b_k(0) = 0.$$

Substituting (40) into the Schroedinger equation we obtain the following equation for the coefficients, which we consider equal to zero for $t < 0$ (see for example ref. [9]):

$$i\hbar\dot{b}_n(t) = \sum_m (H_\gamma+H_n)_{nm} e^{i\frac{(E_n-E_m)t}{\hbar}} b_m(t)+i\hbar\delta(t)\sum_\lambda C_{\lambda p}\delta_{n\lambda}, \tag{41}$$

where n and m denote sets of subscripts λ, ν and k. Let us make the Fourier transformation of the coefficients b_n:

$$\begin{aligned} b_\lambda &= -\frac{1}{2\pi i}\int_{-\infty}^{+\infty} G_\lambda(E)e^{i(E_\lambda-E)t/\hbar}dE, \\ b_\nu &= -\frac{1}{2\pi i}\int_{-\infty}^{+\infty} G_\nu(E)\zeta(E-E_\nu)e^{i(E_\nu-E)t/\hbar}dE, \\ b_k &= -\frac{1}{2\pi i}\int_{-\infty}^{+\infty} G_k(E)\zeta(E-E_k)e^{i(E_k-E)t/\hbar}dE, \end{aligned} \tag{42}$$

where

$$\zeta(x) = \lim_{\sigma\to+0}\frac{1}{x+i\sigma}.$$

We are interested in the total probability W_γ of emission of a quantum by a

muon, which is obviously given by $W_\gamma = \sum_\nu |b_\nu(\infty)|^2$. Similarly the probability W_n of the non-radiative nuclear excitation, with subsequent decay of the nucleus, is given by $W_n = \sum_k |b_k(\infty)|^2$. On the other hand we have [9])

$$b_\nu(\infty) = G_\nu(E)|_{E=E_\nu}, \qquad b_k(\infty) = G_k(E)|_{E=E_k}.$$

Substituting (42) into (41) we obtain the equations for G_λ, G_ν and G_k:

$$\begin{aligned} (E-E_\lambda)G_\lambda &= \sum_\nu H^{(\gamma)}_{\lambda\nu}\zeta(E-E_\nu)G_\nu + \sum_k H^{(n)}_{\lambda,k}\zeta(E-E_k)G_k + C_{\lambda p}, \\ G_\nu &= \sum_\lambda H^{(\gamma)}_{\nu\lambda} G_\lambda, \qquad G_k = \sum_\lambda H^{(n)}_{k\lambda} G_\lambda, \end{aligned} \tag{43}$$

where

$$\begin{aligned} H^{(\gamma)}_{\lambda\nu} &= \langle \Psi_\lambda | H_\gamma | \Phi_\nu \rangle = C_{\lambda p} H_\nu, \qquad & H_\nu &= \langle \varphi_p | H_\gamma | \varphi_s \rangle, \\ H^{(n)}_{\lambda k} &= \langle \Psi_\lambda | H_n | \Phi_k \rangle = \sum_c C_{\lambda c} H_{ck}, \qquad & H_{ck} &= \langle \psi_c | H_n | \Phi_k \rangle. \end{aligned}$$

Let us assume that H_ν does not depend on the energy E_ν in the interval $\approx \Gamma_\gamma + \Gamma_{r.l.}$. This assumption is quite justified since $\Gamma_\gamma + \Gamma_{r.l.} \ll E_p$. For the same reason H_{ck} does not depend on E_k. In that case G_ν and G_k do not depend on E_ν and E_k either, while the subscripts ν and k are only the indices on the decay channel of the muon-nucleus system. Bearing this in mind the sums in ν and k in (43) can be performed and after eliminating G_λ we obtain the following set of equations for G_ν and G_k:

$$\begin{aligned} G_\nu\left\{1+\tfrac{1}{2}i\Gamma_\gamma \sum_\lambda \frac{G^2_{\lambda p}}{E-E_\lambda}\right\} + C_k\left\{i\pi H_\nu^* \rho_k \sum_{\lambda c} \frac{C_{\lambda c} H_{ck} C_{\lambda p}}{E-E_\lambda}\right\} &= H_\nu^* \sum_\lambda \frac{C^2_{\lambda p}}{E-E_\lambda}, \\ G_\nu\left\{i\pi H_\nu \rho_\nu \sum_{\lambda c} \frac{C^*_{\lambda c} H^*_{ck} C_{\lambda p}}{E-E_\lambda}\right\} + G_k\left\{1+\tfrac{1}{2}i\Gamma_n \sum_\lambda \frac{1-C^2_{\lambda p}}{E-E_\lambda}\right\} &= \sum_{\lambda c} \frac{C^*_{\lambda c} H^*_{ck} C_{\lambda p}}{E-E_\lambda}, \end{aligned} \tag{44}$$

where $\Gamma_\gamma = 2\pi|H_\nu|^2\rho_\nu$ and $\Gamma_n = 2\pi\overline{|H_{ck}|^2}\rho_k$ and ρ_ν, ρ_k are the densities of the final states ν and k.

In solving (44) we come across double sums over c. For calculating them we use the assumption that the phases of the terms of the sum are random. As a result we obtain

$$\begin{aligned} |\sum_c C_{\lambda c} H_{ck}|^2 &\approx \sum_c |C_{\lambda c}|^2 |H_{ck}|^2 = \overline{|H_{ck}|^2} \sum_c |C_{\lambda c}|^2, \\ \sum_{cc'} H_{ck} H^*_{c'k} C_{\lambda c} C^*_{\lambda' c'} &\approx \sum_c |H_{ck}|^2 C_{\lambda c} C_{\lambda' c} = \overline{|H_{ck}|^2}(\delta_{\lambda\lambda'} - C_{\lambda p} C_{\lambda' p}) \end{aligned} \tag{45}$$

The assumption of random phases is reasonable for non-overlapping nuclear levels.

Since $C_{\lambda c} H_{ck} = [C_{\lambda p}/(E_\lambda - E_c)]\, V_c H_{ck}$, the phase of this product is determined by that of the matrix elements $\langle \psi_0 | V_c | \psi_c \rangle \langle \psi_c | H_n | \psi_k \rangle$. Summed over C, the

number of the effective terms is of the order $\rho\Gamma_{\text{r.l.}} \gg 1$, and therefore even a slight change of the phase from the level to level $\Delta\varphi \approx 1/\rho\Gamma_{\text{r.l.}} \ll 1$ reduces the sum of the cross-terms to zero

In this approximation we obtain from (44) and (45)

$$G_\nu(E) = \frac{\sum_\lambda \frac{C_{\lambda p}^2}{E-E_\lambda} - i\frac{\Gamma_n}{2}\left[\sum_\lambda \frac{C_{\lambda p}^2}{(E-E_\lambda)^2} - \sum_\lambda \frac{C_{\lambda p}^2}{E-E_\lambda}\sum_\lambda \frac{1}{E-E_\lambda}\right]}{1+\frac{\Gamma_\gamma\Gamma_n}{4}\left[\sum_\lambda \frac{C_{\lambda p}^2}{E-E_\lambda} - \sum_\lambda \frac{C_{\lambda p}^2}{E-E_\lambda}\sum_\lambda \frac{1}{E-E_\lambda}\right] + \frac{i}{2}\left[\Gamma_\gamma \sum_\lambda \frac{C_{\lambda p}^2}{E-E_\lambda} + \Gamma_n \sum_\lambda \frac{1}{E-E_\lambda}\right]} H_\nu^*,$$

$$G_k(E) = \frac{\sum_{\lambda c} \frac{C_{\lambda c}^* H_{ck}^* C_{\lambda p}}{E-E_\lambda}}{1+\frac{\Gamma_\gamma\Gamma_n}{4}\left[\sum_\lambda \frac{C_{\lambda p}^2}{E-E_\lambda} - \sum_\lambda \frac{C_{\lambda p}^2}{E-E_\lambda}\sum_\lambda \frac{1}{E-E_\lambda}\right] + \frac{i}{2}\left[\Gamma_\gamma \sum_\lambda \frac{C_{\lambda p}^2}{E-E_\lambda} + \Gamma_n \sum_\lambda \frac{1}{E-E_\lambda}\right]}. \tag{46}$$

Hence we have for the probability of decay of the muon-nucleus system through the nuclear channels

$$W_n = \frac{\Gamma_n}{2\pi}\int_{-\infty}^{+\infty} dE \frac{\sum_\lambda \frac{C_{\lambda p}^2}{E-E_\lambda} - \left(\sum_\lambda \frac{C_{\lambda p}^2}{E-E_\lambda}\right)^2}{\left[1-\frac{\Gamma_\gamma\Gamma_n}{4}\sum_{\lambda\lambda'}\frac{C_{\lambda p}^2}{(E-E_\lambda)(E-E_{\lambda'})}(1-\delta_{\lambda\lambda'})\right]^2 + \frac{1}{4}\left(\sum_\lambda \frac{\Gamma_\gamma C_{\lambda p}^2 + \Gamma_n}{E-E_\lambda}\right)^2}. \tag{47}$$

For W_γ we obtain a more complicated integral. Therefore W_γ is better derived from the normalization condition $W_\gamma = 1 - W_n$. Substituting (36) into (47) and summing over λ we can calculate the intergal in (47) in the general form under the sole condition $\rho\Gamma_{\text{r.l.}} \gg 1$. The method of calculating this integral is set down in ref. [10]). We shall confine ourselves to quating the final result:

$$W_n = \left[1+\frac{\Gamma_\gamma}{\Gamma_{\text{r.l.}}}\frac{1+(\frac{1}{2}\pi\rho\Gamma_n)^2}{\frac{1}{2}\pi\rho\Gamma_n} + \left(\frac{\Gamma_\gamma}{\Gamma_{\text{r.l.}}}\right)^2\right]^{-\frac{1}{2}}, \tag{48}$$

$$\frac{W_\gamma}{W_n} = \sqrt{1+\frac{\Gamma_\gamma}{\Gamma_{\text{r.l.}}}\frac{1+(\frac{1}{2}\pi\rho\Gamma_n)^2}{\frac{1}{2}\pi\rho\Gamma_n} + \left(\frac{\Gamma_\gamma}{\Gamma_{\text{r.l.}}}\right)^2} - 1. \tag{49}$$

If the condition

$$\Gamma_{\text{r.l.}} \gg \frac{\Gamma_\gamma}{\rho\Gamma_n} \tag{50}$$

is fulfilled, it follows from (49) that

$$\frac{W_\gamma}{W_n} \approx \frac{\Gamma_\gamma}{\Gamma_{\text{r.l.}}}\frac{1}{\pi\rho\Gamma_n}. \tag{51}$$

Eq. (51) coincides with the result obtained in ref. [2]) under the assumption

$\Gamma_{\text{r.l.}} \gg \Gamma_\gamma$. From the calculation given above it follows that (50) is a more rigorous criterion of the validity of eq. (51). Schematically the yield of γ-quanta from the muon 2p-1s transition is represented in fig. 1 as a function of $\rho\Gamma_n$.

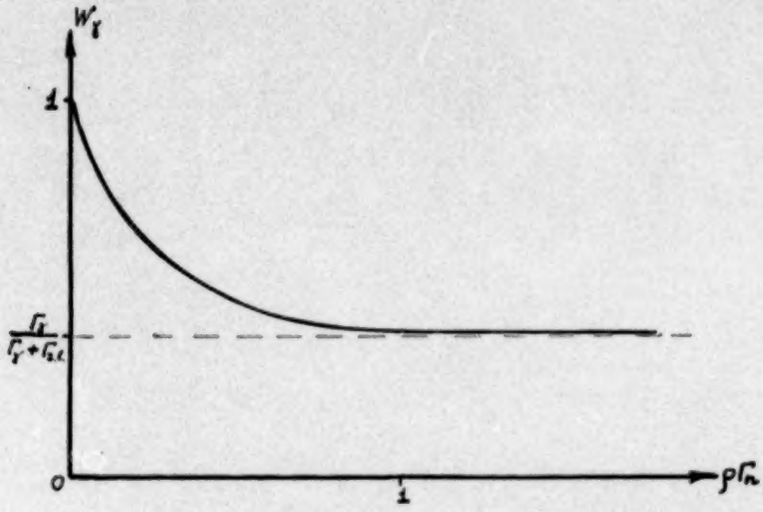

Fig. 1. The yield of γ-quanta from the 2p-1s transition as a function of $\rho\Gamma_n$ (schematically).

The curve for $\rho\Gamma_n \approx 1$ is found by interpolating from the values given by (49) at $\rho\Gamma_n \ll 1$ to the magnitude $\Gamma_\gamma/(\Gamma_\gamma+\Gamma_{\text{r.l.}})$ at $\rho\Gamma_n \gg 1$. From fig. 1 it is clear that the yield of γ-quanta at $\rho\Gamma_n \approx 1$ differs little from the case of totally overlapping nuclear levels, in agreement with ref. [1]). For very small $\rho\Gamma_n$ the decrease of the yield of γ-quanta is proportional to $\sqrt{\rho\Gamma_n}$.

5. Influence of Muon on Nuclear Fission

The nucleus excited in the transition of a muon from the 2p- into the 1s-state may decay in particular through the fission channel. Yet the probability of nuclear fission in the presence of a muon in the K-shell willl differ from that of the bare nucleus. Qualitatively this effect is explained by the fact that the muon while in the K-shell close to the nucleus (the Bohr radius of the muon in U is $a_\mu \approx \frac{1}{2}R$) prevents the deformation of the nucleus leading to fission. The influence of the presence of a muon in the K-shell on the probability of fission is the larger the closer the threshold fission energy to the nuclear excitation energy.

It can easily be seen that the nuclear rotation and fission effects are adiabatic with respect to the motion of the muon. The influence of the muon on nuclear fission can therefore be taken into account with a fixed orientation of the nuclear axes. In the deformation of the nucleus the muon binding energy decreases in the ground state and the energy threshold for nuclear fission increases accordingly. The potential curve for nuclear fission in the presence of

the muon E^{μ}_{nucl} is $E^{\mu}_{\text{nucl}} = E^{0}_{\text{nucl}} + E_{\mu}$, where E^{0}_{nucl} is the potential curve in the absence of the muon and E_{μ} is the muon binding energy as a function of nuclear deformation parameters. To find E_{μ}, the Schroedinger equation should be solved for the muon in the Coulomb field of the deformed nucleus. We shall make no appreciable error if we consider that the shape of the nucleus is an ellipsoid up to the saddle point. The Coulomb potential of a uniformly charged rotation, ellipsoid with semi-axes a and b is

$$\varphi(\alpha,\beta) = \frac{Ze}{C} \times \begin{cases} [1-p_2(\operatorname{ch}\alpha)p_2(\cos\beta)]\ln \operatorname{cth}\frac{\alpha_0}{2} + \frac{3}{2}\frac{\operatorname{ch}^2\alpha}{\operatorname{ch}^2\alpha_0}p_2(\cos\beta) + \frac{3}{4}\left(1-\frac{\operatorname{sh}^2\alpha}{\operatorname{sh}^2\alpha_0}\right)\frac{\sin^2\beta}{\operatorname{ch}\alpha_0} \\ \qquad\qquad \text{if} \quad \operatorname{ch}\alpha \leqq \operatorname{ch}\alpha_0 = \frac{a}{c}, \quad (52) \\ [1-p_2(\operatorname{ch}\alpha)p_2(\cos\beta)]\ln \operatorname{cth}\frac{\alpha}{2} + \frac{3}{2}\operatorname{ch}\alpha p_2(\cos\beta) \quad \text{if} \quad \operatorname{ch}\alpha \geqq \frac{a}{c}, \end{cases}$$

where Ze is the nuclear charge, $c^2 = a^2 - b^2$, p_2 the Legendre polynomial of the second order and α and β are the degenerate elliptical coordinates.

The Schroedinger equation with the potential (52) was numerically integrated for the ground state of the muon by an electronic computor. The magnitude of the muon binding energy in U^{238} as a function of the ratio of the nuclear semi-axes is represented in table 1.

TABLE 1

The magnitude of the muon binding energy in U^{238} as a function of the ratio of the nuclear semi-axes

$\frac{a}{b}$	1.2	1.4	1.6	1.8	2	2.2	2.5
E (MeV)	11.89	11.79	11.66	11.53	11.36	11.21	11.01

Using the hydrodynamic model for fission [11]), we can find the ratio of the nuclear semi-axes $(a/b)_{\text{s.p.}}$ corresponding to the saddle point. This ratio and the increasing barrier of fission ΔE_{thr} for several nuclei are represented in table 2 where $(a/b)_{\text{st}}$ is the static deformation [12]) and E_{thr} is the fission energy threshold [13]).

TABLE 2

The ratio of the nuclear semi-axes and the barrier of fission

Nucleus	$\left(\frac{a}{b}\right)_{\text{st}}$	$\left(\frac{a}{b}\right)_{\text{s.p.}}$	E_{thr} (MeV)	ΔE_{thr} (MeV)
U^{238}	1.3	2.24	5.8	0.6
U^{235}	1.25	2.2	5.75	0.6
Pu^{239}	1.3	2.17	5.48	0.5

From table 2 it is clear that in the case of U^{238} the fission threshold in the presence of a muon lies above the excitation energy and in the case of Pu^{239} it is roughly 0.3 MeV below the excitation energy.

6. Conclusion

The calculation given in the present paper shows that $\Gamma_{\text{r.l.}} \approx \Gamma_\gamma$. To know the magnitude $\Gamma_{\text{r.l.}}/\Gamma_\gamma$ more accurately, the photo-capture cross-section in the nuclei of interest to us should be measured directly. The calculation of the photo-capture cross section on the basis of data on photo-fission and photo-neutron yield is not highly reliable since the processes involving the elastic and inelastic scattering of γ-quanta are not taken into consideration. With the ratio of the widths indicated, the $\rho\Gamma_n$ dependence of the γ-quantum yield of the 2p-1s transition for one muon is weak. As is clear from (49), for example, the change of the magnitude $\rho\Gamma_n$ from 0.1 to 0.05 at $\Gamma_{\text{r.l.}} = \Gamma_\gamma$ leads to an increase of the γ-quantum yield from 0.71 to 0.79. The dependence of W_γ on $\rho\Gamma_n$ can be more essential only in the case when $\Gamma_{\text{r.l.}} \gg \Gamma_\gamma/\rho\Gamma_n$. The experimental results obtained in ref. [14]) show that W_γ depends rather weakly on $\rho\Gamma_n$. This result is in qualitative agreement with the theory. The quantitative treatment of the experiments to obtain the magnitude $\rho\Gamma_n$ will only be possible if W_γ is measured more accurately for different nuclei.

Let us now consider the experimental data on the fission due to radiationless nuclear excitation. Let us assume that the presence of a muon in the K-shell does not affect the magnitude of the fission barrier. Since the probability of the radiationless excitation of U^{238} is of the order of [14]) 20 %, the probability of energy yield through the fission channel is $\approx$ 5 %. The probability of fission after the capture of a muon by the nucleus U^{238} is $\approx$ 10 % (ref. [15])). Radiationless excitation can also be accompanied by the emission of a neutron from the excited nucleus. The residual nucleus may also capture a muon and fission. With allowances for these processes, the ratio of fissions due to radiationless excitation to those due to muon capture proves to be of the order of 20 % to 50 %. Experimentally this quantity was measured in ref. [16]) and proved equal to 5.6 ± 2.7 %. Thus the assumption that the presence of a muon in the K-shell does not affect the magnitude of the fission barrier is contradicted by experiment. As is clear from table 2, a more suitable nucleus for the study of fission due to radiationless excitation is Pu^{239}. It should also be borne in mind that in Np^{237} and Am^{241} the threshold of neutron emission is above the radiationless excitation energy and therefore the above nuclei may decay only through the radiative and fission channels.

In conclusion the authors express their gratitude to D. P. Grechukhin for the discussion of the influence of the muon on nuclear fission, V. K. Saulyev,

for programming and electronic computation as well as to B. M. Pontecorvo, M. Ya. Balats, L. G. Landsberg and L. N. Kondratyev for discussing the experimental data.

References

1) D. F. Zaretsky, Proc. Second United Nations Int. Conf. on the peaceful uses of atomic energy, (Geneva, 1958), Vol. **15**, p. 175
2) D. F. Zaretsky and V. M. Novikov, Nuclear Physics **14** (1960) 540
3) D. P. Grechukhin, private communication
4) D. Blatt and V. Weisskopf, Theoretical nuclear physics (Weley, New York-London, 1952)
5) V. M. Novikov, JETP **41** (1961) 276
6) G. E. Pustovalov, JETP **36** (1959) 1806
7) R. A. Schmitt and R. B. Duffield, Phys. Rev. **105** (1957) 1277
8) L. E. Lazareva *et al.*, The Session of the USSR Academy of Sciences on the peaceful uses of atomic energy (USSR Academy of Sciences Publishing House, Moscow, 1955)
9) V. Heitler, The quantum theory of radiation (Oxford, University Press, 1954)
10) D. F. Zaretsky and V. M. Novikov, JETP **41** (1961) 214
11) W. J. Swniateski, Proc. Second United Nations Int. Conf. on the peaceful uses of atomic energy, (Geneva, 1958) Vol. **15**, p. 248
12) K. Alder, A. Bohr, T. Huns. B. Mottleson and A. Winter, Rev. Mod. Phys. **28** (1956) 432
13) A. Cameron, Proc. symposium of the physics of fission (Ontario, 1956) p. 189
14) N. Ya. Balats *et al.*, JETP **39** (1960) 1168
15) G. E. Belovitsky *et al.*, JETP **38** (1960) 404
16) J. Diaz, S. N. Kaplan, B. MacDonald and R. V. Pyle, Phys. Rev. Lett. **3** (1959) 234

1.C:
1.D.4

Nuclear Physics **28** (1961) 192—209; © *North-Holland Publishing Co., Amsterdam*
Not to be reproduced by photoprint or microfilm without written permission from the publisher

PAIRING FORCES AND PAIR CORRELATIONS IN Pb^{206}, Pb^{210} AND Po^{210}

V. N. GUMAN, Yu. I. KHARITONOV, L. A. SLIV and G. A. SOGOMONOVA
Leningrad Physical-Technical Institute, Academy of Sciences, Leningrad, USSR

Received 21 December 1960

Abstract: Pairing forces acting between nucleons in a nucleus are studied. Nuclei with two identical nucleons (holes) over the closed shells are investigated for this purpose. Both pairing interaction and the nucleon interaction with the surface of the nuclear core are taken into account by diagonalizing the energy matrix. The need of evaluating pair correlation not only for $I = 0$ but also for other values of I is shown. Study is made of the sensitivity of the pairing potential to different physical characteristics of nuclei. The energy levels up to 3 MeV are obtained for the Pb^{206}, Pb^{210} and Po^{210} nuclei and the transition probabilities calculated.

1. Introduction

The nuclear forces affecting an individual nucleon close to the Fermi energy surface can, in their principal part, be represented by a self-consistent field, responsible for the formation of nuclear shells. Yet the residual short-range forces after the subtraction of the self-consistent field are not small enough to be allowed for as a minor correction. The importance of the residual forces proves to be much larger than it was supposed before, which has become especially conspicuous after the application of the modern superconductivity theory to the investigation of nuclear excitations.

The present investigation has been undertaken to find the explicit form of the residual forces acting between two nucleons in a nucleus and known as pairing forces. Another aim of the investigation is to see to what extent the self-consistent field together with pairing forces can explain and describe all properties of the nuclear states up to an excitation energy of ≈ 3 MeV.

2. Choice of the Forces

The simplest system for investigating nuclear forces is a nucleus with closed neutron and proton shells $\pm$ one nucleon. In this case the forces acting on an external particle (or a hole) are expressed through the central potential $V_C(r, \mathbf{s}\cdot\mathbf{l})$ and the quadrupole potential $V_S(r, \theta, \varphi)$. To be more exact, V_C and V_S are the two leading terms of the expansion of a self-consistent potential for an external nucleon. This can be exemplified best of all by two-particle forces. Having expanded the potential acting on the i-th particle $V(\mathbf{r}_i) = \sum_{k\neq i}^{A} V(\mathbf{r}_i - \mathbf{r}_k)$ in a series of Legendre polynomials $P_l(\cos\omega_{ik})$ and

averaging it over the states of all particles except the i-th, we find that the term of the series with $l = 0$ gives the central potential V_C and the term with $l = 2$ the quadrupole potential V_S. So far there has been conclusive evidence in favour of taking no account of the terms with $l > 2$ in considering low excitations and therefore these terms are discarded. The residual forces in the case of one particle have a negligible effect.

In ref. [1]) an analysis of the spectra of the excitations of nuclei with one nucleon (or a hole) over the closed shells provided the basis for determining the parameters of the potential

$$V_C(r, \mathbf{s}\cdot\mathbf{l}) = V(r) - \lambda\left(\frac{\hbar}{2Mc}\right)^2 \frac{\mathbf{s}\cdot\mathbf{l}}{r}\frac{\mathrm{d}V(r)}{\mathrm{d}r}, \tag{1}$$

where

$$V(r) = \frac{V_0}{1+\mathrm{e}^{\alpha(r-r_0)}}. \tag{2}$$

The parameters V_0, α and λ proved to be rather stable for the nuclei from O^{17} to Bi^{209}. Therefore V_S may be regarded as known.

The quadrupole potential V_S is usually represented in the form

$$V_S = \mp\kappa(r)\sum_\mu \alpha_{2\mu} Y_{2\mu}(\theta, \varphi), \tag{3}$$

where the $-$ sign is to be taken for the particles and the $+$ sign for the holes.

The potential V_S can formally be regarded as such an interaction of an external particle with the others which is described by the deformation of the potential surface. For small deformations we have

$$\kappa(r) = r\frac{\partial V(r)}{\partial r}. \tag{4}$$

The radial matrix elements can be calculated:

$$\langle nl|\kappa(r)|n'l'\rangle = \int_0^\infty R_{nl}(r)R_{n'l'}(r)r^3\frac{\partial V}{\partial r}\,\mathrm{d}r, \tag{5}$$

where $R_{nl}(r)$ are the radial wave functions of a particle in the potential (1). It appears that with small deviations we have for all states of the external nucleons in the lead region

$$\langle nl\,|\kappa(r)|n'l'\rangle \approx (-1)^{n+n'}\ 40\ \text{MeV}. \tag{5'}$$

It is this value that is accepted in the following.

The other parameters of interaction with the surface α_μ are represented in the form [2])

$$\alpha_\mu = \sqrt{\frac{\hbar\omega}{2C}}\,(b_\mu + (-1)^\mu b^+_{-\mu}). \tag{6}$$

It is assumed that the core surface characterized by the effective surface tension C is subject to quadrupole oscillations with the phonon energy $\hbar\omega$, while b_μ and b_μ^+ are the operators of the annihilation and creation of a phonon with spin 2 and projection μ.

In nuclei with two external nucleons (holes) it is necessary to take into account the effective pairing potential V_p of the interaction of the two nucleons, apart from the potentials V_C and V_S. The potential V_p cannot be included in the two others, for its principal short-range part is essential. In the case of two external nucleons it is precisely the potential V_p which gives an addition to the energy of states as well as changes their properties.

Let us assume for V_p the following form:

$$V_p(1, 2) = -[v_t\pi_t+v_s\pi_s] \exp\left\{-\frac{|\mathbf{r}_1-\mathbf{r}_2|^2}{\rho^2}\right\}. \tag{7}$$

Here ρ is the effective pairing interaction range, v_t and v_s are the parameters of triplet and singlet forces and $\pi_t = \frac{1}{4}(3+\boldsymbol{\sigma}_1\cdot\boldsymbol{\sigma}_2)$ and $\pi_s = \frac{1}{4}(1-\boldsymbol{\sigma}_1\cdot\boldsymbol{\sigma}_2)$ are the projection operators.

Taking account of only spin forces and excluding tensors is due to the fact that at small excitation energies there are no distinct effects making it possible to separate the tensors and the usual spin forces.

The choice of the Gaussian form for the radial dependence of pairing forces is somewhat arbitrary, for any other rapidly diminishing function is also suitable. Yet since the results depend on the integral effect, it is the qualitative characteristics of the forces and not details that really matter. No account was taken of the possible repulsion between the nucleons at the distances $|\mathbf{r}_1-\mathbf{r}_2| \leqq 0.5$ fm (of the so-called "core"). Taking account of the repulsion and the respective correction of the functions, with the aid of a cut-off factor of the type $1-\exp\{-|\mathbf{r}_1-\mathbf{r}_2|^2/r_C^2\}$ for example, yields a negligible contribution to the level energy. Consequently, this kind of forces at small distances plays no part in the problem under consideration.

3. Calculation Method

In the present paper the nucleus is regarded as a system consisting of a core capable of oscillation, and two interacting nucleons (holes). The Hamiltonian of this system can be written as

$$\hat{H} = \hat{H}_S+\hat{H}_0(1)+\hat{H}_0(2)+\hat{V}_S(1)+\hat{V}_S(2)+\hat{V}_p(1, 2), \tag{8}$$

$$H_S = \hbar\omega(\tfrac{5}{2}+\sum_\mu b_\mu^+ b_\mu), \tag{8'}$$

$$H_0(i) = -\frac{\hbar^2}{2M}\Delta_i+V_C(i). \tag{8''}$$

The potentials V_C, V_S and V_p are given by eqs. (1), (3) and (7).

The problem is to determine the eigenvalues and eigenfunctions of the Schrödinger equation

$$\hat{H}\,|IM\nu\rangle = E\,|IM\nu\rangle. \tag{9}$$

As basis functions we shall accept the well-known eigenfunctions

$$|[(n_1 l_1 j_1, n_2 l_2 j_2)J]_a;\ NR;\ IM\nu\rangle \tag{10}$$

of the operator

$$\hat{H}' = \hat{H}_S + \hat{H}_0(1) + \hat{H}_0(2).$$

Here J is the resulting angular momentum of the two nucleons which, vectorially connected with the angular momentum R formed by N photons, gives the total spin of the nucleus I and the projection M. The subscript a denotes that the function of the two nucleons is antisymmetrized. The parity of the function is $\nu = (-1)^{l_1+l_2}$. The eigenvalues of the Hamiltonian H' are equal to $E' = N\hbar\omega + E_1^{(0)} + E_2^{(0)}$. Let us solve eq. (9) in the form of an expansion in the basis functions (10):

$$\begin{aligned} |IM\nu\rangle = &\sum_{\substack{n_1 l_1 j_1,\ n_2 l_2 j_2,\\ J,N,R}} c^J(n_1 l_1 j_1,\ n_2 l_2 j_2,\ J, N, R) \\ &\times |[(n_1 l_1 j_1, n_2 l_2 j_2)J]_a; NR; IM\nu\rangle. \end{aligned} \tag{11}$$

Then $\langle|H|\rangle$ becomes a symmetrical matrix, and the matrix elements can be calculated by the well-known methods of the algebra of irreducible tensor operators.

Let us write the principal formulas for calculating the matrix elements of the operators V_S and V_p with non-antisymmetrized basis functions. Taking account of the identity of particles does not introduce anything new in the formulas but make them more cumbersome.

The operator $V_S(i)$ can be written as a scalar product of two tensor operators of the second rank:

$$V_S(i) = \mp\kappa(r_i)\sqrt{\frac{5}{4\pi}}\,(\alpha^+ \cdot \mathbf{T}^2(\theta_i\varphi_i)). \tag{12}$$

Then the matrix elements of the interaction of the external nucleons with the core surface are equal to

$$\begin{aligned} &\langle (n_1 l_1 j_1, n_2 l_2 j_2)J; NR; IM|\sum_{i=1}^{2} V_S(i)|(n'_1 l'_1 j'_1, n'_2 l'_2 j'_2)J', N'R'; IM\rangle \\ &= (-1)^{\alpha+n_1+n_2+n'_1+n'_2+J+R'-I+j_2-j'_1} 40\left[\frac{5}{4\pi}\frac{\hbar\omega}{2C}(2J+1)(2J'+1)\right]^{\frac{1}{2}} \\ &\times \langle NR||b||N'R'\rangle W(JRJ'R'; I2) \\ &\times \{\delta_{n_1 l_1 j_1,\ n'_1 l'_1 j'_1}(-1)^{J'}\langle l_2 j_2||\mathbf{T}^2||l'_2 j'_2\rangle W(j_2 J j'_2 J'; j_1 2) \\ &+ \delta_{n_2 l_2 j_2,\ n'_2 l'_2 j'_2}(-1)^{J}\langle l_1 j_1||\mathbf{T}^2||l'_1 j'_1\rangle W(j_1 J j'_1 J'; j_2 2)\}. \end{aligned} \tag{13}$$

Here we used

$$\alpha = \begin{cases} 1 & \text{for the particles,} \\ 0 & \text{for the holes.} \end{cases}$$

Furthermore, $W(abcd; ef)$ is the Racah-coefficient, and $\langle NR \,||b||\, N'R' \rangle$ and $\langle lj \,||\mathbf{T}^2||\, l'j' \rangle$ are the reduced matrix elements [4]).

To calculate the matrix elements of the operator $V_p(1, 2)$, we shall first expand the coordinate part into the series

$$e^{-\frac{|r_1-r_2|^2}{\rho}} = \sum_{k=0}^{\infty} f_k(r_1 r_2) P_k(\cos \omega_{12})$$

$$= \sum_{k=0}^{\infty} f_k(r_1, r_2) \frac{4\pi}{2k+1} \sum_{m=-k}^{m=k} Y^*_{km}(1) Y_{km}(2) = \sum_{k=0}^{\infty} f_k(r_1 r_2)(\mathbf{T}^k(1) \cdot \mathbf{T}^k(2)). \quad (14)$$

After which we have

$$V_p(1, 2) = -(v_t \pi_t + v_s \pi_s) \sum_{k=0}^{\infty} f_k(r_1 r_2)(\mathbf{T}^k(1) \cdot \mathbf{T}^k(2)) = V_p^{\,t}(1, 2) + V_p^{\,s}(1, 2). \quad (15)$$

In calculating the matrix elements it is convenient to pass from the $j-j$ coupling to the $L-S$ coupling. Then $\langle |V_p^{\,s}| \rangle$ is easily calculated as

$$\langle (n_1 l_1 j_1, n_2 l_2 j_2) J, NR; IM | V_p^{\,s}(1, 2) | (n'_1 l'_1 j'_1, n'_2 l'_2 j'_2) J', N'R'; IM \rangle$$

$$= -v_s \delta_{JNR, J'N'R'} A \begin{pmatrix} l_1 & \frac{1}{2} & j_1 \\ l_2 & \frac{1}{2} & j_2 \\ J & 0 & J \end{pmatrix} A \begin{pmatrix} l'_1 & \frac{1}{2} & j'_1 \\ l'_2 & \frac{1}{2} & j'_2 \\ J & 0 & J \end{pmatrix} \sum_k F^k(n_1 l_1 j_1, n_2 l_2 j_2; n'_1 l'_1 j'_1; n'_2 l'_2 j'_2)$$

$$\times (-1)^{l_1 + l'_2 - J} \langle l_1 || \mathbf{T}^k || l'_1 \rangle \langle l_2 || \mathbf{T}^k || l'_2 \rangle W(l_1 l_2 l'_1 l'_2; Jk). \quad (16)$$

In the matrix element for $V_p^{\,t}(1, 2)$ there appears an additional sum for the total angular momentum of two particles:

$$\langle (n_1 l_1 j_1, n_2 l_2 j_2) J; NR; IM | V_p^{\,t}(1, 2) | (n'_1 l'_1 j'_1, n'_2 l'_2 j'_2) J'; N'R'; IM \rangle$$

$$= -v_t \delta_{JNR, J'N'R'} \sum_L A \begin{pmatrix} l_1 & \frac{1}{2} & j_1 \\ l_2 & \frac{1}{2} & j_2 \\ L & 1 & J \end{pmatrix} A \begin{pmatrix} l'_1 & \frac{1}{2} & j'_1 \\ l'_2 & \frac{1}{2} & j'_2 \\ L & 1 & J \end{pmatrix} \sum_k F^k(n_1 l_1 j_1, n_2 l_2 j_2, n'_1 l'_1 j'_1, n'_2 l'_2 j'_2)$$

$$\times (-1)^{l_1 + l'_2 - L} \langle l_1 || \mathbf{T}^k || l'_1 \rangle \langle l_2 || \mathbf{T}^k || l'_2 \rangle W(l_1 l_2 l'_1 l'_2; Lk). \quad (17)$$

Here

$$A \begin{pmatrix} l & \frac{1}{2} & j \\ l' & \frac{1}{2} & j' \\ L & S & J \end{pmatrix}$$

is the coefficient of the transition from $j-j$ to $L-S$ coupling and furthermore

we have used the relation

$$\langle l||\mathbf{T}^k||l'\rangle = \sqrt{2l'+1}C^{l0}_{l'0\,k0},$$

where $C^{l0}_{l'0\,k0}$ is the Clebsch-Gordan coefficient. Finally, we used in eq. (17) the integral

$$F^k(n_1l_1j_1,\ n_2l_2j_2;\ n'_1l'_1j'_1,\ n'_2l'_2j'_2)$$
$$= \int R_{n_1l_1j_1}(r_1)R_{n_2l_2j_2}(r_2)f_k(r_1r_2)R_{n'_1l'_1j'_1}(r_1)R_{n'_2l'_2j'_2}(r_2)r_1^2r_2^2\,\mathrm{d}r_1\,\mathrm{d}r_2 \quad (18)$$

It should be noted that taking account of antisymmetrization also leads to the appearance of exchange integrals of the type

$$G^k(n_1l_1j_1,\ n_2l_2j_2,\ n'_1l'_1j'_1;\ n'_2l'_2j'_2)$$
$$= \int R_{n_1l_1j_1}(r_1)R_{n_2l_2j_2}(r_2)f_k(r_1r_2)R_{n'_1l'_1j'_1}(r_2)R_{n'_2l'_2j'_2}(r_1)r_1^2r_2^2\,\mathrm{d}r_1\,\mathrm{d}r_2. \quad (18')$$

After calculating the matrix elements the problem of determining the eigenvalues and eigenfunctions reduces itself to diagonalizing the matrix (9). The method is approximate as the infinite matrix cuts off at a certain level. If we demand, for example, that in the wave function (11) of a given level the terms with the coefficients $c^I > 0.03$ should only be preserved, we shall have to reject all levels for which the ratio $\{\langle a\,|V_S+V_p|b\rangle/(E_a-E_b)\} < 0.03$ with selected parameters. In the following the order of the matrix is chosen so that the first three levels for each I are determined with high accuracy.

The level energies and the coefficients c^I in (11) will depend on the three parameters ρ, v_t and v_s of pairing forces and the two parameters $\hbar\omega$ and C involved in the interaction with the core †. Not all experimentally measured values are equally sensitive to these parameters. Thus the distance between the first level 2^+ and the ground state 0^+ are mainly determined by the quantities v_s and v_t. A small variation of the parameter ρ results in a strong change in the binding energy but has a small effect on the distance between the levels 2^+ and 0^+. The E2 transition probabilities ($2 \to 0$, $2 \to 2$, etc.) determine the choice of the parameters $\hbar\omega$ and C. Thus, there is a possibility to make a rough estimate of the values of the unknown parameters prior to diagonalization.

4. Determining Parameters for Pb^{206}

The first study-object was Pb^{206}, a nucleus with two deficient nucleons. The choice of Pb^{206} was motivated by its spectrum having been well studied. About 30 levels are known in the nucleus of Pb^{206} with the spins and parities established and the transition probabilities or relative intensities determined.

† The parameters $\hbar\omega$ and C can be determined independently from the E2 transitions and quadrupole moments of nuclei with closed shells ± one nucleon.

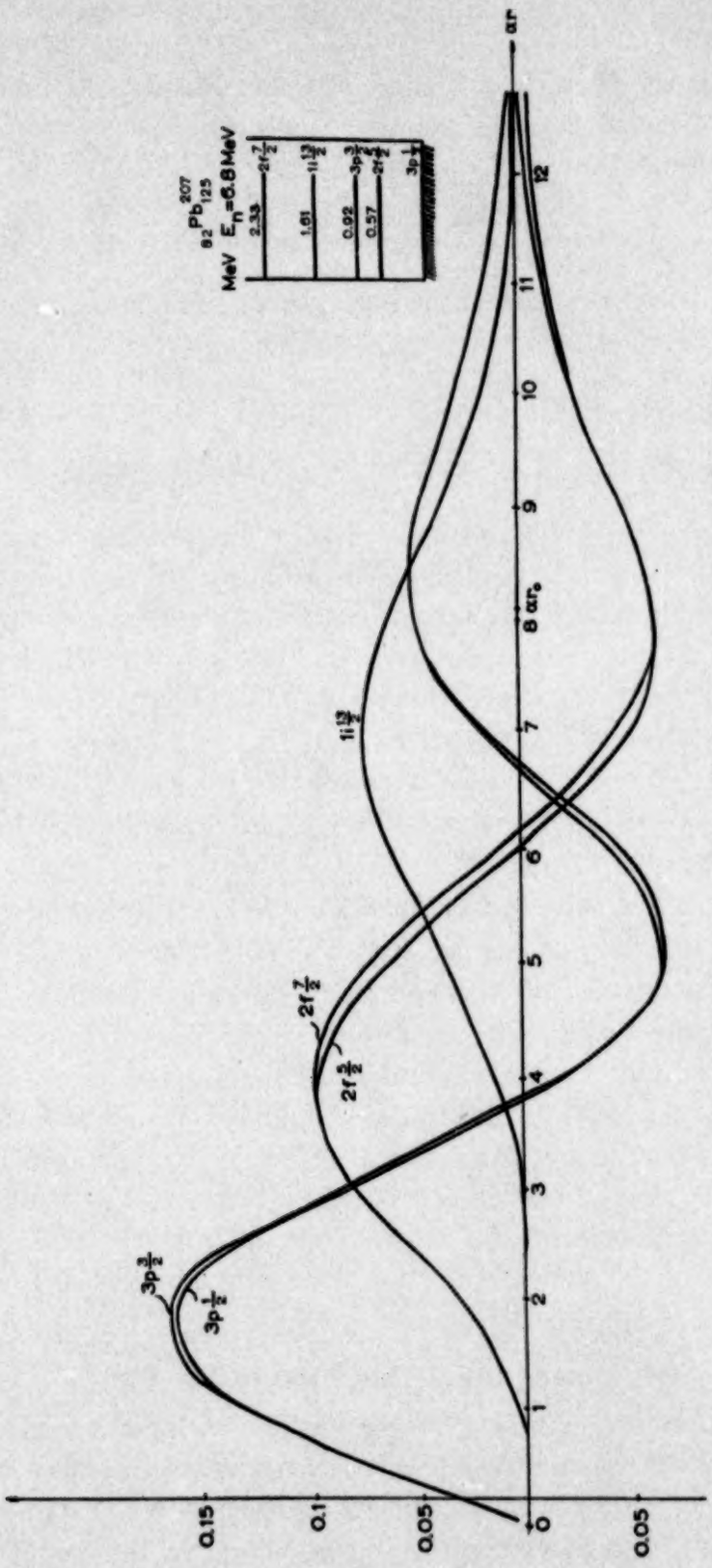

Fig. 1. Single-particle wave functions and energy levels of Pb^{207}.

The Pb^{206} nucleus has been studied in several theoretical investigations with an analysis of the levels which can be used for reference in our calculations. The energies and functions of the single-particle state in the Pb^{207} nucleus were taken from ref. [1]). Fig. 1 represents the data on Pb^{207} levels necessary for the following. Then we calculated the matrix elements of the pair and surface interactions. The calculation of the radial integrals F^k and G^k and the subsequent diagonalization of the matrices were performed on the Strela electronic computor.

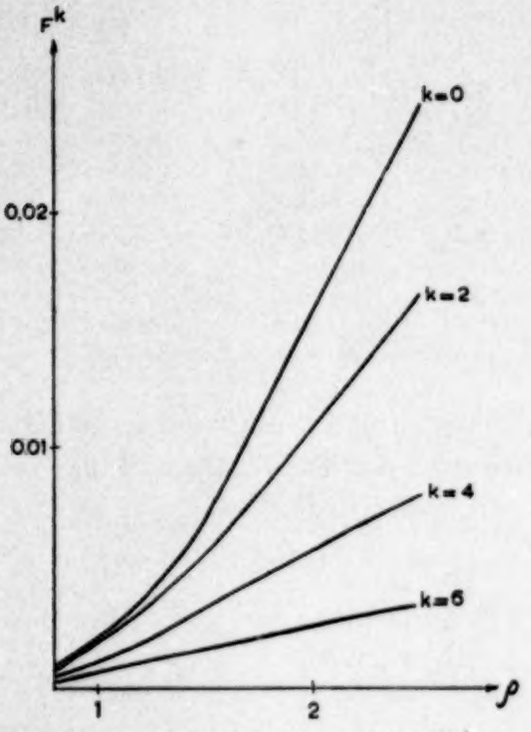

Fig. 2. Dependence of the radial integrals $F^k(n_1l_1j_1, n_2l_2j_2, n'_1l'_1j'_1, n'_2l'_2j'_2)$ in Pb^{206} on the parameter ρ for different k.

Fig. 2 represents the dependence of the radial integrals $F^k(n_1l_1j_1, n_2l_2j_2; n'_1l'_1j'_1, n'_2l'_2j'_2)$ on the parameter ρ for different values of k. It is interesting to compare our matrix elements of pairing interactions with those calculated with the functions of the oscillator potential. Table 1 makes this comparison with the data from ref. [3]) after reducing all data to the same ρ and v_s. It is clear that the oscillator functions yield overestimated matrix elements.

The following fact should be borne in mind in determining the parameters for the Pb^{206} nucleus. All principal matrix elements of Pb^{206} contain v_s and v_t approximately in the same ratio $a(2v_s+v_t)$, where a is a certain number. This being the case it is difficult to determine both parameters at once, and it is expedient to leave only one of them, v_s for example, which will express the effective sum of both. Calculations will then be shorter though a small error is introduced thereby. Thus we ought to determine the four parameters ρ, v_s, $\hbar\omega$ and C.

First we shall take account of only pairing interaction to see what effects it yields.

TABLE 1

Comparison of pairing interaction matrix elements when the radial wave functions of oscillator and diffuse potentials are used for Pb^{206}

Configuration	Oscillator potential	Diffuse potential	Ratio
$(p_{\frac{1}{2}})^2 0^+$	−0.427	−0.349	0.817
$(f_{\frac{5}{2}})^2 0^+$	−0.685	−0.581	0.848
$(p_{\frac{1}{2}} f_{\frac{5}{2}}) 1^+$	0	0	
$(p_{\frac{3}{2}} f_{\frac{5}{2}}) 2^+$	−0.329	−0.236	0.717
$(p_{\frac{3}{2}} p_{\frac{1}{2}}) 2^+$	−0.520	−0.399	0.767
$(p_{\frac{1}{2}})^2 2^+$	−0.260	−0.199	0.765
$(f_{\frac{5}{2}})^2 2^+$	−0.235	−0.195	0.830
$(p_{\frac{1}{2}} f_{\frac{5}{2}}) 2^+$	−0.094	−0.069	0.734
$(p_{\frac{3}{2}} f_{\frac{5}{2}}) 3^+$	−0.037	−0.025	0.676
$(p_{\frac{3}{2}} f_{\frac{5}{2}}) 4^+$	−0.046	−0.036	0.783
$(f_{\frac{5}{2}})^2 4^+$	−0.101	−0.083	0.822
$(p_{\frac{3}{2}} f_{\frac{5}{2}}) 4^+$	−0.364	−0.265	0.728

Figs. 3 and 4 represent the results of diagonalizing the corresponding matrices at different values of ρ and v_s. Analysis of the results obtained warrants the following important conclusions:

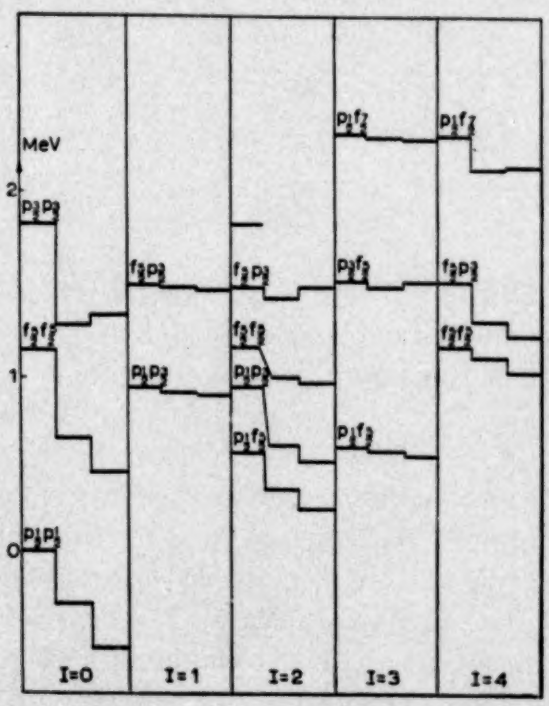

Fig. 3. Change in the position of levels as a result of taking into account the pairing forces in Pb^{206}. In each column, the levels on the left are single-particle levels, those in the middle are levels calculated after the inclusion of only the diagonal term of pairing interaction and those on the right are levels calculated taking into account pair correlation.

a) The matrix elements of pairing interaction are large for the levels with spin $I = 0$, less, approximately by a factor 2, for the levels $I = 2$, still less for $I = 4$, and very small indeed for the other levels.

b) Taking account of the non-diagonal terms of the matrix, that is of pairing correlations, leads to the appearance of considerable repulsion between the levels and a mixture in the resulting wave functions.

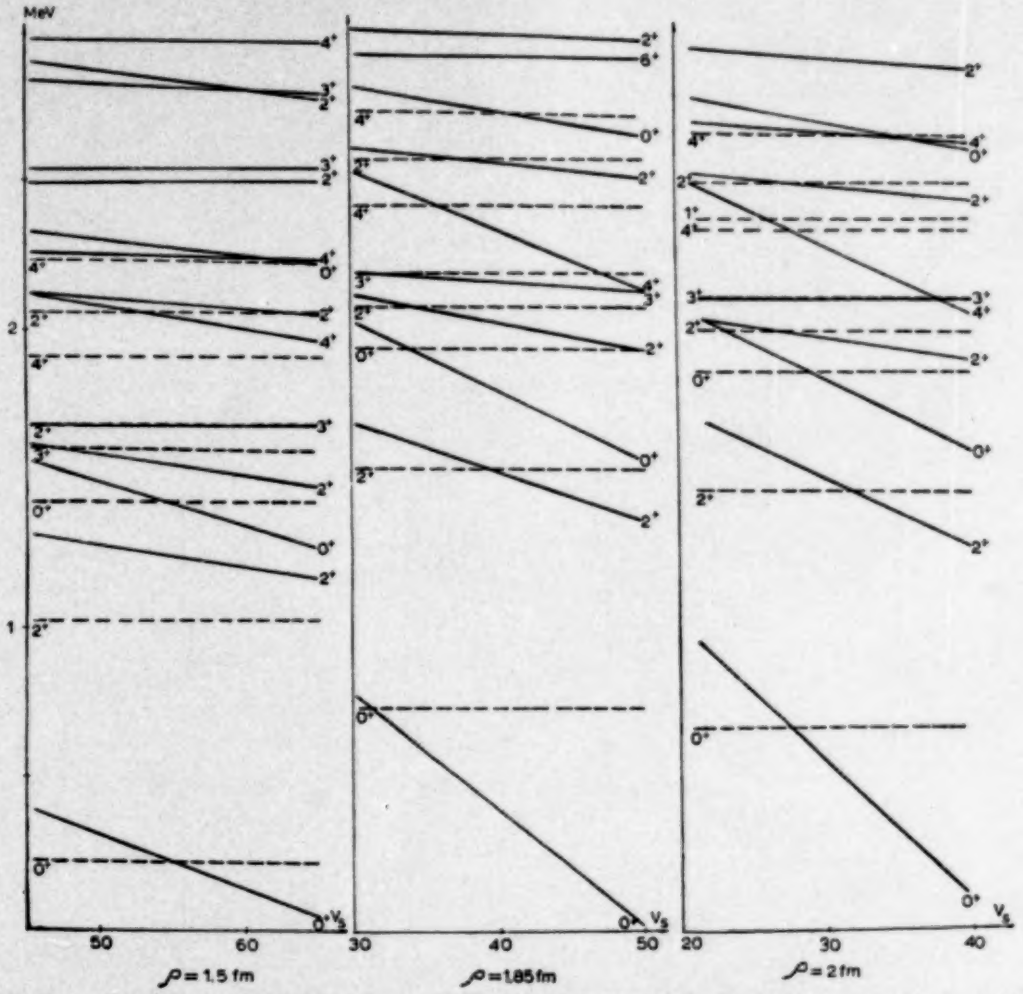

Fig. 4. Relative spacing of Pb^{208} energy levels for different values of the parameters ρ and v_0. Experimental levels are shown by dashed lines.

c) Since the pairing interaction has the largest effect on the ground level $I = 0$ an energy gap of ≈ 0.8 MeV is formed between the ground state $I = 0$ and the other levels.

d) The level energy and spacing at $\rho < 1.5$ fm and $\rho > 2.5$ fm differ from experiment so widely that the subsequent evaluation of the interaction with the surface cannot rectify the situation. Hence it follows in particular that δ-forces can be used, on account of their simplicity, for obtaining different qualitative results, but they are not suitable for obtaining quantitative results.

e) The E2 transition probabilities deviate from experiment especially widely.

Let us now introduce the additional quadrupole interaction. In choosing the parameters $\hbar\omega$ and C it should be taken into account that up to an excitation energy 2 MeV the number of possible single-particle levels with $I = 2^+$ is equal to that of experimentally known levels of this kind. Therefore $\hbar\omega$ cannot be less than 2 MeV.

Study was made of the values $\hbar\omega$ from 2 to 10 MeV and C from 800 to 2000 MeV. The best agreement with experimental data was obtained with the parameters † $v_s = 25$ MeV, $\rho = 2$ fm, $\hbar\omega = 3$ MeV and $C = 1000$ MeV.

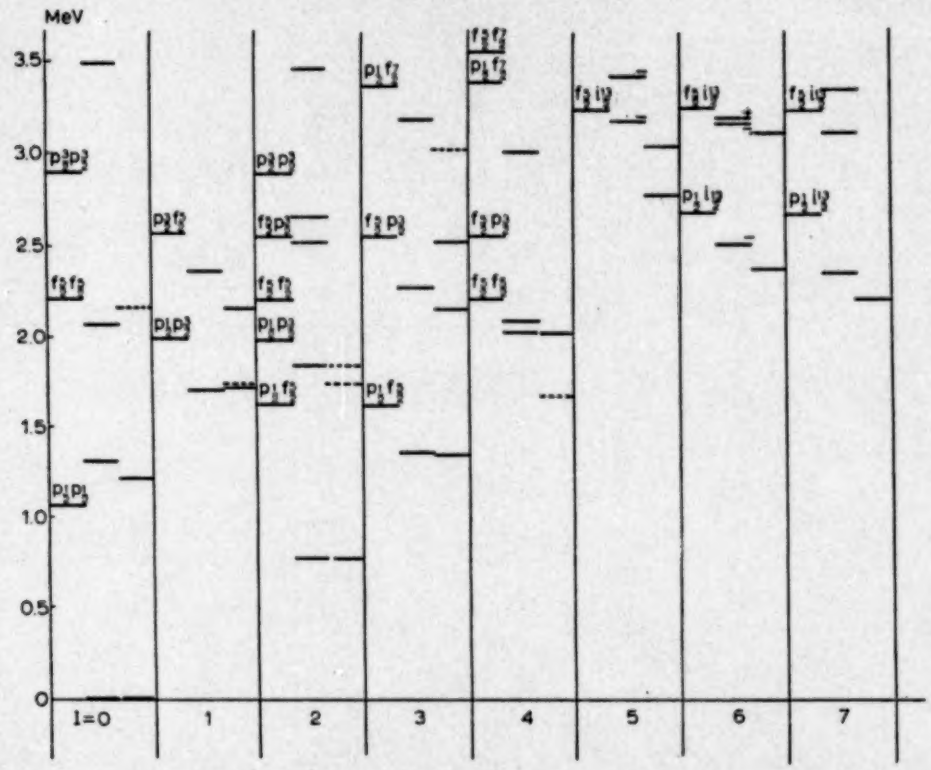

Fig. 5. Comparison of the results obtained for Pb^{206} energy levels with experimental data. In each column, to the left are shown position and configuration of single-particle levels, in the middle the final position of levels after taking account of the pairing forces and interaction with the core surface and on the right the experimental levels. The levels determined unreliably are represented by a dashed line.

Fig. 5 and table 2 represent the principal results of calculating the Pb^{206} levels with spins from $I = 0$ to $I = 7$. The energies of the first three levels with a given I were determined with accuracy to several units of the third decimal place. To ensure this accuracy it was usually necessary to diagonalize a matrix of the 14th order, and it was only for $I = 0$ that a matrix of the

† The experimental levels of Pb^{207} are not purely single-particle levels, for the energy of interaction of a nucleon with a core surface should be detracted. If we allow for this small correction the results obtained will not change, except for the parameter v_s increasing up to $\neq 30$ MeV.

TABLE 2

The energies and principal coefficients $c^I(n_1 l_1 j_1,\ n_2 l_2 j_2,\ J, N, R)$ of the components of wave functions of Pb^{206} levels

$I = 0$	$p_{\frac{1}{2}}p_{\frac{1}{2}}0;$ 00	$f_{\frac{1}{2}}f_{\frac{1}{2}}0;$ 00	$p_{\frac{1}{2}}p_{\frac{1}{2}}0;$ 00	$i_{\frac{13}{2}}i_{\frac{13}{2}}0;$ 00	$f_{\frac{7}{2}}f_{\frac{7}{2}}0;$ 00	$p_{\frac{1}{2}}p_{\frac{1}{2}}0;$ 20	$f_{\frac{1}{2}}f_{\frac{1}{2}}0;$ 20	$p_{\frac{1}{2}}f_{\frac{1}{2}}2;$ 12	$p_{\frac{1}{2}}p_{\frac{1}{2}}2;$ 12	$f_{\frac{1}{2}}f_{\frac{1}{2}}2;$ 12	$f_{\frac{1}{2}}p_{\frac{1}{2}}2;$ 12	$p_{\frac{1}{2}}p_{\frac{1}{2}}2;$ 12	$f_{\frac{1}{2}}f_{\frac{1}{2}}4;$ 24	$f_{\frac{1}{2}}p_{\frac{1}{2}}4;$ 24
−1.07	0.836	0.283	0.264	−0.051	0.073	0.045	0.023	0.271	−0.216	0.099	−0.048	0.056	0.029	−0.051
0.26	−0.355	0.838	0.014	−0.077	0.110	0.002	0.040	0.067	0.076	0.368	−0.069	0.004	0.037	−0.009
1.00	−0.267	−0.089	0.898	−0.047	0.038	−0.003	−0.013	−0.139	−0.151	−0.071	−0.102	0.226	−0.030	−0.024
2.40	−0.026	−0.113	0.053	0.859	−0.148	0.033	0.070	0.077	−0.089	0.441	−0.010	0.046	0.073	−0.041
$I = 2$	$p_{\frac{1}{2}}p_{\frac{1}{2}}0;$ 12	$f_{\frac{1}{2}}f_{\frac{1}{2}}0;$ 12	$p_{\frac{1}{2}}p_{\frac{1}{2}}0;$ 12	$p_{\frac{1}{2}}f_{\frac{1}{2}}2;$ 00	$p_{\frac{1}{2}}p_{\frac{1}{2}}2;$ 00	$f_{\frac{1}{2}}f_{\frac{1}{2}}2;$ 00	$f_{\frac{1}{2}}p_{\frac{1}{2}}2;$ 00	$p_{\frac{1}{2}}p_{\frac{1}{2}}2;$ 00	$p_{\frac{1}{2}}f_{\frac{1}{2}}2;$ 12	$p_{\frac{1}{2}}p_{\frac{1}{2}}2;$ 12	$f_{\frac{1}{2}}f_{\frac{1}{2}}2;$ 12	$p_{\frac{1}{2}}f_{\frac{1}{2}}2;$ 20	$f_{\frac{1}{2}}f_{\frac{1}{2}}4;$ 12	$f_{\frac{1}{2}}p_{\frac{1}{2}}4;$ 12
−0.030	0.200	0.094	0.067	0.766	−0.440	0.209	−0.143	0.144	0.152	−0.102	0.097	0.036	0.103	−0.166
0.38	−0.043	0.044	−0.085	0.508	0.803	0.064	0.041	−0.222	0.046	0.109	0.072	0.004	0.077	0.074
0.76	−0.064	0.109	−0.008	−0.240	0.055	0.935	0.003	−0.004	0.154	0.018	−0.124	0.003	0.097	0.020
1.48	0.071	−0.041	−0.056	0.105	−0.196	0.033	0.933	−0.184	−0.052	0.105	−0.023	0	0.122	0.072
1.60	−0.056	−0.014	0.081	0.016	0.255	−0.003	0.252	0.912	−0.039	−0.162	−0.005	−0.002	0.032	0.007
2.71	0.921	0.147	0.235	−0.141	0.154	0.012	−0.017	0.012	−0.099	0.080	−0.057	0.059	−0.039	0.085
$I = 3$	$p_{\frac{1}{2}}f_{\frac{1}{2}}3;$ 00	$p_{\frac{1}{2}}f_{\frac{1}{2}}3;$ 00	$p_{\frac{1}{2}}f_{\frac{7}{2}}3;$ 00	$f_{\frac{1}{2}}f_{\frac{7}{2}}3;$ 00	$p_{\frac{1}{2}}f_{\frac{7}{2}}3;$ 00	$p_{\frac{1}{2}}p_{\frac{3}{2}}1;$ 12	$f_{\frac{1}{2}}p_{\frac{3}{2}}1;$ 12	$f_{\frac{1}{2}}f_{\frac{7}{2}}1;$ 12	$p_{\frac{1}{2}}f_{\frac{1}{2}}2;$ 12	$p_{\frac{1}{2}}p_{\frac{3}{2}}2;$ 12	$p_{\frac{1}{2}}f_{\frac{1}{2}}3;$ 12	$p_{\frac{1}{2}}f_{\frac{7}{2}}3;$ 12	$f_{\frac{1}{2}}f_{\frac{7}{2}}4;$ 12	
0.32	0.969	−0.037	−0.012	−0.007	0.013	0.025	−0.067	0	−0.061	0.062	−0.134	0.081	0.149	
1.20	0.057	0.955	−0.091	0.024	0.023	−0.109	0.099	−0.013	0.107	0.148	0.132	−0.044	0.043	
2.14	0.022	0.116	0.945	−0.032	−0.017	0.227	0.013	0.073	0.153	−0.100	−0.022	−0.001	0.010	
$I = 4$	$f_{\frac{1}{2}}f_{\frac{1}{2}}4;$ 00	$f_{\frac{1}{2}}p_{\frac{1}{2}}4;$ 00	$p_{\frac{1}{2}}f_{\frac{7}{2}}4;$ 00	$f_{\frac{1}{2}}f_{\frac{7}{2}}4;$ 00	$p_{\frac{3}{2}}f_{\frac{7}{2}}4;$ 00	$f_{\frac{1}{2}}f_{\frac{1}{2}}4;$ 12	$f_{\frac{1}{2}}p_{\frac{3}{2}}4;$ 12	$p_{\frac{1}{2}}f_{\frac{7}{2}}4;$ 12	$p_{\frac{1}{2}}f_{\frac{1}{2}}2;$ 12	$p_{\frac{1}{2}}p_{\frac{3}{2}}2;$ 12	$f_{\frac{1}{2}}f_{\frac{7}{2}}2;$ 12	$p_{\frac{1}{2}}p_{\frac{1}{2}}0;$ 24	$f_{\frac{1}{2}}f_{\frac{1}{2}}0;$ 24	$p_{\frac{1}{2}}f_{\frac{7}{2}}2;$ 22
0.965	0.977	0.080	−0.038	−0.063	0.011	0.100	0.088	0.011	0.002	0.005	0.120	−0.001	0.012	0.005
1.02	−0.088	0.941	0.229	0.049	−0.107	0.063	0.186	−0.010	−0.005	−0.046	0.007	0.006	0.001	−0.001
1.95	0.071	−0.226	0.903	0.115	−0.052	−0.001	−0.076	−0.134	−0.393	−0.291	0.007	0.049	0.006	−0.004
2.69	0.066	0.004	−0.119	0.959	0.028	0.135	−0.107	−0.110	0.022	0.086	−0.103	−0.021	−0.018	0.010

20th order was taken. Fig. 5 also represents the comparison of the results obtained with the levels known experimentally. The comparison shows that the forces assumed in the present paper as acting on a nucleon in the nucleus account for all levels known up to an excitation energy of 3 MeV. Only one 1.66 MeV experimental level 4^+ proved to be misplaced. It is possible that experimental data are not so reliable and should be checked. The theoretical spectrum is richer in levels than the experimental one. This can be expected, for it is difficult to observe certain levels against the background of others. The calculated levels with large I lie somewhat higher than the corresponding experimental levels. Yet, if a single-particle $f_{\frac{5}{2}}$ level is reduced a little, the agreement improves.

A very sensitive criterion of checking the character of the forces is the determination of the probability of transitions. For the γ-radiation of the multipolarity λ the probability T is given by

$$T(\lambda) = \frac{8\pi(\lambda+1)}{\lambda[(2\lambda+1)!!]^2} \frac{1}{\hbar} \left(\frac{\Delta E}{\hbar c}\right)^{2\lambda+1} B(\lambda), \tag{19}$$

$$B(\lambda) = \frac{1}{2I+1} |\langle \alpha I || \mathbf{M}_\lambda || \beta I' \rangle|^2. \tag{19'}$$

Here I and I' are the spin of the nucleus in the initial and final state, α and β are the additional quantum numbers characterizing the states, $\mathbf{M}_\lambda$ is the multipole transition operator and ΔE the transition energy. The explicit form of the operator $\mathbf{M}_\lambda$ and the reduced probability of the transition $B(\lambda)$ for electric and magnetic transitions are given in refs. [2–4]) for different values of the initial and final quantum numbers. We define the reduced probability as

$$B(\lambda) = \frac{T(\lambda)}{(\Delta E)^{2\lambda+1}}, \tag{19''}$$

where ΔE is measured in MeV †. Table 3 lists the results of calculations for $B(\lambda)$ according to eq. (19'') and $T(\lambda)$ in sec^{-1}. For understanding the probabilities obtained it will be recalled that the functions of the initial and final states are a mixture of single-particle and collective levels. The transition probability will therefore have the form of the square of the modulus of the summed matrix elements of the transition between the components of the mixture of both levels. This sum usually alternates in sign and it is not surprising that two levels of the same type may have transition probabilities

† Then the reduced probability $B'(\lambda)$ usually measured in $e^2 \cdot b^\lambda$ is for electric E2-type transitions equal to

$$B'(\mathrm{E2}) \text{ in } e^2 \cdot b^2 = \frac{B(\mathrm{E2})}{1.23 \times 10^{13}} \frac{2I_f+1}{2I_i+1}.$$

differing by two order. The E2 transition probabilities are especially sensitive to the parameters $\hbar\omega$ and C, the E2-transition from the first 2^+ level being less sensitive to these parameters than that from the other 2^+ levels. Thus the experimentally observed transition probability $2_1 \to 0_1$ can be obtained with $\hbar\omega = 3$ MeV and $C = 1{,}000$ MeV as well as with $\hbar\omega = 10$ MeV and $C = 1000$ MeV. Yet the transition probability $2_2 \to 0_1$ with the latter set of parameters will be one fifth of the former. The E2-transition $2_2 \to 2_1$ will be less by 3 orders than with our choice of the parameters if the interaction with the core surface is not taken into account, and less by an order if it is taken into account by the perturbation method. The transition probabilities from the second, third, etc. levels with the given I are sensitive to all parameters of the forces, since it is on the latter that the character of the mixture of states depends. As a result, the E2-transitions $2_3 \to 0_1$ and $0_3 \to 2_1$ have a vanishing transition probability despite an admixture of collective states.

TABLE 3

Transition probabilities between Pb^{206} levels

Number	Initial state	Final state	Type of transition	ΔE in MeV	B	T
1	2^+, 1	0^+, 1	E2	0.815	0.254	0.092
2	2^+, 2	0^+, 1	E2	1.46	0.008	0.053
3	2^+, 2	2^+, 1	M1	0.65	2.125	0.57
4	0^+, 2	2^+, 1	E2	0.36	0.033	0
5	0^+, 3	2^+, 1	E2	1.25	0.001	0.002
6	2^+, 3	0^+, 1	E2	1.8	0.005	0.095
7	2^+, 4	0^+, 1	E2	2.4	0.003	0.252
8	2^+, 5	0^+, 1	E2	2.65	0.002	0.327
9	3^+, 1	2^+, 1	E2	0.56	0.010	0.001
10	3^+, 2	2^+, 1	E2	1.43	0.001	0.004
11	4^+, 1	2^+, 1	E2	1.20	0.015	0.037

T is the transition probability in $\sec^{-1}$. $B(\lambda) = T(\lambda)/(\Delta E)^{2\lambda+1}$, where ΔE is measured in MeV. The transition probability $T_{E2}(2_1 \to 0_1) = 0.103 \times 10^{12}\,\sec^{-1}$ as is known experimentally. For transitions from the level 2_2 the following relation holds: $T_{E2}(2_2 \to 2_1) : T_{E2}(2_2 \to 0_1) = 4 : 1$. Relative intensities for other levels are given in ref. [5]).

In particular, as a result of the mixture of states, the E2-transitions from high levels will not be enhanced.

5. The Nucleus Pb^{210}

The Pb^{210} nucleus has two extra neutrons. Since the forces for two neutrons and two holes may differ, it is necessary to investigate the parameters in Pb^{210} irrespectively of the results obtained in Pb^{206}. Unfortunately, the Pb^{210} nucleus has been investigated considerably less than Pb^{206}. Actually, the binding energy of a neutron pair in the ground state and the distance between the

levels 2_1 and 0_1 are known. These data will suffice for determining only two parameters ρ and v_s. Therefore, the parameters $\hbar\omega$ and C have to be chosen from the results obtained for Bi^{209} and Pb^{209}.

The further course of calculations is well known: we take single-particle energies and functions of Pb^{209} (ref. [1])), calculate the matrix elements by eqs. (13) and (16), build energy matrices for each spin I separately and perform diagonalizing. The results are obtained as functions of the parameters. Table 4 gives the energies of the levels 0^+ and 2^+ for different sets of parameters. The best agreement with experiment is obtained at $\rho = 1.95$ fm, $v_s = 35$ MeV, $\hbar\omega = 3$ MeV and $C = 2000$ MeV. Fig. 6 lists the calculated and experimental levels with spins $I = 0,2$. The binding energy of a pair in the ground state minus single-particle energy is equal 1.45 MeV. This result also agrees well with experiment †.

TABLE 4

Pb^{210} energy levels 0^+ and 2^+ for different sets of parameters

Parameters	Level number	$I = 0$	$I = 2$
$V_1 = 35$ $\hbar\omega = 2$ $C = 2000$	1 2 3	−1.43 0.473 2.16	−0.630 0.589 0.952
$V_1 = 35$ $\hbar\omega = 3$ $C = 1000$	1 2 3	−1.64 0.266 2.06	−0.722 0.369 0.871
$V_1 = 28$ $\hbar\omega = 3$ $C = 2000$	1 2 3	−1.17 0.64 2.38	−0.533 0.586 1.07
$V_1 = 28$ $\hbar\omega = 2$ $C = 2000$	1 2 3	−1.14 0.653 1.75	−0.524 0.600 1.27
single particle energy (MeV) $V_1 = 0, \hbar\omega = 0$	1 2 3	0.00 1.50 3.12	0.00 0.75 1.50

The reduced probability $B(E2)$ for the transition $2_1 \to 0_1$ is equal to 0.7×10^{11} sec^{-1} for $C = 2000$ MeV and is approximately twice as large for $C = 1000$ MeV. For the transition $2_2 \to 2_1$ the reduced probability $B(E2)$ is less by a factor 30.

† In comparing with experimental binding energy it should be borne in mind that the single-particle energy of a neutron is equal to the binding energy of the odd (127th) neutron minus the energy of its interaction with the core surface ($\approx$ 100 keV).

6. The Nucleus Po^{210}

Let us now determine the pairing forces for two protons in Po^{210}. A specific point of the experimental spectrum of Po^{210} is the high location of the first level 2^+ (1.18 MeV). The distance between the levels 2^+ and 0^+ is determined mainly by the quantity v_s. Consequently, this parameter seems anomalously large in Po^{210}. If indeed we perform calculations using single-particle energies and functions of Bi^{210} and assume the level $i_{\frac{13}{2}}$ at a height of 1.65 MeV, we shall obtain 55 MeV for v_s. But for such a value of v_s, the other parameters being equal, the binding energy of a proton pair will be larger by 400 keV than that of a neutron pair. Yet from the β-decay of Pb^{210}, Bi^{210} and Po^{210} it follows that the nucleon pair binding energies in Pb^{210} and Po^{210} are nearly

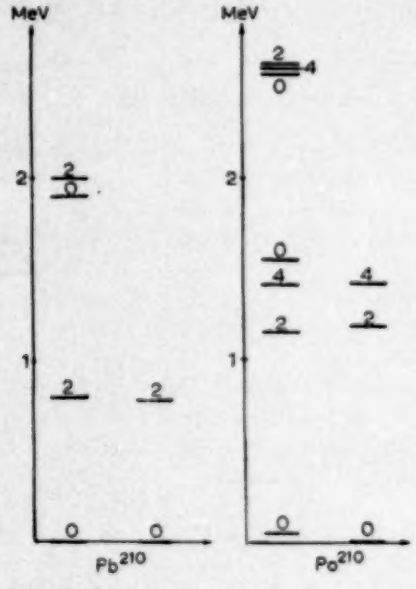

Fig. 6. Comparison of the results obtained for Pb^{210} and Po^{210} levels with experimental data. For both nuclei, the levels on the left are calculated levels, those on the right experimental levels.

the same †. The way out of this contradiction consists in allowing for a possible shift of $i_{\frac{13}{2}}$ downward. Firstly, the exact location of the $i_{\frac{13}{2}}$ level in the Bi^{209} nucleus is unknown and possibly it lies considerably lower. Secondly, the $i_{\frac{13}{2}}$ level may get lower as the second proton joins the Bi^{209} nucleus. Now we have substantial evidence pointing to the shift of the $i_{\frac{13}{2}}$ and $i_{\frac{11}{2}}$ levels when nucleons join the Pb^{209} and Bi^{209} nuclei (see ref. [5])) converned with Bi^{210}). As the $i_{\frac{13}{2}}$ level lowers, its interaction with the $h_{\frac{9}{2}}$ level increases and as a result the ground level 0^+ in Po^{210} will lower even more than before. This shift will have a minor effect on the 2^+ level, for the $i_{\frac{13}{2}}$ and $h_{\frac{9}{2}}$ levels differ in parity. Herein lies the peculiarity of Po^{210}, for a similar shift of the $i_{\frac{13}{2}}$ level in the Pb^{210} nucleus will affect the 0_1 and 2_1 levels in the same way and will

† The experimental binding energy of Po^{210} is less than that of Pb^{210}. But their energies tend to be equal if the proton Coulomb energy is taken into account.

not change the distance between the 2_1 and 0_1 levels. If the $i_{\frac{13}{2}}$ level in Po^{210} lies at a height of 0.9 MeV, we have the observed distance between the levels at $v_s = 40$ MeV. The detection of the second level 0^+ or the first level 2^- would be an experimental of the energy of the $i_{\frac{13}{2}}$ level.

Fig. 6 represents the spectrum of Po^{210}. To determine the parameter v_s and the position of the $i_{\frac{13}{2}}$ level use was made of the experimental data on the proton pair ibinding energy in the ground state and the distance between the 2_1 and 0_1 levels. Table 5 lists functions of the states of Po^{210}. The reduced spectrum contains levels with spins $I = 0, 2, 4$. The other levels and transition probabilities could be calculated but so far there is nothing to compare them with.

TABLE 5

The energies and principal coefficients $c^I(n_1 l_1 j_1, n_2 l_2 j_2, J, N, R)$ of the wave function components of Po^{210} levels

I	Energy	$h_{\frac{9}{2}}h_{\frac{9}{2}}0;$ 00	$f_{\frac{7}{2}}f_{\frac{7}{2}}0;$ 00	$i_{\frac{13}{2}}i_{\frac{13}{2}}0;$ 00	$p_{\frac{1}{2}}p_{\frac{1}{2}}0;$ 00	$h_{\frac{9}{2}}h_{\frac{9}{2}}2;$ 12	$h_{\frac{9}{2}}f_{\frac{7}{2}}2;$ 12	$f_{\frac{7}{2}}f_{\frac{7}{2}}2;$ 12
0_1	−1.54	0.854	0.047	0.495	0.012	−0.148	0.023	−0.009
0_2	−0.01	−0.304	−0.680	0.628	−0.150	0.088	−0.037	0.109
0_3	1.02	0.859	0.687	0.597	0.057	0.137	0.017	−0.182
		$h_{\frac{9}{2}}h_{\frac{9}{2}}2;$ 00	$h_{\frac{9}{2}}f_{\frac{7}{2}}2;$ 00	$f_{\frac{7}{2}}f_{\frac{7}{2}}2;$ 00	$h_{\frac{9}{2}}h_{\frac{9}{2}}0;$ 12	$i_{\frac{13}{2}}i_{\frac{13}{2}}0;$ 12	$h_{\frac{9}{2}}h_{\frac{9}{2}}2;$ 12	$h_{\frac{9}{2}}h_{\frac{9}{2}}4;$ 12
2_1	−0.51	0.977	−0.014	0.059	−0.130	−0.046	0.098	−0.181
2_2	0.87	0.024	0.991	−0.030	0.092	0.047	0.006	−0.035
2_3	1.42	−0.073	0.048	0.986	−0.108	−0.081	0.020	0.020
		$h_{\frac{9}{2}}h_{\frac{9}{2}}4;$ 00	$h_{\frac{9}{2}}f_{\frac{7}{2}}4;$ 00	$f_{\frac{7}{2}}f_{\frac{7}{2}}4;$ 00	$h_{\frac{9}{2}}f_{\frac{7}{2}}4;$ 00	$h_{\frac{9}{2}}h_{\frac{9}{2}}2;$ 12	$h_{\frac{9}{2}}h_{\frac{9}{2}}3;$ 12	$h_{\frac{9}{2}}h_{\frac{9}{2}}6;$ 12
4_1	−0.31	0.977	−0.128	0.089	0.023	−0.112	0.052	−0.102
4_2	0.82	0.146	0.950	0.007	−0.270	−0.066	−0.065	−0.020
4_3	1.27	0.082	0.277	0.015	0.914	0.054	0.196	0.210

7. Conclusions

1) Effective pairing forces affecting a nucleon in its motion in a self-consistent potential can be characterized by a range $\rho = 2$ fm and a depth of ≈ 35 MeV.

2) It is impossible to obtain a correct spectrum of levels and transition probabilities without taking account of pairing forces and pair correlation.

3) Quadrupole interaction is not small and is described in the nuclei under consideration by quadrupole oscillations with a frequency of $\hbar\omega = 3$ MeV and surface tension $C = 1000$ to 2000 MeV.

4) Pairing and quadrupole interactions taken together considerably enrich the description of shell model levels with important peculiarities and fragments. As a result, the description becomes closer to reality.

5) Experimental accumulation of data on the detailed investigation of levels in the 1 to 3 MeV region for heavy nuclei must pass the verdict on the completeness of the picture now emerging and decide whether other forces should be taken into account.

In future papers similar investigations will be treated for nuclei with three, four and more particles in excess of the closed shells.

References

1) L. A. Sliv and B. A. Volchok, JETP **36** (1959) 539
2) A. Bohr and B. Mottelson, Mat. Fys. Medd. Dan. Vid. Selsk. **27**, No. 16 (1953)
3) W. W. True and K. W. Ford, Phys. Rev. **109** (1958) 1675
4) J. Raz, Phys. Rev. **114** (1959) 1116
5) D. E. Alburger and M. H. L. Pryce, Phys. Rev. **95** (1954) 1482
6) Handbuch der Physik (Springer Verlag, Berlin, 1957) Vol. **39**, p. 327

1.C:
1.D.4

Nuclear Physics **28** (1961) 210—219; © *North-Holland Publishing Co., Amsterdam*
Not to be reproduced by photoprint or microfilm without written permission from the publisher

PAIRING FORCES AND PAIR CORRELATION IN Tl^{206} AND Bi^{210}

Yu. I. KHARITONOV, L. A. SLIV and G. A. SOGOMONOVA
Leningrad Physical-Technical Institute, Academy of Sciences, Leningrad, USSR

Received 21 December 1960

Abstract: The residual pairing forces between a neutron and proton in a nucleus are determined. The energies, eigenfunctions and transition probabilities in the Tl^{206} and Bi^{210} are obtained and compared with the experiments.

1. Introduction

The present work was undertaken with the aim of determining the residual forces acting between neutrons and protons moving in a self-consistent nuclear field. The nuclei most suitable for this purpose are those which posses nucleon configurations differing from doubly closed shells by the presence of two "holes" or of two "extra" nucleons. The Tl^{206} and Bi^{210} nuclei are such nuclei in the heavy nuclei region. At first glance it might appear that a neutron and a proton from different shells should interact only weakly. That this is not the case can be seen by comparing the β-decay energy of the Tl^{207} and Tl^{206} nuclei or the Pb^{209} and Pb^{210} nuclei. In the $Tl^{207} \rightarrow Pb^{207}$ β-decay an energy of 1440 keV is liberated. This energy consists of the difference of the proton and neutron level energies in the nuclei and the mass difference equal to 780 keV. The β-decay energy of Tl^{206} differs from that of Tl^{207} by the difference between the pairing energy ε_{np} and ε_{nn}. If the interaction between the neutron and proton is assumed to be small ($\varepsilon_{np} \ll \varepsilon_{nn}$), the β-decay energies of the Tl^{207} and Tl^{206} nuclei should differ by approximately 700 keV. Experimentally the β-decay energy difference is observed to be only 70 keV. Hence $\varepsilon_{np} \approx \varepsilon_{nn}$ and the neutron-proton interaction is of the same order of magnitude as the neutron-neutron interaction. Analogously, an examination of the $Pb^{210} \rightarrow Bi^{210}$ β-decay also shows that the n-p binding energy in the Bi^{210} nucleus should not be smaller than 700 keV. Therefore investigation of n-p interaction in the Tl^{206} and Bi^{210} nuclei was carried out in the same way as was the investigation of n—n forces in the Pb^{206} nucleus [1]).

The motion of the outer nucleons can be described by the potential

$$V = \sum_{i=1,2} V_C(i) + \sum_{i=1,2} V_S(i) + V_p(1, 2). \tag{1}$$

Here

$$V_C(i) = V(r_i) - \lambda \left(\frac{\hbar}{2Mc}\right)^2 \frac{\mathbf{l}_i \cdot \mathbf{s}_i}{r_i} \frac{\partial V(r_i)}{\partial r_i}, \quad V(r_i) = \frac{V_0}{1 + e^{\alpha(r_i - r_0)}} \tag{2}$$

is the diffuse single-particle central potential for an external particle, the parameters of which have been determined in ref. [2]). Furthermore,

$$V_S(i) = -\kappa(r_i) \sum_\mu \alpha_{2\mu} Y_{2\mu}(\vartheta_i, \varphi_i) \tag{3}$$

is the quadrupole interaction potential between the i-th external particle and the particles of the core. Finally,

$$V_p(1,2) = -e^{-\frac{(r_1-r_2)^2}{\rho^2}} (v_t \pi_t + v_s \pi_s) \tag{4}$$

is the residual pair interaction potential between the proton and neutron. The parameter ρ corresponds to an effective nuclear force range and v_s and v_t determine the depth of the singlet and triplet forces [1]). The excited state spectrum of the Tl^{206} and Bi^{210} nuclei was calculated with the help of potential (1) with the purpose of determining the pairing interaction parameters.

2. Spectrum of the Tl^{206} Nucleus

Single-particle levels and the corresponding wave functions of the Pb^{207} and Tl^{207} nuclei were used to calculate the Tl^{206} spectrum. The Pb^{207} nuclear levels have been determined in ref. [2]). For the Tl^{207} nucleus the proton coupling energy is known in the $s_{\frac{1}{2}}$ ground state. The position of the first excited level $d_{\frac{3}{2}}$ can be determined by examining this level in the various Tl isotope levels. This indicates that the $d_{\frac{3}{2}}$ level in Tl^{206} should lie at about 150 keV. The following levels are determined by the solution of the Schroedinger equation with potential V_C in the same form as (2). The level $d_{\frac{5}{2}}$, in particular, is found to be at 1150 keV and the other levels yet higher.

The experimental spectrum of the Tl^{206} nucleus has been studied in detail in ref. [3]), the main results of which are presented in fig. 1. Attention is drawn to the presence of narrow doublets.

Passing over to the theoretical interpretation of the Tl^{206} spectrum it should first of all be mentioned that the observed level spacing cannot be explained without taking into account n—p interaction. Consequently, the Schroedinger equation must be solved with the complete potential (1). A method of solving the equation has been described in ref. [1]). Briefly it consists in diagonalizing the energy matrices evaluated for definite total angular momenta and a given parity. Linear combinations of products of neutron and proton single-particle functions and the wave function describing quadrupole oscillations of the core, namely

$$|(l_1 j_1, l_2 j_2) J;\ NR;\ IM\rangle \tag{5}$$

are used as the basis functions.

Diagonalization of the energy matrix yields the energy level spacing for a nucleus with a given spin and parity and also the coefficients $c^J(l_1j_1, l_2j_2, J, N, R)$ in the linear combinations of basis functions (5) defining the corresponding wave functions

$$\Psi_{IM} = \sum_{l_1j_1, l_2j_2, J, N, R} c^J(l_1j_1, l_2j_2, I, N, R)|\,(l_1j_1, l_2j_2)J;\ NR;\ IM\rangle. \qquad (6)$$

The order of the energy matrix is restricted by the condition that the energy and wave functions of the lower levels are determined with a sufficient degree

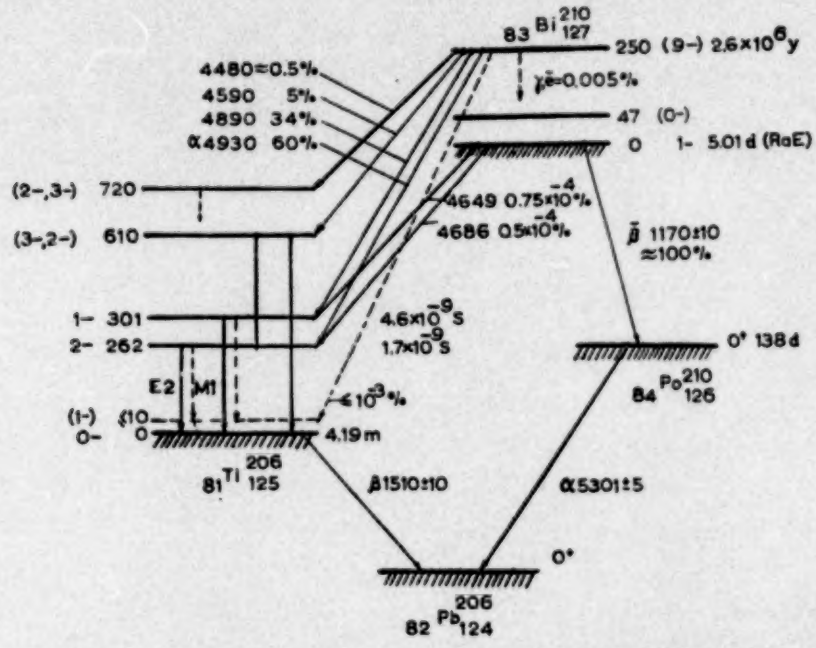

Fig. 1. The experimental spectra of Tl^{206} and Bi^{210} nuclei.

of accuracy. Comparison of the results of the calculations with the experimental spectrum permits one to determine the optimum values of the parameters entering the potential.

The doublet in the Tl^{206} spectrum was found to be particularly sensitive to the parameters v_t and v_s and this facilitates the determination of these parameters. The values deduced by analyzing the spectrum of the Pb^{206} nucleus were employed for the parameters $\hbar\omega$ and C on which $\alpha_{2\mu}$ depends and also for ρ since these parameters cannot be much different in the neighbouring nuclei.

Energy levels calculated for fixed values of parameters v_t and v_s without taking into account the surface interaction are presented in table 1. It can be seen from the table that there are three doublets in the Tl^{206} spectrum. Variation of parameters v_t and v_s and also surface interaction, as table 2 shows, leads to various distances between the doublets and to various splitting of the doublets

TABLE 1

Energy of Tl^{206} levels in the case when only pair interaction is taken into account

Parameters	Level number	$I = 0^-$		$I = 1^-$		$I = 2^-$		$I = 3^-$	
		Single particle energy (MeV)	Calculated energy (MeV)	Single particle energy (MeV)	Calculated energy (MeV)	Single particle energy (MeV)	Calculated energy (MeV)	Single particle energy (MeV)	Calculated energy (MeV)
$V_t = 20$	1	0.00	−0.520	0.00	−0.500	0.150	−0.280	0.570	0.210
$V_s = 20$	2	1.070	0.460	0.150	−0.340	0.570	0.180	0.720	0.510
	3	1.720	1.040	0.920	0.200	0.720	0.370	1.070	0.590

TABLE 2

Energy of Tl^{206} and Bi^{210} levels for various values of the interaction potential

	Parameters	Level number	$I = 0^-$	$I = 1^-$	$I = 2^-$	$I = 3^-$	$I = 9^-$
Tl^{206}	$v_t = 20$, $v_s = 20$, $\hbar\omega = 3$, $C = 1000$	1	−0.770	−0.810	−0.462	0.010	
		2	0.350	−0.490	−0.060	0.300	
		3	0.980	0.100	0.190	0.510	
	$v_t = 25$, $v_s = 25$, $\hbar\omega = 3$, $C = 1000$	1	−0.900	−0.950	−0.580	−0.100	
		2	0.190	−0.630	−0.040	0.340	
		3	0.820	0.240	0.050	0.400	
	$v_t = 25$, $v_s = 35$, $\hbar\omega = 3$, $C = 1000$	1	−0.900	−0.880	−0.570	−0.010	
		2	0.190	−0.490	−0.025	0.370	
		3	0.820	0.390	0.060	0.430	
	$v_t = 20$, $v_s = 35$, $\hbar\omega = 3$, $C = 1000$	1	−0.770	−0.970	−0.490	−0.140	
		2	0.350	−0.600	−0.031	0.330	
		3	0.980	−0.110	0.170	0.370	
	$v_t = 20$, $v_s = 20$, $\hbar\omega = 3$, $C = 2000$	1	−0.650	−0.660	−0.380	0.110	
		2	0.310	−0.410	0.120	0.450	
		3	1.000	0.120	0.280	0.550	
Bi^{210}	$v_t = 20$, $v_s = 20$, $\hbar\omega = 3$, $C = 1000$	1	−0.970	−0.690	−0.590		−0.620
		2	2.600	−0.790	−0.540		−0.270
		3	2.890	0.310	0.520		0.570
	$v_t = 20$, $v_s = 35$, $\hbar\omega = 3$, $C = 1000$	1	−0.970	−1.010	−0.750		−0.760
		2	2.400	−0.810	−0.560		−0.290
		3	2.900	0.050	0.400		0.450
	$v_t = 20$, $v_s = 20$, $\hbar\omega = 3$, $C = 2000$	1	−0.840	−0.560	−0.500		−0.510
		2	2.600	−0.670	−0.460		−0.200
		3	2.760	0.320	0.520		0.580
	$v_t = 20$, $v_s = 35$, $\hbar\omega = 3$, $C = 2000$	1	−0.840	−0.910	−0.680		−0.650
		2	2.400	−0.680	−0.470		−0.230
		3	2.760	0.060	0.410		0.450

The energy is measured relative to the ground single-particle level 0^-. All values are in MeV.

themselves, but does not result in their overlapping. Thus there can be no doubt that an excited level $I = 1^-$ exists near the ground state.

In fig. 2 is shown the level scheme of the Tl^{206} nucleus for parameter values $v_t = 22$ MeV and $v_s = 27$ MeV as determined from the splitting energy of the second doublet (40 keV) and the binding energy of the pair in the ground state. The wave functions for the levels, i.e., the coefficients $c^I(l_1 l_1, l_2 j_2, J, N, R)$ presented in table 3 are calculated for the same values of the parameters. The theoretical level scheme is in satisfactory agreement with the experimental data and even better agreement can be attained by decreasing the parameter ρ by 3 to 5 %. However, since the energy of the single-particle levels is not accurately known it was not the aim of the calculations to obtain better egreement with the experimental distances between the doublets.

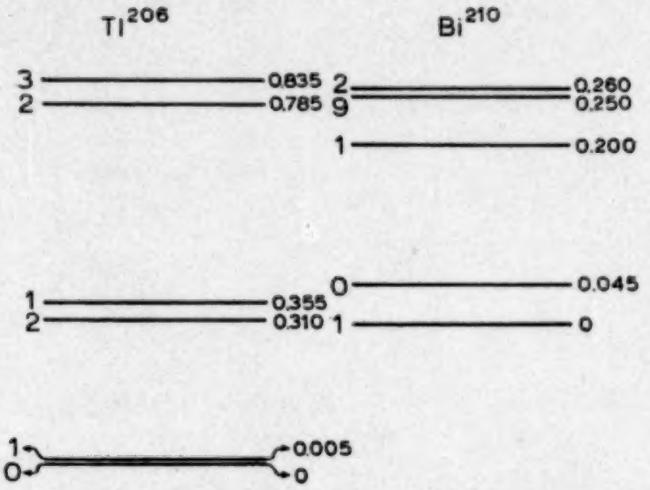

Fig. 2. The level scheme of Tl^{206} and Bi^{210}. All values in MeV.
Tl^{206} for $v_t = 22$, $v_s = 27$, $\hbar\omega = 3$, $C = 1000$. Bi^{210} for $v_t = 20$, $v_s = 35$, $\hbar\omega = 3$, $C = 1000$.

The reduced γ-transition probabilities $B(\lambda)$ (see eq. (19′′) of ref. [1])) were calculated with the aid of the wave functions found for the Tl^{206} levels. The results are presented in table 4. The theoretical values of $B(E2)$ for the electric transitions $2^- \to 0^-$ and $2^- \to 1^-$ are in good agreement with the experimental values. This means that the values of parameters $\hbar\omega$ and C were chosen correctly. According to the single-particle model the magnetic transitions $1^- \to 0^-$ and $1^- \to 1^-$ are forbidden ($d_{\frac{3}{2}} \to s_{\frac{1}{2}}$) and the reduced M1 transition probabilities do not vanish only in the presence of other admixtures of states. Nevertheless, the theoretical value of $B(M1)$ turns out to be 10^3 times larger than the experimental value. Variation of parameters v_t and v_s within reasonable limits permits one to decrease the value of $B(M1)$ but not more than by one order of magnitude. Those values of v_t and v_s which yield agreement between the theoretical values of $B(M1)$ and the experimental values cannot be used to obtain the observed energy spectrum or pair binding energy. Thus we have here an unexplained contradiction with the experimental data.

TABLE 3

Coefficients $c^I(l_1 j_1, l_2 j_2, J, N, R)$ of the expansion of the eigenfunctions of Tl^{206} and Bi^{210}

I	$p_{\frac{1}{2}}s_{\frac{1}{2}}0;$ 00	$p_{\frac{1}{2}}d_{\frac{3}{2}}0;$ 00	$f_{\frac{5}{2}}d_{\frac{3}{2}}0;$ 00	$p_{\frac{1}{2}}d_{\frac{3}{2}}2;$ 12	$f_{\frac{5}{2}}s_{\frac{1}{2}}2;$ 12						
0_1	0.953	−0.102	0.134	0.159	0.194						
	$p_{\frac{1}{2}}s_{\frac{1}{2}}1;$ 00	$p_{\frac{1}{2}}d_{\frac{3}{2}}1;$ 00	$p_{\frac{3}{2}}s_{\frac{1}{2}}1;$ 00	$f_{\frac{5}{2}}d_{\frac{3}{2}}1;$ 00	$p_{\frac{3}{2}}d_{\frac{3}{2}}1;$ 00	$f_{\frac{5}{2}}d_{\frac{5}{2}}1;$ 00	$p_{\frac{1}{2}}s_{\frac{1}{2}}1;$ 12	$p_{\frac{1}{2}}d_{\frac{3}{2}}1;$ 12	$p_{\frac{1}{2}}d_{\frac{3}{2}}2;$ 12	$f_{\frac{5}{2}}s_{\frac{1}{2}}2;$ 12	$f_{\frac{5}{2}}s_{\frac{1}{2}}3;$ 12
1_1	0.914	0.034	0.008	−0.260	0.093	0.103	−0.006	−0.135	0.137	0.086	0.177
1_2	−0.030	0.899	0.247	0.110	0.251	0.019	−0.166	0.114	0.109	0.021	−0.026
	$p_{\frac{1}{2}}d_{\frac{3}{2}}2;$ 00	$f_{\frac{5}{2}}s_{\frac{1}{2}}2;$ 00	$f_{\frac{5}{2}}d_{\frac{3}{2}}2;$ 00	$p_{\frac{3}{2}}d_{\frac{3}{2}}2;$ 00	$f_{\frac{5}{2}}d_{\frac{5}{2}}2;$ 00	$p_{\frac{1}{2}}s_{\frac{1}{2}}0;$ 12	$p_{\frac{1}{2}}s_{\frac{1}{2}}1;$ 12	$p_{\frac{1}{2}}d_{\frac{3}{2}}1;$ 12	$p_{\frac{1}{2}}d_{\frac{3}{2}}2;$ 12	$f_{\frac{5}{2}}s_{\frac{1}{2}}2;$ 12	$f_{\frac{5}{2}}s_{\frac{1}{2}}3;$ 12
2_1	0.898	0.279	0.209	−0.101	0.039	0.112	−0.132	−0.083	0.131	0.047	−0.038
2_2	0.379	0.749	0.504	0.013	0.072	0.061	−0.033	−0.035	−0.004	0.136	−0.107
	$f_{\frac{5}{2}}s_{\frac{1}{2}}3;$ 00	$f_{\frac{5}{2}}d_{\frac{3}{2}}3;$ 00	$p_{\frac{3}{2}}d_{\frac{3}{2}}3;$ 00	$p_{\frac{1}{2}}d_{\frac{3}{2}}3;$ 00	$f_{\frac{5}{2}}d_{\frac{5}{2}}3;$ 00	$p_{\frac{1}{2}}s_{\frac{1}{2}}1;$ 12	$p_{\frac{1}{2}}d_{\frac{3}{2}}1;$ 12	$p_{\frac{1}{2}}d_{\frac{3}{2}}2;$ 12	$f_{\frac{5}{2}}s_{\frac{1}{2}}2;$ 12	$f_{\frac{5}{2}}s_{\frac{1}{2}}3;$ 12	
3_1	0.855	−0.317	0.031	0.267	0.166	0.199	−0.031	0.065	0.038	0.160	
3_2	0.314	0.877	0.289	0	0.015	0.068	0.148	−0.091	0.104	−0.055	
	$g_{\frac{7}{2}}h_{\frac{9}{2}}0;$ 00	$g_{\frac{7}{2}}h_{\frac{9}{2}}2;$ 12	$i_{\frac{13}{2}}h_{\frac{9}{2}}2;$ 12								
0_1	0.966	−0.259	0.032								
	$g_{\frac{7}{2}}h_{\frac{9}{2}}1;$ 00	$i_{\frac{13}{2}}h_{\frac{9}{2}}1;$ 00	$g_{\frac{7}{2}}f_{\frac{7}{2}}1;$ 00	$g_{\frac{7}{2}}h_{\frac{9}{2}}1;$ 12	$g_{\frac{7}{2}}h_{\frac{9}{2}}2;$ 12	$g_{\frac{7}{2}}h_{\frac{9}{2}}3;$ 12	$i_{\frac{13}{2}}h_{\frac{9}{2}}1;$ 12	$i_{\frac{13}{2}}h_{\frac{9}{2}}2;$ 12	$i_{\frac{13}{2}}h_{\frac{9}{2}}3;$ 12		
1_1	−0.237	0.934	0.019	−0.062	0.020	0.038	−0.083	0.178	−0.163		
1_2	0.934	0.238	0.043	0.166	0.006	−0.193	−0.044	0.053	−0.017		
	$g_{\frac{7}{2}}h_{\frac{9}{2}}2;$ 00	$i_{\frac{13}{2}}h_{\frac{9}{2}}2;$ 00	$g_{\frac{7}{2}}f_{\frac{7}{2}}2;$ 00	$g_{\frac{7}{2}}h_{\frac{9}{2}}2;$ 12	$g_{\frac{7}{2}}h_{\frac{9}{2}}3;$ 12	$g_{\frac{7}{2}}h_{\frac{9}{2}}4;$ 12	$i_{\frac{13}{2}}h_{\frac{9}{2}}2;$ 12	$i_{\frac{13}{2}}h_{\frac{9}{2}}3;$ 12	$i_{\frac{13}{2}}h_{\frac{9}{2}}4;$ 12		
2_1	−0.490	0.840	−0.017	−0.082	0.016	0.083	0.070	0.094	−0.160		
	$g_{\frac{7}{2}}h_{\frac{9}{2}}9;$ 00	$i_{\frac{13}{2}}h_{\frac{9}{2}}9;$ 00	$i_{\frac{13}{2}}f_{\frac{7}{2}}9;$ 00	$g_{\frac{7}{2}}h_{\frac{9}{2}}7;$ 12	$g_{\frac{7}{2}}h_{\frac{9}{2}}8;$ 12	$g_{\frac{7}{2}}h_{\frac{9}{2}}9;$ 12	$i_{\frac{13}{2}}h_{\frac{9}{2}}7;$ 12	$i_{\frac{13}{2}}h_{\frac{9}{2}}8;$ 12	$i_{\frac{13}{2}}h_{\frac{9}{2}}9;$ 12	$i_{\frac{13}{2}}h_{\frac{9}{2}}10;$ 12	
9_1	0.967	0	0.006	−0.042	0	0.249	−0.001	−0.005	−0.014	−0.031	

TABLE 4

Reduced transition probabilities for Tl^{206} levels

Transition	B (single particle)	B (collective)	B (total)	B (experimental)
M1, $1_2 \to 1_1$	2.13×10^{12}		2.13×10^{12}	1.7×10^{9}
M1, $1_2 \to 0_1$	1.89×10^{12}		1.89×10^{12}	0.33×10^{10}
E2, $2_1 \to 0_1$	0.266×10^{11}	0.659×10^{11}	1.76×10^{11}	1.6×10^{11}
E2, $2_1 \to 1_1$	0.196×10^{11}	0.981×10^{11}	2.05×10^{11}	2.3×10^{11}

3. Spectrum of the Bi^{210} Nucleus

The nucleon configurations of Bi^{210} combine with the single-particle levels of Pb^{209} and Bi^{209}. The resulting multiplets are characterized by a high degeneracy which disappears when the interactions V_s and V_p are turned on. This is accompanied by splitting and overlapping of the levels. The problem is to determine the parameters which yield agreement with the experimental spectrum. The first task is to make the 1^- level lie below the 0^- level. The 0^- level decreases more than any other of those of the $(g_{\frac{9}{2}} h_{\frac{9}{2}})$ multiplet under the action of V_s and V_p. This is a general result which is valid for any values of the potential parameters. This signifies that the 1^- level belongs to another multiplet, or more precisely, to the $i_{\frac{11}{2}} h_{\frac{9}{2}}$ multiplet. In order to become the ground state the 1^- level must decrease by 800 keV more than the 0^- level and this is impossible for any reasonable values of the parameters v_t and v_s. The 1^- level may become the ground one if the single-particle level $i_{\frac{11}{2}}$ in the Bi^{210} nucleus is lower than in the Pb^{209} nucleus. The property of the $i_{\frac{11}{2}}$ level noted in ref. [2]) should be mentioned here. It was found that the $i_{\frac{11}{2}}$ levels is very sensitive to variation of the diffuseness parameter α of the potential V_C. An increase of α by 0.1 leads to a decrease of the $i_{\frac{11}{2}}$ level by 0.5 MeV whereas the remaining levels practically do not change. It therefore seems reasonable to assume that when a proton is added to the Pb^{209} nucleus and the Bi^{210} nucleus is formed a small change of diffuseness of the potential boundary for a neutron occurs, the result being that the $i_{\frac{11}{2}}$ level approaches the $g_{\frac{9}{2}}$ level. In the present calculations the single-particle $i_{\frac{11}{2}}$ level of the Pb^{209} nucleus decreased by 500 keV.

The 9^- level decreases more than any other level of those possessing large values of the spin I. This is also a general result which does not depend on the choice of the parameters.

A theoretical level scheme of the Bi^{210} nucleus calculated for parameter values $v_t = 20$ MeV and $v_s = 35$ MeV which correspond to the experimental energy difference between the levels $I = 1_1^-$, and $I = 0_1^-$, and also to the binding energy of the neutron-proton pair in the ground state of the nucleus as found from the $Pb^{210} \rightarrow Bi^{210}$ β-decay is shown in fig. 2. The existence of a second level $I = 1_2^-$ near the $I = 9^-$ level does not contradict the experiments since it is difficult to detect this level due to the large spin difference and small energy of the γ-transition from the $I = 9^-$ level to the $I = 1_2^-$ level.

The probability for a M1 transition from the $I = 0_1^-$ level to the $I = 1_1^-$ level was calculated by using the wave functions of the corresponding states in the Bi^{210} nucleus obtained by diagonalization of the energy matrix. The reduced M1 transition probabilities depending on the character of the $I = 1_1^-$ level are presented in table 5. The character of the multiplet mixture $i_{\frac{11}{2}} h_{\frac{9}{2}}$ and $g_{\frac{9}{2}} h_{\frac{9}{2}}$ corresponds to the optimum parameters found above. It can be

seen from table 5 that the probability for a given transition is very sensitive to the composition of the mixture. An exact experimental measurement of the M1 transition probability would permit one to determine the character

TABLE 5

Probability for transition between levels $0_1^- \to 1_1^-$ under various concerning the nature of the level 1_1^-

Level	B	T (sec^{-1})
Pure state $i_{\frac{13}{2}} h_{\frac{9}{2}}$	0	0
Pure state $g_{\frac{9}{2}} h_{\frac{9}{2}}$	1×10^{14}	4.4×10^{11}
Mixing state (this paper)	6.4×10^{12}	3.2×10^{9}

of the $I = 1_1^-$ level. It should be mentioned that when the parameter C is doubled (for $C = 2000$ MeV) the energy spectrum does not change but the interaction energy decreases by 150 keV.

4. General Examination of n-p Interaction

The foregoing calculations show that the effects due to pair interaction in a neutron-proton system significantly differ from the corresponding effects in a system of two identical particles. Singlet forces give the main contribution to the pair interaction in a system of identical particles but in an n–p system triplet forces predominate. If the ground state (0^+) in an n–n (or p–p) system is separated from the remaining states by an appreciable energy gap, the pair energy in a n–p system varies more smoothly with variation of I and obeys a different law. Moreover, since one or two levels with other spin values (e.g., $I = 1^-$ and $I = 9^-$ for Bi^{210}) may be located between the levels $I = 0^-$ and $I = 2^-$, the average distance between the levels turns out to be equal 100—150 keV.

It is convenient to use δ forces for a qualitative examination of the role of singlet and triplet interaction in a n–p system. The pair interaction operator can be written down in the following form:

$$V_{12} = V_{12}^t + V_{12}^s = -\delta(\mathbf{r}_1 - \mathbf{r}_2)[v_t \pi_t + v_s \pi_s], \tag{7}$$

where

$$\pi_t = \tfrac{1}{4}(3 + \boldsymbol{\sigma}_1 \cdot \boldsymbol{\sigma}_2), \tag{8}$$

$$\pi_s = \tfrac{1}{4}(1 - \boldsymbol{\sigma}_1 \cdot \boldsymbol{\sigma}_2). \tag{9}$$

The general nature of level splitting of a given multiplet can be clarified by inspecting the diagonal matrix elements of the n–p interaction. The

diagonal matrix elements of $\delta(\mathbf{r}_1-\mathbf{r}_2)$ and $\delta(\mathbf{r}_1-\mathbf{r}_2)\boldsymbol{\sigma}_1\cdot\boldsymbol{\sigma}_2$ were computed in ref. [4]); they are given by

$$\langle(n_1l_1j_1,\ n_2l_2j_2)JM\ |\delta(\mathbf{r}_1-\mathbf{r}_2)|(n_1l_1j_1,\ n_2l_2j_2)JM\rangle$$
$$=\tfrac{1}{2}F\langle l_1j_1||\mathbf{T}^J||l_2j_2\rangle^2\left\{1+\frac{[(2j_1+1)+(-1)^{j_1+j_2+J}(2j_2+1)]^2}{4J(J+1)}\right\}, \quad (10)$$

$$\langle(n_1l_1j_1,\ n_2l_2j_2)JM\ |\delta(\mathbf{r}_1-\mathbf{r}_2)\boldsymbol{\sigma}_1\cdot\boldsymbol{\sigma}_2|(n_1l_1j_1,\ n_2l_2j_2)JM\rangle \quad (11)$$
$$=\tfrac{1}{2}F\langle l_1j_1\,||\mathbf{T}^J||l_2j_2\rangle^2\left\{\frac{[(2j_1+1)+(-1)^{j_1+j_2+J}(2j_2+1)]^2}{4J(J+1)}-[1+2(-1)^{l_1+l_2+J}]\right\}.$$

Here F is the Slater integral and

$$\langle l_1j_1\,||\mathbf{T}^J||l_2j_2\rangle^2=\tfrac{1}{2}\{1+(-1)^{l_1+l_2+J}\}\,\frac{(2j_1+1)(2j_2+1)}{(2J+1)}\,[C^{J0}_{j_1\frac{1}{2}\,j_2-\frac{1}{2}}]^2. \quad (12)$$

The numerical values of the coefficients $[C^{J0}_{j_1\frac{1}{2}\,j_2-\frac{1}{2}}]^2$ for $j=\frac{1}{2},\ \frac{3}{2},\ \ldots,\ \frac{9}{2}$ are also presented in ref. [4]).

Using eqs. (8) to (11) we find that the diagonal matrix elements of the triplet interaction operator V^{t}_{12} and singlet interaction operator V^{s}_{12} are given by

$$\langle(n_1l_1j_1,n_2l_2j_2)JM|V^{\mathrm{t}}_{12}|(n_1l_1j_1,\ n_2l_2j_2)JM\rangle \quad (13)$$
$$=-\tfrac{1}{2}v_{\mathrm{t}}F\langle l_1j_1||\mathbf{T}^J||l_2j_2\rangle^2\left\{\frac{[(2j_1+1)+(-1)^{j_1+j_2+J}(2j_2+1)]^2}{4J(J+1)}+\tfrac{1}{2}[1-(-1)^{l_1+l_2+J}]\right\},$$

$$\langle(n_1l_1j_1,\ n_2l_2j_2)JM|V^{\mathrm{s}}_{12}|(n_1l_1j_1,\ n_2l_2j_2)JM\rangle=-\tfrac{1}{2}v_{\mathrm{s}}F\langle l_1j_1\,||\mathbf{T}^J||\,l_2j_2\rangle^2. \quad (14)$$

In the following only negative parity states which are most frequent in neutron-proton pairs in heavy nuclei will be considered. Eqs. (13) and (14) can be written separately for even and odd values of the angular momentum J.

(A) Even values of J:

$$\langle|V^{\mathrm{t}}_{12}|\rangle=-\tfrac{1}{2}v_{\mathrm{t}}F\langle l_1j_1\,||\mathbf{T}^J||l_2j_2\rangle^2\left\{1+\frac{[2j_1+1)+(-1)^{j_1+j_2}(2j_2+1)]^2}{4J(J+1)}\right\}, \quad (13A)$$

$$\langle|V^{\mathrm{s}}_{12}|\rangle=0. \quad (14A)$$

(B) Odd values of J:

$$\langle|V^{\mathrm{t}}_{12}|\rangle=-\tfrac{1}{2}v_{\mathrm{t}}F\langle l_1j_1\,||\mathbf{T}^J||l_2j_2\rangle^2\frac{[(2j+1)-(-1)^{j_1+j_2}(2j_2+1)]^2}{4J(J+1)}, \quad (13B)$$

$$\langle|V^{\mathrm{s}}_{12}|\rangle=-\tfrac{1}{2}v_{\mathrm{s}}F\langle l_1j_1\,||\mathbf{T}^J||\,l_2j_2\rangle^2. \quad (14B)$$

Straightforward calculations performed for $v_{\mathrm{s}}=2v_{\mathrm{t}}$ show that in case (A) as well as in case (B) the dependence of the pairing energy can be qualitatively represented by the two curves shown in fig. 3. For a multiplet with $j_1=l_1\pm\frac{1}{2}$

and $j_2 = l_2 \mp \frac{1}{2}$, curve (a) refers to the pairing energy for even values of the angular momentum J and curve (b) to odd values of J. Conversely, for multiplets with $j_1 = l_1 \pm \frac{1}{2}$ and $j_2 = l_2 \pm \frac{1}{2}$, curve (a) refers to odd values of J and curve (b) to even values. It follows from these curves that, just as in the case of identical particles, the level with $J_{\min}$ is the lowest of all but any other level including that with $J_{\max}$ may be the second level.

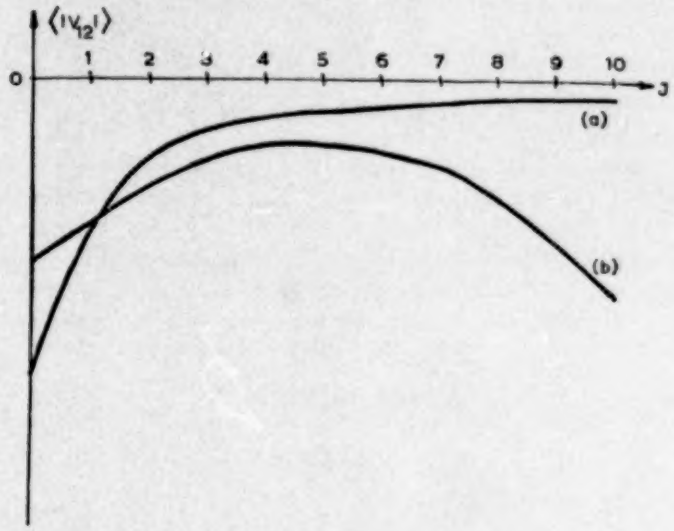

Fig. 3. The dependence of the n–p interaction energy on the angular momentum J.

An analysis of the results based on the assumption of finite range forces leads to the conclusion that the general nature of the multiplet splitting is the same as for δ-forces. However for v_t the coefficient is larger and for v_s smaller than the corresponding coefficients in the case of δ-forces. As a consequence, for finite range forces triplet interaction predominates even when singlet interaction makes the main contribution in the case of δ-forces.

In conclusion it should be noted that the values of v_t and v_s for Tl^{206} and Bi^{210} are quite close although hole interaction takes place in the first case and particle interaction in the second. Additional data on these nuclei may be helpful for a more precise determination of the interaction parameters. However, it is already clear that a complete picture of the properties of the lower levels of odd nuclei can be obtained by taking into account n–p interaction.

References

1) V. N. Guman, Yu. I. Kharitonov, L. A. Sliv and G. A. Sogomonova, Nuclear Physics **28** (1961) 192
2) L. A. Sliv and B. A. Volchok, JETP **36** (1959) 539
3) L. I. Rusinov *et al.*, JETP **40** (1961) 1007
4) A. de-Shalit, Phys. Rev. **91** (1953) 1479

1.B

Nuclear Physics 28 (1961) 220—243; © *North-Holland Publishing Co., Amsterdam*

Not to be reproduced by photoprint or microfilm without written permission from the publisher

DIFFUSION DE PROTONS POLARISÉS PAR UNE CIBLE DE PROTONS POLARISÉS

J. RAYNAL

Centre d'Études Nucléaires de Saclay

Reçu le 15 mai 1961

Abstract: The proton-proton scattering problem, in the helicity formalism, is studied for a polarized target and a polarized incident beam. Exact expressions are given as well as their approximations when one considers only S, P and D waves for the four sets of phase-shifts fitting the cross section in the range of 10-40 MeV. One finds that the polarization is a higher order effect compared to the correlation coefficients and it is shown that the four sets of solutions give only two different angular distributions of the spin correlation coefficient C_{nn}.

1. Introduction

L'analyse des résultats expérimentaux de la diffusion proton-proton n'a pas permis jusqu'ici de déterminer avec précision les déphasages des ondes partielles même pour des énergies inférieures à 25 MeV. Dans ce domaine où il est raisonnable de ne faire intervenir que des ondes S, P et D, Clementel et Villi [1]) ont montré qu'en utilisant uniquement la section efficace on obtient quatre ensembles de valeurs pour les déphasages P pour chaque choix de déphasages S et D, et l'analyse des résultats expérimentaux a fait ressortir une très large indétermination de ces derniers déphasages [2]). L'ambiguïté peut être levée pour l'onde P par des mesures des coefficients de corrélation de spin qui ne mélangent pas les déphasages des ondes paires et des ondes impaires, puisque le spin de la voie est un bon nombre quantique.

Mais les coefficients de corrélation de spin sont plus difficiles à mesurer que des sections efficaces de diffusion élastique de protons polarisés par une cible de protons polarisés. La possibilité de produire des cibles partiellement polarisées permet d'envisager ces expériences et d'obtenir des paramètres équivalents aux coefficients de corrélation de spin.

La méthode envisagée à Saclay pour polariser une cible de protons rend l'utilisation expérimentale assez délicate. La source est placée dans l'entrefer d'un électroaimant et sa polarisation, qui est normale aux pôles, peut être renversée par une faible variation du champ. Il est donc difficile d'observer en dehors du plan normal à la polarisation de la cible et la présence du champ magnétique introduit des corrections pour comparer les sections efficaces à droite et à gauche; il est plus simple de comparer les sections efficaces à un angle donné pour des valeurs opposées de la polarisation de la cible.

On peut envisager quatre séries de mesures:

1) La polarisation du faisceau est transversale et celle de la cible lui est parallèle; on observe dans le plan perpendiculaire. On obtient ainsi un coefficient $A_{yy}(\theta)$ qui n'est autre que le coefficient de corrélation de spin $C_{nn}(\theta)$ de Wolfenstein [3]) (fig. 1a).

2) Avec la même disposition du faisceau et de la cible on observe dans le plan parallèle aux polarisations: on obtient le coefficient $A_{xx}(\theta)$ (fig. 1b).

3) La polarisation du faisceau incident est longitudinale, sa direction est perpendiculaire à la polarisation de la cible et on observe dans le plan parallèle aux polarisations: on obtient le coefficient $A_{zx}(\theta)$ (fig. 1c). On peut permuter les directions de polarisation de la cible et du faisceau incident.

4) Les polarisations sont parallèles à la direction de propagation du faisceau et on observe dans un plan arbitraire: on obtient $A_{zz}(\theta)$ (fig. 1d).

L'ensemble des coefficients A_{xx}, A_{zz}, A_{xz} est équivalent à celui du coefficient de corrélation de spin C_{kp} (introduit par Wolfenstein) et de C_{kk} et C_{pp} qui peuvent être définis avec les mêmes notations. En fait la seule différence provient du système de référence; la corrélation de spin est exprimée dans le système du laboratoire alors qu'il y a réciprocité exacte entre les deux genres de mesures exprimées dans le système du centre de masse.

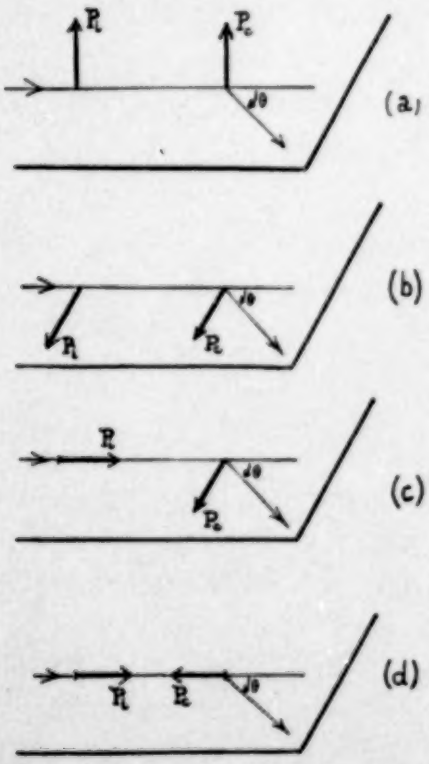

Fig. 1. Disposition des polarisations correspondant aux coefficients A_{yy}, A_{xx}, A_{xz} et A_{zz}.

Il est donc intéressant de calculer la section efficace différentielle de diffusion élastique d'un faisceau sur une cible, tous deux polarisés de façon quelconque et d'exprimer le résultat avec les paramètres A liés aux coefficients de corrélation de spin. Il est également intéressant de calculer explicitement ces coefficients en fonction des déphasages S, P et D, et d'étudier leurs valeurs pour chaque ensemble de déphasages tirés de l'étude de la section efficace. A cette approximation toutes ces quantités peuvent s'exprimer sous une forme analogue à celle donnée par Clementel et Villi pour la section efficace.

Remarquons que parmi les quatre séries de mesures proposées plus haut, les trois premières ne nécessitent pas l'emploi de champ magnétique pour faire tourner la polarisation du faisceau incident. Mais la quatrième série est absolument nécessaire si on veut obtenir la section efficace de diffusion élastique dans l'état singulet à un angle quelconque; la difficulté est du même ordre en employant les coefficients de corrélation de spin puisqu'il faut connaître la corrélation de la polarisation longitudinale du proton sortant avec la polarisation transversale du proton de recul.

2. Amplitudes de Diffusion

Pour écrire les amplitudes de diffusion nous devons tenir compte de l'invariance par réflexion d'espace et par renversement du temps. La statistique impose une partie d'espace paire pour la fonction d'onde dans l'état singulet et impaire pour l'état triplet; puisque la parité est un bon nombre quantique, le spin de la voie, S, l'est aussi. Nous pouvons donc étudier séparément les diffusions singulet et triplet.

La diffusion singulet est décrite par une seule amplitude qui s'écrit directement

$$a(\theta) = f_c(\theta)+f_c(\pi-\theta)+\sum_{l \text{ pair}} \frac{i}{k}(2l+1)e^{2i\sigma_l}(1-e^{2i\delta_l})P_l(\cos\theta), \qquad (1)$$

avec

$$f_c(\theta) = -\frac{\gamma}{2k\sin^2\frac{1}{2}\theta} e^{-i\gamma \ln \sin^2 \frac{1}{2}\theta + 2i\sigma_0}, \qquad (2)$$

où σ_0, σ_l sont les déphasages coulombiens, δ_l le déphasage nucléaire de l'onde partielle correspondante.

La diffusion triplet est décrite par $f(\theta)$ qui est une matrice 3×3. Pour exprimer ces amplitudes il est plus simple d'utiliser le formalisme de l'hélicité [4]). Nous prenons (voir fig. 2) pour axe de quantification dans l'état initial la direction Oz_1 du faisceau incident et dans l'état final la direction Oz_f de l'un des protons sortants; l'axe Oy est commun et tel que le trièdre Oz_1, Oz_f, Oy soit direct (direction du produit vectoriel $\mathbf{k}_1 \wedge \mathbf{k}_f$ des impulsions du proton incident et du proton sortant choisi). Avec ces notations, il n'y a que quatre amplitudes différentes alors que le formalisme habituel conduit à considérer

cinq amplitudes liées par une relation. L'expression générale de l'amplitude

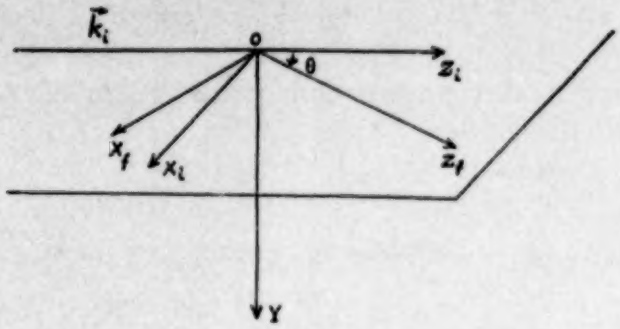

Fig. 2. Référentiels utilisés dans le formalisme de l'hélicité.

correspondant à l'état initial d'hélicité μ_1 et à l'état final d'hélicité μ_f s'écrit

$$\begin{aligned} f_{\mu_f\mu_1}(\theta) = {} & \{f_c(\theta)-f_c(\pi-\theta)\}r^1_{\mu_f\mu_1}(\theta) \\ & + \frac{i}{k}\sum_{J\,\text{pair}}(2J+1)\left\{(2J-1)\begin{pmatrix}J-1 & 1 & J\\ 0 & \mu_f & -\mu_f\end{pmatrix}\begin{pmatrix}J-1 & 1 & J\\ 0 & \mu_1 & -\mu_1\end{pmatrix}C_-{}^J\right. \\ & -\sqrt{(2J-1)(2J+3)}\left[\begin{pmatrix}J-1 & 1 & J\\ 0 & \mu_f & -\mu_f\end{pmatrix}\begin{pmatrix}J+1 & 1 & J\\ 0 & \mu_1 & -\mu_1\end{pmatrix}\right. \\ & \left.+\begin{pmatrix}J+1 & 1 & J\\ 0 & \mu_f & -\mu_f\end{pmatrix}\begin{pmatrix}J-1 & 1 & J\\ 0 & \mu_1 & -\mu_1\end{pmatrix}\right]C^J \\ & \left.+(2J+3)\begin{pmatrix}J+1 & 1 & J\\ 0 & \mu_f & -\mu_f\end{pmatrix}\begin{pmatrix}J+1 & 1 & J\\ 0 & \mu_1 & -\mu_1\end{pmatrix}C_+{}^J\right\}(-)^{\mu_f-\mu_1}r^J_{\mu_f\mu_1}(\theta) \\ & + \frac{i}{k}\sum_{J\,\text{impair}}(2J+1)^2\begin{pmatrix}J & 1 & J\\ 0 & \mu_f & -\mu_f\end{pmatrix}\begin{pmatrix}J & 1 & J\\ 0 & \mu_1 & -\mu_1\end{pmatrix}C_0{}^J(-)^{\mu_f-\mu_1}r^J_{\mu_f\mu_1}(\theta). \end{aligned} \tag{3}$$

Les $r^J_{\mu\mu'}$ sont les éléments de matrice de rotation réduits, c'est-à-dire relatifs aux angles d'Euler 0, θ, 0†. L'invariance par réflexion et par renversement du temps correspond aux relations entre les différents éléments de matrice $r^J_{\mu\mu'}$, qui entraînent

$$f_{11} = f_{-1-1}, \qquad f_{10} = f_{0-1} = -f_{01} = -f_{-10}, \quad f_{1-1} = f_{-11}. \tag{4}$$

La condition d'unitarité de la matrice de diffusion se traduit par des conditions sur les C introduits dans la formule (3). Si le moment total J est impair, il n'y a qu'un seul déphasage

$$C_0{}^J = \exp(2i\sigma_J)\,(1-\exp(2i\delta_{JJ})) \tag{5}$$

où δ_{JJ} doit être réel. Si le moment total J est pair il y a trois paramètres

$$\begin{gathered} C_-{}^J = \exp(2i\sigma_{J-1})(1-S_-{}^J), \quad C_+{}^J = \exp(2i\sigma_{J+1})(1-S_+{}^J), \\ C^J = -\exp(i\sigma_{J+1}+i\sigma_{J-1})S_J, \end{gathered} \tag{6}$$

† Nous suivons les notations de A. Messiah [8]).

avec les conditions

$$|S_-{}^J|^2+|S^J|^2 = |S_+{}^J|^2+|S^J|^2 = 1, \qquad S_-^{J*}S^J+S_+{}^J S^{J*} = 0. \tag{7}$$

Il y a diverses façons d'introduire trois paramètres réels pour exprimer les S [5]). L'une d'entre elles est

$$\begin{aligned} S_-{}^J &= \cos^2\varepsilon_J \exp(2i\delta_J{}^1)+\sin^2\varepsilon_J \exp(2i\delta_J{}^2), \\ S_+{}^J &= \sin^2\varepsilon_J \exp(2i\delta_J{}^1)+\cos^2\varepsilon_J \exp(2i\delta_J{}^2), \\ S^J &= \sin\varepsilon_J \cos\varepsilon_J \{\exp(2i\delta_J{}^1)-\exp(2i\delta_J{}^2)\}. \end{aligned} \tag{8}$$

Pour la diffusion singulet la condition d'unitarité est analogue à l'équation (5): δ_l doit être réel.

La condition d'unitarité peut s'exprimer globalement sur les amplitudes. Pour cela, il faut les généraliser en introduisant une rotation quelconque autour des axes Oz_1 et Oz_f. On remplace les éléments de matrice réduits $r^J_{\mu_f\mu_1}$ par les éléments de matrice $R^J_{\mu_f\mu_1}$ $(\mathbf{k}_1 \to \mathbf{k}_f)$ de la rotation qui fait passer du repère initial ayant Oz_1 comme axe de quantification au repère final autour de Oz_f) La condition d'unitarité s'écrit alors

$$\frac{4\pi i}{k}\{f(\mathbf{k}_1 \to \mathbf{k}_f)-f^\dagger(\mathbf{k}_f \to \mathbf{k}_1)\} = \int f^\dagger(\mathbf{k}_f \to \mathbf{k}')f(\mathbf{k}_1 \to \mathbf{k}')\,\mathrm{d}\mathbf{k}'. \tag{9}$$

Sans séparer la partie coulombienne on peut poser

$$f_{\mu_f\mu_1}(\mathbf{k}_f \to \mathbf{k}_1) = \sum_J \lambda^J_{\mu_f\mu_1} R^J_{\mu_f\mu_1}(\mathbf{k}_1 \to \mathbf{k}_f). \tag{10}$$

En effectuant l'intégration sur $\mathbf{k}'$ on obtient †

$$\frac{4\pi i}{k}\{\lambda^J_{\mu_f\mu_1}-\lambda^{J*}_{\mu_f\mu_1}\} = \frac{4\pi}{2J+1}\sum_{\mu'} \lambda^{J*}_{\mu'\mu_f}\lambda^J_{\mu'\mu_1}. \tag{11}$$

En utilisant les relations entre les coefficients $3j$ et en séparant la diffusion coulombienne on retrouve les conditions (5), (6) et (7).

Nous pouvons expliciter les coefficients $3j$ qui interviennent dans la formule (3) et exprimer les $r^J_{\mu\mu'}$ à l'aide des polynomes de Legendre et de leurs dérivées.

† Remarquons que nous pouvons effectuer l'intégration de la formule (9) en n'utilisant que les éléments de matrice de rotation réduits, c'est-à-dire avec les amplitudes telles que nous les avons primitivement écrites:

$$\frac{4\pi i}{k}\{f_{\mu_f\mu_1}(\theta)-(-)^{\mu_f+\mu_1}f^*_{\mu_f\mu_1}(\theta)\} = \int \sum_{\mu'} \mathrm{e}^{i\mu_1\varphi'-i\mu_f\varphi}(\varphi',\theta')f_{\mu'\mu_1}(\theta)\,f^*_{\mu'\mu_f}(\theta''(\theta',\varphi'))\sin\theta'\,\mathrm{d}\theta'\,\mathrm{d}\varphi', \tag{9'}$$

avec

$$\cos\theta'' = \cos\theta\cos\theta'+\sin\theta\sin\theta'\cos\varphi', \quad \sin\theta''\sin\varphi = \sin\theta'\cos\varphi',$$
$$\sin\theta''\cos\varphi = -\sin\theta\cos\theta'+\cos\theta\cos\theta'\cos\varphi'.$$

En fait nous obtenons des expressions plus simples en considérant

$$b = f_{11} + f_{1-1} = \{f_c(\theta) - f_c(\pi-\theta)\} + \frac{i}{k} \sum_{J\text{impair}} (2J+1) C_0^J \left\{ \frac{-\cos\theta}{J(J+1)} P'_J + P_J \right\}$$

$$+ \frac{i}{k} \sum_{J\text{pair}} \{(J+1) C_-^J + J C_+^J - 2\sqrt{J(J+1)}\, C^J\} \frac{P'_J}{J(J+1)},$$

$$c = f_{11} - f_{1-1} = \{f_c(\theta) - f_c(\pi-\theta)\} \cos\theta + \frac{i}{k} \sum_{J\text{impair}} (2J+1) C_0^J \frac{P'_J}{J(J+1)} \qquad (12)$$

$$+ \frac{i}{k} \sum_{J\text{pair}} \{(J+1) C_-^J + J C_+^J - 2\sqrt{J(J+1)}\, C^J\} \left\{ \frac{-\cos\theta}{J(J+1)} P'_J + P_J \right\},$$

$$d = f_{10}\sqrt{2} = \{f_c(\theta) - f_c(\pi-\theta)\} \sin\theta + \frac{i}{k} \sum_{J\text{pair}} \left\{ C_-^J - C_+^J + \frac{C^J}{\sqrt{J(J+1)}} \right\} P'_J \sin\theta,$$

$$e = f_{00} = \{f_c(\theta) - f_c(\pi-\theta)\} \cos\theta + \frac{i}{k} \sum_{J\text{pair}} \{J C_-^J + (J+1) C_+^J + 2\sqrt{J(J+1)}\} P_J.$$

Cette simplification est uniquement due à l'invariance par réflexion: en effet si on prend pour états de base de l'état triplet les composantes suivant les axes x, y, z des repères respectifs de l'état initial et de l'état final, nous avons

$$f(\theta) = \begin{vmatrix} c & 0 & -d \\ 0 & b & 0 \\ d & 0 & e \end{vmatrix}. \qquad (13)$$

En fait, dans l'état final nous avons pris la direction de propagation de l'un des deux protons comme axe de quantification. Comme ce choix est arbitraire il doit exister certaines relations entre les amplitudes pour les angles θ et $\pi-\theta$. Pour échanger le rôle des deux protons il faut faire une rotation de π autour de l'axe Ox pour l'état final et une rotation de π autour de l'axe Oz pour l'état initial. Ces opérations entraînent

$$\begin{aligned} b(\theta) &= -b(\pi-\theta), \qquad c(\theta) = c(\pi-\theta), \\ d(\theta) &= -d(\pi-\theta), \qquad e(\theta) = e(\pi-\theta). \end{aligned} \qquad (14.a)$$

Ces relations sont évidentes sur les formules (12). Pour l'état singulet on a simplement

$$a(\theta) = a(\pi-\theta). \qquad (14.b)$$

L'ensemble des diffusions singulet et triplet est décrit par la matrice de diffusion $M(\theta)$. Nous pouvons l'écrire en „représentation hélicité" pour les

particules couplées (les vecteurs de base sont les états $S = 0$ et $S = 1$, $M = 1$, 0, -1 sur la direction de propagation):

$$M(\theta) = \begin{vmatrix} a & 0 & 0 & 0 \\ 0 & \frac{1}{2}(b+c) & \frac{1}{2}\sqrt{2}d & \frac{1}{2}(b-c) \\ 0 & -\frac{1}{2}\sqrt{2}d & e & \frac{1}{2}\sqrt{2}d \\ 0 & \frac{1}{2}(b-c) & \frac{1}{2}\sqrt{2}d & \frac{1}{2}(b+c) \end{vmatrix}, \tag{15}$$

ou bien en représentation hélicité pour les particules découplées (avec les vecteurs de base $\frac{1}{2}\ \frac{1}{2}$, $\frac{1}{2}\ -\frac{1}{2}$, $-\frac{1}{2}\ \frac{1}{2}$, $-\frac{1}{2}\ -\frac{1}{2}$, où le premier nombre désigne l'hélicité du proton dont on a pris la direction de propagation comme axe de quantification et le deuxième la projection du spin de l'autre proton sur le même axe):

$$M(\theta) = \begin{vmatrix} \frac{1}{2}(b+c) & \frac{1}{2}d & \frac{1}{2}d & \frac{1}{2}(b-c) \\ -\frac{1}{2}d & \frac{1}{2}(a+e) & \frac{1}{2}(e-a) & \frac{1}{2}d \\ -\frac{1}{2}d & \frac{1}{2}(e-a) & \frac{1}{2}(a+e) & \frac{1}{2}d \\ \frac{1}{2}(b-c) & \frac{1}{2}d & \frac{1}{2}d & \frac{1}{2}(b+c) \end{vmatrix}. \tag{16}$$

3. Section Efficace et Coefficients de Corrélation de Spin

Connaissant les matrices densités ρ_1 et ρ_c du faisceau incident et de la cible, nous voulons calculer la section efficace différentielle de diffusion élastique à l'angle θ, φ. Pour raison de simplicité, nous avons calculé les amplitudes de diffusion pour l'angle $\varphi = 0$ seulement; il faut donc exprimer ρ_1 et ρ_c dans le système d'axes tourné de l'angle φ autour de la direction de propagation du proton incident, puis calculer

$$M(\theta)[\rho_1(\varphi) \otimes \rho_c(\varphi)]M^\dagger(\theta). \tag{17}$$

La trace de cette matrice est la section efficace différentielle $\mathrm{d}\sigma(\theta, \varphi)/\mathrm{d}\Omega$ et ses éléments décrivent la polarisation des deux protons sortants et leur corrélation de spin. En particulier, l'étude de la section efficace seule avec état initial polarisé ne fait intervenir que les éléments de la matrice $M^\dagger(\theta)\, M(\theta)$ et l'étude de la polarisation et de la corrélation de spin avec un état initial non polarisé ne dépend que de ceux de $M(\theta)\, M^\dagger(\theta)$. Les deux matrices sont très voisines puisqu'on passe de l'une à l'autre par transposition et renversement du sens du temps ($d(\theta)$ change de signe et les autres éléments sont invariants). Ainsi avec la base ($S = 0$; $S = 1$, x, y, z) déjà employée en (13) elles s'écrivent

$$M^\dagger(\theta)M(\theta) = \begin{vmatrix} |a|^2 & 0 & 0 & 0 \\ 0 & |c|^2+|d|^2 & 0 & -dc^*+d^*e \\ 0 & 0 & |b|^2 & 0 \\ 0 & -d^*c+de^* & 0 & |c|^2+|d|^2 \end{vmatrix}, \quad M(\theta)M^\dagger(\theta) = \begin{vmatrix} |a|^2 & 0 & 0 & 0 \\ 0 & |c|^2+|d|^2 & 0 & cd^*-e^*d \\ 0 & 0 & |b|^2 & 0 \\ 0 & dc^*-ed^* & 0 & |c|^2+|d|^2 \end{vmatrix}. \tag{18}$$

Considérons un faisceau incident décrit par un vecteur polarisation de projection p_0 sur la direction de propagation et dont la partie transversale, de longueur p, fait un angle φ avec la normale au plan de diffusion. Supposons que la cible est décrite de la même manière par les composantes p'_0, p' et l'angle φ' (fig. 3). Nous pouvons écrire la matrice densité de l'état initial dans la

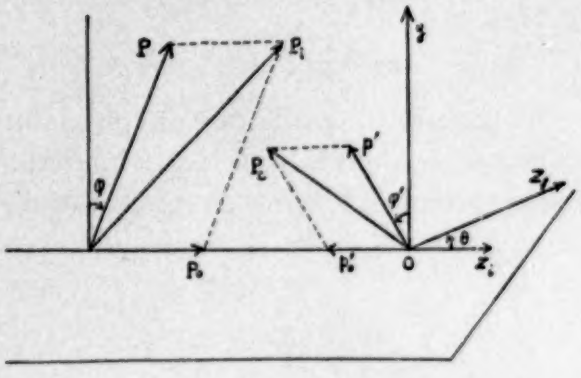

Fig. 3. Coordonnées utilisées pour décrire des polarisations quelconques.

représentation employée pour $M^\dagger(\theta)\ M(\theta)$ et calculer la trace de $\rho M^\dagger M$. On obtient

$$\frac{\mathrm{d}\sigma(\theta,\varphi)}{\mathrm{d}\Omega} = \left(\frac{\mathrm{d}\sigma(\theta)}{\mathrm{d}\Omega}\right)_{\text{n.p.}} \{1+P(p\cos\varphi+p'\cos\varphi')+A_{xx}(p_0p'\sin\varphi'+p'_0p\sin\varphi)$$
$$+[\tfrac{1}{2}(A_{yy}-A_{zz})\cos(\varphi+\varphi')+\tfrac{1}{2}(A_{yy}+A_{zz})\cos(\varphi-\varphi')]pp'+A_{zz}p_0p'_0), \quad (19)$$

avec

$$\left(\frac{\mathrm{d}\sigma(\theta)}{\mathrm{d}\Omega}\right)_{\text{n.p.}} = \tfrac{1}{4}\{|a|^2+|b|^2+|c|^2+2|d|^2+|e|^2\},$$
$$4A_{xx}\left(\frac{\mathrm{d}\sigma(\theta)}{\mathrm{d}\Omega}\right)_{\text{n.p.}} = |b|^2+|c|^2-|a|^2-|e|^2,$$
$$4A_{yy}\left(\frac{\mathrm{d}\sigma(\theta)}{\mathrm{d}\Omega}\right)_{\text{n.p.}} = |c|^2+|e|^2+2|d|^2-|a|^2-|b|^2, \quad (20)$$
$$4A_{zz}\left(\frac{\mathrm{d}\sigma(\theta)}{\mathrm{d}\Omega}\right)_{\text{n.p.}} = |b|^2+|e|^2-|c|^2-|a|^2,$$
$$4A_{xz}\left(\frac{\mathrm{d}\sigma(\theta)}{\mathrm{d}\Omega}\right)_{\text{n.p.}} = d^*(e-c)+d(e^*-c^*),$$
$$4P\left(\frac{\mathrm{d}\sigma(\theta)}{\mathrm{d}\Omega}\right)_{\text{n.p.}} = i\{d(c^*+e^*)-d^*(c+e)\}.$$

Dans la formule (19) $(\mathrm{d}\sigma(\theta)/\mathrm{d}\Omega)_{\text{n.p.}}$ est la section efficace différentielle pour un état initial non polarisé et P est la polarisation telle qu'elle est obtenue en n'observant qu'un seul des protons sortants. Réciproquement nous pouvons

écrire $M(\theta)\,M^{\dagger}(\theta)$ à l'aide de ces paramètres et exprimer cette matrice comme une combinaison linéaire des produits $\sigma_i^1 \otimes \sigma_j^2$ construites à l'aide des spins σ^1 du proton sortant dont la direction est prise pour axe de quantification et σ^2 du proton de recul. On obtient ainsi

$$M(\theta)M^{\dagger}(\theta) = \left(\frac{\mathrm{d}\sigma(\theta)}{\mathrm{d}\Omega}\right)_{\text{n.p.}} \{1+P(\sigma_y^1\otimes 1+1\otimes\sigma_y^2)+A_{xx}(\sigma_x^1\otimes\sigma_x^2+\sigma_z^1\otimes\sigma_z^2) + A_{xx}\sigma_x^1\otimes\sigma_x^2+A_{yy}\sigma_y^1\otimes\sigma_y^2+A_{zz}\sigma_z^1\otimes\sigma_z^2\}. \quad (21)$$

Pour retrouver les coefficients de corrélation de spin habituels il faut projeter sur les directions des particules dans le système du laboratoire. Si les impulsions initiale et finale dans le système du centre de masse sont $\mathbf{k}_i$ et $\mathbf{k}_f$, les nouveaux axes sont suivant $\mathbf{P} = \mathbf{k}_i+\mathbf{k}_f$, $\mathbf{K} = \mathbf{k}_f-\mathbf{k}_i$ et $\mathbf{n}$ qui a la même direction que

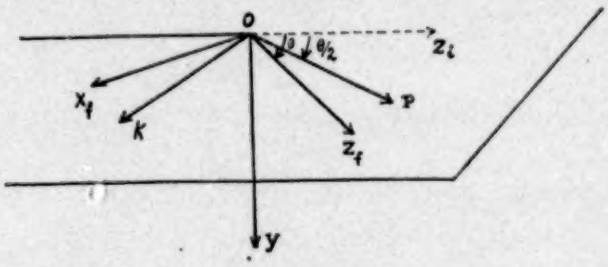

Fig. 4. Passage du système du centre de masse au système du laboratoire.

Oy. La direction $\mathbf{K}$ est en fait opposée à celle du proton de recul dans le système du laboratoire (fig. 4). On doit donc substituer

$$\begin{aligned}
\sigma_x^1 &= -\cos\tfrac{1}{2}\theta\,\sigma_k^1-\sin\tfrac{1}{2}\theta\,\sigma_p^1, & \sigma_x^2 &= -\sin\tfrac{1}{2}\theta\,\sigma_p^2-\cos\tfrac{1}{2}\theta\,\sigma_k^2,\\
\sigma_z^1 &= -\sin\tfrac{1}{2}\theta\,\sigma_k^1+\cos\tfrac{1}{2}\theta\,\sigma_p^1, & \sigma_z^2 &= \cos\tfrac{1}{2}\theta\,\sigma_p^2-\sin\tfrac{1}{2}\theta\,\sigma_k^2,\\
\sigma_y^1 &= \sigma_n^1, & \sigma_y^2 &= \sigma_n^2.
\end{aligned}$$

On obtient ainsi

$$\begin{aligned}
C_{kp} &= C_{pk} = \tfrac{1}{2}\sin\theta(A_{zz}-A_{xx})+\cos\theta\,A_{xz},\\
C_{kk} &= \sin^2\tfrac{1}{2}\theta\,A_{zz}+\cos^2\tfrac{1}{2}\theta\,A_{xx}+\sin\theta\,A_{xz}, \qquad (22)\\
C_{pp} &= \cos^2\tfrac{1}{2}\theta\,A_{zz}+\sin^2\tfrac{1}{2}\theta\,A_{xx}-\sin\theta\,A_{xz}, \qquad C_{nn} = A_{yy}.
\end{aligned}$$

Par des expériences de corrélation de spin, on cherche à mesurer C_{nn} et C_{kp} qui correspondent à des corrélations de polarisation transversales, mais alors que $A_{yy} = C_{nn}$, les coefficients A_{xx}, A_{zz} et A_{xz} dépendent simultanément de C_{kp}, C_{kk} et C_{pp}:

$$\begin{aligned}
A_{xx} &= -\sin\theta\,C_{kp}+\cos^2\tfrac{1}{2}\theta\,C_{kk}+\sin^2\tfrac{1}{2}\theta\,C_{pp},\\
A_{zz} &= \sin\theta\,C_{kp}+\sin^2\tfrac{1}{2}\theta\,C_{kk}+\cos^2\tfrac{1}{2}\theta\,C_{pp}, \qquad (23)\\
A_{xz} &= \cos\theta\,C_{kp}+\tfrac{1}{2}\sin\theta\,(C_{kk}-C_{pp}).
\end{aligned}$$

Les relations (14) se traduisent sur les coefficients de la section efficace différentielle de l'équation (19) par des égalités analogues:

$$\begin{aligned} \left(\frac{d\sigma(\theta)}{d\Omega}\right)_{n.p.} &= \left(\frac{d\sigma(\pi-\theta)}{d\Omega}\right)_{n.p.}, & A_{zz}(\theta) &= A_{zz}(\pi-\theta), \\ P(\theta) &= -P(\pi-\theta), & A_{yy}(\theta) &= A_{yy}(\pi-\theta), \\ A_{xz}(\theta) &= -A_{xz}(\pi-\theta), & A_{xx}(\theta) &= A_{xx}(\pi-\theta). \end{aligned} \tag{24}$$

Pour les coefficients de corrélation de spin on a

$$C_{nn}(\theta) = C_{nn}(\pi-\theta), \qquad C_{kp}(\theta) = C_{kp}(\pi-\theta), \qquad C_{pp}(\theta) = C_{kk}(\pi-\theta). \tag{25}$$

Les relations (25) sont évidentes d'après la signification de ces coefficients.

En exprimant la matrice $M^{\dagger}(\theta)\, M(\theta)$ à l'aide des paramètres A et P définis en (20) dans la base ($S = 0$; $S = 1$, $M = 1, 0, -1$) déjà utilisée pour écrire (15) on voit directement que la diffusion singulet est égale à

$$|a|^2 = \left(\frac{d\sigma(\theta)}{d\Omega}\right)_{n.p.} \{1-A_{xx}-A_{yy}-A_{zz}\} \tag{26}$$

quel que soit l'angle θ. Il serait donc très intéressant d'obtenir ces trois coefficients à tous les angles pour connaître la distribution angulaire de la diffusion singulet. La mesure de A_{zz} nécessite un faisceau incident à polarisation longitudinale et elle est donc la plus délicate à effectuer. On peut aussi obtenir la diffusion singulet par des mesures de corrélation de spin puisque

$$|a|^2 = \left(\frac{d\sigma(\theta)}{d\Omega}\right)_{n.p.} \{1-C_{nn}-C_{kk}-C_{pp}\}. \tag{27}$$

La difficulté est du même ordre puisqu'il faut mesurer la corrélation entre la polarisation transversale du proton sortant et la polarisation longitudinale du proton de recul à tous les angles.

L'expérience la plus facile à réaliser pratiquement consiste à envoyer un faisceau perpendiculairement à la polarisation de la cible, les deux vecteurs de polarisation étant parallèles. La section efficace différentielle est alors

$$\left(\frac{d\sigma(\theta,\varphi)}{d\Omega}\right)_1 = \left(\frac{d\sigma(\theta)}{d\Omega}\right)_{n.p.} \{1+P(p+p')\cos\varphi+[\tfrac{1}{2}(A_{yy}-A_{xx})\cos 2\varphi + \tfrac{1}{2}(A_{yy}+A_{xx})]pp'\}, \tag{28}$$

où φ est l'angle de la normale au plan de diffusion avec la direction des polarisations. On peut ensuite changer le signe de p' et obtenir

$$\left(\frac{d\sigma(\theta,\varphi)}{d\Omega}\right)_2 = \left(\frac{d\sigma(\theta)}{d\Omega}\right)_{n.p.} \{1+P(p-p')\cos\varphi-[\tfrac{1}{2}(A_{yy}-A_{xx})\cos 2\varphi + \tfrac{1}{2}(A_{yy}+A_{xx})]pp'\}, \tag{29}$$

et définir l'assymétrie $R(\theta, \varphi)$ par

$$R(\theta,\varphi)=\frac{\left(\frac{d\sigma(\theta,\varphi)}{d\Omega}\right)_1-\left(\frac{d\sigma(\theta,\varphi)}{d\Omega}\right)_2}{\left(\frac{d\sigma(\theta,\varphi)}{d\Omega}\right)_1+\left(\frac{d\sigma(\theta,\varphi)}{d\Omega}\right)_2}$$

$$=p'\,\frac{P\cos\varphi+[\frac{1}{2}(A_{yy}-A_{xx})\cos 2\varphi+\frac{1}{2}(A_{yy}+A_{xx})]p}{1+Pp\cos\varphi}. \quad (30)$$

En particulier, en observant à l'angle $\varphi = 0$, on obtient

$$R(\theta,0)=\left\{\frac{P+A_{yy}p}{1+Pp}\right\}p',$$

d'où on peut tirer A_{yy} connaissant P. Comme on sait que P est faible à basse énergie on a approximativement

$$R(\theta,0)\approx A_{yy}pp'=C_{nn}pp'. \quad (31)$$

Pour l'angle $\varphi=\frac{1}{2}\pi$ on a

$$R(\theta,\tfrac{1}{2}\pi)=A_{xx}pp'. \quad (32)$$

Ce coefficient a des propriétés analogues à celles de C_{nn} et on est en droit d'en attendre autant de renseignements.

4. Approximation des Ondes S, P, D

A faible énergie on peut supposer que les ondes de moment angulaire le plus bas interviennent seules. Nous nous limiterons dans ce paragraphe aux cinq paramètres qui sont les déphasages des ondes S et D et les trois déphasages d'onde P. Nous supposerons qu'il n'y a pas de couplage avec l'onde F pour un moment total $J = 2$ [$\varepsilon_2 = 0$ dans les formules (11)].

Les déphasages S et D interviennent seulement dans l'amplitude de diffusion singulet qui s'écrit

$$a=f_c(\theta)+f_c(\pi-\theta)+\frac{i}{k}\{e^{2i\sigma_0}(1-e^{2i\delta_S}) \quad (33)$$
$$+e^{2i\sigma_2}(1-e^{2i\delta_D})\tfrac{5}{2}(3\cos^2\theta-1)\}.$$

Nous pouvons donc considérer a comme une fonction donnée pour des valeurs fixées de δ_S et de δ_D.

Les déphasages P, δ^0, δ^1 et δ^2 interviennent seuls dans les quatre autres amplitudes:

$$
\begin{aligned}
b &= f_c(\theta)-f_c(\pi-\theta)+\frac{ie^{2i\sigma_1}}{k}\{3\cos\theta-\tfrac{3}{2}e^{2i\delta^2}\cos\theta-\tfrac{3}{2}e^{2i\delta^1}\cos\theta\},\\
c &= \{f_c(\theta)-f_c(\pi-\theta)\}\cos\theta+\frac{ie^{2i\sigma_1}}{k}\{3\cos^2\theta-(3\cos^2\theta-\tfrac{3}{2})e^{2i\delta^2}-\tfrac{3}{2}e^{2i\delta^1}\},\\
d &= \{f_c(\theta)-f_c(\pi-\theta)\}\sin\theta+\frac{ie^{2i\sigma_1}}{k}3\sin\theta\cos\theta(1-e^{2i\delta^2}),\\
e &= \{f_c(\theta)-f_c(\pi-\theta)\}\cos\theta+\frac{ie^{2i\sigma_1}}{k}\{3\cos^2\theta-e^{2i\delta^0}-(3\cos^2\theta-1)e^{2i\delta^2}\}.
\end{aligned}
\tag{34}
$$

Suivant Clementel et Villi [1]) nous pouvons exprimer la section efficace et les différents paramètres introduits en (20) par des fonctions de θ multipliées par des coefficients qui ne dépendent que des déphasages. Nous posons donc

$$
\begin{aligned}
A(\theta) &= 3\cos^2\theta+\tfrac{1}{2}(\gamma\cos\theta)\left\{\frac{\sin(2\gamma\ln\sin\frac{1}{2}\theta+2(\sigma_1-\sigma_0))}{\sin^2\frac{1}{2}\theta}-\frac{\sin(2\gamma\ln\cos\frac{1}{2}\theta+2(\sigma_1-\sigma_0))}{\cos^2\frac{1}{2}\theta}\right\},\\
B(\theta) &= -\tfrac{1}{2}(\gamma\cos\theta)\left\{\frac{\cos(2\gamma\ln\sin\frac{1}{2}\theta+2(\sigma_1-\sigma_0))}{\sin^2\frac{1}{2}\theta}-\frac{\cos(2\gamma\ln\cos\frac{1}{2}\theta+2(\sigma_1-\sigma_0))}{\cos^2\frac{1}{2}\theta}\right\},
\end{aligned}
\tag{35}
$$

ce qui diffère des notations de Clementel et Villi par la présence du terme $3\cos^2\theta$ dans la définition de $A(\theta)$ au lieu de 1 et revient à avoir ajouté deux fois le polynome de Legendre $P_2(\cos\theta)$. (On remplace ainsi le coefficient z_3 dans les expressions ci-dessous par z_3-2z_1 qui a une expression plus simple.) Nous obtenons ainsi les trois expressions suivantes:

$$
\begin{aligned}
\left(\frac{d\sigma(\theta)}{d\Omega}\right)_{n.p.} &= \tfrac{1}{4}|a|^2+\tfrac{3}{4}|f_c(\theta)-f_c(\pi-\theta)|^2+\frac{1}{k^2}\{z_1A(\theta)+z_2B(\theta)+z_3P_2(\cos\theta)\},\\
4\left(\frac{d\sigma(\theta)}{d\Omega}\right)_{n.p.}A_{zz} &= -|a|^2+|f_c(\theta)-f_c(\pi-\theta)|^2+\frac{1}{k^2}\{z_1'A(\theta)+z_2'B(\theta)+z_3'P_2(\cos\theta)\},\\
4\left(\frac{d\sigma(\theta)}{d\Omega}\right)_{n.p.}\tfrac{1}{2}(A_{xx}+A_{yy}) &= -|a|^2+|f_c(\theta)-f_c(\pi-\theta)|^2\\
&\quad+\frac{1}{k^2}\{z_1''A(\theta)+z_2''B(\theta)+z_3''P_2(\cos\theta)\},
\end{aligned}
\tag{36}
$$

où les coefficients z ont pour définition

$$
\begin{aligned}
z_1 &= \tfrac{1}{2}\{9-\cos 2\delta^0-3\cos 2\delta^1-5\cos 2\delta^2\}=\sum_J(2J+1)\sin^2\delta^J,\\
z_2 &= \tfrac{1}{2}\{\sin 2\delta^0+3\sin 2\delta^1+5\sin 2\delta^2\}=\sum_J(2J+1)\sin\delta^J\cos\delta^J,\\
z_3 &= \tfrac{1}{4}\{9\cos 2(\delta^2-\delta^1)+4\cos 2(\delta^2-\delta^0)-13\}=-\tfrac{1}{2}\sum_J(J+2)^2\sin^2(\delta^J-\delta^2),
\end{aligned}
\tag{37}
$$

$$z'_1 = 2(3+\cos 2\delta^0-3\cos 2\delta^1-\cos 2\delta^2),$$
$$z'_2 = 2(-\sin 2\delta^0+3\sin 2\delta^1+\sin 2\delta^2), \tag{38}$$
$$z'_3 = 9\cos 2(\delta^2-\delta^1)-4\cos 2(\delta^2-\delta^0)-5,$$

$$z''_1 = 2(3-\cos 2\delta^0-2\cos 2\delta^2),$$
$$z''_2 = 2(\sin 2\delta^0+2\sin 2\delta^2), \tag{39}$$
$$z''_3 = 4\cos 2(\delta^2-\delta^0)-4.$$

Ces coefficients ne sont pas indépendants: la relation (26) qui donne la diffusion singulet entraîne évidemment que

$$4z_1 = z'_1+2z''_1, \qquad 4z_2 = z'_2+2z''_2, \qquad 4z_3 = z'_3+2z''_3. \tag{40}$$

Connaissant la section efficace à plusieurs angles, on peut se donner les déphasages δ_S et δ_D et déterminer de manière univoque les coefficients z_1, z_2, z_3 qui donnent la valeur de la section efficace la plus voisine de la courbe expérimentale. Les valeurs des déphasages δ_S et δ_D sont très mal déterminées et pour chacune d'elles la résolution en δ^0, δ^1, δ^2 admet toujours 4 solutions (voir appendice 1) qui se correspondent deux à deux par la transformation suivante:

$$\delta^0-\delta^2 \to \delta^2-\delta^0, \qquad \delta^1-\delta^2 \to \delta^2-\delta^1,$$
$$\delta^2 \to -\delta^2+2\,\text{arctg.}\left(\frac{2z_2}{9-2z_1}\right). \tag{41}$$

Nous pouvons constater que les coefficients z_3, z'_3 et z''_3 sont invariants dans cette transformation. En particulier pour $\theta = \frac{1}{2}\pi$ pour lequel $A(\theta) = B(\theta) = 0$, les valeurs de A_{zz} ou de $(A_{xx}+A_{yy})$ ne permettent pas de distinguer entre deux de ces solutions.

A la même approximation une autre expression très intéressante est celle de $A_{xx}-A_{yy}$:

$$4\left(\frac{d\sigma(\theta)}{d\Omega}\right)_{n.p.} \tfrac{1}{2}(A_{xx}-A_{yy}) = \frac{\sin^2\theta}{k^2} \times \tfrac{9}{2}\{\cos 2(\delta^2-\delta^1)-1\}. \tag{42}$$

Elle prend la même valeur pour les deux solutions déduites l'une de l'autre par (41). De plus elle indique une méthode directe pour obtenir la différence $\delta^2-\delta^1$ de deux des déphasages P.

Enfin les deux derniers paramètres A_{zz} et P s'expriment aussi à l'aide de $A(\theta)$ et $B(\theta)$, mais c'est le polynome de Legendre associé $P_2^1(\cos\theta) = 3\sin\theta$

$\cos\theta$ qui intervient ici:

$$4\left(\frac{d\sigma(\theta)}{d\Omega}\right)_{n.p.} A_{xx} = \frac{1}{k^2}\,\mathrm{tg}\theta A(\theta)\{3\cos 2\delta^1 - \cos 2\delta^2 - 2\cos 2\delta^0\} + \frac{1}{k^2}\,\mathrm{tg}\theta B(\theta)\{2\sin 2\delta^0 - 3\sin 2\delta^1 + \sin 2\delta^2\} + \frac{3}{k^2}\sin\theta\cos\theta\{2\cos 2(\delta^2-\delta^0) - 3\cos 2(\delta^2-\delta^1) + 1\},$$

$$4\left(\frac{d\sigma(\theta)}{d\Omega}\right)_{n.p.} P = \frac{1}{k^2}\,\mathrm{tg}\theta A(\theta)\{5\sin 2\delta^2 - 3\sin 2\delta^1 - 2\sin 2\delta^0\} + \frac{1}{k^2}\,\mathrm{tg}\theta B(\theta)\{5\cos 2\delta^2 - 3\cos 2\delta^1 - 2\cos 2\delta^0\} + \frac{3}{k^2}\sin\theta\cos\theta\{2\sin 2(\delta^0-\delta^2) + 3\sin 2(\delta^1-\delta^2)\}. \tag{43}$$

Pour A_{xx} les deux premiers coefficients sont

$$\tfrac{1}{2}(z''_1 - z'_1), \qquad \tfrac{1}{2}(z''_2 - z'_2), \tag{44}$$

et le troisième a les mêmes propriétés que les z_3.

Remarquons que toutes ces expressions se simplifient à l'angle $\theta = \frac{1}{2}\pi$ puisque

$$\mathrm{tg}\theta A(\theta) = \mathrm{tg}\theta B(\theta) = f_c(\theta) - f_c(\pi-\theta) = 0. \tag{45}$$

On obtient donc

$$\begin{aligned}
\left(\frac{d\sigma(\theta)}{d\Omega}\right)_{n.p.} &= \tfrac{1}{4}\left\{|a|^2 - \frac{1}{2k^2}\,(9\cos 2(\delta^2-\delta^1) + 4\cos 2(\delta^2-\delta^0) - 13)\right\},\\
4\left(\frac{d\sigma(\theta)}{d\Omega}\right)_{n.p.} A_{zz} &= -|a|^2 - \frac{1}{2k^2}\,(9\cos 2(\delta^2-\delta^1) - 4\cos 2(\delta^2-\delta^0) - 5),\\
4\left(\frac{d\sigma(\theta)}{d\Omega}\right)_{n.p.} A_{yy} &= -|a|^2 - \frac{1}{2k^2}\,(9\cos 2(\delta^2-\delta^1) + 4\cos 2(\delta^2-\delta^0) - 13),\\
4\left(\frac{d\sigma(\theta)}{d\Omega}\right)_{n.p.} A_{xx} &= -|a|^2 + \frac{1}{2k^2}\,(9\cos 2(\delta^2-\delta^1) - 4\cos 2(\delta^2-\delta^0) - 5)\\
A_{xx} = 0, \qquad P &= 0.
\end{aligned} \tag{46}$$

La mesure de A_{yy} à l'angle $\theta = \frac{1}{2}\pi$ permet de séparer les diffusions des états singulet et triplet mais pour cet angle seulement. Ceci a été signalé comme méthode pour déterminer avec plus de précision le déphasage S. Des calculs sont en cours pour étudier la dépendance des valeurs prises par A_{yy} et A_{xx} a $\theta = \frac{1}{2}\pi$ en fonction des déphasages S et D.

5. Calculs et Discussions

Le calcul de toutes les quantités envisagées a été fait pour plusieurs ensembles de déphasages donnés par Mac Gregor [2]). En fait, on a calculé z_1, z_2, z_3 à partir de la solution 1 de cet article, pour retrouver les autres solutions suivant la méthode donnée à l'appendice 1.

Pour retrouver approximativement la dépendance du genre de solution, nous pouvons résoudre de façon approchée les équations qui donnent les déphasages P et remplacer partout les fonctions trigonométriques par leur développement. On obtient à l'ordre le plus bas

$$\delta^0 = \tfrac{1}{9}(c-6x+10y), \qquad \delta^1 = \tfrac{1}{9}(c-3x-5y), \qquad \delta^2 = \tfrac{1}{9}(c+3x+y), \quad (47)$$

où c, x, y sont des constantes définies par

$$c = z_2, \qquad x = \pm\sqrt{\tfrac{1}{8}(z_2^2-9z_1-5z_3)}, \qquad y = \pm\sqrt{\tfrac{1}{8}(9z_1-z_2^2+3z_3)}, \quad (48)$$

La solution 1 correspond aux valeurs positives de x et de y, la solution 2 aux valeurs négatives de x et positives de y; la solution 3 aux valeurs positives de x et négatives de y; et la solution 4 aux valeurs négatives de x et y.

La section efficace est

$$\left(\frac{d\sigma(\theta)}{d\Omega}\right)_{n.p.} = \tfrac{1}{4}|a|^2+\tfrac{3}{4}|f_c(\theta)-f_c(\pi-\theta)|^2+\frac{1}{k^2}A(\theta)\times\tfrac{1}{9}\{c^2+12x^2+20y^2\} + \frac{1}{k^2}B(\theta)c-\frac{4P_2(\cos\theta)}{k^2}\{x^2+y^2\}. \quad (49)$$

Elle est indépendante de la solution envisagée. Dans le calcul des coefficients A_{zz}, A_{yy}, A_{xx}, A_{zx} et P nous pouvons séparer une partie invariante et des parties qui changent de signe d'une solution à l'autre. Pour mieux mettre en évidence les différences entre les solutions, nous remplacerons $A(\theta)$ et $B(\theta)$ par des expressions approchées. En effet pour une énergie du proton incident variant de 10 à 40 MeV le paramètre coulombien γ décroît de 0.05 à 0.025 ce qui permet de remplacer $f_c(\theta)$ par le premier terme de son développement en puissances de γ dans un assez large domaine de θ. En effet, pour que

$$|2\gamma Ln\sin\tfrac{1}{2}\theta+2(\sigma_1-\sigma_0)| \approx 2\gamma|Ln\sin\tfrac{1}{2}\theta+1| \leqq 0.1,$$

il faut que

$$\theta > 2/e^2 \text{ radians soit } 16° \text{ à } 10 \text{ MeV},$$
$$\theta > 2/e^3 \text{ radians soit } 6° \text{ à } 40 \text{ MeV}.$$

Les formules obtenues couvriront donc tout le domaine pratiquement observable.

Dans ces conditions, on a

$$k^2 A_{zz}\left(\frac{d\sigma}{d\Omega}\right)_{n.p.} = \left\{-\frac{k^2}{4}|a|^2+\tfrac{1}{4}k^2|f_c(\theta)-f_c(\pi-\theta)|^2+A(\theta)\tfrac{1}{27}(c^2-8y^2)+B(\theta)\frac{c}{3}\right\} + \left\{\tfrac{16}{9}\cos^2\theta\left(\frac{3\gamma}{\sin^2\theta}-c\right)\right\}y \quad +\{4\sin^2\theta\}xy, \quad (50)$$

$$k^2 A_{yy}\left(\frac{d\sigma}{d\Omega}\right)_{n.p.} = \left\{-\tfrac{1}{4}k^2|a|^2+\tfrac{1}{4}k^2|f_c(\theta)-f_c(\pi-\theta)|^2+A(\theta)\tfrac{1}{27}(c^2+18x^2+34y^2)\right.$$
$$\left.+B(\theta)\frac{c}{3}+(x^2+y^2)(2-4\cos^2\theta)\right\}+\left\{\tfrac{8}{9}\cos^2\theta\left(c-\frac{3\gamma}{\sin^2\theta}\right)\right\}y,$$

$$k^2 A_{xx}\left(\frac{d\sigma}{d\Omega}\right)_{n.p.} = \left\{-\frac{k^2}{4}|a|^2+\tfrac{1}{4}k^2|f_c(\theta)-f_c(\pi-\theta)|^2+A(\theta)\tfrac{1}{27}(c^2+18x^2+34y^2)\right.$$
$$\left.+B(\theta)\frac{c}{3}-2\cos^2\theta(x^2+y^2)\right\}+\left\{\tfrac{8}{9}\cos^2\theta\left(c-\frac{3\gamma}{\sin^2\theta}\right)\right\}y+\{-4\sin^2\theta\}xy,$$

$$k^2 A_{xx}\left(\frac{d\sigma}{d\Omega}\right)_{n.p.} = \{A(\theta)\,\mathrm{tg}\,\theta\tfrac{1}{9}(3x^2+7y^2)-\sin\theta\cos\theta(x^2+y^2)\} \tag{50}$$
$$+\left\{\tfrac{4}{3}\sin\theta\cos\theta\left(c-\frac{3\gamma}{\sin^2\theta}\right)\right\}y \quad +\{4\cos\theta\sin\theta\}xy,$$
$$P=0.$$

Dans les trois premières expressions, nous pouvons remarquer que les solutions (1), (2) diffèrent des solutions (3), (4) seulement par un terme de la forme

$$\tfrac{8}{9}\cos^2\theta\left(c-\frac{3\gamma}{\sin^2\theta}\right), \tag{51}$$

qui s'annule pour $\theta = \frac{1}{2}\pi$ mais qui peut être très important dans la zone d'interférence avec la diffusion coulombienne. Les calculs de la fig. 5 correspondent à une valeur de c très faible, ce qui semble être le cas à 20 MeV, car tous les systèmes de déphasages donnés par Mac Gregor à 19.8 MeV correspondent à une valeur de c négligeable. Ce paramètre a une interprétation physique très importante: il détermine la possibilité de connaître le signe des déphasages P par mesure de la section efficace dans la région d'interférence avec la diffusion coulombienne puisque lorsqu'il est nul on passe des solutions (1) et (2) aux solutions (3) et (4) en changeant tous les signes. La fig. 6 représente un cas fictif c'est-à-dire un calcul avec des déphasages de départ arbitraires, mais pour lesquels le coefficient c est très grand pour mettre son influence en évidence.

Les solutions (1), (4) diffèrent des solutions (2), (3) par un terme en $\sin^2\theta$ et ce terme est absent de l'expression de A_{yy}. Donc à l'approximation envisagée il n'y a que deux valeurs différentes de A_{yy} et une mesure à un angle de l'ordre de 30° permet de rejeter les solutions (1), (2) ou les solutions (3), (4); ensuite une mesure de A_{xx} à 90° permet de déterminer quelle solution parmi les quatre est la meilleure, sauf accident tel que des valeurs trop faibles de c, x ou y. La mesure de A_{yy} à $\frac{1}{2}\pi$ a un grand intérêt car elle permet de déterminer les déphasages singulets.

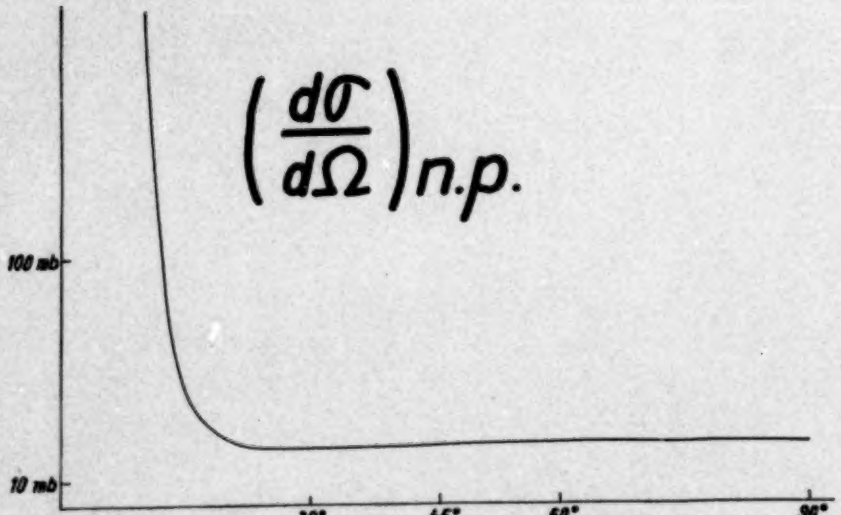
$\left(\frac{d\sigma}{d\Omega}\right)_{n.p.}$
100 mb
10 mb
30°
45°
60°
90°

(1)

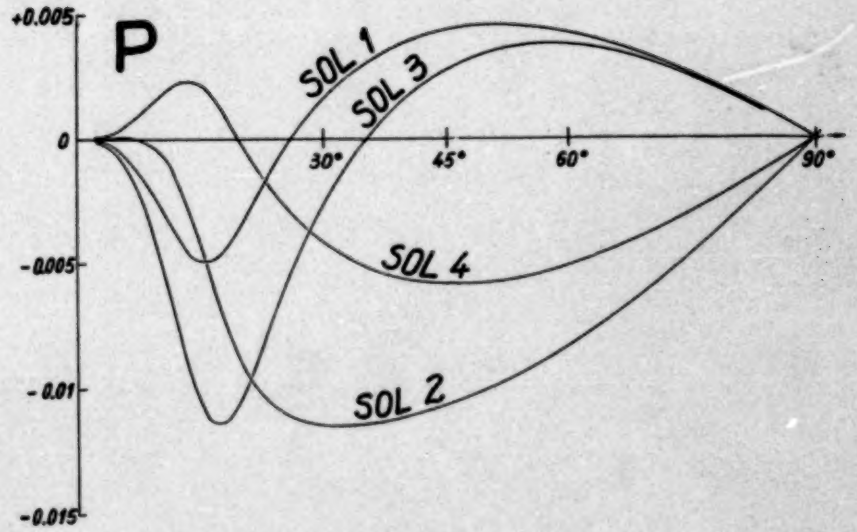
P
+0.005
0
-0.005
-0.01
-0.015
SOL 1
SOL 3
SOL 4
SOL 2
30°
45°
60°
90°

(2)

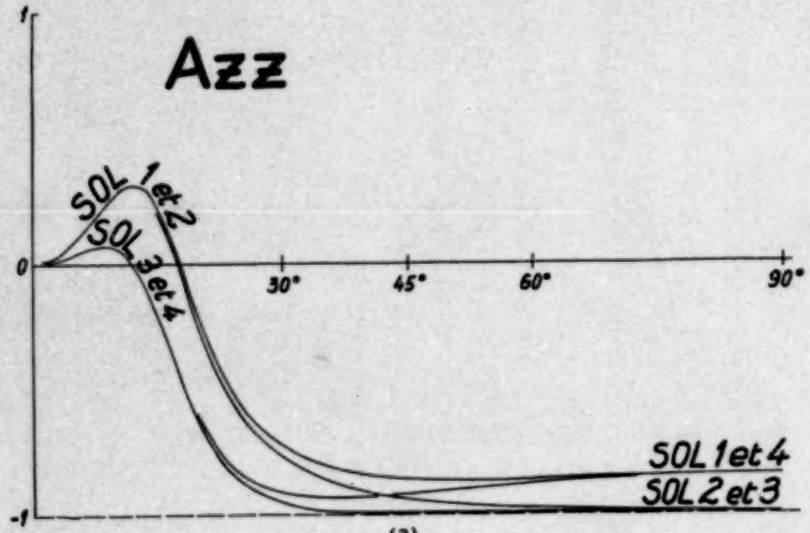
Azz
1
0
-1
SOL 1 et 2
SOL 3 et 4
30°
45°
60°
90°
SOL 1 et 4
SOL 2 et 3

(3)

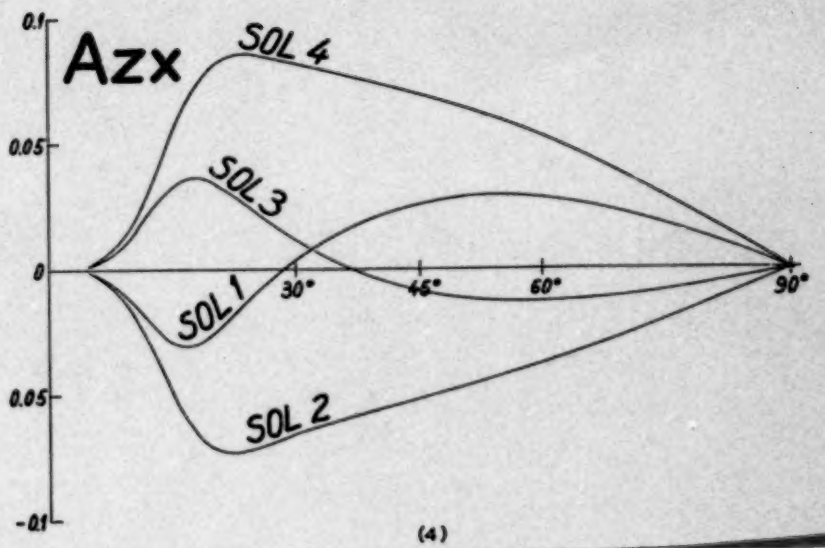
Azx
0.1
0.05
0
0.05
-0.1
SOL 4
SOL 3
SOL 1
SOL 2
30°
45°
60°
90°

(4)

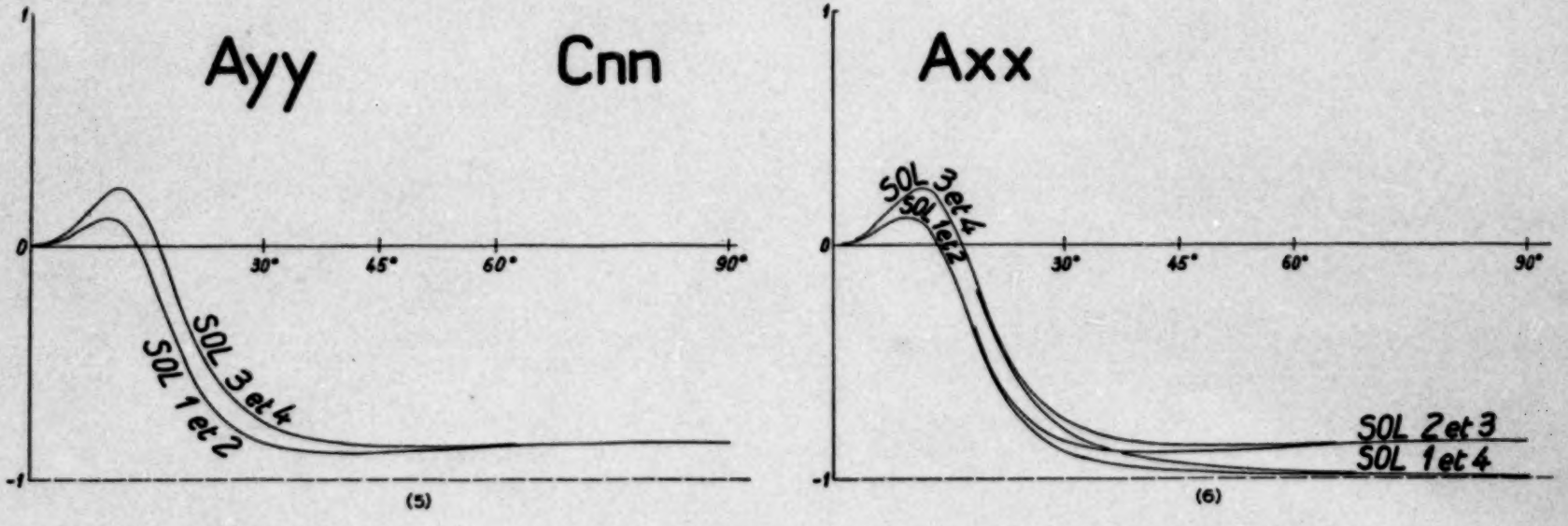

Fig. 5. Distributions angulaires pour les quatre solutions donnant la section efficace différentielle observée à 19.8 MeV pour S (50°) et D (0° · 40). Les déphasages P sont:

solution 1: $\delta^0 = 0.44$, $\delta^1 = -5.25$, $\delta^2 = 3.03$;
solution 2: $\delta^0 = 10.51$, $\delta^1 = -0.20$, $\delta^2 = -1.95$;
solution 3: $\delta^0 = -10.54$, $\delta^1 = 0.18$, $\delta^2 = 1.93$;
solution 4: $\delta^0 = -0.46$, $\delta^1 = 5.23$, $\delta^2 = -3.05$;

ce qui correspond à $c = -0.16$, $x = 7.5$, $y = 4.5$.

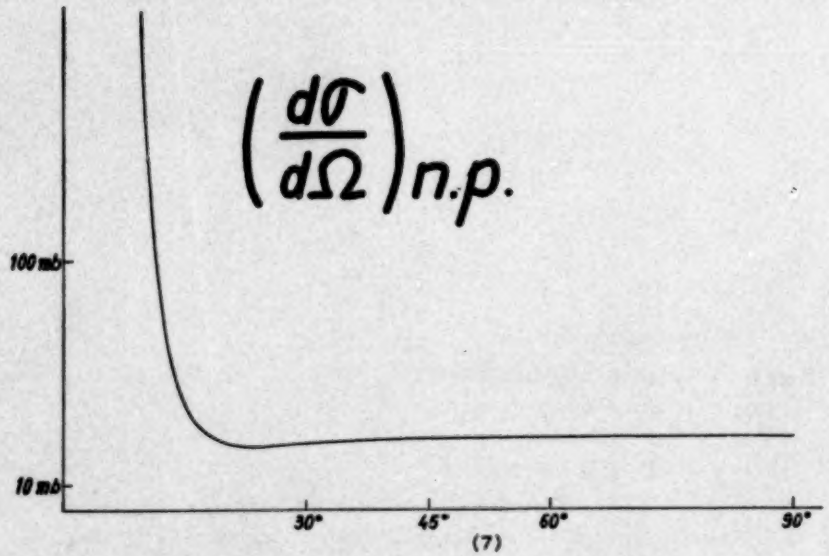
$\left(\frac{d\sigma}{d\Omega}\right)_{n.p.}$
100 mb
10 mb
30°
45°
60°
90°

(7)

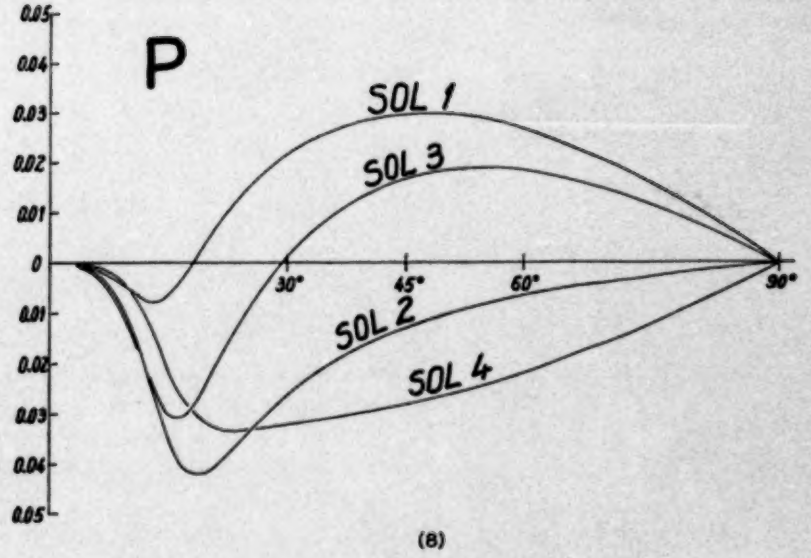
P
SOL 1
SOL 3
SOL 2
SOL 4
0.05
0.04
0.03
0.02
0.01
0
30°
45°
60°
90°

(8)

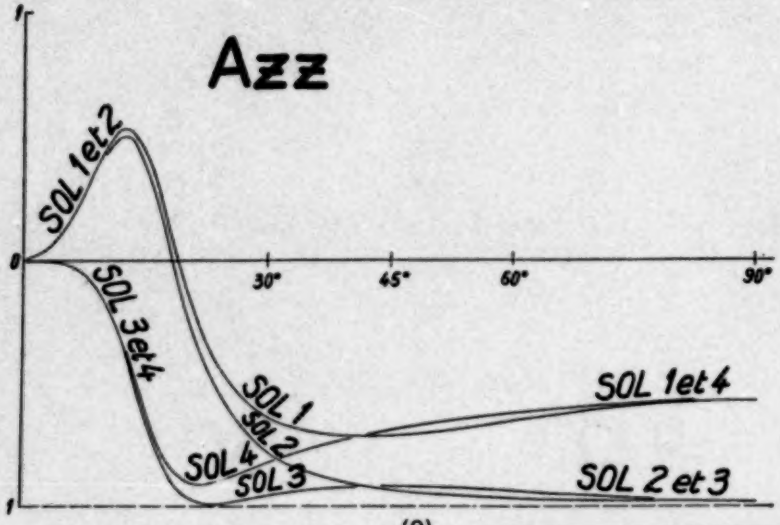
Azz
SOL 1et2
SOL 3et4
SOL 1
SOL 2
SOL 4
SOL 3
SOL 1et4
SOL 2et3
1
0
30°
45°
60°
90°

(9)

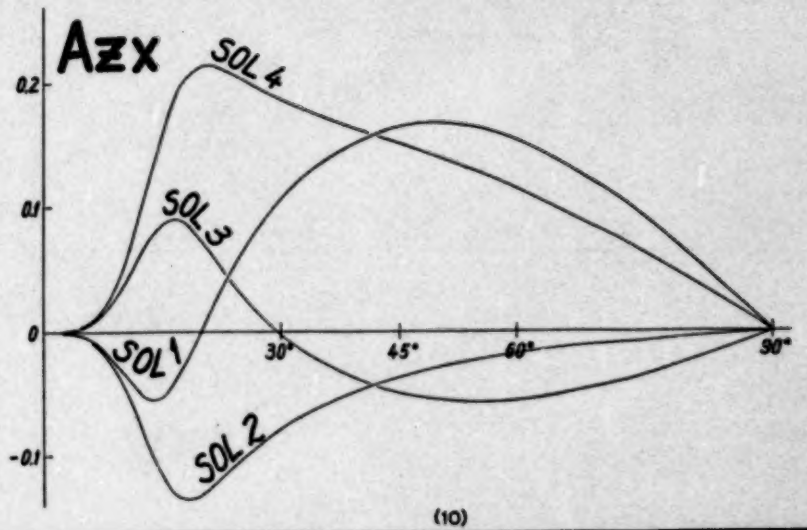
Azx
SOL 4
SOL 3
SOL 1
SOL 2
0.2
0.1
0
-0.1
30°
45°
60°
90°

(10)

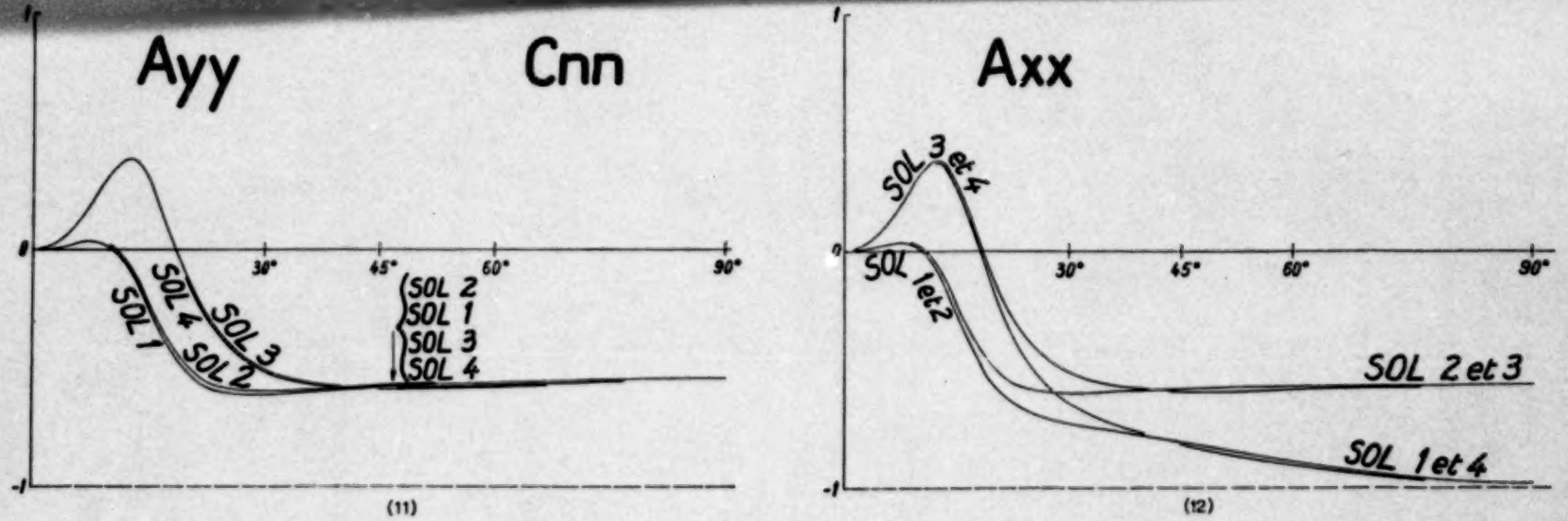

Fig. 6. Distributions angulaires pour les quatre solutions donnant la même section efficace différentielle à 19.8 MeV pour S (50°) et D (0° · 40). Les déphasages sont:

solution 1:	$\delta^0 = 10.50$,	$\delta^1 = -9.00$,	$\delta^2 = 6.00$;
solution 2:	$\delta^0 = 23.08$,	$\delta^1 = -2.87$,	$\delta^2 = 0.28$;
solution 3:	$\delta^0 = -19.97$,	$\delta^1 = 5.97$,	$\delta^2 = 2.82$;
solution 4:	$\delta^0 = -7.39$,	$\delta^1 = 12.11$,	$\delta^2 = -2.89$;

ce qui correspond à $c = 13.50$, $x = 9$, $y = 13.50$.

Si nous formons l'expression de C_{kp} nous trouvons seulement le terme ayant xy en facteur, ce qui entraîne que les valeurs de C_{kp} calculées pour les solutions (1) et (4) sont identiques entre elles, ainsi que celles des solutions (2) et (3).

Pour A_{zz}, l'expression est analogue aux précédentes avec la seule différence du remplacement de $\cos^2\theta$ ou $\sin^2\theta$ par $\sin\theta\cos\theta$. La différence entre les solutions (1), (2) et les solutions (3), (4) est donc plus importante pour les angles voisins de 90°.

A cette approximation la polarisation est nulle. Nous pouvons calculer les termes suivants:

$$\begin{aligned} k^2P\left(\frac{\mathrm{d}\sigma(\theta)}{\mathrm{d}\Omega}\right)_{\text{n.p.}} &= \left\{\tfrac{2}{9}\sin\theta\cos\theta(5y^2+x^2)\left(c-\frac{3\gamma}{\sin^2\theta}\right)\right\} \\ &+\left\{2\gamma^2\left(\frac{\ln\sin\frac{1}{2}\theta+1}{\sin^2\frac{1}{2}\theta}-\frac{\ln\cos\frac{1}{2}\theta+1}{\cos^2\frac{1}{2}\theta}\right)\sin\theta+\tfrac{8}{9}\gamma c\,\mathrm{cotg}\,\theta\right. \\ &\left.+\tfrac{2}{27}\sin\theta\cos\theta(37y^2+27x^2-2c^2)\right\}x \\ &+\{\tfrac{10}{9}\sin\theta\cos\theta(y^2-x^2)\}y-\left\{\tfrac{20}{27}\sin\theta\cos\theta\left(c-\frac{3\gamma}{\sin^2\theta}\right)\right\}xy. \end{aligned} \tag{52}$$

La polarisation est donc très sensible aux déphasages puisque les expressions en facteur de x, y ou xy dépendent elles mêmes des déphasages P. La dépendance de la solution est compliquée ici par la présence d'un terme ayant x en facteur. Cependant, même en supposant γ très petit le terme

$$\tfrac{2}{27}\sin\theta\cos\theta(15y^2+3x^2-10xy)\left(c-\frac{3\gamma}{\sin^2\theta}\right) \tag{53}$$

indique une polarisation plus importante aux petits angles et ayant pour origine l'interférence avec la diffusion Coulombienne.

Les figs. 5 et 6 donnent les résultats des calculs effectués avec les expressions complètes. Le cas 5 correspond à des déphasages qui ont été calculés par Mac Gregor à 19.8 MeV; le cas 6 est fictif.

Je tiens à remercier Monsieur Thirion, dont les expériences sont à l'origine de ce travail et Messieurs Bloch et Messiah qui m'ont aidé de leurs conseils.

Appendice

1. DÉTERMINATION DES DÉPHASAGES P

La section efficace dépend des déphasages P par l'intermédiaire des paramètres

$$\begin{aligned} 2z_1-2iz_2 &= 9-\mathrm{e}^{2i\delta^0}-3\mathrm{e}^{2i\delta^1}-5\mathrm{e}^{2i\delta^2}, \\ 4z_3 &= 9\cos 2(\delta^2-\delta^1)+4\cos 2(\delta^2-\delta^0)-13. \end{aligned} \tag{A.1}$$

Si nous posons

$$\delta^2-\delta^0=\alpha, \qquad \delta^2-\delta^1=\beta, \tag{A.2}$$

ces relations deviennent

$$\begin{aligned} Ae^{i\gamma} &= 9-2z_1-2iz_2 = (5+e^{2i\alpha}+3e^{2i\beta})e^{-2i\delta^2}, \\ 4z_3 &= 9\cos 2\beta+4\cos 2\alpha-13, \end{aligned} \tag{A.3}$$

avec

$$A^2 = 35+10\cos 2\alpha+30\cos 2\beta+6\cos 2(\alpha-\beta).$$

Si $\alpha=\alpha_0$, $\beta=\beta_0$ est la solution du système (A.3), $\alpha=-\alpha_0$, $\beta=-\beta_0$ est aussi une solution: la relation entre les deux déphasages δ^2 correspondants est

$$2(\delta^2+\delta^{2'})=2\gamma=2\,\mathrm{arctg}\,\frac{2z_2}{9-2z_1}. \tag{A.4}$$

Pour résoudre le système (A.3) nous posons

$$X=\mathrm{tg}\alpha, \qquad Y=\mathrm{tg}\beta,$$

et nous obtenons

$$\begin{aligned} &2z_3(1+X^2)(1+Y^2)+4X^2+9Y^2+13X^2Y^2=0, \\ &\tfrac{1}{8}(81-A^2)(1+X^2)(1+Y^2)-4X^2-9Y^2-10X^2Y^2+3XY=0. \end{aligned} \tag{A.5}$$

L'élimination de X entre les deux équations (A.5) donne une équation du quatrième degré en Y^2, mais on doit éliminer la racine $Y^2=-1$. Il reste alors

$$\begin{aligned} Y^6(4z_0-2z_3-9)^2+Y^4(48z_0^2+8z_3^2-32z_0z_3+44z_3-72z_0+36) \\ +Y^2(48z_0^2+4z_3^2-16z_0z_3+8z_3)+16z_0^2=0, \end{aligned} \tag{A.6}$$

avec

$$z_0=\tfrac{1}{24}(81-A^2)+\tfrac{2}{3}z_3=\tfrac{3}{2}z_1-\tfrac{1}{6}(z_1^2+z_2^2)+\tfrac{2}{3}z_3.$$

De même en éliminant Y on obtient l'équation

$$\begin{aligned} X^6(9z_0-2z_3-4)^2+X^4(243\,z_0^2+8z_3^2-72z_0z_3-72z_0+34z_3+36) \\ +X^2(243z_0^2+4z_3^2-36z_0z_3+18z_3)+81z_0^2=0. \end{aligned} \tag{A.7}$$

Les deux équations ont toujours une racine négative. Les deux autres racines, ont le même signe si elles sont réelles puisque les coefficients du terme du sixième degré et le terme constant sont des carrés. Par conséquent s'il y a une solution du système il en existe quatre également valables. En écrivant que ces deux racines existent et qu'elles sont positives on obtient dans le plan de z_0, z_3 le domaine "physique" des points auxquels correspondent des solutions.

Si $z_0>0$, les solutions (1), (2), (3), (4)[2]) correspondent aux racines en Y de l'équation (A.6) de valeur algébrique décroissante. Si $z_0<0$, l'ordre des

solutions (2) et (3) est inversé. Le système (A.4) détermine la valeur de X correspondante et les équations (A.2) et (A.3) donnent les déphasages.

Si nous supposons une solution connue et donnée par les valeurs x et y de X et Y nous pouvons exprimer z_0 et z_3 dans (A.6) et (A.7) à l'aide de x et y. On obtient alors

$$X^4(4+9xy-5y^2)+(36+20x^2-81y^2+72xy + 121x^2y^2+45y^4-252xy^3-61x^2y^4)X^2-81y^2(1+xy)^2=0, \quad \text{(A.8)}$$

ou

$$Y^4(9+4xy+5x^2)^2+Y^2(36-16x^2+72xy- 45y^2-20x^4+8x^3y-74x^2y^2-61x^4y^2)-16x^2(1+xy)^2=0. \quad \text{(A.9)}$$

Les solutions qui ne se déduisent pas de la solution connue par la transformation (A.4) correspond aux racines des équations (A.8) et (A.9).

2. RELATION ENTRE LES AMPLITUDES EMPLOYÉES ET CELLES QUI SONT LES PLUS USITÉES

1) Formalisme à un seul axe de quantification [5]):

$$M_{11} = \frac{b}{2}+\tfrac{1}{2}(c\cos\theta)+\tfrac{1}{2}(d\sin\theta), \qquad b = M_{11}+M_{1-1},$$

$$M_{10} = \frac{1}{\sqrt{2}}(d\cos\theta-e\sin\theta), \qquad c = (M_{11}-M_{1-1})\cos\theta+M_{01}\sqrt{2}\sin\theta,$$

$$M_{1-1} = \tfrac{1}{2}b-\tfrac{1}{2}(c\cos\theta)-\tfrac{1}{2}(d\sin\theta), \qquad d = M_{10}\sqrt{2}\cos\theta+M_{00}\sin\theta$$

$$M_{01} = \frac{1}{\sqrt{2}}(c\sin\theta-d\cos\theta), \qquad = (M_{11}-M_{1-1})\sin\theta-M_{01}\sqrt{2}\cos\theta,$$

$$M_{00} = d\sin\theta+e\cos\theta, \qquad e = -M_{10}\sqrt{2}\sin\theta+M_{00}\cos\theta,$$

$$M^S = a.$$

Les formules de passage ci-dessus sont celles qui sont obtenues en employant les matrices de rotation.

2) Formalisme des invariants [5]):

$$a(\theta) = \tfrac{1}{4}(b+(c+e)\cos\theta+2d\sin\theta+a), \qquad a = a(\theta)-2g(\theta))-m(\theta),$$

$$c(\theta) = \tfrac{i}{4}(2d\cos\theta-(c+e)\sin\theta), \qquad b = a(\theta)+2g(\theta)-m(\theta),$$

$$m(\theta) = \tfrac{1}{4}(-b+(c+e)\cos\theta+2d\sin\theta-a), \qquad c = 2h(\theta)+a(\theta)+m(\theta)\cos\theta - 2ic(\theta)\sin\theta,$$

$$g(\theta) = \tfrac{1}{4}(b-a), \qquad d = a(\theta)\sin\theta+m(\theta)\sin\theta - 2ic(\theta)\sin\theta,$$

$$h(\theta) = \tfrac{1}{4}(c-e), \qquad e = -2h(\theta)+(a(\theta)+m(\theta))\cos\theta + 2ic(\theta)\sin\theta.$$

3) Amplitudes données par l'échange d'un pion [6]):

$$a = -\frac{g^2}{4E}(A+B),$$

$$b = -\frac{g^2}{4E}(A-B),$$

$$c = -\frac{g^2}{4E}(A+B),$$

$$d = 0,$$

$$e = \frac{g^2}{4E}(A+B),$$

avec

$$A = \frac{1+\cos\theta}{x_0+\cos\theta},$$

$$B = \frac{1-\cos\theta}{x_0-\cos\theta}.$$

Bibliographie

1) E. Clementel et C. Villi, Nuovo Cim. **2** (1955) 1165
2) M. H. Mac Gregor, Phys. Rev. **113** (1959) 1559;
   M. P. Noyes et M. H. Mac Gregor, Phys. Rev. **111** (1958) 223
3) L. Wolfenstein, Ann. Rev. Nuclear Sci. **6** (1956) 43
4) M. Jacob et G. C. Wick, Annals of Physics **7** (1959) 404
5) H. P. Stapp, University of California, Radiation Laboratory report UCRL-3098 (1955)
6) P. Cziffra, M. H. Mac Gregor, M. J. Moravcsik et H. P. Stapp, Phys. Rev. **114** (1959) 880
7) M. H. Mac Gregor, M. J. Moravcsik et H. P. Stapp, Ann. Rev. Nuclear Sci. **10** (1960) 291
8) A. Messiah, Mécanique quantique (Dunod, Paris, 1960)

2.F:2.G *Nuclear Physics* **28** (1961) 244—257; © *North-Holland Publishing Co., Amsterdam*
Not to be reproduced by photoprint or microfilm without written permission from the publisher

ON THE DISPERSION THEORY OF DIRECT NUCLEAR REACTIONS

I. S. SHAPIRO

Theoretical and Experimental Physics Institute, Academy of Sciences, Moscow, USSR

Received 1 May 1961

Abstract: The Feynman graphs with singularities closest to the physical region of variables are assumed to be responsible for the main contribution to the amplitude of a direct nuclear process.

Using the dispersion relations with respect to energy a singular integral equation is obtained for calculating interactions in the initial and final states. This equation admits an accurate solution and simple iteration, the first-order iteration corresponding to the method of distorted waves.

It is found that a substantial contribution to the direct process mechanism may come not only from pole graphs corresponding to the Butler mechanism, exchange stripping and heavy pick-up reactions, but from more complex graphs as well. The reactions $Be^9(d, n)B^{10}$, $Be^9(\alpha, t)B^{10}$ and $C^{12}(d, p)C^{13}$ are considered to illustrate this point. Some reactions of the type (x, yz) and in particular, the "knock out" of nuclear clusters, are analyzed from the same angle.

1. Introduction

1.1. STATEMENT OF THE PROBLEM

Ample experimental data warrant the assumption that direct reactions of the types

$$A+x \rightarrow B+y, \tag{1}$$

$$A+x \rightarrow B+y+z \tag{2}$$

can be described satisfactorily by Feynman graphs with few internal lines. The simplest pole graph for deuteron stripping was considered by Amado [1]) and corresponds to the Butler stripping theory.

The present paper is concerned with further applications of dispersion relations to the direct-process theory and especially with processes of the type of eq. (1). This section introduces notations and formulates general premises.

1.2. KINEMATIC RELATIONS

The reaction (1) is described by two independent kinematic variables. Two of the following three quantities can be selected for this purpose:

a) the kinetic energy of the colliding particles E;

b) the square of the momentum transfer

$$q^2 = (p_y - p_x)^2, \tag{3}$$

where p_x and p_y are the momenta of the particles x and y;

c) the square of the sum of the momenta of the particles x and y:

$$p^2 = (p_x + p_y)^2. \tag{3a}$$

In the centre-of-mass system of colliding particles to be used in the following, the three variables are connected by the simple relation

$$q^2+p^2 = 4(m_{xA}+m_{yB})E+4m_{yB}Q. \tag{4}$$

Here m_{xA} and m_{yB} are the reduced masses of the particles x and y and Q is the energy released in the reaction or its threshold

$$Q = m_A+m_x-m_B-m_y \tag{5}$$

(it will be assumed that $\hbar = c = 1$).

As independent variables, q^2 and E will be selected except for some cases (exchange stripping and heavy pick-up) when it is convenient to use the variable p^2 instead of q^2.

1.3. UNITARITY AND ANALYTICITY

The unitarity relation

$$SS^\dagger = 1 \tag{6}$$

for the S-matrix, which is written in the form

$$S = 1+i(2\pi)^4T, \tag{7}$$

where

$$T = \mathscr{B}+i\mathscr{A}, \qquad \mathscr{A} = \mathscr{A}^\dagger, \qquad \mathscr{B} = \mathscr{B}^\dagger, \tag{8}$$

leads to the well-known formula

$$\mathscr{A}_{if} = \tfrac{1}{2}(2\pi)^4 \sum_n T_{in}T_{nf}^\dagger. \tag{9}$$

In eq. (9) summation (integration) is performed over all intermediate states of n for which the transitions $i \to n$ and $n \to f$ are allowed by the conservation laws. The matrices T and $\mathscr{A}$ are of the form

$$T_{kl}(q^2, E) = M_{kl}(q^2, E)\delta_{\lambda_k\lambda_l}\delta^4(l-m), \tag{10}$$

$$\mathscr{A}_{kl}(q^2, E) = A_{kl}(q^2, E)\delta_{\lambda_k\lambda_l}\delta^4(l-m). \tag{11}$$

In eqs. (10) and (11) the arguments of the δ-function are the momenta and energies of the states k and l, and the subscript λ denotes an aggregate of discrete quantum numbers. The quantity A_{kl} is the absorptive part of the amplitude M_{kl}. The principal postulate of the dispersion relation theory is the assumption that the amplitudes $M_{kl}(q^2, E)$ are analytical functions of their arguments. The amplitude $M_{kl}(q^2, E)$ has singularities: poles or branch points, and therefore $M_{kl}(q^2, E)$ is, in general, a many-valued function. In the dispersion relation theory we deal with only one of its sheets known as the physical sheet. For $M_{kl}(z)$ the following relation holds true:

$$M_{kl}(z^*) = M_{kl}^\dagger(z), \tag{12}$$

where

$$z = q^2, E.$$

2. Reactions A+x → B+y

2.1. POLE GRAPHS

The fraction of the sum (9) corresponding to the transition $n \to f$, in which one particle b is absorbed out of those emitted in the transition $i \to n$, can be written as

$$A_{if} = 2\pi m_b \delta(p_b^2 - 2m_b E_b) \sum_{s_b} M_{ib} M_{bf}^{\dagger}. \tag{13}$$

In eq. (13) summation is performed over the spin variable S_b of the particle b; the quantities m_b, p_b and E_b are the mass, momentum and energy of the intermediate particle b. Using (13) it is easy to establish that at

$$p_b^2 = 2m_b E_b$$

the amplitude M_{if} has a pole, and close to the pole we have

$$M_{if} = 2m_b \frac{\sum_{s_b} M_{ib} M_{bf}^{\dagger}}{p_b^2 - 2m_b E_b - i\eta}, \qquad \eta \to 0. \tag{14}$$

The Feynman graphs with one internal line correspond to the pole amplitude (14). Fig. 1(a) represents Amado's graph corresponding to the Butler stripping theory. For

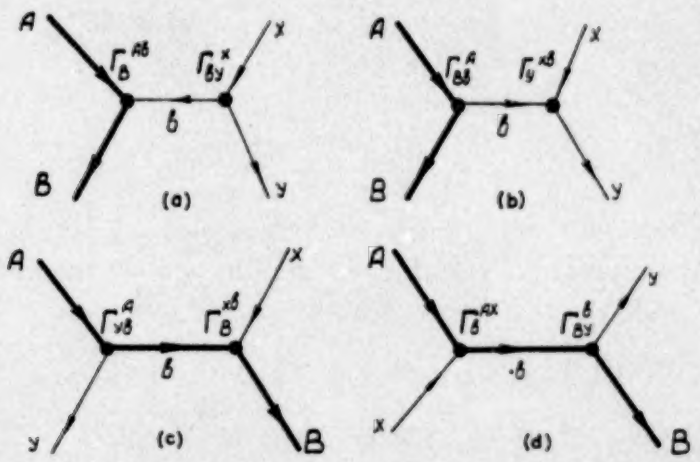

Fig. 1. Feynman graphs with one internal line. (a) Pole graph for stripping reaction. (b) Pole graph for pick-up reaction. (c) Pole graph for exchange stripping and heavy pick-up reactions. (d) Quasi-compound process.

instance, in the reaction (d, p) one has b = n, in the reaction (He^3, p), b = d, etc. Graph 1(b) corresponds to a pick-up process. In the reaction (p, d), b = n, in the reaction (n, d) b = He^3 etc. Fig. 1(c) represents a graph corresponding to exchange stripping and heavy pick-up. In the reaction B^{11}(d, n)C^{12}, for example, the particle b is B^{10}. The graph in fig. 1(d) resembles the production and disintegration of a compound nucleus, but actually the pattern is somewhat more involved. The compound nucleus corresponds to complex poles lying in the unphysical sheet. In the physical sheet, on the other hand, the compound nucleus corresponds to involved Feynman

graphs the singularities of which are branch points rather than poles. In this context it should be emphasized that the poles of graphs 1(a)—1(d) lie on the real axis and correspond to such states of the nuclei b from which the decay with nuclear particle emission is impossible (though β-decay or radiative transitions are not ruled out). In this sense graph 1(d) corresponds to a direct reaction which may be termed a quasi-compound process. Graphs 1(a)—1(d) exhaust all pole terms of the amplitudes of direct reactions of the type (1). Several important peculiarities of direct processes of the type (1) follow directly from eq. (14) corresponding to these graphs.

For the usual stripping reaction (fig. 1(a)) we have from energy and momentum conservation

$$p_b^2 - 2m_b E_b = q^2 + 2m_b[\mu_{yB}\varepsilon_{Ab}^B + (1-\mu_{yB})\varepsilon_{yb}^x + (\mu_{yB}-\mu_{xA})E]. \tag{15}$$

Here

$$\varepsilon_{\beta\gamma}^{\alpha} = m_\beta + m_\gamma - m_\alpha \tag{16}$$

is the binding energy of β and γ in the nucleus α, and $\mu_{\alpha\beta}$ is given by

$$\mu_{\alpha\beta} = m_{\alpha\beta}/m_\alpha. \tag{17}$$

If $m_{\alpha\beta} \approx m_\alpha$, eq. (15) turns into a simpler relation

$$p_b^2 - 2m_b E_b \approx q^2 + 2m_b \varepsilon_{Ab}^B. \tag{18}$$

From eqs. (15) and (18) it is clear that the stripping reaction amplitude has a pole for the unphysical values of the variable $q^2 (q^2 < 0)$. Hence it follows that the amplitude reaches a maximum at the smallest physical q^2, which happens when the particles y are emitted in the direction of the incident particles x.

In the pick-up reaction (graph 1(b)) there is also a pole when the values of q^2 are unphysical:

$$q^2 = -2m_b[\mu_{yB}\varepsilon_{Bb}^A + (1-\mu_{yB})\varepsilon_{xb}^y + (\mu_{xA}-\mu_{yB})E]. \tag{19}$$

The closest proximity to the pole is attained at the smallest physical q^2 and the angular distribution is peaked forward.

In exchange stripping and heavy pick-up reactions (graph 1(c)) a pole arises when the values of the variable p^2 are unphysical:

$$p^2 = -2m_b[(1-\mu_{By})\varepsilon_{xb}^B + \mu_{By}\varepsilon_{yb}^A + (\mu_{xA}-\mu_{By})E]. \tag{20}$$

If m_A, $m_B \ll m_x, m_y$, then one has $\mu_{By} \ll 1$, $\mu_{xA} \approx 1$ and

$$p^2 = -2m_b E(E + \varepsilon_{xb}^B). \tag{21}$$

From eqs. (20) and (21) it follows that exchange stripping and heavy pick-up must bulk largest in exothermal reactions when E is small. Clearly, angular distribution will be peaked backward in this case.

For a quasi-compound process (graph 1b) there is a pole when the values of E are negative:

$$E = -\varepsilon_{xA}^b. \tag{22}$$

Hence it follows that the angular distribution in the quasi-compound process is isotropic. It is difficult therefore to distinguish the contribution of the quasi-compound process from the compound nucleus reactions.

The above inferences would be accurate if the amplitude $M_{if}(q^2, E)$ had no other singularities than a pole corresponding to a particle (in this case the numerator of eq. (14), being the residue of an analytical function, would be a constant). If there are other singularities, but we still write the amplitude in the form (14) the numerator of this formula will no longer be a constant, but in fact a slowly varying function of the variables q^2 and E, provided other singularities are situated much farther from the limit of the physical region than the pole in question. Otherwise the change of the numerator in eq. (14) as q^2 and E vary in the physical region may prove to be at least as essential as the change of the denominator. It should be emphasized that singularities on sheets other than the physical one are of importance (for example, close to the pole corresponding to the level of the compound nucleus the amplitude of the reaction is a sensitive function of E though singularities on the physical sheet can lie far from the region of values of E under consideration). Since the nucleus possesses a radius R the point $|q^2| = 1/R^2$ stands out physically. In terms of dispersion relation theory this must indicate that the amplitude of the process has a singu larity in the above region of the variable q^2. Yet it is rather difficult to point out the Feynman graph leading to this singularity. This can be done only for a deuteron while the sizes of heavier nuclei are probably determined by the singularities with respect to the variable q^2 lying on the unphysical sheet†. This last proposition is given here as a hypothesis essential mainly for writing dispersion relations in q^2 on the basis of the graphs considered in subsect. 2.3. In considering pole graphs, on the other hand, it is sufficient to bear in mind that, firstly, a singularity determined by the sizes of the nucleus is not a pole on the physical sheet, and secondly, that the numerator of eq. (14) should be regarded as a function of qR. The above situation corresponds to the Butler theory. Thus, the latter corresponds to the pole graphs 1(a) and 1(b).

Eq. (14) can conveniently be modified by introducing the vertex parts Γ averaged over the spin variable s_b. Thus, for graph 1(a) we shall introduce the notations

$$\overline{M_{ib} M_{bf}^{\dagger}} \equiv \frac{\pi}{m_b} \Gamma_{by}^{x}(qR_x, s_x, s_y) \Gamma_{B}^{Ab}(qR_B, s_A, s_B). \tag{23}$$

The superscripts of Γ designate the variables of the particles entering the vertex and the subscripts the particles issuing from it. In eq. (23), R_x and R_B are the effective radii of the vertices, and s_A, s_B, s_x and s_y are the spin variables of the particles A, B, x and y. In the new notations eq. (14) for graph 1(a) assumes the form

$$M_{if} = 2\pi \frac{\Gamma_{B}^{Ab} \Gamma_{by}^{x}}{q^2 + \kappa_b^2}, \tag{24}$$

† See *Note added in proof* at the end of this article.

where the quantity κ_b^2 is determined by eq. (15). The differential cross section will be of the form

$$\frac{d\sigma}{d\Omega_y} = m_{xA} m_{yB} \frac{(2I_B+1)(2I_y+1)}{(2I_A+1)(2I_x+1)} \frac{p_y}{p_x} \frac{\overline{(\Gamma_{Ab}^B)^2}\,\overline{(\Gamma_{by}^x)^2}}{(q^2+\kappa_b^2)^2}. \tag{25}$$

Here we use the notation

$$\overline{(\Gamma_{b\beta}^{\alpha})^2} = \overline{(\Gamma_{\alpha}^{b\beta})^2} = \sum_{s_\alpha s_\beta} |\Gamma_{b\beta}^{\alpha}|^2, \tag{26}$$

where by definition $\Gamma_{\beta\gamma}^{\alpha} = (\Gamma_{\alpha}^{\beta\gamma})^*$.

In eq. (25), $d\Omega_y$ is an element of solid angle in the space of the momenta of the particles y. The values of $[\overline{(\Gamma_{b\beta}^{\alpha})^2}]^{\frac{1}{2}}$ at the pole (i.e., at $q^2 = -\kappa_b{}^2$) shall be referred to as the reduced vertex parts and designated by $\gamma_{b\beta}^{\alpha}$:

$$\gamma_{b\beta}^{\alpha} = [\overline{(\Gamma_{b\beta}^{\alpha})^2}]_{q^2=-\kappa_b{}^2}^{\frac{1}{2}}. \tag{27}$$

The reduced vertex part γ_{Ab}^{B} in deuteron stripping and pick-up reactions (b = p, n) are expressed through the reduced width of the reaction, and the reduced vertex part γ_{pn}^{d} through the normalizing factor of the internal wave function of the deuteron. Parametrization of direct process theory becomes uniform due to the introduction of the reduced vertex parts. It is essential that the cross sections for different processes can contain the same reduced vertex parts (for example, the same reduced vertex part γ_{Ap}^{B} enters into the cross sections for the reactions A(d, n)B and A(α, t)B). Thus, there arises a possibility of establishing a quantitative connection between direct nuclear reactions of different types, though it should be noted that this programme is not easy to realize since the pole mechanism of direct processes is not the only one and sometimes not even the chief one (see subsect. 2.3). In those cases when the contribution of the pole graph to the amplitude of the reaction predominates, the reduced vertex parts can be extrapolated from experimental data in accordance with eq. (25)†. In eq. (25) summation is performed over the spin variables of the outgoing particles y. It can readily be seen, however, that in pole approximation the polarization of the particles y will be equal to zero if the beam of particles x and the target nucleus A are not polarized, and the polarization of the residual nucleus B is not registered in experiment. This result lends itself to simple physical interpretation. It is clear from eq. (25) that the entire process can be represented as an aggregate of two independent processes determined by each vertex.

† Preliminarily, it is necessary to "weaken" the dependence of the vertex parts on qR. Experiment shows that $d\sigma/d\Omega_y$ should be divided by $[j_{l_B}(qR_B)/j_{l_x}(qR_x)]^2$ for this purpose. Orders of the spherical Bessel functions l_B and l_x as well as the radii R_B and R_x are selected so as to flatten the angular distribution curve, after which extrapolation to the unphysical region can be performed using eq. (25). The requirement that R_B and R_x should be close to the radii of the nuclei B and x may serve as a clue in the choice of these quantities. The numbers l_B and l_x can be interpreted as orbital momenta of the particle b in the nuclei B and x. It will be emphasized that this interpretation is essential for finding the momenta and parities of states of the nucleus B, while for the extrapolation proper it is rather a clue in the choice of the flattening factor.

One of these vertices corresponds to the decay of a non-polarized particle. For the decay products therefore we have the correlation of polarizations, and summation over the spin variable of one of these particles (b) cancels the polarization of the other particle (y or B).

It should also be noted that the interference of different pole graphs should as a rule have a small effect since the poles corresponding to the interfreing graphs lie in the non-coinciding regions of the change of variables (with the exception of the interference of graphs 1(c) and 1(d)).

2.2. INTERACTION IN THE INITIAL AND FINAL STATES

The interaction in the initial and final states corresponds, in unitarity relation, to the terms corresponding to the transitions

$$(\mathrm{i} \to n) = (\mathrm{A}+\mathrm{x} \to \mathrm{A}'+\mathrm{x}'), \quad (n \to \mathrm{f}) = (\mathrm{A}'+\mathrm{x}' \to \mathrm{B}+\mathrm{y}),$$
$$(\mathrm{i} \to n) = (\mathrm{A}+\mathrm{x} \to \mathrm{B}'+\mathrm{y}'), \quad (n \to \mathrm{f}) = (\mathrm{B}'+\mathrm{y}' \to \mathrm{B}+\mathrm{y}).$$

The graphs corresponding to these transitions are represented in figs. 2(a) and 2(b). In the first case we have the scattering of the particle x on the nucleus A followed by a

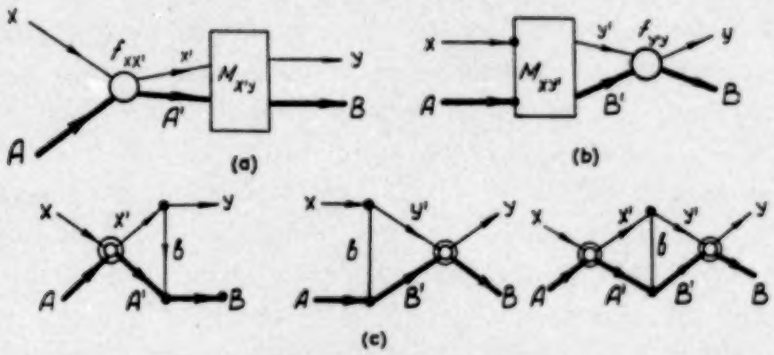

Fig. 2. General graphs for estimating the interactions in (a) the initial and (b) the final states. Special cases, taking into account interactions in the initial and final states for the simplest (pole) mechanism of the reaction, are shown in fig. 2(c).

nuclear reaction. In the second case (2b) the first transition is a nuclear reaction with the subsequent scattering of the particle y on the nucleus B. In both cases there are two virtual particles in intermediate states. Integration over the momenta and energy of the intermediate particles leads to the formula

$$A_{xy} = \frac{p_x}{4\pi}\int f^*_{x'x} M_{x'y}\, d\Omega_{x'} + \frac{p_y}{4\pi}\int M^*_{y'x} f_{y'y}\, d\Omega_{y'}, \tag{28}$$

where $A_{xy} \equiv A_{if}$, $M_{xy} \equiv M_{if}$, while $f_{x'x}$ and $f_{y'y}$ are the scattering amplitudes

$$f_{x'x} = \frac{m_{xA}}{2\pi} M_{x'x}, \qquad f_{y'y} = \frac{m_{yB}}{2\pi} M_{y'y}, \tag{29}$$

and

$$p_x = \sqrt{2m_{xA}E}, \qquad p_y = \sqrt{2m_{yB}(E+Q)}, \tag{30}$$

while $d\Omega_{x'}$ and $d\Omega_{y'}$ are the solid angles in the space of momenta of the intermediate particles x′ and y′. The integral in eq. (28) incorporates summation over the spins of the intermediate particles. If the non-elastic process $A+x \leftrightarrow B+y$ makes a small contribution to the scattering amplitudes $f_{x'x}$ and $f_{y'y}$ so that these can be treated as independent quantities, the following relation holds:

$$\int f^*_{x'x} M_{x'x} d\Omega_{x'} = \int f_{xx'} M^*_{yx'} d\Omega_{x'} \tag{28a}$$

(under the assumption made this equation is a corollary of the interchangeability of the matrices T and $T^\dagger$ in eq. (9)).

To restore the entire amplitude by its absorptive part (28) we must know the location of the branch points of the amplitude $M_{xy}(E)$ with regard to the variable E. We shall assume that these branch points are determined by the simplest Feynman graphs represented in fig. 2c. The first of them gives a branch point at $E=0$, the second at $E=-Q$ and the third corresponds to two branch points $E=0$ and $E=-Q$. Hence it follows that at $Q<0$ the wanted amplitude is analytical in the plane of the complex variable E with a cut along the real axis from 0 to ∞. If $Q>0$, the initial point of the cut is $E=-Q$. Starting from this fact we arrive at the following dispersion relations in the variable E:

$$M_{xy}(E) = M^0_{xy}(E) + \frac{1}{\pi}\int_{E_0}^{\infty} \frac{A_{xy}(E')}{E'-E-i\eta}\, dE'. \tag{31}$$

Here $M^0_{xy}(E)$ denotes the sum of all pole terms, and

$$E_0 = \begin{cases} 0, & Q<0, \\ -Q, & Q>0. \end{cases} \tag{32}$$

Eq. (31) is an integral equation for $M_{xy}(E)$, the kernel of which is expressed through the scattering amplitudes $f_{x'x}$ and $f_{y'y}$. These can be taken from experiment or calculated on the basis of an optical model. Omnès [2]) suggested some accurate solutions for equations of the type (30). Using the iterations of eq. (30) we can establish the connection of this equation with the distorted wave method (DWM) usually employed in the theory of direct nuclear reactions. The zero-order iteration

$$M_{xy} = M^0_{xy} \tag{33}$$

leads to the Butler theory. The first-order iteration gives the terms corresponding to the DWM:

$$\begin{aligned} M^{(1)}_{xy} = M^0_{xy} &+ \frac{1}{4\pi^2}\int_{E_0}^{\infty}\int \frac{dE'\, d\Omega_{x'}}{E'-E-i\eta}\, p_x(E') f_{xx'}(E') M^0_{x'y}(E') \\ &+ \frac{1}{4\pi^2}\int_{E_0}^{\infty}\int \frac{dE'\, d\Omega_{y'}}{E'-E-i\eta}\, p_y(E') f_{y'y}(E') M^0_{xy'}(E'). \end{aligned} \tag{34}$$

To obtain eq. (34) the fact that the pole term M^0_{xy} is real was taken into account and

eq. (28a) used. The amplitude of the processes in the DWM can be represented as

$$M_{xy}(\mathrm{DWM}) = \int \psi_y^*(\boldsymbol{p}_y, \boldsymbol{p}_y') M^0_{x'y'}(\boldsymbol{p}_x', \boldsymbol{p}_y') \psi_x(\boldsymbol{p}_x, \boldsymbol{p}_x') \mathrm{d}^3\boldsymbol{p}_x' \mathrm{d}^3\boldsymbol{p}_y' \tag{35}$$

where ψ_x and ψ_y are the wave functions of the particles x and y. The identity of eq. (34) and the corresponding terms (35) can easily be established if we take into account that

$$\psi_x = \delta(\boldsymbol{p}_x - \boldsymbol{p}_x') + \frac{1}{2\pi^2} \frac{f_{xx'}(\boldsymbol{p}_x, \boldsymbol{p}_x')}{p_x'^2 - p_x^2 - i\eta}, \tag{36}$$

$$\psi_y = \delta(\boldsymbol{p}_y - \boldsymbol{p}_y') + \frac{1}{2\pi^2} \frac{f^*_{yy'}(\boldsymbol{p}_y, \boldsymbol{p}_y')}{p_y'^2 - p_y^2 + i\eta}. \tag{36a}$$

Apart from the terms of (34) the amplitude of eq. (35) contains a term obtained from eq. (31) as a result of second order iteration and incorporating the product of the scattering amplitudes $f_{xx'}$ and $f_{y'y}$. There arise, however, other terms containing the products of the same amplitudes $f_{xx'} f_{x'x''}$ and $f_{y'y''} f_{y''y}$, and corresponding, therefore, to the "double scattering" of the particles x and y on the nuclei A and B. Since there are no such terms in (35) it follows from the analysis at hand that taking into account the product $f_{xx'} f_{y'y}$ in the DWM approximation is, in general, in excess of its accuracy. The degree of accuracy of the DWM can be estimated by comparing the numerical solution of eq. (31) and the amplitude (35). Here we shall confine ourselves to a rough (and probably too rigid) condition for the rapid convergence of the iteration procedure. The following inequality will be this condition:

$$\frac{\bar{k}|\bar{f}|}{4\pi^2} \ll 1 \tag{37}$$

where $\bar{k}$ and $\bar{f}$ are certain effective values of the wave number and the scattering amplitude responsible for the main contribution to the integrals of eq. (31) and (34). After expressing $|\bar{f}|$ through the scattering cross section $\bar{\sigma}_s$ we have the inequality

$$\frac{\bar{k}\sqrt{\bar{\sigma}_s}}{4\pi^2} \ll 1. \tag{38}$$

If we put $\bar{\sigma}_s \approx \pi R^2$ as an estimate in the case of neutrons, the condition (38) leads to

$$\frac{\bar{k}R}{4\pi^{\frac{1}{2}}} \ll 1, \tag{38a}$$

which is equivalent to the long wave approximation. Eqs. (31) and (28) determine the conditions under which taking into account the interactions in the initial and final states does not distort appreciably the angular distribution of the outgoing particles. It does not, in fact, in those cases when the scattering amplitudes $f_{xx'}$ and $f_{y'y}$ are

δ-like functions of the scattering angles, i.e., most of the scattering angles are small. A not dissimilar situation exists for nucleons upwards of 10 MeV.

Out of all observed quantities the polarization of outgoing particles is most sensitive to the estimation of the interaction in the initial and final states. Nor is the interaction the only source of polarization in direct processes. An essential contribution to the polarization of outgoing particles may come from more complex graphs to be considered in subsect. 2.3.

2.3. TRIANGULAR SINGULARITIES

The pole mechanism of direct processes discussed in the preceding sections may predominate if the amplitude $M_{xy}(q^2)$ has no singularities for the variable q^2 (apart from the poles) lying closer to the physical region or lying not far from the poles. Actually this condition is by no means fulfilled in all cases, and the direct process mechanism can therefore differ essentially from the pole mechanism, and in particular, from the Butler mechanism. In this section we shall consider some Feynman graphs corresponding to the branch points for q^2. We shall confine ourselves to graphs with three internal lines. The general type of these graphs is represented in fig. 3.

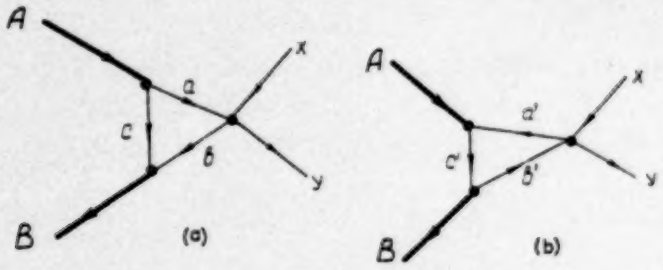

Fig. 3. Simplest triangle graphs for the reactions A(x, y)B.

For instance, the direct process corresponding to graph 3(a) reduces to this mechanism: the nucleus A emits the particle a colliding with the particle x. The reaction

$$a+x \rightarrow y+b \tag{39}$$

gives rise to the particle b which is captured by the nucleus c with the production of the final nucleus B. In this graph the three-ray vertices are functions of $q' R$ (just as in case of pole graphs), where q' is the momentum transferred in the vertex, and the four-ray vertex is the amplitude of the reaction (39) also depending, in general, on q^2. The above singularities of the graphs of fig. 3 are not connected with the dependence of the vertices on q^2 and are determined exclusively by the masses of the particles A, B, x, y, a, b and c. The branch point closest to the physical region and corresponding to the graph of fig. 3 is found according to the general rules set down by Landau [3]) and developed by Okun and Rudik [4]). In the case at hand these rules lead to the equation

$$\tfrac{1}{2}q^2 = -(m_y-m_x)[Q'-\mu_{yB}Q+(\mu_{yB}-\mu_{xA})E]-m_a m_b(\sqrt{\varepsilon^A_{ac}/m_{ac}}+\sqrt{\varepsilon^B_{bc}/m_{bc}})^2, \tag{40}$$

where

$$Q' = m_a + m_x - m_b - m_y. \tag{41}$$

A similar formula for graphs of the type 3(b) is obtained from (40) by the substitutions $x \leftrightarrow A$ and $y \leftrightarrow B$.

The singularity determined by eq. (40) belongs to the class of "anomalous thresholds", first considered by Karplus, Sommerfield and Wichman [5]). These singularities appear if certain inequalities are fulfilled for the vertices; for the vertex $A \to a+c$, for example, these inequalities are

$$m_A < m_a + m_c, \tag{42}$$

$$m_A^2 > m_a^2 + m_c^2. \tag{42a}$$

This is precisely what happens in nuclear reactions. The branch points of (40) appear because the energy-momentum relation for intermediate particles, for the values of q^2 given by eq. (40), proves to be the same as that for free particles. Since the real decay $A \to a+c$ is impossible in this case because of the inequality (42), the singularity (40) always lies in the region of unphysical (negative) values of q^2.

TABLE 1

Singularities of graphs 3(a) with different virtual particles a and b for the reaction $Be^9(\alpha, t)B^{10}$

a		n	p	d	t
b	p	d	p+p	He^3	α
(MeV · amu)	23.6 (pole)	62.8	299	467	432

Starting from the above, let us now turn to some specific nuclear reactions. Table 1 lists the values of $-q^2$ for the reaction $Be^9(\alpha, t)B^{10}$ calculated by eq. (40) for $E=27.7$ MeV. The first figure of the table is the value of $-q^2$ at the pole (graph 1(a), eq. (15), b being a proton). The other figures of the table are the branch points of graph 3(a) for different virtual particles a, b and c. All data listed refer to the ground states of the nuclei A, B and C (the singularities corresponding to the excited states of the virtual nucleus c exist for larger values of $-q^2$). It is clear from table 1 that the branch point closest to the pole is determined by the graph in which a is a neutron, b a deuteron and c the Be^8 nucleus. The proximity of the branch point to the pole indicates that the reaction $Be^9(\alpha, t)B^{10}$ is certainly not the Butler mechanism pure and simple: the contribution from graph 3(a) to the amplitude of the process is comparable with the pole graph. Actually, the limit of the physical region lies at $q^2 = 16.8$ MeV · amu and consequently the ratio of the square of the pole amplitude to the interference term appearing due to graph 3(a) may be of the order of unity, since the part of the amplitude corresponding to this graph diminishes roughly as $1/q^2+q_0^2$, where $-q_0^2$ is a singularity determined by eq. (40). A similar situation holds for the deuteron stripping

reaction $Be^9(d, n)B^{10}$. In this case the amplitude of the reaction has a pole at $q^2 = -13.2$ MeV · amu and a branch point corresponding to graph 3(a) with a = n, b = d and c = Be^8 at $q^2 = -48.4$ MeV · amu. Thus, there is no reason to expect that the Butler mechanism predominates in the reaction $Be^9(d, n)B^{10}$ either. Against this background the result obtained by Vlasov *et al.* [6]) becomes quite comprehensible qualitatively. They showed that the ratio of the reduced widths of the reactions corresponding to the production of the nucleus B^{10} in different states proves different in the reactions $Be^9(\alpha, t)B^{10}$ and $Be^9(d, n)B^{10}$.

In a number of cases the closet branch points lie much farther from the pole than in the reactions $Be^9(\alpha, t)B^{10}$ and $Be^9(d, n)B^{10}$. For example in the reaction $C^{12}(d, p)C^{13}$ the pole value $q^2 = -12$ MeV · amu while the closest branch point (graph 3(a), a being a proton, b a deuteron and c the B^{11} nucleus) lies at $q^2 = -200$ MeV · amu. Yet even in this case the final judgement on the relative quantities of the contribution of the pole graph and graph 3(a) is possible only if there are data on reduced vertex parts and the amplitude of the reaction (39). Thus knowledge of the amplitudes of nuclear reactions with nucleon-deficient systems is of primary importance for understanding the mechanism of direct processes in complex nuclei.

An essential factor in studying the direct process mechanism is the measurement of the polarization of the reaction products. Unlike the pole mechanism, the polarization of the particles y in cases like that of graph 3 will be determined not only by interaction in the initial and final states but also by the polarization arising in the reaction (39). It should be emphasized that the angular distribution of outgoing particles is a less sensitive criterion of the direct process mechanism.

3. On the Reactions A+x → B+y+z

The simplest graphs for the reactions (2) and (1) are pole graphs. These, for the processes (x, dx), (π^-, 2n) and (K^-, Λ^0n), are represented in figs. 4(a) and 4(b).

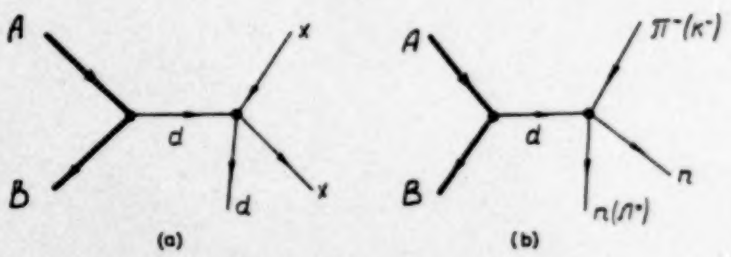

Fig. 4(a). Pole graph of the reaction (x, xd). (b) Pole graph of the reactions (π^-, 2n) and (K^-, Λ^0n).

Some experimental data available at present testify in favour of the pole mechanism though it cannot be ruled out on the basis of these data that other graphs may also be essential. For example, in the work of Ozaki *et al.*[7]) it is found that neutrons formed in the reaction (π^-, 2n) fly out mostly in opposite directions. This result corresponds to the pole graph 4(b) though it can also be obtained from the graph of fig. 5

incorporating the emission by the nucleus A of a neutron and proton in a singlet state. Clearly, the study of the mechanism of the reaction calls for comparing data on different processes. If the contribution of pole graphs predominates there must be quantitative agreement between the cross sections for the processes corresponding to graphs 4(a), 4(b) and 4(c) for the same reduced vertex parts γ^{A}_{Bd}. In this context it

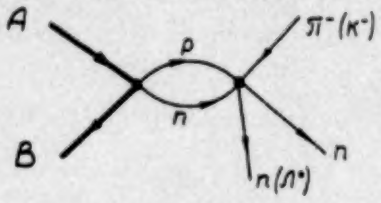

Fig. 5. Simplest non-pole graph of the reactions (π^-, 2n) and (K^-, Λ^0n).

should be noted that the "knock-out" of deuterons from nuclei does not seem surprising if viewed in terms of dispersion theory since there are no grounds to suppose that the reduced vertex parts γ^{A}_{Bd} are equal to zero. At the same time the quantitative description of this process requires knowledge of at least the scattering cross sections of particles on a free deuteron in a broad interval of energies and reduced vertex parts γ^{A}_{Bd}, which in turn calls for comparing data (very scarce so far) on other processes.

What has been said above concerning the knock out of deuterons applies to other knock-out reactions, i.e., to processes like (x, xy). This makes for a uniform approach to the study of the mechanism of knock-out clusters from nuclei of different types. We shall not give here any formulae for the cross sections of processes of the type (2) in pole approximation, since these formulae can be found in the well-known work by Chew and Low [8]).

In case of the reactions (2) taking account of graphs more involved than those of figs. 4 and 5 leads in general to several difficulties. These arise chiefly because five independent kinematic variables correspond to each graph with five external lines, and the position of singularities with respect to each of these variables depends on the values of the others. Nevertheless, the interaction in the initial and final states can

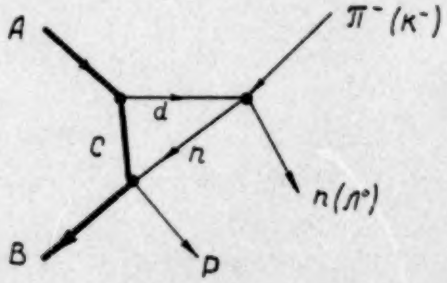

Fig. 6. Simplest graph of the reactions (π^-, pn) and (K^-, Λ^0p).

be evaluated for many processes at non-relativistic energies, as was done in sect. 2. It is of interest in particular to consider the reactions (π^-, pn) and (K^-, Λ^0p) with

the aid of this method. The simplest graph for these reactions is represented in fig. 6. The integral equation (31) in which the scattering amplitude $f_{\gamma'\gamma}$ should be replaced (according to eq. (29)) by the amplitude M_{np} of the reaction c(n, p)B holds for the amplitude of the process corresponding to graph 6. More experimental data are required, however, than those available at present for the fulfilment of this programme.

4. Conclusive Remarks

The method under consideration has several advantages: a) it is graphic, b) it does not involve perturbation theory and c) it leads to formulae transparent in their physical content and connecting the amplitudes of different reactions. The latter point entails an experimental programme for checking the initial concept (the possibility of describing direct processes in terms of Feynman graphs). The construction is in fact a phenomenological theory of direct processes similar to the Breit-Wigner theory of the compound nucleus. The two are in fact twins since they deal with the singularities of different sheets of the same analytical function. Just as the Breit-Wigner theory of the compound nucleus the method under consideration lays no claim to the calculation of the reduced widths of nuclear reactions, but points to a uniform procedure for deriving these widths from experimental data and establishing quantitative connections between nuclear reactions that at first glance might seem to have nothing in common.

The author expresses gratitude to L. D. Landau and K. A. Ter-Martirosyan for valuable suggextions.

Note added in proof: As was mentioned by V. N. Gribov (private communication) the singularity corresponding to the nuclear radius may be due to the final radius of nucleon-nucleon forces. It is possible therefore that complex Feynman graphs with internal π-meson lines correspond to this singularity. This viewpoint seems to be favoured by the fact that, unlike the case of deuteron, the nuclear problem of three bodies has no solution in the approximation of inter-nucleon δ-forces.

References

1) R. D. Amado, Phys. Rev. Letters **2** (1959) 399
2) R. Omnès, Nuovo Cim. **8** (1958) 316
3) L. D. Landau, Nuclear Physics **13** (1959) 181
4) L. B. Okun and A. P. Rudik, Nuclear Physics **15** (1960) 261
5) R. Karplus, C. M. Sommerfield and E. H. Wichman, **111** (1958) 1187; **114** (1959) 376
6) N. A. Vlasov *et al.*, JETP **39** (1960) 1468
7) S. Ozaki *et al.*, Phys. Rev. Letters **4** (1960) 533
8) G. F. Chew and F. E. Low, Phys. Rev. **113** (1959) 1640

1.C

Nuclear Physics **28** (1961) 258—269; © *North-Holland Publishing Co., Amsterdam*

Not to be reproduced by photoprint or microfilm without written permission from the publisher

A STUDY OF SOME APPROXIMATIONS OF THE PAIRING FORCE

J. HÖGAASEN-FELDMAN

Laboratoire de Physique Nucléaire, Orsay, France

and

Institute for Theoretical Physics, University of Copenhagen, Denmark

Received 24 April 1961

Abstract: The quasi-particle and the boson approximation are used in the study of the first 0+ excited state of the pairing force: a special case is chosen for its simplicity, which allows us to study quantitatively the validity of these approximations. This validity shows a strong dependence with respect to the coupling constant and to the degeneracy of the shell-model levels.

1. Introduction

The pairing force, which was first introduced by Racah in 1943 as a convenient mathematical tool for the classification of the atomic levels, has been shown in the last few years to be a very good approximation of the short-range part of the nuclear forces for several problems of nuclear physics. Both these reasons, physical interest and mathematical simplicity, led us to study the quasi-particle approximation which is generally used to account for the pairing force [1]), and the boson approximation [2]) which is used for more general problems (especially for the so-called collective vibrations) but which will be shown to be a logical extension of the first one †.

We shall limit ourselves to the study of the first 0+ excited state. The Hamiltonian of a system of nucleons interacting in an average potential by a pairing force is

$$H = \sum_{jm} \varepsilon_j a^\dagger_{jm} a_{jm} + \tfrac{1}{4} G \sum_{\substack{jm \\ j'm'}} (-)^{j-m} (-)^{j'-m'} a^\dagger_{jm} a^\dagger_{j-m} a_{j'-m'} a_{j'm'}, \qquad (1)$$

where j labels a shell. We get rid of the magnetic quantum numbers m by defining the following operators:

$$A_j^\dagger = \frac{1}{\sqrt{\Omega_j}} \sum_{m>0} (-)^{j-m} a^\dagger_{jm} a^\dagger_{j-m}, \qquad A_j = \frac{1}{\sqrt{\Omega_j}} \sum_{m>0} (-)^{j-m} a_{j-m} a_{jm},$$
$$N_j = \sum_m a^\dagger_{jm} a_{jm}, \qquad (2)$$

† See also a similar study by P. W. Anderson [5]), made in the frame of the random-phase approximation in superconductivity.

where Ω_j is the half-degeneracy of the j-shell. These operators obey the following commutation relations:

$$[A_i, A_j^\dagger] = \delta_{ij}\left(1-\frac{N_i}{\Omega_i}\right), \tag{3}$$

$$[N_i, A_j^\dagger] = \delta_{ij} 2A_i^\dagger. \tag{4}$$

Thus one has

$$H = \sum_i \varepsilon_i N_i + G\sum_{ij}\sqrt{\Omega_i}\sqrt{\Omega_j}A_i^\dagger A_j. \tag{1'}$$

Exact solutions are known in two cases:

I. *The degenerate case.* As is well known [3]), the ground state is proportional to $(\sum_i \sqrt{\Omega_i} A_i^\dagger)^{\frac{1}{2}n}|0\rangle$. The first excited 0+ states (seniority 2) are proportional to $(\sum_i \sqrt{\Omega_i} A_i^\dagger)^{\frac{1}{2}n-1}(\sum c_i \sqrt{\Omega_i} A_i^\dagger)|0\rangle$ with $\sum_i c_i\Omega_i = 0$. If p is the number of shells, there are $p-1$ such states, all degenerate, the energy of which is $W = |G|\sum_i \Omega_i$.

II. *The two-particle case.* Looking for an operator $\Gamma^\dagger = \sum_i c_i A_i^\dagger$ such that $H\Gamma^\dagger|0\rangle = W\Gamma^\dagger|0\rangle$, we are led to write

$$[H, \Gamma^\dagger] = \sum_i c_i 2\varepsilon_i A_i^\dagger + G\sum_j \sqrt{\Omega_j} A_j^\dagger \sum_i c_i\sqrt{\Omega_i}\left(1-\frac{N_i}{\Omega_i}\right).$$

The operators N_i acting on the vacuum give no contribution and we find the following eigenvalue equation:

$$\frac{1}{G} = \sum_i \frac{\Omega_i}{W-2\varepsilon_i}, \tag{5}$$

which may be solved graphically. This suggests the following approximation: if we have few particles in rather large shells, we may forget about the Pauli principle, in other words neglect the term N_i/Ω_i in eq. (3). In this approximation, pairs of fermions are just bosons and the Hamiltonian (1') describes a system of bosons in a one-body potential. This problem admits solutions given by eq. (5). However, when we have too many particles, we have first to perform a canonical transformation in order to get a good approximation.

2. The Quasi-Particle and the Quasi-Boson Approximations

2.1 THE QUASI-PARTICLE SCHEME

We define quasi-particles by the Bogoliubov-Valatin transformation

$$\alpha_{jm}^\dagger = u_j a_{jm}^\dagger - v_j(-)^{j-m}a_{j-m}, \qquad u_j^2+v_j^2 = 1, \tag{6}$$

and, as in the case of particles, we define the following operators:

$$\mathscr{A}_j^\dagger = \frac{1}{\sqrt{\Omega_j}} \sum_{m>0} (-)^{j-m} \alpha_{jm}^\dagger \alpha_{j-m}^\dagger, \qquad \mathscr{A}_j = \frac{1}{\sqrt{\Omega_j}} \sum_{m>0} (-)^{j-m} \alpha_{j-m} \alpha_{jm},$$
$$\mathscr{N}_j = \sum_m \alpha_{jm}^\dagger \alpha_{jm}, \tag{7}$$

satisfying the commutator relations

$$[\mathscr{A}_i, \mathscr{A}_j^\dagger] = \delta_{ij}\left(1 - \frac{\mathscr{N}_i}{\Omega_i}\right), \tag{8}$$

$$[\mathscr{N}_i, \mathscr{A}_j^\dagger] = \delta_{ij} 2\mathscr{A}_i^\dagger. \tag{9}$$

We rewrite the pairing Hamiltonian (introducing a chemical potential λ) in terms of these new operators:

$$H = U + H_{11} + (H_{20} + H_{02}) + H_c + H_{res},$$
$$U = \sum_i (\varepsilon_i - \lambda) 2v_i^2 \Omega_i + G(\sum_i \Omega_i u_i v_i)^2,$$
$$H_{11} = \sum_i [(\varepsilon_i - \lambda)(u_i^2 - v_i^2) - 2G u_i v_i (\sum_j \Omega_j u_j v_j)] \mathscr{N}_i,$$
$$H_{20} + H_{02} = \sum_i [(\varepsilon_i - \lambda) 2u_i v_i \sqrt{\Omega_i} + G(\sum_j \Omega_j u_j v_j)\sqrt{\Omega_i}(u_i^2 - v_i^2)](\mathscr{A}_i^\dagger + \mathscr{A}_i), \tag{10}$$
$$H_c = G \sum_{ij} \sqrt{\Omega_i}\sqrt{\Omega_j}(u_i^2 \mathscr{A}_i^\dagger - v_i^2 \mathscr{A}_i)(u_j^2 \mathscr{A}_j - v_j^2 \mathscr{A}_j^\dagger),$$
$$H_{res} = G \sum_{ij} \sqrt{\Omega_j}(-u_i v_i)\{\mathscr{N}_i(u_j^2 \mathscr{A}_j - v_j^2 \mathscr{A}_j^\dagger) + (u_j^2 \mathscr{A}_j^\dagger - v_j^2 \mathscr{A}_j)\mathscr{N}_i\}$$
$$+ G \sum_{ij} u_i v_i u_j v_j \mathscr{N}_i \mathscr{N}_j.$$

The parameters u and v are chosen in order to cancel $H_{20} + H_{02}$. The parameter λ is chosen so that the "vacuum" of the quasi-particle space, defined by $\alpha_i|\phi_0\rangle = 0$, will be an approximation for a system of n particles:

$$\langle \phi_0(\lambda)|N|\phi_0(\lambda)\rangle = n.$$

Consequently, we obtain the well-known equations

$$u_i^2 = \tfrac{1}{2}\left(1 + \frac{\varepsilon_i - \lambda}{E_i}\right), \qquad v_i^2 = \tfrac{1}{2}\left(1 - \frac{\varepsilon_i - \lambda}{E_i}\right), \tag{12}$$

$$\sum_i \frac{\Omega_i}{E_i} = -\frac{2}{G}, \tag{13a}$$

$$\sum_i \Omega_i \left(1 - \frac{\varepsilon_i - \lambda}{E_i}\right) = n \tag{13b}$$

$$E_i = \sqrt{\Delta^2 + (\varepsilon_i - \lambda)^2}, \qquad \Delta = -G\sum_i \Omega_i u_i v_i. \tag{14}$$

Now the Hamiltonian (10) describes a system of quasi-particles interacting in an average potential by means of a two-body force.

The quasi-particle approximation consists in keeping only the free quasi-particle Hamiltonian $H'_0 = U+H_{11}$. The 0+ excited states are $|\phi_i\rangle = \mathscr{A}_i^\dagger|\phi_0\rangle$, the energy of which is $W_i = 2E_i = 2\sqrt{\Delta^2+(\varepsilon_i-\lambda)^2}$. There are p of them, one more than the right value: this "spurious" state, the existence of which arises from the non-conservation of the number of particles, is mixed up with the others. In the limit where G is very large, we find the degenerate case, and the value $|G|\sum_i \Omega_i$ for the excited states, but we have still a spurious state.

2.2. THE QUASI-BOSON APPROXIMATION

From eq. (10) we see that H_{11} and H_c are of the order of magnitude $G\Omega$ (where Ω is the total degeneracy of the system), while terms of H_{res} are of the order of $G\sqrt{\Omega}$ or even 1 and, besides, include the $\mathscr{N}_i$ operators. If the quasi-particle scheme is a rather good approximation, the low lying states will have only a few quasi-particles. Also if Ω is large, a *consistent* approximation will be to keep only H_c for the interaction of the quasi-particles and neglect the Pauli principle for the pairs of quasi-particles, i.e., use the following approximate commutator rules instead of (8):

$$[\mathscr{A}_i, \mathscr{A}_j^\dagger] = \delta_{ij}. \tag{8'}$$

Now we are led again to a system of bosons with a one-body force. To find the canonical transformation which diagonalizes the Hamiltonian it is convenient to go to the "space" variables. We define

$$q_i = \tfrac{1}{2}\sqrt{2}(\mathscr{A}_i+\mathscr{A}_i^\dagger), \qquad p_i = -\tfrac{1}{2}i\sqrt{2}(\mathscr{A}_i-\mathscr{A}_i^\dagger). \tag{15}$$

Then we get

$$\begin{aligned} H_{11}+H_c &= \tfrac{1}{2}G\sum_i \Omega_i \frac{\varepsilon_i-\lambda}{E_i} + \tilde{H}(q_i, p_i), \\ \tilde{H}(q_i, p_i) &= \sum_i E_i\mathscr{N}_i + \tfrac{1}{2}G\left\{\left(\sum_i \sqrt{\Omega_i}\,\frac{\varepsilon_i-\lambda}{E_i}\,q_i\right)^2 + \left(\sum_i \sqrt{\Omega_i}\,p_i\right)^2\right\}. \end{aligned} \tag{16}$$

We are looking for

$$Q_j = \sum_i \lambda_{ji} q_i, \qquad P_j = \sum_i \mu_{ji} p_i, \tag{17}$$

so that

$$[Q_i, P_j] = i\delta_{ij}, \qquad [Q_i, \tilde{H}] = iB_iP_i, \qquad [P_i, \tilde{H}] = -iC_iQ_i. \tag{18}$$

The energies we are looking for are $W_i = \sqrt{B_iC_i}$.

By straightforward calculations one finds

$$\lambda_{ji} = -\frac{G\sqrt{\Omega_i}}{2E_i}\frac{4E_i^2\Lambda_j^{(1)}+2(\varepsilon_i-\lambda)B_j\Lambda_j^{(2)}}{4E_i^2-W_j^2}$$
$$\mu_{ji} = -G\sqrt{\Omega_i}\frac{C_j\Lambda_j^{(1)}+2(\varepsilon_i-\lambda)\Lambda_j^{(2)}}{4E_i^2-W_j^2}, \tag{19}$$

where $\Lambda_j^{(1)}$ and $\Lambda_j^{(2)}$ are two constants defined by the following equations:

$$\Lambda_j^{(1)} = \sum_i \lambda_{ji}\sqrt{\Omega_i}, \qquad \Lambda_j^{(2)} = \sum_i \mu_{ji}\sqrt{\Omega_i}\frac{\varepsilon_i-\lambda}{E_i}. \tag{20}$$

Inserting (19) into (20), we obtain the following equations for $\Lambda_j^{(1)}$ and $\Lambda_j^{(2)}$:

$$\left(1+G\sum_i \frac{\Omega_i 2E_i}{4E_i^2-W_j^2}\right)\Lambda_j^{(1)}+G\left(\sum_i \frac{\Omega_i(\varepsilon_i-\lambda)}{E_i(4E_i^2-W_j^2)}\right)B_j\Lambda_j^{(2)} = 0, \tag{21}$$
$$G\left(\sum_i \Omega_i \frac{\varepsilon_i-\lambda}{E_i(4E_i^2-W_j^2)}\right)C_j\Lambda_j^{(1)}+\left(1+G\sum_i \frac{2(\varepsilon_i-\lambda)^2}{E_i(4E_i^2-W_j^2)}\right)\Lambda_j^{(2)} = 0.$$

Defining

$$a_j = \sum_i \frac{\Omega_i}{2E_i(4E_i^2-W_j^2)}, \qquad b_j = \sum_i \frac{\Omega_i(\varepsilon_i-\lambda)}{E_i(4E_i^2-W_j^2)}, \tag{22}$$

and using (13a), we can write (21) in a simpler way, viz.,

$$W_j^2 a_j\Lambda_j^{(1)}+b_jB_j\Lambda_j^{(2)} = 0, \qquad C_jb_j\Lambda_j^{(1)}+(W_j^2-4\Delta^2)a_j\Lambda_j^{(2)} = 0. \tag{21'}$$

The condition of solvability of this equation gives the eigenvalue equation

$$W_j^2(W_j^2-4\Delta^2)a_j^2 = b_j^2W_j^2. \tag{23}$$

There are two cases to be considered.

1) $W_j \neq 0$

Let us put

$$y_j^2 = W_j^2-4\Delta^2. \tag{24}$$

Using (23) and (22) one finds

$$\sum_i \frac{\Omega_i}{E_i(y_j+2(\varepsilon_i-\lambda))} = 0. \tag{25}$$

If Δ and λ are known, these equations can be solved graphically. Let us notice the important fact that there are just $p-1$ solutions. This is the right number of our excited states. We shall see below that the whole spurious state has been taken up by the $W = 0$ solution. The case when the ε_i are symmetrical with

respect to the λ-value is of special interest: because of the symmetry, the $y = 0$ solution leads to the lowest eigenvalue $W = 2\Delta$: this is just the gap. From eq. (13b), we see that, in order to obtain this situation, we need two things: a symmetrical distribution of the shell model energy levels, and a number of particles which is just half the total degeneracy of the system †. In the limit where all the levels are degenerate, it is a half-filled shell. In sect. 3, we shall study the case of two levels. One can write (19) in thefollowing form:

$$\lambda_{ji} = \left[\frac{W_j^2\sqrt{\Omega_i}}{E_i(2(\varepsilon_i-\lambda)+y_j)} - y_j\frac{\sqrt{\Omega_i}}{E_i}\right]\frac{-G\Lambda_j^{(2)}}{2W_j}, \quad \mu_{ji} = \frac{\sqrt{\Omega_i}\,(-G\Lambda_j^{(2)})}{2(\varepsilon_i-\lambda)+y_j}; \quad (26)$$

$\Lambda_j^{(2)}$ is a normalisation constant so that $\sum_i \lambda_{ji}\mu_{ji} = 1$.

2) $W = 0$

This solution can occur only for $\Delta \neq 0$ and corresponds to $B = 0$. This extra degree of freedom which introduces a continuous spectrum clearly does not belong to our physical problem. In fact, it is easy to see that the wave function $Q_0|\phi_0\rangle$ describes a linear combination of the ground states of the neighbouring nuclei such that the average value of the number of particles is nevertheless equal to n. Eq. s(19) give

$$\lambda_i^0 = \Delta\frac{\sqrt{\Omega_i}}{E_i}, \qquad \mu_i^0 = K_0\sqrt{\Omega_i}\,\frac{\Delta^2 a_3+(\varepsilon_i-\lambda)b_3}{E_i^2}, \quad (27)$$

with

$$a_3 = \sum_i \frac{\Omega_i}{E_i^3}, \qquad b_3 = \sum_i \frac{\Omega_i(\varepsilon_i-\lambda)}{E_i^3}, \qquad K_0\Delta(\Delta^2 a_3^2+b_3^2) = 1.$$

The Hamiltonian can be rewritten as follows:

$$\tilde{H} = \tfrac{1}{2}C_0Q_0^2+\tfrac{1}{2}\sum_{j=1}^{p-1} W_j(P_j^2+Q_j^2). \quad (28)$$

The canonical transformation is given by formulas (17), (26), (27). Thus, including H_c in the Hamiltonian leads to the elimination of the spurious state. However, the number of particles is not yet a good quantum number, some terms in H_{res} are playing an important role in this respect.

2.3. THE AVERAGE NUMBER OF PARTICLES IN THE QUASI-BOSON APPROXIMATION

The Bogoliubov-Valatin transformation has been chosen so that the average number of particles in the quasi-particle vacuum has the correct value n:

$$\langle\phi_0|N|\phi_0\rangle = n.$$

† This is precisely the case in superconductivity.

This is not true any more for an excited state. If this excited state is built up with 2 quasi-particles from the j-shell, we have

$$\langle\phi_j|N|\phi_j\rangle = n+2\frac{\varepsilon_j-\lambda}{E_j}.$$

For G large, i.e. Δ large, the extra-term is small. But for $\Delta = 0$, it is just ± 2: the state ϕ_j describes a system with $n+2$ or $n-2$ particles.

In the quasi-boson approximation, let us consider the operators of creation and annihilation of the system of bosons which diagonalize the Hamiltonian

$$\Gamma_j^+ = \tfrac{1}{2}\sqrt{2}(Q_j+iP_j), \qquad \Gamma_j = \tfrac{1}{2}\sqrt{2}(Q_j-iP_j),$$

The number of particles in terms of $\mathscr{A}$ and $\mathscr{A}^\dagger$ operators is

$$N = \sum_i \frac{\varepsilon_i-\lambda}{E_i}\mathscr{N}_i + \Delta\sum_i \frac{\sqrt{\Omega_i}}{E_i}(\mathscr{A}_i^\dagger+\mathscr{A}_i). \tag{29}$$

The ground state is the vacuum of the new bosons: $\Gamma_j|\psi_0\rangle = 0$. The first excited states are $|\psi_j\rangle = \Gamma_j^+|\psi_0\rangle$, and by straightforward calculations (see Appendix 2) one gets

$$\begin{aligned}\langle\psi_0|N-n|\psi_0\rangle &= \sum_{ij}(\mu_{ji}^2+\lambda_{ji}^2)\frac{\varepsilon_i-\lambda}{2E_i} - \sum_i \frac{\varepsilon_i-\lambda}{E_i},\\ \langle\psi_j|N-n|\psi_j\rangle &= \langle\psi_0|N-n|\psi_0\rangle + \sum_i \frac{\varepsilon_i-\lambda}{E_i}(\mu_{ji}^2+\lambda_{ji}^2).\end{aligned} \tag{30}$$

As the $(\varepsilon_i-\lambda)$ have no definite signs, these quantities are rather small in general. One can see that they are identically 0 for the symmetrical case.

If we look at the limit of the degenerate case, we realize that, concerning the average number of particles, the approximation improves as the number of particles increases in the shell, and is best in the middle of the shell.

2.4. THE CASE OF THE COMPLETE SHELLS

As can be seen from eq. (13b), in this case and only in this case, $\Delta = 0$, when $|G|$ is smaller than a critical value $|G_c|$. Then the quasi-particles just define particles and holes, as usually. The eigenvalue equation is

$$\frac{1}{G} = \sum \frac{\Omega_n}{\omega-2(\varepsilon_n-\lambda)} - \frac{\Omega_m}{\omega-2(\varepsilon_m-\lambda)}, \tag{31}$$

where ε_n is above the Fermi surface and ε_m is under the Fermi surface. In this case, one boson creates two particles or two holes, and two bosons are necessary to get the right number of particles. Fig. 1 represents the solution of eq. (31). The energy of the first excited state is indicated by arrows. When $|G|$ increases

from 0 to $|G_c|$, the energy of the first excited state decreases, and is 0 when $G = G_c$. Then Δ becomes different from 0 and the quasi-particle scheme starts. This is an illustration of the general relation between the stability of the Hartree Fock solution and the boson approximation (4).

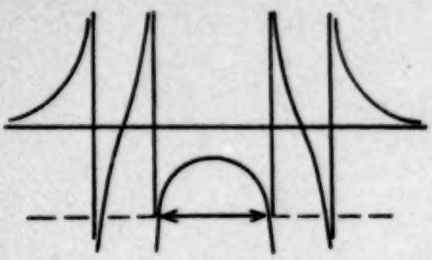

Fig. 1. The solution of eq. (31).

3. The Two-Shell Symmetrical Case

We use this case in order to compare the approximations studied in the last section with the actual solution. Let ε be the distance of the shells, $\pm\frac{1}{2}\varepsilon$ their energy and Ω the common degeneracy; we have $n = 2\Omega$. In the limit of $G = 0$, we have a complete shell, in the limit of $G = -\infty$, a half-filled shell.

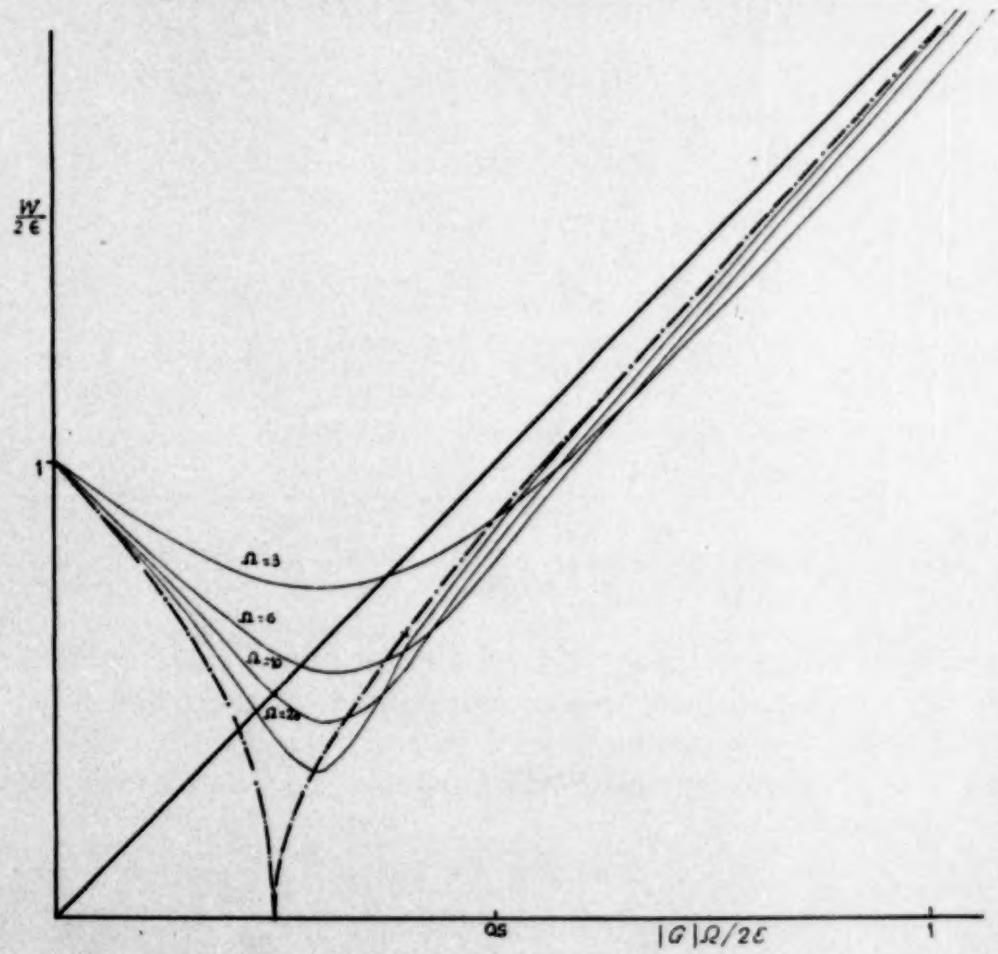

Fig. 2. $W/2\varepsilon$ as a function of $|G|\Omega/2\varepsilon$ for different values of Ω.

The quasi-particle approximation gives 2 degenerate excited states $2E_1 = 2E_2 = 2|G|\Omega$. The critical value G_c, for which $\Delta = 0$, is given by $|G_c|\Omega = \frac{1}{2}\varepsilon$. For $|G| < |G_c|$, the Boson approximation gives $W_b = 2\varepsilon(1-2|G|\Omega/2\varepsilon)^{\frac{1}{2}}$; for $|G| > |G_c|$, the quasi-Boson approximation removes the spurious state. One remains with a one-shell problem, the Hamiltonian of which is

$$H = 2|G|\Omega B^\dagger B - \frac{\varepsilon^2}{8|G|\Omega}(B^\dagger + B)^2, \text{ with } B^\dagger = \tfrac{1}{2}\sqrt{2}(\mathscr{A}_1^\dagger - \mathscr{A}_2^\dagger). \quad (32)$$

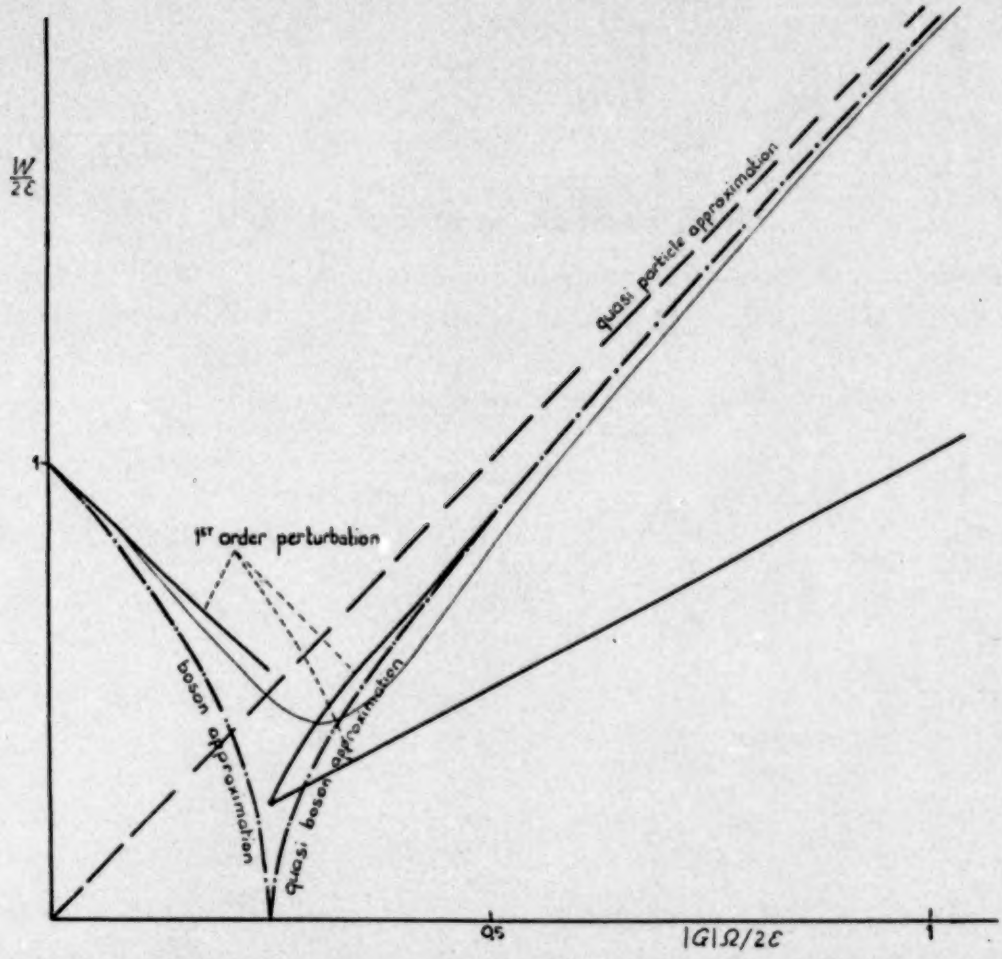

Fig. 3. Comparison of the different approximations (the thin curve is the case $\Omega = 10$ taken from fig. 2).

One clearly sees the interchange of the roles of $|G|\Omega$ and ε as a result of the quasi-particle transformation. Diagonalization leads to the energy $W_{qb} = 2(|G|^2\Omega^2 - \frac{1}{4}\varepsilon^2)^{\frac{1}{2}}$. These curves are plotted in dotted lines on fig. 2. The exact solution was obtained with electronic computors (in Lund and in Paris), for the following values of Ω:

$$\Omega = 3,\ 6,\ 10,\ 20.$$

One can see how the approximation improves when Ω increases. One sees also how good the quasi-boson approximation is for $|G| > |G_c|$. On the other hand,

the agreement is not as good for the boson approximation when $|G|<|G_c|$. This might be explained by the fact that, to construct our state, we must here use two bosons instead of one. In fact, a first-order perturbation

$$W_p = 2\varepsilon - 2|G|\Omega\left(1-\frac{1}{\Omega}\right)$$

is even better in this region, as can be seen from fig. 3 (the case $\Omega = 10$). Fig. 3 shows also the result of a first-order perturbation on the free quasi-particle Hamiltonian: the degeneracy is removed, the spurious state is isolated, and the result for the physical state is almost the same as the one obtained by the quasi-boson approximation:

$$W_p = \begin{cases} |G|\Omega, \\ |G|\Omega\left(2-\dfrac{\varepsilon^2}{4|G|^2\Omega^2}\right) \text{ in the limit where } \Omega \text{ is large.} \end{cases}$$

There remains a region around the critical value G_c where no approximation is valid. One could see that, in that region, the average value of the number of quasi-particles in the ground state of the quasi-boson approximation becomes infinite, stressing the fact that the Pauli principle plays a decisive role in this region.

4. Conclusion

We have seen that for the treatment of the pairing force when no exact solution is known, a quasi-particle method with a first order perturbation or a boson approximation gives very satisfactory results, apart for values of the coupling constant in an intermediate region.

The advantage of the boson approximation over the perturbation method is that it removes completely the spurious state of the quasi-particle approximation, and that it can be applied to quite different problems than the one discussed here, for which a perturbation would not give any satisfactory results.

This work was begun during the author's stay at the Institute for Theoretical Physics of Copenhagen. It is a pleasure for her to thank Professors Niels Bohr and Aage Bohr for their kind hospitality, and Professor Mottelson for suggesting this problem, and several illuminating discussions.

Appendix 1.

THE MATRIX ELEMENTS OF THE PAIRING FORCE

We are studying the space generated by A_i operators. An orthonormal set of vectors for this space is

$$|\ldots n_i \ldots\rangle = \prod_i \frac{1}{\sqrt{[n_i]!}} A_i^{\dagger n_i}|0\rangle,$$

with

$$[n_i] = \frac{n_i}{\Omega_i}(\Omega_i - n_i + 1),$$

$$[n_i]! = [n_i][n_i-1]\dots[1] = \frac{1}{\Omega_i^{n_i}}\frac{n_i!\,\Omega_i!}{(\Omega_i-n_i)!}.$$

Then we have

$$A_i^\dagger|\dots n_k\dots\rangle = \sqrt{[n_i+1]}\quad|\dots n_k+\delta_{ki}\dots\rangle,$$

$$A_i|\dots n_k\dots\rangle = \sqrt{[n_i]}\quad|\dots n_k-\delta_{ki}\dots\rangle.$$

These equations are very similar to those of real bosons, the difference being in the second term in the definition of $[n_i]$, which comes from the Pauli principle. One finds for the pairing force

$$H|\dots n_k\dots\rangle = (\sum_k 2\varepsilon_k n_k)|\dots n_k\dots\rangle$$

$$+ G\sum_{ij}\sqrt{\Omega_j[n_j-\delta_{ij}+1]\Omega_i[n_i]}|\dots n_k+\delta_{kj}-\delta_{ki}\dots\rangle.$$

Appendix 2.

THE OPERATOR N IN THE QUASI-BOSON APPROXIMATION

We start from the definition of the Q and P operators with respect to the p and q operators:

$$Q = \Lambda q, \qquad P = \mu p, \qquad \text{with } \Lambda\mu^\dagger = 1.$$

We then get the inverse formulas

$$q = \mu^\dagger Q, \qquad p = \Lambda^\dagger P,$$

which lead to the following expression for the $\mathcal{A}$ operators:

$$\mathcal{A} = \tfrac{1}{2}(\mu^\dagger+\Lambda^\dagger)\Gamma + \tfrac{1}{2}(\mu^\dagger-\Lambda^\dagger)\Gamma^\dagger.$$

Thus, we rewrite

$$N = \sum_i \frac{2(\varepsilon_i-\lambda)}{E_i}\mathcal{A}_i^\dagger\mathcal{A}_i + \sqrt{2}\,Q_0 = \mathcal{A}^\dagger v\mathcal{A} + \sqrt{2}Q_0$$

as a function of the Γ operators:

$$N = \tfrac{1}{2}\Gamma^\dagger(\mu v\mu^\dagger + \Lambda v\Lambda^\dagger)\Gamma + \tfrac{1}{4}\Gamma^\dagger(\mu+\Lambda)v(\mu^\dagger-\Lambda^\dagger)\Gamma^\dagger$$

$$+ \tfrac{1}{4}\Gamma(\mu-\Lambda)v(\mu^\dagger+\Lambda^\dagger)\Gamma + \tfrac{1}{4}\mathrm{Tr}(\mu v\mu^\dagger + \Lambda v\Lambda^\dagger - 2v) + \Gamma_0 + \Gamma_0^\dagger.$$

References

1) S. T. Belyaev, Mat. Fys. Medd. Dan Vid. Selsk. **31**, No. 11 (1959)
2) R. Arvieu et M. Véneroni, Comptes Rendus **252** (1961) 670;
M. Baranger, Phys. Rev. **120** (1960) 957
3) B. R. Mottelson, The many-body problem (Dunod, Paris, 1959) p. 295
4) D. J. Thouless, Nuclear Physics **21** (1960) 225
5) P. W. Anderson, Phys. Rev. **112** (1958) 1900

1.D.1:2.1 *Nuclear Physics* **28** (1961) 270—292; © *North-Holland Publishing Co., Amsterdam*
Not to be reproduced by photoprint or microfilm without written permission from the publisher

THEORY OF COLLECTIVE EXCITATIONS OF SPHERICAL NUCLEI WITH PARTICULAR APPLICATION TO THE GIANT DIPOLE STATE

JERZY SAWICKI and TOSHIO SODA
University of California, Berkeley, California †

Received 12 May 1961

Abstract: The system of equations of motion for the components of the one-particle density matrix is linearized for a finite system of fermions interacting through a two-body "residual" force. Exchange terms are included. Equations corresponding to those of the "extended shell model" method are obtained for calculating collective states of spherical nuclei of definite angular momentum, parity, spin and isobaric spin, both in the j-j and L-S coupling scheme. Particular application and solution of such equations is obtained for the case of the giant dipole state of O^{16} by the use of finite range potentials with two different mixtures of exchange forces and radial shapes. The matrix elements are antisymmetrized and the "backward-going graphs" are included. Satisfactory agreement with experiment is obtained.

The left over terms bilinear in the density operator are then "minimized" by extracting their lowest order linear contribution. The resulting correction terms are estimated for the giant dipole state in O^{16} and found small, giving support to the Random Phase Approximation.

1. Introduction

Recently, a popular approach to the problem of collective oscillations in systems of fermions has been founded on the Random Phase Approximation (RPA). The usual formalism follows the early papers of Sawada and his collaborators [1]), but the density matrix formulation of Ehrenreich and Cohen [2])†† seems to be more convenient in certain applications. The density matrix formulation of a somewhat extended RPA for finite systems was presented in a previous paper [3]) (referred to hereafter as I). In the following we shall essentially follow the lines of I in a somewhat modified form and shall present extensions and applications of this theory. In particular, certain corrections of the deviations from linearity are discussed in a way somewhat similar to the method indicated by Sawada and Soda [4]).

2. General Formulation

2.1. EQUATIONS FOR THE DENSITY MATRIX

The second quantized Hamiltonian discussed in I can be written as

$$\hat{H} = \sum_{s} E_s^0 c_s^\dagger c_s + \tfrac{1}{2} \sum_{ss'\kappa\kappa'} \Delta V_{ss'\kappa\kappa'} c_{s'}^\dagger c_{\kappa'}^\dagger c_\kappa c_s, \tag{1}$$

where $\{E_s^0\}$ is the complete set of eigenvalues of a phenomenological (shell

† This work was supported in part by the Office of Naval Research.

†† Similar equations for the density matrix were first introduced in atomic physics by Dirac [5])

model) single particle model Hamiltonian $H_0(\mathbf{r})$, and $\Delta V(\mathbf{r}_1\sigma^{(1)}\tau^{(1)}, \mathbf{r}_2\sigma^{(2)}\tau^{(2)})$ is a phenomenological (pure two-body), as yet unspecified interaction potential; its matrix elements are

$$\Delta V_{\alpha\beta,\gamma\delta} = \langle\varphi_\delta^*(2)\varphi_\beta^*(1)|\Delta V(1,2)|\varphi_\alpha(1)\varphi_\gamma(2)\rangle,$$

where $\{\varphi_s(i)\}$ is a complete set of eigenfunctions of $H_0(\mathbf{r})$; c_s and $c_s^\dagger$ are the usual fermion destruction and creation operators.

The exact equation of motion for a component of the single particle density matrix of the system described by eq. (1) was obtained in I in the form †

$$\Delta_{\nu\nu'}\hat{\varrho}_{\nu\nu'} = \sum_{\kappa\kappa'\delta}(\Delta V_{\delta\nu,\kappa\kappa'}\hat{\varrho}_{\kappa\kappa'}\hat{\varrho}_{\delta\nu'} - \Delta V_{\nu'\delta,\kappa\kappa'}\hat{\varrho}_{\nu\delta}\hat{\varrho}_{\kappa\kappa'}), \tag{2}$$

where

$$\hat{\varrho}_{\alpha\alpha'} \equiv c_{\alpha'}^\dagger c_\alpha, \qquad \Delta_{\nu\nu'} = E_{\nu'}^0 - E_\nu^0 + i\hbar\frac{\partial}{\partial t}.$$

We can now approach the problem of linearization of eq. (2) in a manner slightly different from that of I. Let us represent each $\hat{\varrho}_{\alpha\alpha'}$ in the form

$$\hat{\varrho}_{\alpha\alpha'} = \hat{\varrho}_{\alpha\alpha}\delta_{\alpha\alpha'} + \hat{\varrho}_{\alpha\alpha'}(1-\delta_{\alpha\alpha'}). \tag{3}$$

Our hypothesis will be that certain collective states which we describe here are approximately linear combinations of single-particle excitations from the "true" ground state. It will be assumed, therefore, that the contributions of the terms quadratic in the off-diagonal components are of higher order; further, it will be assumed that the amplitudes of each of the single-particle excitations are small; the potential ΔV is also weak enough for the wave functions of the "true" ground state and the collective states not to be extremely different from the non-interacting Fermi sea. Therefore, the terms with the fluctuation of particle number operators $(\hat{\varrho}_{\alpha\alpha} - n_\alpha)$ are also assumed to contribute in higher order. Here n_α is the occupation factor in the Fermi sea appropriate to the non-interacting system ($n_\alpha = 1$ if state α is a hole, $n_\alpha = 0$ if it is a particle). In the following we shall attempt to give estimates of the effect of some of these higher order terms.

Using eq. (3) we can now rewrite eq. (2) for the off-diagonal ($\nu \neq \nu'$) com-

† In addition to the two methods of deriving eq. (2) mentioned in I, we might point out another method utilizing the equations of motion for the single destruction and creation operators. One can also obtain eq. (2) in the following form using the antisymmetrized matrix elements:

$$\Delta_{\nu\nu'}\hat{\varrho}_{\nu\nu'} = \sum_{\kappa\kappa'\delta}[\tfrac{1}{2}(\Delta V_{\delta\nu,\kappa\kappa'} - \Delta V_{\delta\kappa',\kappa\nu})\hat{\varrho}_{\kappa\kappa'}\hat{\varrho}_{\delta\nu'} - \tfrac{1}{2}(\Delta V_{\nu'\delta,\kappa\kappa'} - \Delta V_{\kappa\delta,\nu'\kappa'})\hat{\varrho}_{\nu\delta}\hat{\varrho}_{\kappa\kappa'}].$$

In view of the anticommutation relations of the fermion operators this form is exactly equivalent to eq. (2). This form is also equivalent to eq. (2) with respect to the Hartree-Fock factorization of eq. (7) of I. However, when linearized, it is not equivalent to eq. (2) if the less accurate Hartree factorization [eq. (6) of I] is used instead.

ponents in the form

$$\begin{aligned}\Delta_{\nu\nu'}\hat{\varrho}_{\nu\nu'} &= \sum_{\kappa\neq\kappa'}\Delta V_{\nu'\nu,\kappa\kappa'}(\hat{\varrho}_{\kappa\kappa'}\hat{\varrho}_{\nu'\nu'}-\hat{\varrho}_{\nu\nu}\hat{\varrho}_{\kappa\kappa'}) \\ &+\sum_{\kappa}\Big(\sum_{\kappa'\neq\nu'}\Delta V_{\kappa'\nu,\kappa\kappa}\hat{\varrho}_{\kappa\kappa}\hat{\varrho}_{\kappa'\nu'}-\sum_{\kappa'\neq\nu}\Delta V_{\nu'\kappa',\kappa\kappa}\hat{\varrho}_{\nu\kappa'}\hat{\varrho}_{\kappa\kappa}\Big) \qquad (4) \\ &+\sum_{\kappa\neq\kappa'}\Big(\sum_{s\neq\nu'}\Delta V_{s\nu,\kappa\kappa'}\hat{\varrho}_{\kappa\kappa'}\hat{\varrho}_{s\nu'}-\sum_{s\neq\nu}\Delta V_{\nu's,\kappa\kappa'}\hat{\varrho}_{\nu s}\hat{\varrho}_{\kappa\kappa'}\Big).\end{aligned}$$

We shall now go over from the operators to their matrix elements. In doing this, we shall take into account the antisymmetry properties of Fermi operators by writing the Hartree-Fock exchange matrix elements explicitly. Next we can write the diagonal components as $\hat{\varrho}_{\alpha\alpha}=n_\alpha+(\hat{\varrho}_{\alpha\alpha}-n_\alpha)$. All the matrix elements involving the $\hat{\varrho}_{\alpha\alpha}-n_\alpha$ operators are of higher order. Finally, we define the first order density fluctuations as those corresponding to retaining only the first two lines of the right-hand side of eq. (4) and involving n_α in the place of $\hat{\varrho}_{\alpha\alpha}$. Consequently, we can write

$$\begin{aligned}\Delta_{\nu\nu'}\varrho'_{\nu\nu'} &= (n_{\nu'}-n_\nu)\sum_{\kappa\neq\kappa'}(\Delta V_{\nu'\nu,\kappa\kappa'}-\Delta V_{\kappa\nu,\nu'\kappa'})\rho'_{\kappa\kappa'} \\ &+\sum_{\kappa}n_\kappa\Big[\sum_{\kappa'\neq\nu'}(\Delta V_{\kappa'\nu,\kappa\kappa}-\Delta V_{\kappa\nu,\kappa'\kappa})\rho'_{\kappa'\nu'}-\sum_{\kappa'\neq\nu}(\Delta V_{\nu'\kappa',\kappa\kappa}-\Delta V_{\nu'\kappa,\kappa\kappa'})\varrho'_{\nu\kappa'}\Big]. \qquad (5)\end{aligned}$$

This equation differs from eq. (10) of I only by the removal of all the diagonal components $\rho'_{\alpha\alpha}$ which correspond here to a higher order. The leading term is the RPA term; the presence of the second line "self-energy" terms corresponds to the fact that here we are not doing any self-consistency calculation with respect to ΔV, i.e., we first do not separately "renormalize" the zero-order energies $\{E_\nu^0\}$ by solving the secular equation involving those "self-energy" terms. Rather, we shall use, in most of the early discussion, the consequently "purely phenomenological" ΔV formalism, and the "systematic linearization" of the form of eq. (5). If we used the other approach, we would write

$$\bar{\Delta}_{\nu\nu'}\bar{\varrho}'_{\nu\nu'} = (n_{\nu'}-n_\nu)\sum_{\kappa\neq\kappa'}(\Delta\bar{V}_{\nu'\nu,\kappa\kappa'}-\Delta\bar{V}_{\kappa\nu,\nu'\kappa'})\bar{\varrho}'_{\kappa\kappa'}, \qquad (6)$$

where all the "bar" quantities refer to the new spectrum being the solution of the secular equation with the bottom line of eq. (5).

It is probably most consistent from a theoretical point of view to choose the "residual" two-body potential in such a way that it has no diagonal matrix elements: $\Delta V_{\alpha\alpha,\beta\gamma}=0=\Delta V_{\alpha\alpha,\beta\beta}$. A more complete discussion of this point will be given later in this paper.

2.2. SECULAR PROBLEM FOR SYSTEMS OF SPHERICAL SYMMETRY

Let us now discuss the problem of physical states of systems of spherical symmetry. The single fermion total angular momentum j and its z-projection m are good quantum numbers. The collective states of interest here are charac-

terized by the angular momentum L, its z-projection M and isobaric spin T. In our linearized theory they are described as linear superpositions of single-particle excitations i.e., linear combinations of fermion pair states generated from the true ground state. As the true ground state contains not only "hole" states (as in the "vacuum") but also admixtures of states above the Fermi level we can have, in general, also particle-particle and hole-hole pairs in addition to the particle-hole pairs. In fact, and this is most important, we have in this case particle-destruction and hole-creation amplitudes (the "backward going" graphs), in contrast to the case of the Fermi model ground state. If we retain only the first line of the right-hand side of eq. (5) (the RPA), we retain solely the particle-hole pairs. The energies of the collective states (eigenfrequencies of the density fluctuations ρ') are counted relative to the ground state.

Let us now introduce the pair operators with projected angular momentum states, appropriate to the j–j coupling scheme,

$$\hat{A}^{+}_{LM}(\nu\nu') = \sum_{m_\nu m_{\nu'}} (-)^{m_\nu} (j_\nu j_{\nu'}; -m_\nu m_{\nu'}|LM)\hat{\varrho}_{\nu\nu'}. \tag{7}$$

The phase factor $(-)^{m_\nu}$ corresponds to the Condon-Shortley convention for the transformation of angular momentum eigenfunctions under rotations; $(j_\alpha j_{\alpha'}; -m_\alpha m_{\alpha'}|LM)$ is a Clebsch-Gordan coefficient. Using eq. (5) we can first derive the system of equations for the matrix elements of the $\hat{A}^{+}_{LM}(\nu\nu')$ operators with the collective state, denoted $A^{*}_{LM}(\nu\nu')$.

We can consider first a general two-body potential of the form

$$\begin{aligned}&\Delta V(1,2)\\ &= \Delta V(\mathbf{r}_1, \mathbf{r}_2)[(g_0+g'_0\boldsymbol{\sigma}_1\cdot\boldsymbol{\sigma}_2)\tfrac{1}{4}(1-\boldsymbol{\tau}_1\cdot\boldsymbol{\tau}_2)+(g_1+g'_1\boldsymbol{\sigma}_1\cdot\boldsymbol{\sigma}_2)\tfrac{1}{4}(3+\boldsymbol{\tau}_1\cdot\boldsymbol{\tau}_2)],\end{aligned} \tag{8}$$

where g_i, g'_i are coupling constants, $\frac{1}{4}(1-\boldsymbol{\tau}_1\cdot\boldsymbol{\tau}_2)$ and $\frac{1}{4}(3+\boldsymbol{\tau}_1\cdot\boldsymbol{\tau}_2)$ are the projection operators of the singlet ($T=0$) and triplet ($T=1$) isobaric spin states, and $\Delta V(\mathbf{r}_1, \mathbf{r}_2)$ is of a pure Wigner form and can be expanded in Legendre polynomials in the usual form

$$\Delta V(\mathbf{r}_1, \mathbf{r}_2) = \sum_{L'} v_{L'}(r_1, r_2) P_{L'}(\cos\omega). \tag{9}$$

We can now consider a system of two kinds of fermions: protons and neutrons. Let us denote by τ_ν the third component of the isobaric spin (we define $\tau_\nu = +$ for the proton and $\tau_\nu = -$ for the neutron). We denote by ν (for brevity) the set of quantum numbers $\{n_\nu, l_\nu, j_\nu\}$ unless otherwise explicitly specified. Let us now consider the pair (ν, ν') and assume both members of this pair to be proton states, say $(\tau_\nu = \tau_{\nu'} = +)$. The final system of equations we obtain

for such off-diagonal components is

$$\Delta_{\nu\nu'}A^{*}_{LM}(\nu\nu';++)$$
$$=-\sum_{\substack{\kappa\kappa'\\(\tau_\kappa=\tau_{\kappa'}=+)}}\sum_{L'}\{R_{LL}(\nu'\nu,\kappa\kappa')\delta_{L'L}(f^{(1)}_{L'}(\nu'\nu,\kappa\kappa')+g^{(1)}_{L'}(\nu'\nu,\kappa\kappa'))+R'_{LL'}(\nu'\nu,\kappa\kappa')\}$$
$$\times(f^{(1)}_{L'}(\kappa\nu,\nu'\kappa')+g^{(1)}_{L'}(\kappa\nu,\nu'\kappa'))A^{*}_{LM}(\kappa\kappa';++)-\sum_{\substack{\kappa\kappa'\\(\tau_\kappa=\tau_{\kappa'}=-)}}\{R_{LL}(\nu'\nu,\kappa\kappa')$$
$$\times\tfrac{1}{2}(f^{(0)}_{L}(\nu'\nu,\kappa\kappa')+f^{(1)}_{L}(\nu'\nu,\kappa\kappa')+g^{(0)}_{L}(\nu'\nu,\kappa\kappa')+g^{(1)}_{L}(\nu'\nu,\kappa\kappa')) \tag{10}$$
$$-\sum_{L'}R'_{LL'}(\nu'\nu,\kappa\kappa')\tfrac{1}{2}(f^{(1)}_{L'}(\kappa\nu,\nu'\kappa')-f^{(0)}_{L'}(\kappa\nu,\nu'\kappa')+g^{(1)}_{L'}(\kappa\nu,\nu'\kappa')$$
$$-g^{(0)}_{L'}(\kappa\nu,\nu'\kappa'))\}A^{*}_{LM}(\kappa\kappa';--)\ \text{plus self-energy terms.}$$

The self-energy terms are

$$+\sum_{\substack{s\kappa\\(\tau_s=\tau_\kappa=+)}}\{\sum_{L'=0}s_{L'}(\nu s\kappa)(f^{(1)}_{L'}+g^{(1)}_{L'})(s\nu,\kappa s)A^{*}_{LM}(\kappa\nu';++)-\sum_{L'=0}s_{L'}(\nu' s\kappa)$$
$$\times(f^{(1)}_{L'}+g^{(1)}_{L'})(s\nu',\kappa s)A^{*}_{LM}(\nu\kappa;++)+s_0(\nu s\kappa)(f_0{}^{(1)}+g_0{}^{(1)})(\nu\nu,ss)A^{*}_{LM}(\kappa\nu';++)$$
$$-s_0(\nu' s\kappa)(f_0{}^{(1)}+g_0{}^{(1)})(\kappa\nu',ss)A^{*}_{LM}(\nu\kappa;++)\}+\sum_{\substack{s\kappa\\(\tau_s=-,\tau_\kappa=+)}}\{\sum_{L'=0}s_{L'}(\nu s\kappa)$$
$$\times\tfrac{1}{2}(f^{(1)}_{L'}-f^{(0)}_{L'}+g^{(1)}_{L'}-g^{(0)}_{L'})(s\nu,\kappa s)A^{*}_{LM}(\kappa\nu';++)-\sum_{L'=0}s_{L'}(\nu' s\kappa) \tag{10a}$$
$$\times\tfrac{1}{2}(f^{(1)}_{L'}-f^{(0)}_{L'}+g^{(1)}_{L'}-g^{(0)}_{L'})(s\nu',\kappa s)A^{*}_{LM}(\nu\kappa;++)+s_0(\nu s\kappa)$$
$$\times\tfrac{1}{2}(f_0{}^{(1)}+f_0{}^{(0)}+g_0{}^{(1)}+g_0{}^{(0)})(\kappa\nu,ss)A^{*}_{LM}(\kappa\nu';++)-s_0(\nu' s\kappa)$$
$$\times\tfrac{1}{2}(f_0{}^{(1)}+f_0{}^{(0)}+g_0{}^{(1)}+g_0{}^{(0)})(\kappa\nu',ss)A^{*}_{LM}(\nu\kappa;++)\}.$$

Here we introduce the following quantities:

$$R_{LL}(\nu'\nu,\kappa\kappa')=(n_{\nu'}-n_\nu)\delta(j_\nu j_{\nu'}L),$$
$$R'_{LL'}(\nu'\nu,\kappa\kappa')=(n_{\nu'}-n_\nu)(-)^{L'-L}[L']\begin{Bmatrix}j_\nu & j_\kappa & L'\\ j_{\kappa'} & j_{\nu'} & L\end{Bmatrix},$$
$$s_L(\mu s\kappa)=n_s[L][j_\mu]^{-1}\delta(j_\mu j_s L),$$
$$f^{(T)}_{L}(\alpha\beta,\gamma\delta)=g_T[L]^{-1}\{[j_\alpha][j_\beta][j_\gamma][j_\delta]\}^{\frac{1}{2}}\begin{pmatrix}j_\alpha & j_\beta & L\\ \frac{1}{2} & -\frac{1}{2} & 0\end{pmatrix}\begin{pmatrix}j_\gamma & j_\delta & L\\ \frac{1}{2} & -\frac{1}{2} & 0\end{pmatrix}v_L(\alpha\beta,\gamma\delta), \tag{11}$$
$$g^{(T)}_{L'}(\alpha\beta,\gamma\delta)=6g'_T\sum_{L''}(-)^{L'+L''+1}\{[j_\alpha][j_\beta][j_\gamma][j_\delta]\}^{\frac{1}{2}}\{[l_\alpha][l_\beta][l_\gamma][l_\delta]\}^{\frac{1}{2}}$$
$$\times(-)^{l_\alpha+l_\gamma+j_\alpha+j_\gamma}\begin{pmatrix}l_\alpha & l_\beta & L''\\ 0&0&0\end{pmatrix}\begin{pmatrix}l_\gamma & l_\delta & L''\\ 0&0&0\end{pmatrix}\begin{Bmatrix}l_\alpha & \frac{1}{2} & j_\alpha\\ l_\beta & \frac{1}{2} & j_\beta\\ L'' & 1 & L'\end{Bmatrix}\begin{Bmatrix}l_\gamma & \frac{1}{2} & j_\gamma\\ l_\delta & \frac{1}{2} & j_\delta\\ L'' & 1 & L'\end{Bmatrix}v_{L''}(\alpha\beta,\gamma\delta).$$

In these definitions, $\delta(j_\alpha j_\beta L)$ stands for the vectorial triangular condition,

$\begin{pmatrix} j_\alpha & j_\beta & L \\ m_\alpha & m_\beta & M \end{pmatrix}$ is a 3–j symbol, $\begin{Bmatrix} j_\alpha & j_\beta & L \\ j_\gamma & j_\delta & L' \end{Bmatrix}$ a 6–j symbol, $\begin{Bmatrix} j_\alpha & j_\beta & J \\ j_\gamma & j_\delta & J' \\ L & L' & L'' \end{Bmatrix}$ a Wigner 9–j symbol and $v_L(\alpha\beta, \gamma\delta)$ is a radial matrix element of $v_L(r_1, r_2)$ as in I†. The terms involving the R_{LL} and $R'_{LL'}$ symbols correspond to the RPA [top line of eq. (5)], and the self-energy terms to the bottom line of eq. (5). Further, we used the notation $[x] \equiv 2x+1$.

If we exchange the + and − signs we obtain analogous equations for the neutron-neutron (ν, ν') pairs. Notice that the neutron-neutron pairs are coupled to proton-proton pairs. The equations simplify if we allow for no charge dependence of the ΔV operator ($g_0 \neq g_1$, $g'_0 \neq g'_1$). Very similar equations obtain for the mixed neutron-proton and proton-neutron pairs. Those are coupled only between themselves.

If we use for the isobaric spin projection operator the convention analogous to that of eq. (7) for the angular momentum, we see that the combinations $\sqrt{2}A^{0(1)*}_{LM}(\nu\nu') = A^*_{LM}(\nu\nu'; ++)(\pm)\ A^*_{LM}(\nu\nu'; --)$ correspond to isobaric spin states $T=0$ (+ sign) and $T=1$, $T_3=0$ (− sign). A particularly simple case obtains for systems with equal numbers of two kinds of particles (e.g., nuclei with $A = 2Z$). For such systems we can write

$$\Delta_{\nu\nu'} A^{0(1)*}_{LM}(\nu\nu') = \sum_{\kappa,\kappa'} \sum_{L'} (M_{LL'}(\nu\nu', \kappa\kappa') \pm N_{LL'}(\nu\nu', \kappa\kappa')) A^{0(1)*}_{LM}(\kappa\kappa'), \quad (12)$$

where

$$\begin{aligned} M_{LL'}(\nu\nu', \kappa\kappa') &= -R_{LL}(\nu'\nu, \kappa\kappa')\delta_{LL'}(f^{(1)}_{L'}+g^{(1)}_{L'})(\nu'\nu, \kappa\kappa') - R'_{LL'}(\nu'\nu, \kappa\kappa')(f^{(1)}_{L'}+g^{(1)}_{L'})(\kappa\nu, \nu'\kappa') \\ &+ \sum_s s_{L'}(\nu s\kappa)\delta_{\kappa'\nu'}[(\tfrac{3}{2}f^{(1)}_{L'} - \tfrac{1}{2}f^{(0)}_{L'} + \tfrac{3}{2}g^{(1)}_{L'} - \tfrac{1}{2}g^{(0)}_{L'})(s\nu, \kappa s) \\ &+ \delta_{L'0}(\tfrac{3}{2}f_0^{(1)} + \tfrac{1}{2}f_0^{(0)} + \tfrac{3}{2}g_0^{(1)} + \tfrac{1}{2}g_0^{(0)})(\kappa\nu, ss)] \qquad (13a) \\ &- \sum_s s_{L'}(\nu' s\kappa')\delta_{\kappa\nu}[(\tfrac{3}{2}f^{(1)}_{L'} - \tfrac{1}{2}f^{(0)}_{L'} + \tfrac{3}{2}g^{(1)}_{L'} - \tfrac{1}{2}g^{(0)}_{L'})(s\nu', \kappa' s) \\ &+ \delta_{L'0}(\tfrac{3}{2}f_0^{(1)} + \tfrac{1}{2}f_0^{(0)} + \tfrac{3}{2}g_0^{(1)} + \tfrac{1}{2}g_0^{(0)})(\kappa'\nu', ss)], \end{aligned}$$

$$\begin{aligned} N_{LL'}(\nu\nu', \kappa\kappa') = &-R_{LL}(\nu'\nu, \kappa\kappa')\delta_{LL'}\tfrac{1}{2}(f^{(0)}_L + f^{(1)}_L + g^{(0)}_L + g^{(1)}_L)(\nu'\nu, \kappa\kappa') \\ &- R'_{LL'}(\nu'\nu, \kappa\kappa')\tfrac{1}{2}(f^{(1)}_{L'} - f^{(0)}_{L'} + g^{(1)}_{L'} - g^{(0)}_{L'})(\kappa\nu, \nu'\kappa'). \qquad (13b) \end{aligned}$$

The matrices M and N simplify greatly if $g_0 = g'_0$ and $g_1 = g'_1$. In the summations over κ, κ' and s, which occur in eqs. (12) and (13), for the special case of $A = 2Z$, we have to sum over the single-particle states of one kind of particle (say proton states). Formulae (12) and (13) prove useful, e.g. in the problem of the giant dipole state observed in photo-nuclear reactions (see sect. 3). The energy of the collective state $\hbar\omega$ can be found by solving the secular

† The parity conditions as $l_\alpha + l_\beta + L$ = even, $l_\gamma + l_\delta + L$ = even must be also remembered.

equation

$$\mathrm{Det}||\Delta_{\nu\nu'}\delta_{\nu\kappa}\delta_{\nu'\kappa'}-\sum_{L'}\left(M_{LL'}(\nu\nu',\,\kappa\kappa')\pm N_{LL'}(\nu\nu',\,\kappa\kappa')\right)||=0. \tag{14}$$

A great simplification of the system of equations for $A^{*}_{LM}(\nu\nu')$ can be obtained in the special case of a harmonic oscillator single-particle potential, and also where $\Delta V(\mathbf{r}_1,\,\mathbf{r}_2)\equiv\Delta V(|\mathbf{r}_1-\mathbf{r}_2|)$. Then the well-known Talmi method of reduction of the integration problem to the centre of mass and relative coordinates can be applied. This becomes particularly simple when we neglect the spin-orbit coupling in the single-particle wave functions (or use the representation in which l and s are good quantum numbers). For the Talmi transformation it is very useful to use the brackets $\langle nl,\,N\mathscr{L}\lambda|n_1l_1,\,n_2l_2,\,\lambda\rangle$ extensively tabulated by Moshinsky and Brody [5]. The spatial wave functions transform as

$$\psi_{n_1l_1m_{l_1}}(\mathbf{r}_1)\psi_{n_2l_2m_{l_2}}(\mathbf{r}_2)=\sum_{\lambda\mu}(l_1l_2;\,m_{l_1}m_{l_2}|\lambda\mu)\langle nl,\,N\mathscr{L}\lambda|n_1l_1,\,n_2l_2,\,\lambda\rangle|nl,\,N\mathscr{L}\lambda\mu\rangle, \tag{15}$$

where $|nl,\,N\mathscr{L}\lambda\mu\rangle=\sum_{m,M}(l\mathscr{L};\,mM|\lambda\mu)\psi_{nlm}(\mathbf{r})\psi_{N\mathscr{L}M}(\mathbf{R})$, while $\mathbf{r}=\mathbf{r}_1-\mathbf{r}_2$ and $\mathbf{R}=\frac{1}{2}(\mathbf{r}_1+\mathbf{r}_2)$ are the relative and centre-of-mass coordinates. We shall now use the conventional notation for the Wigner, Majorana, Bartlett and Heisenberg interactions, so that $\Delta V\equiv\Delta V(r)(w+mP^{r}+bP^{\sigma}+hP^{r}P^{\sigma})$; the constants w, m, b and h are related to the previously used coupling constants by the equations $g_1=w-\frac{1}{2}m-h+\frac{1}{2}b$, $g'_1=\frac{1}{2}(b-m)$, $g_0=w+\frac{1}{2}m+h+\frac{1}{2}b$, $g'_0=\frac{1}{2}(b+m)$. First we can write out the equations for the pairs with definite charge (τ) and spin projection (σ) states. We obtain the equations

$$\begin{aligned}
\Delta_{\nu\nu'}\rho'_{\nu\nu'}(\tau\tau,\,\sigma\sigma)=(n_{\nu'}-n_{\nu})\sum_{\kappa\neq\kappa'}\{&\Delta V_{\nu'\nu,\,\kappa\kappa'}[(w-m+b-h)\rho'_{\kappa\kappa'}(\tau\tau,\,\sigma\sigma)\\
&+(w+b)\rho'_{\kappa\kappa'}(-\tau-\tau,\,\sigma\sigma)+(w-h)\rho'_{\kappa\kappa'}(\tau\tau,\,-\sigma-\sigma)+w\rho'_{\kappa\kappa'}(-\tau-\tau,\,-\sigma-\sigma)]\\
&-\Delta V_{\kappa\nu,\,\nu'\kappa'}[(w-m+b-h)\rho'_{\kappa\kappa'}(\tau\tau,\,\sigma\sigma)-(m+h)\rho'_{\kappa\kappa'}(-\tau-\tau,\,\sigma\sigma)\\
&+(b-m)\rho'_{\kappa\kappa'}(\tau\tau,\,-\sigma-\sigma)-m\rho'_{\kappa\kappa'}(-\tau-\tau,\,-\sigma-\sigma)]\}\\
+\sum_{\kappa}n_{\kappa}\{&\sum_{s\neq\nu'}\Delta V_{s\nu,\,\kappa\kappa}[(2w-m+2b-h)\rho'_{s\nu'}(\tau\tau,\,\sigma\sigma)+(2w-h)\rho'_{\nu s'}(\tau\tau,\,-\sigma-\sigma)]\\
&-\sum_{s\neq\nu}\Delta V_{\nu's,\,\kappa\kappa}[(2w-m+2b-h)\rho'_{\nu s}(\tau\tau,\,\sigma\sigma)+(2w-h)\rho'_{\nu s}(\tau\tau,\,-\sigma-\sigma)]\\
&-\sum_{s\neq\nu'}\Delta V_{\kappa\nu,\,s\kappa}[(w-2m+b-2h)\rho'_{s\nu'}(\tau\tau,\,\sigma\sigma)+(b-2m)\rho'_{\nu s'}(\tau\tau,\,-\sigma-\sigma)]\\
&+\sum_{s\neq\nu}\Delta V_{\nu'\kappa,\,\kappa s}[(w-2m+b-2h)\rho'_{\nu s}(\tau\tau,\,\sigma\sigma)+(b-2m)\rho'_{\nu s}(\tau\tau,\,-\sigma-\sigma)]\}.
\end{aligned} \tag{16}$$

Here the subscripts of ΔV refer to spatial states only.

As in the L-S coupling scheme we can first construct (project out) the states of a definite total intrinsic spin S by taking the combinations $\sqrt{2}\rho'^{S}(\tau\tau)=\rho'(\tau\tau,\,\sigma\sigma)\pm\rho'(\tau\tau,\,-\sigma-\sigma)$, where the upper sign corresponds to $S=0$ and the lower to $S=1$ ($S_3=0$). Here the projection S_3 is the difference in the spin

projections of the members of a pair in analogy to the rule $M = m_{\nu'} - m_{\nu}$ of eq. (7). Equations similar to those arrived at below can be obtained in this scheme for the completely decoupled $S = 1$, $S_3 = \pm 1$ states [corresponding to spin combinations $(\sigma, -\sigma)$]. The states with $T = 1$, $T_3 = \pm 1$ (corresponding to proton-neutron and neutron-proton pairs) are not discussed below. In the following equations, whenever we have $S = 1$ or $T = 1$, we mean also $S_3 = 0$, $T_3 = 0$. In fact, such states as discussed below are of greatest physical interest, e.g., the giant dipole state in nuclei ($L = 1$, $S = 0$, $T = 1$, $T_3 = 0$).

As the next step, we can project out the isobaric spin T by introducing the combinations $2\chi^{ST}_{\nu\nu'} \equiv \rho'^{S}_{\nu\nu'}(\tau\tau) + (-)^T \rho'^{S}_{\nu\nu'}(-\tau-\tau)$. As a final result, we obtain the system of equations

$$\begin{aligned}
\Delta_{\nu\nu'}\chi^{ST}_{\nu\nu'} = {} & (n_{\nu'} - n_{\nu}) \sum_{\kappa \neq \kappa'} \{\Delta V_{\nu'\nu,\kappa\kappa'}[(w-m+b-h) + (-)^S(w-h) \\
& + (-)^T(w+b+(-)^S w)] - \Delta V_{\kappa\nu,\nu'\kappa'}[(w-m+b-h) + (-)^S(b-m) \\
& - (-)^T(m+h+(-)^S m)]\}\chi^{ST}_{\kappa\kappa'} + \sum_{\kappa} n_{\kappa}\{[(2w-m+2b-h) + (-)^S(2w-h)] \\
& \times [\sum_{s \neq \nu'} \Delta V_{s\nu,\kappa\kappa}\chi^{ST}_{s\nu'} - \sum_{s \neq \nu} \Delta V_{\nu' s,\kappa\kappa}\chi^{ST}_{\nu s}] - [(w-2m+b-2h) + (-)^S(b-2m)] \\
& \times [\sum_{s \neq \nu'} \Delta V_{\kappa\nu,s\kappa}\chi^{ST}_{s\nu'} - \sum_{s \neq \nu} \Delta V_{\nu'\kappa\ \kappa s}\chi^{ST}_{\nu s}].
\end{aligned} \tag{17}$$

In the case of special interest where $S = 0$, $T = 1$ (the giant dipole state), we have

$$\begin{aligned}
\Delta_{\nu\nu'}\chi^{01}_{\nu\nu'} = {} & -(n_{\nu'} - n_{\nu}) \sum_{\kappa \neq \kappa'} [\Delta V_{\nu'\nu,\kappa\kappa'}(m+2h) + \Delta V_{\kappa\nu,\nu'\kappa'}(w+2b)]\chi^{01}_{\kappa\kappa'} \\
& + \sum_{\kappa} n_{\kappa}\{(4w-m+2b-2h)[\sum_{s \neq \nu'} \Delta V_{s\nu,\kappa\kappa}\chi^{01}_{s\nu'} - \sum_{s \neq \nu} \Delta V_{\nu' s,\kappa\kappa}\chi^{01}_{\nu s}] \\
& - (w-4m+2b-2h)[\sum_{s \neq \nu'} \Delta V_{\kappa\nu,s\kappa}\chi^{01}_{s\nu'} - \Delta V_{\nu'\kappa,\kappa s}\chi^{01}_{\nu s}]\}.
\end{aligned} \tag{18}$$

Finally, we project out the collective state angular momentum (L, M) by means of an operator analogous to that of eq. (7):

$$\hat{F}^{ST}_{LM}(\nu\nu') = \sum_{m_{l\nu}} (-)^{m_{l\nu}}(l_{\nu} l_{\nu'}; -m_{l_{\nu}} m_{l_{\nu'}} | LM)\hat{\chi}^{ST}_{\nu\nu'}. \tag{19}$$

Using the Moshinsky-Brody transformation brackets for the harmonic oscillator eigenfunctions [5]), we obtain the system of equations

$$\begin{aligned}
\Delta_{\nu\nu'} F^{ST}_{LM}(\nu\nu') = {} & (n_{\nu'} - n_{\nu}) \sum_{\kappa \neq \kappa'} \sum_{l} u_l^{ST} D_{Ll}(\nu\nu', \kappa\kappa') F^{ST}_{LM}(\kappa\kappa') \\
& + \sum_{\kappa} \sum_{l} s_l^{ST}\{\sum_{s \neq \nu'} E_{Ll}(\nu\kappa s)\delta_{l_{\nu} l_s} F^{ST}_{LM}(s\nu') - \sum_{s \neq \nu} E_{Ll}(\nu'\kappa s)\delta_{l_{\nu'} l_s} F^{ST}_{LM}(\nu s)\},
\end{aligned} \tag{20}$$

$$\begin{aligned}
u_l^{ST} = {} & (w-m+b-h) + (-)^S(w-h) + (-)^T(w+b+(-)^S w) \\
& - (-)^l[w-m+b-h+(-)^S(b-m) - (-)^T(m+h+(-)^S m)], \\
s_l^{ST} = {} & 2w-m+2b-h+(-)^S(2w-h) - (-)^l[w-2m+b-2h+(-)^S(b-2m)],
\end{aligned}$$

$$D_{Ll}(\nu\nu', \kappa\kappa') = \sum_{\lambda nn'N\mathscr{L}} (-)^{l_\nu + l_{\nu'} - \lambda}[\lambda]\langle nl, n\mathscr{L}, \lambda | n_{\nu'} l_{\nu'}, n_\kappa l_\kappa, \lambda\rangle$$
$$\times \langle n'l, N\mathscr{L}, \lambda | n_\nu l_\nu, n_{\kappa'} l_{\kappa'}, \lambda\rangle \begin{Bmatrix} l_{\nu'} & l_\nu & L \\ l_{\kappa'} & l_\kappa & \lambda \end{Bmatrix} \langle nl||\Delta V(r)||n'l\rangle,$$

$$E_{Ll}(\nu\kappa S) = n_\kappa \sum_{\lambda nn'N\mathscr{L}} \langle nl, N\mathscr{L}, \lambda | n_s l_s, n_\kappa l_\kappa, \lambda\rangle\langle n'l, N\mathscr{L}, \lambda | n_\nu l_\nu, n_\kappa l_\kappa, \lambda\rangle$$
$$\times [\lambda][l_\nu]^{-1}\langle nl||\Delta V(r)||n'l\rangle.$$

Here $\langle nl||\Delta V(r)||n'l\rangle = \sum_p B(nl, n'l, p) I_p$ is the reduced radial matrix element, and $I_p = [2/\Gamma(p+\frac{3}{2})]\int_0^\infty r^{2p} e^{-r^2} \Delta V(r/\sqrt{\nu}) r^2 dr$ is the usual "Talmi integral", where ν is the usual range parameter of the harmonic oscillator wave functions. All the space exchange terms in eq. (20) contain the parity factor of the relative motion $\pi = (-)^l$. In order to evaluate their relative importance, it is sufficient to look at the ratio of the part proportional to π to the "direct" part in u_l^{ST} and s_l^{ST}. In the particular case of $S = 0$, $T = 1$ this ratio is $(w+2b)/(m+2h)$. Finally, the corresponding secular equation obtains in the form

$$\mathrm{Det}||M^{(L,S,T)}_{\nu\nu',\kappa\kappa'}|| = \mathrm{Det}||\Delta_{\nu\nu'}\delta_{\nu\kappa}\delta_{\nu'\kappa'} - (n_{\nu'} - n_\nu)$$
$$\times \sum_l u_l^{ST} D_{Ll}(\nu\nu', \kappa\kappa') - \sum_t \sum_l s_l^{ST}[E_{Ll}(\nu t\kappa)\delta_{l_\kappa l_\nu}\delta_{\kappa' \nu'} \quad (21)$$
$$- E_{Ll}(\nu' t\kappa')\delta_{l_{\kappa'} l_{\nu'}}\delta_{\kappa\nu}]|| = 0.$$

This formula displays the effective strength of the particle-hole interaction in different types of collective states in terms of the coupling constants w, m, b and h of the different exchange mixtures.

In the more realistic case of $H_0(\mathbf{r})$ involving a spin-orbit coupling which accounts for the j-splitting of the shell model single-particle states, it is appropriate to use the j–j coupling representation. This leads to a considerable complication in the coupling of angular momenta. It is common in shell model calculations to use an average well-depth parameter (or harmonic oscillator "spring constant") common for both $j = l \pm \frac{1}{2}$ for each single-particle orbital angular momentum l. Here again one can utilize the Talmi method with the transformation brackets of ref. [5]) for the case of the harmonic oscillator $H_0(\mathbf{r})$.

In analogy to the previous result we find, for the case of $T = 1$, the system of equations for the $A^{1*}_{LM}(\alpha\alpha')$ components:

$$\Delta_{\nu\nu'} A^{1*}_{LM}(\nu\nu') = -(n_{\nu'} - n_\nu) \sum_{\kappa \neq \kappa'} \sum_l \sum_{\lambda nn'N\mathscr{L}} (-)^{l_\kappa + l_{\kappa'} - \lambda}[\lambda]$$
$$\times \langle nl, N\mathscr{L}, \lambda | n_{\nu'} l_{\nu'}, n_\kappa l_\kappa, \lambda\rangle\langle n'l, N\mathscr{L}, \lambda | n_\nu l_\nu, n_{\kappa'} l_{\kappa'}, \lambda\rangle\langle n'l||\Delta V||nl\rangle$$
$$\times \left\{ (-)^{l_\nu + l_{\nu'} + l_\kappa + l_{\kappa'} + j_\nu + j_{\nu'} + j_\kappa + j_{\kappa'}} \begin{Bmatrix} l_\nu & j_\nu & \frac{1}{2} \\ j_{\nu'} & l_{\nu'} & L \end{Bmatrix} \begin{Bmatrix} l_\kappa & j_\kappa & \frac{1}{2} \\ j_{\kappa'} & l_{\kappa'} & L \end{Bmatrix} \begin{Bmatrix} l_{\nu'} & l_\nu & L \\ l_{\kappa'} & l_\kappa & \lambda \end{Bmatrix} \right. \quad (22)$$
$$\times (h + (-)^l b) + \left. \begin{Bmatrix} l_{\nu'} & j_{\nu'} & j_\nu & l_\nu \\ \frac{1}{2} & L & \frac{1}{2} & \lambda \\ l_{\kappa'} & j_{\kappa'} & j_\kappa & l_\kappa \end{Bmatrix} (m + (-)^l w) \right\}$$
$$\times A^{1*}_{LM}(\kappa\kappa') + \text{ self-energy terms.}$$

Here

$$\begin{Bmatrix} l_{\nu'} & j_{\nu'} & j_{\nu} & l_{\nu} \\ \frac{1}{2} & L & \frac{1}{2} & \lambda \\ l_{\kappa'} & j_{\kappa'} & j_{\kappa} & l_{\kappa} \end{Bmatrix}$$

is the 12–j symbol in the notation of Ord-Smith [6]); it can be expressed as a sum of the products of four 6-j symbols

$$(-)^{\tilde{S}} \sum_{x} (-)^{-x}[x] \begin{Bmatrix} j_{\nu} & j_{\kappa} & x \\ j_{\kappa'} & j_{\nu'} & L \end{Bmatrix} \begin{Bmatrix} j_{\kappa'} & j_{\nu'} & x \\ l_{\nu'} & l_{\kappa'} & \frac{1}{2} \end{Bmatrix} \begin{Bmatrix} l_{\nu'} & l_{\kappa'} & x \\ l_{\nu} & l_{\kappa} & \lambda \end{Bmatrix} \begin{Bmatrix} l_{\nu} & l_{\kappa} & x \\ j_{\kappa} & j_{\nu} & \frac{1}{2} \end{Bmatrix},$$

where $\tilde{S}$ is the sum of all 12 elements of the symbol. All the other symbols are the same as above. In the theory of eq. (22) we mix both the $S = 0$ and $S = 1$ states. Here again the relative parity cofactor $\pi = (-)^{l}$ characterizes the space exchange parts of the matrix element.

2.3. WAVE FUNCTION OF THE COLLECTIVE STATE

The theory discussed above corresponds to the construction of an approximate eigenmode $\hat{\mathcal{B}}^{\omega\dagger}_{LM,T}|\psi_0\rangle$, where $|\psi_0\rangle$ is the true ground state, having the following property:

$$([\hat{H}, \hat{\mathcal{B}}^{\omega\dagger}_{LM,T}])_{\text{linearized}} = \hbar\omega \hat{\mathcal{B}}^{\omega\dagger}_{LM,T}. \tag{23}$$

It corresponds to

$$(\hat{H}\hat{\mathcal{B}}^{\omega\dagger}_{LM,T})_{\text{linearized}}|\psi_0\rangle = (E_{\text{ground state}} + \hbar\omega)\hat{\mathcal{B}}^{\omega\dagger}_{LM,T}|\psi_0\rangle. \tag{24}$$

The operator $\hat{\mathcal{B}}^{\omega\dagger}_{LM,T}$ is sought in the form of a linear superposition of single-particle excitations

$$\hat{\mathcal{B}}^{\omega\dagger}_{LM,T} \equiv \sum_{\alpha \neq \alpha'} C^{\omega *}_{LM,T}(\alpha\alpha') \hat{A}^{T\dagger}_{LM}(\alpha\alpha'),$$

or

$$\hat{\mathcal{B}}^{\omega\dagger}_{LM,ST} \equiv \sum_{\alpha \neq \alpha'} C^{\omega *}_{LM,ST}(\alpha\alpha') \hat{F}^{ST}_{LM}(\alpha\alpha'), \tag{25}$$

if the L–S coupling scheme is used, and the above linearization refers to the operators involved in eq. (22). Substituting in eq. (22) and comparing coefficients, we readily obtain a system of equations for the expansion coefficients $C^{\omega}_{LM,T(ST)}(\nu\nu')$. The secular matrix of that equation turns out to be just the transpose of the matrix in eq. (14) or eq. (21).

This new form of the eigenvalue equation equivalent to eq. (12) can be written as

$$\sum_{\kappa \neq \kappa'} \Omega^{(LT)}_{\kappa\kappa',\nu\nu'} C^{\omega *}_{LM,T}(\kappa\kappa') = \hbar\omega C^{\omega *}_{LM,T}(\nu\nu'), \tag{26}$$

where the explicit form of the Ω-matrix can easily be derived from eq. (14)

or eq. (21). Also, we can easily check that $\Omega^{(LT)}_{\kappa\kappa',\nu\nu'} = -\Omega^{(LT)}_{\kappa'\kappa,\nu'\nu}$. It can be seen from the above that the secular problem may be written in the block form

$$\begin{Vmatrix} \Omega_1 & \Omega_2 \\ \Omega_2 & \Omega_1 \end{Vmatrix} \begin{Vmatrix} X \\ Y \end{Vmatrix} = \hbar\omega \begin{Vmatrix} X \\ -Y \end{Vmatrix}, \tag{27}$$

where the column submatrix $||X||$ stands for $||C^{\omega *}_{LM,T\,\nu<\nu'}(\nu\nu')||$, $||Y||$ for $||C^{\omega}_{LM,T\,\nu>\nu'}(\nu\nu')||$, $||\Omega_1||$ for $||\Omega^{(L)}_{\kappa\kappa'\nu\nu'}||_{\kappa<\kappa',\nu<\nu'}$, $||\Omega_2||$ for $||\Omega^{(L)}_{\kappa\kappa',\nu\nu'}||_{\kappa>\kappa',\nu<\nu'}$.

The form of eq. (26) is very similar to that obtained by Brown, Evans and Thouless [7]) and by Thouless [8]) for the case of a pure RPA. In their case, only particle-hole and hole-particle pairs were involved. In our case, in general, contributions from particle-particle and hole-hole pairs are also included, as well as the Hartree-Fock exchange terms. From eq. (26) and even more immediately from the hermitian adjoint of eq. (22), we see that for each eigenmode of energy $+|\hbar\omega|$, there is another solution for the negative energy $-|\hbar\omega|$. In view of their nature of collective excitations from the ground state [cf. eq. (23)], such negative energy solutions cannot represent new physical collective states, since the ground state energy is defined as lying below all states. Both the matrices Ω_1 and Ω_2 are hermitian and the secular problem of eq. (26) is nonhermitian. As a result the solutions of eq. (25) have rather peculiar properties.

First of all, in analogy to Thouless [8]) it can be shown that in the absence of a zero-energy solution, the set of solutions of eq. (25) is complete. In a discussion of a particular case, we have to find the stability condition, i.e., the condition for the reality of the secular equation roots. Next we can establish the relations of completeness and orthonormality for the $C^{\omega *}_{LM,T}(\alpha\alpha')$ coefficients.

The orthonormality condition is

$$\sum_{\alpha<\alpha'} [C^{\omega_n *}_{LM,T}(\alpha\alpha') C^{\omega_m}_{LM,T}(\alpha\alpha') - C^{\omega_n *}_{LM,T}(\alpha'\alpha) C^{\omega_m}_{LM,T}(\alpha'\alpha)] = \frac{\omega_n}{|\omega_n|}\delta_{mn} \tag{28}$$

and the completeness relation is

$$\sum_{\omega_n\neq 0} C^{\omega_n}_{LM,T}(\alpha\alpha') C^{\omega_n *}_{L'M',T}(\beta\beta') \frac{\omega_n}{|\omega_n|} = \delta_{\alpha\beta}\delta_{\alpha'\beta'}\delta_{LL'}\delta_{MM'}. \tag{29}$$

The orthonormality relation can be derived in analogy to refs. [1,9]) or from the obvious condition $\langle\psi_0|[\hat{\mathcal{B}}^{(n)}_{LM,T}, \hat{\mathcal{B}}^{(m)\dagger}_{LM,T}]|\psi_0\rangle = \delta_{mn}$ treated consistently with the approximation assumed for obtaining eq. (5) (cf. also a somewhat similar case discussed by Fallieros [10]) or in ref. [4])). The completeness relation eq. (28) can be verified directly by using the structure of eq. (26) and

by taking into account the fact that †

$$C^{-\omega *}_{LM,T}(\nu'\nu) = -(-)^M C^{\omega}_{L-M,T}(\nu\nu') = -(-)^M C^{\omega}_{LM,T}(\nu\nu').$$

From eqs. (28) and (29) we see that the $C^{\omega}_{LM,T}$ coefficients have certain properties described by an indefinite metric. This is a consequence of the non-hermiticity of the secular problem, eq. (26) following from the approximations of eq. (5). This type of indefinite metric has been discussed for the case of an infinite medium of fermions in the papers by Sawada [11]) and in ref. [4]).

2.4. HIGHER ORDER CORRECTIONS

We can now utilize eq. (29) in a discussion of non-linear terms of the third sum on the right-hand side of eq. (4), which have so far been completely neglected. The following method of "minimizing" the contribution of such terms is taken in analogy with refs. [11, 4]). We shall discuss below the case of a state (L, M) appropriate to a spherical nucleus, although it is obvious that this can be modified to a discussion of other states, e.g., those of deformed nuclei.

With the help of eq. (29) we can expand components of the $\hat{\varrho}$ operator in linear combination of the creation and destruction operation corresponding to the collective eigenmodes, $\hat{\mathscr{B}}^{\omega\dagger}_{LM,T}$ and $\hat{\mathscr{B}}^{\omega}_{LM,T} \equiv \hat{\mathscr{B}}^{-\omega\dagger}_{LM,T}$ respectively. We can then substitute the expressions thus obtained into the terms of the "4-operator non-linear terms" bilinear in $\hat{\varrho}$. By reordering the operators, specifically by bringing the destruction operators $\mathscr{B}^{\omega}_{LM,T}$ systematically to the right and the creation operators $\mathscr{B}^{\omega\dagger}_{LM,T}$ to the left, we can extract the lowest order bulk of contribution of these terms, and thus "minimize" the left-over part with respect to its expectation value on our collective state as discussed previously. These extracted lowest order terms are linear in $\hat{\varrho}$.

Let us first discuss the case of the j–j coupling scheme. We can introduce the operators χ^T, creating pairs with definite isobaric spin: $T = 0$ and $T = 1$ $(T_3 = 0)$. In terms of these operators, we can write

$$\hat{\varrho}_{\alpha\alpha'}(\tau\tau) = \tfrac{1}{2}\sqrt{2}(\hat{\chi}^0_{\alpha\alpha'} + \hat{\chi}^1_{\alpha\alpha'}), \qquad \hat{\varrho}_{\alpha\alpha'}(-\tau-\tau) = \tfrac{1}{2}\sqrt{2}(\hat{\chi}^0_{\alpha\alpha'} - \hat{\chi}^1_{\alpha\alpha'}) \tag{30}$$

where $\tau = \pm$ is the proton (neutron)charge.

Let us now concentrate for definiteness on the case of the $T = 1$ and the negative parity state (the giant dipole state in nuclei). First we can rewrite the nonlinear terms [bottom line of eq. (4)] after summing over τ [i.e., taking the combination $\frac{1}{2}\sqrt{2}(\tau\tau) - (\tau\tau)$] in the form

$$\begin{aligned}\Gamma^{(4)}_{\nu\nu'}(T=1) = \tfrac{1}{2}\sqrt{2} \sum_{L'M'} \sum_{\kappa \neq \kappa'} \{ \sum_{s \neq \nu'} (-)^{m_s + m_\kappa + M'} (j_s j_\nu; m_s - m_\nu | L'M') \\ \times (j_\kappa j_{\kappa'}; m_\kappa - m_{\kappa'} | L' - M') [(\tfrac{3}{2} f^{(1)}_{L'} + \tfrac{1}{2} f^{(0)}_{L'} + \tfrac{3}{2} g^{(1)}_{L'} + \tfrac{1}{2} g^{(0)}_{L'})(s\nu, \kappa\kappa') \hat{\chi}^0_{\kappa\kappa'} \hat{\chi}^1_{s\nu'} \\ + \tfrac{1}{2}(f^{(1)}_{L'} - f^{(0)}_{L'} + g^{(1)}_{L'} - g^{(0)}_{L'})(s\nu, \kappa\kappa') \hat{\chi}^1_{\kappa\kappa'} \hat{\chi}^0_{s\nu'} - \tfrac{1}{2}(f^{(1)}_{L'} - f^{(0)}_{L'} + g^{(1)}_{L'} - g^{(0)}_{L'})(s\nu, \kappa\kappa')\end{aligned} \tag{31}$$

† In the case of the L-S coupling scheme, we do not have the extra $-$ sign on the right-hand side.

$$\times(\hat{\chi}^0_{s\kappa'}\hat{\chi}^1_{\kappa\nu'}-\hat{\chi}^1_{s\kappa'}\hat{\chi}^0_{\kappa\nu'})]-\sum_{s\neq\nu}(-)^{m_{\nu'}+m_\kappa+M'}(j_{\nu'}j_s;\, m_{\nu'}-m_s|L'M')$$

$$\times(j_\kappa j_{\kappa'};\, m_\kappa-m_{\kappa'}|L'-M')[(\tfrac{3}{2}f^{(1)}_{L'}+\tfrac{1}{2}f^{(0)}_{L'}+\tfrac{3}{2}g^{(1)}_{L'}+\tfrac{1}{2}g^{(0)}_{L'})(\nu' s,\, \kappa\kappa')\hat{\chi}^0_{\nu s}\hat{\chi}^1_{\kappa\kappa'} \qquad (31)$$

$$+\tfrac{1}{2}(f^{(1)}_{L'}-f^{(0)}_{L'}+g^{(1)}_{L'}-g^{(0)}_{L'})(\nu' s,\, \kappa\kappa')\hat{\chi}^1_{\nu s}\hat{\chi}^0_{\kappa\kappa'}-\tfrac{1}{2}(f^{(1)}_{L'}-f^{(0)}_{L'}+g^{(1)}_{L'}-g^{(0)}_{L'})$$

$$\times(\nu' s,\, \kappa\kappa')(\hat{\chi}^0_{\kappa s}\hat{\chi}^1_{\nu\kappa'}-\hat{\chi}^1_{\kappa s}\hat{\chi}^0_{\nu\kappa'})]\}.$$

The "mixed terms" — the last (3rd) terms in the respective two sums over s — stem from the rearrangement of products of proton-neutron (neutron-proton) pairs as, e.g., $\hat{\varrho}_{\kappa\kappa'}(\tau-\tau)\hat{\varrho}_{s\nu'}(-\tau\tau)=-\hat{\varrho}_{s\kappa'}(-\tau-\tau)\hat{\varrho}_{\kappa\nu'}(\tau\tau)+\delta_{\kappa\nu'}\hat{\varrho}_{s\kappa'}(-\tau-\tau)$.

As an example, we can now consider the first term in eq. (31). Using eq. (29) we can write

$$\hat{\chi}^0_{\kappa\kappa'}\hat{\chi}^1_{s\nu'}=-\hat{\chi}^0_{\kappa\kappa'}\sum_{L''M''}(-)^{m_s}(j_s j_{\nu'};\, -m_s m_{\nu'}|L''M'')\sum_{\omega_n>0}(C^{\omega_n *}_{L''M'',1}(s\nu')$$

$$\times\hat{\mathscr{B}}^{\omega_n\dagger}_{L''M'',1}-C^{-\omega_n *}_{L''M'',1}(s\nu')\hat{\mathscr{B}}^{\omega_n}_{L''M'',1}). \qquad (32)$$

The linear contribution to be extracted from this expression involves the commutator of $\hat{\chi}^0_{\kappa\kappa'}$ and $\hat{\mathscr{B}}^{\omega_n\dagger}_{L''M'',1}$ and equals

$$-\sum_{L''M''}\sum_{\omega_n>0}\sum_{\alpha\neq\alpha'}C^{\omega_n *}_{L''M'',1}(s\nu')C^{\omega_n *}_{L''M'',1}(\alpha\alpha')(-)^{m_s}(j_s j_{\nu'};\, -m_s m_{\nu'}|L''M'')$$

$$\times(-)^{m_\alpha}(j_\alpha j_{\alpha'};\, -m_\alpha m_{\alpha'}|L''M'')(\delta_{\kappa\alpha'}\hat{\chi}^1_{\alpha\kappa'}-\delta_{\alpha\kappa'}\hat{\chi}^1_{\kappa\alpha'}). \qquad (33)$$

The term with $\hat{\chi}^1_{\kappa\kappa'}\hat{\chi}^0_{s\nu'}$ produces a contribution involving the commutator of $\hat{\mathscr{B}}^{\omega_n}_{L''M'',1}$ with $\hat{\chi}_{s\nu'}$, etc. Out of each such contribution, we can then project out the part appropriate to the state (L, M) in the sense of eq. (7). As a final result, we obtain for the first contribution (of eq. (33))

$$\Delta_1{}^{(4)}(\nu\nu')_{LM,1}=-\tfrac{1}{2}\sqrt{2}\sum_{L'M'L''M''}\sum_{\kappa\neq\kappa'}\sum_{s\neq\nu'}\sum_{\alpha}\sum_{\omega_n>0}(\tfrac{3}{2}f^{(1)}_{L'}+\tfrac{1}{2}f^{(0)}_{L'}+\tfrac{3}{2}g^{(1)}_{L'}+\tfrac{1}{2}g^{(0)}_{L'})$$

$$\times(s\nu,\, \kappa\kappa')(-)^{j_{\nu'}-j_\alpha}\begin{Bmatrix} j_\nu & j_{\nu'} & L\\ L'' & L' & j_s\end{Bmatrix}C^{\omega_n *}_{L''M'',1}(s\nu')\Big[(-)^{L'+L''-L}\begin{Bmatrix} j_{\kappa'} & j_\alpha & L\\ L'' & L' & j_\kappa\end{Bmatrix} \qquad (34)$$

$$\times C^{\omega_n *}_{L''M'',1}(\alpha\kappa)A^{1*}_{LM}(a\kappa')-\begin{Bmatrix} j_\kappa & j_\alpha & L\\ L'' & L' & j_{\kappa'}\end{Bmatrix}C^{\omega_n *}_{L''M'',1}(\kappa'\alpha)A^{1*}_{LM}(\kappa\alpha)\Big].$$

From eq. (34) we see that, in general, knowledge of the solutions of the linear problems for $L'' \neq L$ may be needed for the actual evaluation of these correction terms. In particular cases, however, one is able to obtain a rough estimate of their effect, and this we shall do for one example below. The complete expression for all the linear correction terms coming from all the nonlinear terms of eq. (31) is given in the Appendix.

In the case of the L–S coupling scheme, it is convenient to use the operators

$\hat{\chi}^S$ with $S_3 = T_3 = 0$, defined as

$$2\hat{\chi}^{ST} \equiv \hat{\varrho}(\tau\tau, \sigma\sigma)+(-)^S\hat{\varrho}(\tau\tau, -\sigma-\sigma)+(-)^T\hat{\varrho}(-\tau-\tau, \sigma\sigma) +(-)^{S+T}\hat{\varrho}(-\tau-\tau, -\sigma-\sigma). \quad (35)$$

Out of all the resulting terms containing products $\hat{\chi}^{ST}\hat{\chi}^{S'T'}$, only those involving $\hat{\chi}^{01}$ can be "minimized" for the $S = 0$, $T = 1$ ($T_3 = 0$) state. The complete sum of such terms is equal to

$$\begin{aligned}
&\Gamma^{(4)}_{\nu\nu'}(S=0,\ T=1)\\
&\quad=\tfrac{1}{2}\sum_{\kappa\neq\kappa'}\Big\{\sum_{s\neq\nu'}\Delta V_{s\nu,\kappa\kappa'}[(4w-m+2b-2h)\hat{\chi}^{00}_{\kappa\kappa'}\hat{\chi}^{01}_{s\nu'}-(m+2h)\hat{\chi}^{01}_{\kappa\kappa'}\hat{\chi}^{00}_{s\nu'}]\\
&\quad-\sum_{s\neq\nu}\Delta V_{\nu's,\kappa\kappa'}[(4w-m+2b-2h)\hat{\chi}^{00}_{\nu s}\hat{\chi}^{01}_{\kappa\kappa'}-(m+2h)\hat{\chi}^{01}_{\nu s}\hat{\chi}^{00}_{\kappa\kappa'}]\Big\}\\
&\quad+\tfrac{1}{4}\sum_{\kappa\kappa's}\Delta V_{s\nu,\kappa\kappa'}[(3m-b+h)\hat{\chi}^{00}_{s\kappa'}\hat{\chi}^{01}_{\kappa\nu'}-(m+b+h)\hat{\chi}^{01}_{s\kappa'}\hat{\chi}^{00}_{\kappa\nu'}] \qquad (36)\\
&\quad-\tfrac{1}{4}\sum_{\kappa\kappa's}\Delta V_{\nu's,\kappa\kappa'}[(3m-b+h)\hat{\chi}^{00}_{\kappa s}\hat{\chi}^{01}_{\nu\kappa'}-(m+b+h)\hat{\chi}^{01}_{\kappa s}\hat{\chi}^{00}_{\nu\kappa'}].
\end{aligned}$$

Here again the two bottom lines of eq. (36) correspond to a rearrangement of the revelant "mixed "terms. After using the method of the Moshinsky and Brody transformations brackets [5]) for the harmonic oscillator eigenfunctions, we can, as in the preceding case, extract the (LM) component of the effective linear contribution of eq. (36). For example, we obtain for the first term on the right-hand side of eq. (36) the contribution

$$\begin{aligned}
\Delta_1^{(4)}(\nu\nu')_{LM,01} &= \tfrac{1}{2}(4w-m+2b-2h)\sum_{\kappa\neq\kappa'}\sum_{s\neq\nu'}\sum_{nn'N\mathscr{L}}\sum_{\lambda\beta}\sum_{L''M''}\sum_{\alpha}\sum_{\omega_n>0}\\
&\times\langle nl, N\mathscr{L}, \lambda|n_s l_s, n_{\kappa'} l_{\kappa'}, \lambda\rangle\langle n'l, N\mathscr{L}, \lambda|n_\nu l_\nu, n_\kappa l_\kappa, \lambda\rangle\\
&\times\langle n'l||\Delta V(r)||nl\rangle C^{\omega_n *}_{L''M''}(s\nu')\left[(-)^{l_{\nu'}+l_\alpha}(-)^{L''+\lambda-L}\begin{Bmatrix} L & l_\alpha & l_{\kappa'}\\ l_{\nu'} & L'' & l_s\\ l_\nu & l_\kappa & \lambda\end{Bmatrix}\right. \qquad (37)\\
&\times C^{\omega_n *}_{L''M''}(\alpha\kappa)F^{01*}_{LM}(\alpha\kappa)-(-)^{l_\nu+l_s+l_\kappa+l_{\kappa'}}(-)^{L-L''}\left(\frac{[l_\alpha]}{[l_{\kappa'}]}\right)^{\frac{1}{2}}\begin{Bmatrix} l_{\nu'} & l_s & L''\\ l_{\kappa'} & l_\alpha & \lambda\end{Bmatrix}\\
&\times\left.\begin{Bmatrix} l_\nu & l_\kappa & \lambda\\ l_\alpha & l_{\nu'} & L\end{Bmatrix}C^{\omega_n *}_{L''M''}(\kappa'\alpha)F^{01*}_{LM}(\kappa\alpha)\right].
\end{aligned}$$

Here the subscript $ST = 01$ is omitted for simplicity.

The complete expression for all the linear correction terms resulting from $\Gamma^{(4)}$ of eq. (36) is given in the Appendix. As in the previous case of eq. (31), among the terms calculated there are terms of the self-energy type which may, in general, be included in the zero-order energies in a self-consistent manner.

We have performed a rough estimate of the magnitude of the non-self-energy

terms coming from eq. (36) as given in eq. (A.2) of the Appendix. We have found that such terms can at most contribute only a few percent of the RPA terms of eq. (20) in the case of the giant dipole state of the O^{16} nucleus discussed below. The numerical smallness results from the quadratic expressions of $C^{\omega_n}_{LM,01}$ and from the 6–j and 9–j coefficients. We believe, therefore, that in similar problems the RPA is probably a good approximation. It is possible that, in other cases where the contributions discussed above are important, the inclusion of such contributions restores the self-consistency of the theory and still allows calculations with linear equations involving self-consistent single-particle energies and $H_0(\mathbf{r})$.

The method of ref. [4]) consisted of defining a self-consistent single-particle potential and the appropriate "renormalized" single-particle spectrum by diagonalizing the "self-consistent" energy equations. The effective single-particle potential thus defined involves the "screening" effect produced by the summations of the higher order particle-hole diagrams. We have been able to derive closely analogous self-consistent equations for the case of a finite system. However, the mathematical difficulties in solving that system of equations seem to render the method of little practical value for this case. Here the extension of the simple linearized theory as presented above seems to be the simplest first possible improvement on the usual RPA.

It is probably not impossible also to attack in the future the original non-linear exact eq. (2) by using the spectral representation for the non-linear terms and to use a Tamm-Dancoff type of approximation for them by retaining only terms corresponding to the most important part of the single-particle energy spectrum. It would be interesting to compare the solution of such a problem with the results of our linearized theory.

3. The Giant Dipole State

Recently, Brown and co-workers presented in several papers [12])† a calculation of the giant dipole resonance for the finite nuclei. Their calculation is based on the mechanism of the particle-hole interaction producing the dipole state $J^\pi = 1$, $T = 1^-$. Their calculation is essentially similar to the early calculation by Elliott and Flowers [13]) for the O^{16} nucleus.

However, Brown *et al.* [12]) do not take into account a few features of the actual nuclear problem. Brown and Bolsterli [12]) ignore the exclusion principle by neglecting the exchange parts of the matrix elements of ΔV, which should be properly antisymmetrized. This antisymmetrization, which by itself takes into account one feature of the non-linearity of the problem, leads to most essential terms changing the discussion of the required properties of ΔV.

† A similar theory of infinite nuclear matter has been developed by W. Brenig [12]).

Secondly, Brown *et al.* retain only the hole-particle amplitudes, i.e., those in which one particle is lifted from below the Fermi surface to an originally empty state in the ground state. This approximation reduces the order of the RPA secular problem by a factor of two. This corresponds to the completely uncorrelated ground state. Thirdly, the zero-range approximation is used in ref. [12]). These authors also do not discuss the self-consistency aspect of their choice of ΔV, i.e., the self-energy terms and their relation to the assumed shell model.

We have performed a calculation of the O^{16} problem avoiding the assumptions and approximation of the above three points. Once more, however, our calculation does not use a self-consistent shell model hamiltonian.

Similarly, like Brown *et al.* [12]) we have used the harmonic oscillator wave functions and the empirical single-particle and single-hole excitation energies in O^{16}, as given in their table 1.

The matrix elements were computed numerically, using the method of transformation brackets of ref. [5]) and the secular equation of eq. (22) was solved with the help of the IBM 704 computer at the University of California, Berkeley. The eigenvectors were also determined with the aid of the computer. The secular matrix in our case is a 10×10 matrix in contrast with that of Brown *et al* [12]), which is 5×5. For each test case we have five 10-component eigenvectors corresponding to the five positive excitation energies.

The dipole radiative transition matrix element is given by

$$M_{0\omega_n} = \hat{S} \sum_{\alpha \neq \alpha'} C^{\omega_n *}_{10,1}(\alpha\alpha') D_{\alpha\alpha'},$$
$$D_{\alpha\alpha'} = \{[j_\alpha][j_{\alpha'}]\}^{\frac{1}{2}} (j_\alpha j_{\alpha'}; \tfrac{1}{2} -\tfrac{1}{2}|10) \int R_\alpha R_{\alpha'} r^3 \mathrm{d}r. \tag{38}$$

Here $\hat{S}$ is a constant factor independent of ω_n, and R_α is a radial wave function of the state α. Note that our phase is different from that of ref. [12]). The γ-ray width of each state n is proportional to $\gamma_n = (\hbar\omega_n)^3 |M_{0\omega_n}|^2$.

We have examined two phenomenological interactions ΔV. The first, given by Ferrell and Visscher [14]) and employed by Fallieros [10]), is

(I)
$$\Delta V(r) = -V_0 \mathrm{e}^{-r^2/\alpha^2}, \quad V_0 = 51.9 \text{ MeV}, \quad \alpha = 1.732 \text{ fm},$$
$$w = 0.317, \quad m = 0.5, \quad b = 0, \quad h = 0.183.$$

The other is the Rosenfeld mixture used by Elliott and Flowers [13]):

(II)
$$\Delta V(r) = -V_0[\mathrm{e}^{-r/r_0}/(r/r_0)], \quad V_0 = 43 \text{ MeV}, \quad r_0 = 1.4 \text{ fm},$$
$$w = -0.13, \quad m = 0.93, \quad b = 0.46, \quad h = -0.26.$$

These two examples of ΔV differ markedly in range and radial shape and mainly in their exchange mixtures.

As a preliminary test case we performed the calculation, neglecting the spin-orbit splitting of the single-particle energy levels, by taking the averages of the single-particle and single-hole excitation for each two $j = l \pm \frac{1}{2}$ levels, respectively. We then solved the degenerate 4×4 secular problem with the help of eqs. (20) and (21). If we omit the self-energy term E, we find

for the ΔV of (I): $\hbar\omega_1 = 23.5$ MeV (90.4 % of the dipole strength),
$\hbar\omega_2 = 17.1$ MeV (9.6 % of the dipole strength);

for the ΔV of (II): $\hbar\omega_1 = 22.6$ MeV (98 % of the dipole strength),
$\hbar\omega_2 = 18.2$ MeV (2 % of the dipole strength).

We can see that, although the roots are closer together for the interaction (II), and the dipole strength distribution is somewhat different, both (I) and (II) give essentially similar results. The non-self-consistent inclusion of the E terms "pushes" the roots $\hbar\omega_n$ a few MeV higher. This shows the importance of a self-consistency calculation of the zero-order field. In the numerical results given below the self-energy terms are left out. Such terms, if included "phenomenologically", would always push the roots $\hbar\omega_n$ a few MeV up. Such self-energy terms should already have been included in the zero-order field.

The results of our computations are summarized in tables 1 and 2.

TABLE 1

Computed energies of $T = 1$, $L = 1$ levels in O^{16} and their dipole strengths for the complete RPA.

Ferrell and Visscher force (I)		Elliott and Flowers force (II)	
$\hbar\omega$	% dipole strength	$\hbar\omega$	% dipole strength
25.8	9.5	25.3	48.0
20.9	24.9	21.9	47.3
20.6	59.8	20.6	4.1
16.5	5.5	16.9	0.1
14.0	0.3	11.2	0.5

The results in table 1 correspond to the complete RPA of eq. (22), i.e., with all the effects mentioned above included.

In table 2 the results are given for the RPA with no diagonal matrix elements in the particle-hole (hole-particle) pairs, i.e. with $[\Delta V(1-P^{12})]_{\alpha'\alpha,\alpha\alpha'}$ removed from the diagonal of the secular matrix. This case is considered for the sake of comparison of the consequences of two different definitions of the "residual" interaction ΔV and in order to see whether the main bulk on the "giant dipole" effect stems from the off-diagonal elements. In this case it is assumed that, in addition to the previously defined self-energy terms, the elements $[\Delta V(1-P^{12})]_{\alpha'\alpha,\alpha\alpha'}$ diagonal in pairs are also included in the zero-order self-consistent single-particle energies.

TABLE 2

Computed energies of $T = 1$, $L = 1$ levels in O^{16} and their dipole strenghts for the case of the elements diagonal in the interaction of pairs removed

Ferrell and Visscher force (I)		Elliott and Flowers force (II)	
	% dipole strength		% dipole strength
23.4	13.8	23.2	44.8
18.7	19.1	19.0	54.0
17.4	63.6	18.4	0.4
15.1	3.4	14.6	0.2
12.0	0.1	12.1	0.6

All the above numerical results were obtained for the harmonic oscillator scale parameter $\nu^{-\frac{1}{2}} = 1.68$ fm taken according to Ferrell and Visscher [14]) and ref. [10]). This value of $\nu^{-\frac{1}{2}}$ is not exactly equal to $\nu^{-\frac{1}{2}}$ of refs. [12, 13]). In order to see the effect of the inclusion of the "backward-going graphs", we have also diagonalized the 5×5 matrix for the case of the interaction (II) of Elliott and Flowers [13]) from our table 1, corresponding to no correlation effects in the ground state (only hole states in the ground state occupied as in a pure Fermi sea). The result is given in table 3.

TABLE 3

Computed energies of $T = 1$, $L = 1$ levels in O^{16} and their dipole strengths for interaction (II) and for the RPA with no correlations in the ground state.

$\hbar\omega$	25.4	22.0	20.6	17.0	11.3
% dipole strength	45.9	50.1	3.4	0.1	0.5

The strength distribution in the case of interaction (II) for the two highest energies differs somewhat from the results in refs. [12, 13]). This can perhaps be attributed in part also to the difference in the value of the parameter $\nu^{-\frac{1}{2}}$ used here and in refs. [12, 13]). From the comparison of tables 1 and 3 we see that the inclusion of the correlations in the ground state, i.e., "the backward-going graphs", changes only slightly the distribution of the dipole strength in this particular case.

A typical eigenvector of the giant dipole state is presented in table 4, indicating the relative weight of the "time-reversed "amplitudes. We see that

TABLE 4

The eigenvectors of the giant dipole states in O^{16}, $\hbar\omega_{1,2} = 25.3$, 21.9 MeV, for the interaction (II) (cf. table 1)

pair $(\nu\nu')$	$p_{\frac{1}{2}}^{-1}s_{\frac{1}{2}}$	$p_{\frac{3}{2}}^{-1}s_{\frac{1}{2}}$	$p_{\frac{1}{2}}^{-1}d_{\frac{3}{2}}$	$p_{\frac{3}{2}}^{-1}d_{\frac{3}{2}}$	$p_{\frac{3}{2}}^{-1}d_{\frac{5}{2}}$	$s_{\frac{1}{2}}p_{\frac{1}{2}}^{-1}$	$s_{\frac{1}{2}}p_{\frac{3}{2}}^{-1}$	$d_{\frac{3}{2}}p_{\frac{1}{2}}^{-1}$	$d_{\frac{3}{2}}p_{\frac{3}{2}}^{-1}$	$d_{\frac{5}{2}}p_{\frac{3}{2}}^{-1}$
$C_{1M,1}^{\omega_1 *}(\nu\nu')$	0.018	–0.145	0.263	–0.273	–0.915	–0.006	–0.017	0.027	–0.002	0.013
$C_{1M,1}^{\omega_2 *}(\nu\nu')$	0.087	0.030	–0.399	0.836	–0.368	0.005	–0.003	0.014	0.013	0.021

the particle-hole components corresponding to the correlations in the ground state due to the presence of ΔV are not quite negligible in the case of the giant dipole state. However, they are, of course, generally smaller than the hole-particle components for the other four states also.

We have found in fact that the effect of the giant dipole state in O^{16} is not quite insensitive to the choice of ΔV, and, in particular, to the inclusion of the exchange terms and the finite range of ΔV. In our case the two examples of ΔV used are characterized by very different radial shapes, well depths, and exchange mixture parameters. In particular, our ΔV (I) and (II) have very different "effective" coefficients: $-u_t^{01} = (m+2h)+(-)^t(w+2b)$ in eq. (20), and $(h+(-)^t b)$ and $(m+(-)^t w)$ in eq. (22) for the $T = 1$ state. In fact, the giant dipole state is "pushed" a little higher in energy for case (II). We get a somewhat different distribution of the dipole strengths for cases (I) and (II). The dipole strength is exhausted by the highest three levels in case (I), only by the two highest ("giant") states in case (II). On the whole, the agreement with experiment seems to be better for interaction (II).

From a comparison of tables 1 and 2 we see that the effect of the giant dipole state (the dipole strength distribution) is grossly independent of the matrix elements diagonal in hole-particle (particle-hole) pairs. The removal of these elements only causes the levels to "sink" in energy relative to the case of table 1.

4. Final Comments and Concluding Remarks

A theory of the type described above is a practical extension and generalization of the usual shell model configuration mixing calculations. It provides a better understanding of the relation of the shell-model calculations to a more general theory of the nuclear many-body system.

One of the most important open problems here is the question of the "residual interaction potential ΔV. We cannot claim reliable quantitative results until we have first solved the ground state problem self-consistently, including all the self-energy terms, and extracted what can be termed the "residual" interaction. In this respect the above theory carries all the sins of the usual shell model. One key to the problem is the Brueckner theory of the foundations of the shell model. One attempt to determine ΔV would be to extract the off-diagonal part of the reaction matrix not included in the solution of the ground state problem and the effective contribution of the higher cluster terms. In particular, the components of the reaction matrix involving pairs of particle and hole states are essential.

Thouless [15])† proposes to replace the actual two-body interaction by some effective smoothed-out interaction, chosen in such a way that it gives saturation of nuclear matter at the correct energy and density. An approximate ground

† See also ref. [8]).

state is calculated by solving the Hartree-Fock equations. If the calculation is successful, we find the single-particle shell-model energies, which should agree with experiment. We can then proceed to use the "pure" RPA (without the self-energy terms). A simplified version of such a program, proposed by Thouless, would be based on a variational procedure minimizing the expectation value of the energy by varying a few parameters rather than by solving the complete ground state problem.

In any case, one should try to construct a ΔV having no diagonal matrix elements (at least no ordinary self-energy terms). The version of our calculation involving removal of elements of ΔV diagonal in the hole-particle (particle-hole) pair states corresponds to yet another solution of the ground state problem.

In spite of the difficulty in the choice of ΔV, the results of our numerical calculation are of a qualitative and generally quantitative significance.

The well-known problem of the extended shell-model calculations including the Bardeen-Cooper-Schrieffer-type pairing force, which is of particular importance for the vibrational states of unfilled spherical nuclear subshells, has the extra difficulty connected with the H_{31} and H_{22} parts of the effective "residual" interaction of two quasiparticles, i.e., with the parts involving three destruction (creation) operators with one creation (destruction) operator, and two destruction (creation) operators, respectively. We shall not discuss this problem here.

We are indebted to Drs. G. A. Baker, Jr. and B. Hill of Los Alamos, for making their matrix diagonalization computer programs available to us. We also gratefully acknowledge the cooperation of the IBM 704 computer staff at the University of California, Berkeley. One of us (J. S.) is greatly indebted to Dr. S. G. Nilsson for many stimulating discussions, and to Dr. D. J. Thouless for a private communication.

Note added in proof: As a supplement to our tables 1 and 3 we give in table 5

TABLE 5

The values of f_{0n} and $\Gamma_{\gamma_{0n}}$ (in keV) for the five $T = 1$, $L = 1$ levels in O^{16}

Ferrell and Visscher force (I)			Elliott and Flowers force (II)					
Complete RPA			Complete RPA			No correlations in the ground state		
$\hbar\omega_{0n}$	f_{0n}	$\Gamma_{\gamma_{0n}}$	$\hbar\omega_{0n}$	f_{0n}	$\Gamma_{\gamma_{0n}}$	$\hbar\omega_{0n}$	f_{0n}	$\Gamma_{\gamma_{0n}}$
25.8	0.3	3	25.3	2.4	24	25.4	2.4	24
20.9	1.2	8	21.9	3.1	24	22.0	3.4	25
20.6	2.8	19	20.6	0.3	2	20.6	0.3	2
16.5	0.4	2	16.9	0.0	0	17.0	0.0	0
14.0	0.0	0	11.2	0.1	0	11.3	0.1	0
sums	4.7			5.9			6.2	

the absolute values of the dipole strengths $f_{0n} = (2M\hbar\omega_n/\hbar^2)\langle|M_{0\omega_n}|^2\rangle$, where $\langle\ \rangle$ is the properly weighted average (cf. $\hat{S}$ of eq. (38)), and the corresponding reduced widths $\Gamma_{\gamma_{0n}}$ for the spontaneous γ-emission. Note that what we meant by "dipole strength" in sect. 3 is the percentage distribution of the quantity $\Gamma_{\gamma_{0n}}$.

The corresponding results for the case with the diagonal elements removed (cf. table 2) are almost identical. The average values of $\sum_n f_{0n}$ have to be compared with the single particle dipole sum equal 4.7. The latter differs from 4.0 (the Thomas-Kuhn-Reiche limit) as we have used empirical rather than model single particle excitation energies.

Appendix

In subsection 2.4, we discussed the higher order linear correction terms resulting from a "minimization" of the terms bilinear in the density operator $\hat{\varrho}$.

In the case of the j–j coupling scheme, we find the complete form of such correction terms for a $T = 1$ state to be

$$
\begin{aligned}
\Delta^{(4)}(\nu\nu')_{LM,1} = {} & \tfrac{1}{2}\sqrt{2}\sum_{\omega_n>0}\sum_{\kappa\neq\kappa'}\sum_{s\neq\nu'}\sum_{\alpha}\sum_{L'M',L''M''}[\tfrac{1}{2}(3f^{(1)}_{L'}+f^{(0)}_{L'}+3g^{(1)}_{L'}+g^{(0)}_{L'})(s\nu,\kappa\kappa')\\
&\times O^{\omega_n *}_{L'L''L}(\nu\nu' s,\kappa\kappa'\alpha)+\tfrac{1}{2}(f^{(1)}_{L'}-f^{(0)}_{L'}+g^{(1)}_{L'}-g^{(0)}_{L'})(s\nu,\kappa\kappa')P^{\omega_n}_{L'L''L}(\nu'\nu s,\kappa'\kappa\alpha)]\\
&-\tfrac{1}{2}\sqrt{2}\sum_{\omega_n>0}\sum_{\kappa\neq\kappa'}\sum_{s\neq\nu}\sum_{\alpha}\sum_{L'M',L''M''}[\tfrac{1}{2}(3f^{(1)}_{L'}+f^{(0)}_{L'}+3g^{(1)}_{L'}+g^{(0)}_{L'})(\nu' s,\kappa\kappa')\\
&\times P^{\omega_n *}_{L'L''L}(\nu\nu' s,\kappa\kappa'\alpha)+\tfrac{1}{2}(f^{(1)}_{L'}-f^{(0)}_{L'}+g^{(1)}_{L'}-g^{(0)}_{L'})(\nu' s,\kappa\kappa')O^{\omega_n}_{L'L''L}(\nu'\nu s,\kappa'\kappa\alpha)]\\
&+\tfrac{1}{2}\sum_{\omega_n>0}\sum_{\kappa\kappa'\alpha}\sum_{L'M',L''M''}[\tfrac{1}{2}(f^{(1)}_{L'}-f^{(0)}_{L'}+g^{(1)}_{L'}-g^{(0)}_{L'})(s\nu,\kappa\kappa')(T^{\omega_n *}_{L'L''L}(\nu\nu' s,\kappa\kappa'\alpha)\\
&+S^{\omega_n}_{L'L''L}(\nu\nu' s,\kappa\kappa'\alpha))-\tfrac{1}{2}(f^{(1)}_{L'}-f^{(0)}_{L'}+g^{(1)}_{L'}-g^{(0)}_{L'})(\nu' s,\kappa\kappa')\\
&\times(T^{-\omega_n}_{L'L''L}(\nu'\nu s,\kappa'\kappa\alpha)+S^{-\omega_n *}_{L'L''L}(\nu'\nu s,\kappa'\kappa\alpha))],
\end{aligned}
\tag{A.1}
$$

where

$$
\begin{aligned}
O^{\omega_n *}_{L'L''L}(\nu\nu' s,\kappa\kappa'\alpha) \equiv {} & (-)^{j_{\nu'}-j_\alpha}\begin{Bmatrix} j_\nu & j_{\nu'} & L\\ L'' & L' & j_s\end{Bmatrix}C^{\omega_n *}_{L''M'',1}(s\nu')\Big[(-)^{L'+L''-L}\\
&\times\begin{Bmatrix} j_{\kappa'} & j_\alpha & L\\ L'' & L' & j_\kappa\end{Bmatrix}C^{\omega_n *}_{L''M'',1}(\alpha\kappa)A^{1*}_{LM}(\alpha\kappa')-\begin{Bmatrix} j_\kappa & j_\alpha & L\\ L'' & L' & j_{\kappa'}\end{Bmatrix}C^{\omega_n *}_{L''M'',1}(\kappa'\alpha)A^{1*}_{LM}(\kappa\alpha)\Big],
\end{aligned}
$$

$$
\begin{aligned}
P^{\omega_n *}_{L'L''L}(\nu\nu' s,\kappa\kappa'\alpha) \equiv {} & \delta_{L''L'}\delta_{M''M'}(-)^{j_\kappa+j_{\kappa'}-j_{\nu'}-j_s}C^{\omega_n *}_{L'M',1}(\kappa\kappa')\\
&\times\Big[(-)^{L-L'}\begin{Bmatrix} j_{\nu'} & j_s & L'\\ j_\alpha & j_\nu & L\end{Bmatrix}C^{\omega_n *}_{L'M',1}(\alpha\nu)A^{1*}_{LM}(\alpha s)+[j_{\nu'}]^{-1}\delta_{j_\alpha j_{\nu'}}C^{\omega_n *}_{L'M',1}(s\alpha)A^{1*}_{LM}(\nu\alpha)\Big],
\end{aligned}
$$

$$
\begin{aligned}
S^{\omega_n}_{L'L''L}(\nu\nu' s,\kappa\kappa'\alpha) = {} & -(-)^{L-L'}(-)^{j_\kappa+j_{\kappa'}-j_\nu-j_s}\begin{Bmatrix} j_\nu & j_s & L'\\ j_{\kappa'} & j_\kappa & L''\end{Bmatrix}C^{\omega_n}_{L''M'',1}(\kappa' s)\\
&\times\Big[(-)^{L-L''}[j_\nu]^{-1}C^{\omega_n}_{L''M'',1}(\kappa\alpha)\delta_{j_\alpha j_\nu}A^{1}_{LM}(\alpha\nu')+\begin{Bmatrix} j_{\nu'} & j_\alpha & L''\\ j_\kappa & j_\nu & L\end{Bmatrix}C^{\omega_n}_{L''M'',1}(\alpha\nu')A^{1}_{LM}(\kappa\alpha)\Big],
\end{aligned}
$$

$$T^{\omega_n^*}_{L'L''L}(\nu\nu' s,\ \kappa\kappa'\alpha) \equiv (-)^{j_\kappa+j_{\kappa'}-j_\nu-j_s} C^{\omega_n^*}_{L''M'',1}(\kappa\nu')$$

$$\times\left[[j_\alpha]^{\frac{1}{2}}[j_{\kappa'}]^{-\frac{1}{2}}(-)^{L-L''}\begin{Bmatrix} j_{\nu'} & j_\kappa & L'' \\ j_{\kappa'} & j_\alpha & L'\end{Bmatrix}\begin{Bmatrix} j_\nu & j_s & L' \\ j_\alpha & j_{\nu'} & L\end{Bmatrix} C^{\omega_n^*}_{L''M'',1}(\kappa'\alpha)\, A^{1*}_{LM}(s\alpha)\right.$$

$$\left.-\begin{Bmatrix} L & j_{\kappa'} & j_\alpha \\ j_{\nu'} & j_\kappa & L'' \\ j_\nu & L' & j_s\end{Bmatrix} C^{\omega_n^*}_{L''M'',1}(\alpha s) A^{1*}_{LM}(\alpha\kappa')\right].$$

Here all the symbols are explained in the main text. Similarly, for the case of the L–S coupling scheme, as discussed in subsect. 2.4, we obtain for the state $S = 0, T = 1$:

$$\Delta^{(4)}(\nu\nu')_{LM,01} = \tfrac{1}{2}\sum_{\omega_n>0}\sum_{\kappa\neq\kappa'}\sum_{s\neq\nu'}\sum_{\alpha}\sum_{nn'lN\mathscr{L}}\sum_{\lambda\mu,L''M''} v(s\kappa'\nu\kappa, nn'lN\mathscr{L}\lambda)$$

$$\times[(4w-m+2b-2h)Q^{\omega_n^*}_{L''\lambda L}(\nu\nu' s,\ \kappa\kappa'\alpha)-(m+2h)R^{\omega_n^*}_{L''\lambda L}(\nu'\nu s,\ \kappa'\kappa\alpha)]$$

$$+\tfrac{1}{2}\sum_{\omega_n>0}\sum_{\kappa\neq\kappa'}\sum_{s\neq\nu}\sum_{\alpha}\sum_{nn'lN\mathscr{L}}\sum_{\lambda\mu,L''M''} v(s\kappa\nu'\kappa'; nn'lN\mathscr{L}\lambda)$$

$$\times[(4w-m+2b-2h)R^{\omega_n^*}_{L''\lambda L}(\nu\nu' s,\ \kappa\kappa'\alpha)-(m+2h)Q^{\omega_n^*}_{L''\lambda L}(\nu'\nu s,\ \kappa'\kappa\alpha)] \qquad \text{(A.2)}$$

$$+\tfrac{1}{2}\sum_{\omega_n>0}\sum_{\kappa\kappa' s\alpha}\sum_{nn'lN\mathscr{L}}\sum_{\lambda\mu,L''M''}\{v(s\kappa'\nu\kappa; nn'lN\mathscr{L}\lambda)$$

$$\times[X^{\omega_n^*}_{L''\lambda L}(\nu\nu' s,\ \kappa\kappa'\alpha)+Y^{\omega_n^*}_{L''\lambda L}(\nu\nu' s,\ \kappa\kappa'\alpha)]+v(s\kappa\nu'\kappa'; nn'lN\mathscr{L}\lambda)$$

$$\times[X^{-\omega_n}_{L''\lambda L}(\nu'\nu s,\ \kappa'\kappa\alpha)+Y^{-\omega_n^*}_{L''\lambda L}(\nu'\nu s,\ \kappa'\kappa\alpha)]\},$$

where

$$v(\alpha\beta\gamma\delta, nn'lN\mathscr{L}\lambda) \equiv \langle nl, N\mathscr{L}, \lambda|n_\alpha l_\alpha, n_\beta l_\beta, \lambda\rangle$$

$$\times\langle n'l, N\mathscr{L}, \lambda|n_\gamma l_\gamma, n_\delta l_\delta, \lambda\rangle\langle n'l||\Delta V||nl\rangle,$$

$$Q^{\omega_n^*}_{L''\lambda L}(\nu\nu' s,\ \kappa\kappa'\alpha) \equiv (-)^{l_\kappa+l_{\kappa'}-l_\nu-l_s} C^{\omega_n^*}_{L''M''}(s\nu')\left[\begin{Bmatrix} L & l_{\kappa'} & l_\alpha \\ l_{\nu'} & l_s & L'' \\ l_\nu & \lambda & l_\kappa\end{Bmatrix} C^{\omega_n^*}_{L''M''}(\alpha\kappa) F^*_{LM}(\alpha\kappa')\right.$$

$$\left.-(-)^{L-L''}[l_\alpha]^{\frac{1}{2}}[l_{\kappa'}]^{-\frac{1}{2}}\begin{Bmatrix} l_{\nu'} & l_s & L'' \\ l_{\kappa'} & l_\kappa & \lambda\end{Bmatrix}\begin{Bmatrix} l_\nu & l_\kappa & \lambda \\ l_\alpha & l_{\nu'} & L\end{Bmatrix} C^{\omega_n^*}_{L''M''}(\kappa'\alpha) F^*_{LM}(\kappa\alpha)\right],$$

$$R^{\omega_n^*}_{L''\lambda L}(\nu\nu' s,\ \kappa\kappa'\alpha) \equiv (-)^{L-\lambda}(-)^{l_\kappa+l_{\kappa'}-l_{\nu'}-l_s} C^{\omega_n^*}_{L''M''}(\kappa\kappa')\begin{Bmatrix} l_{\nu'} & l_{\kappa'} & \lambda \\ l_\kappa & l_s & L''\end{Bmatrix}$$

$$\times\left[(-)^{L-L''}[l_{\nu'}]^{-1} C^{\omega_n^*}_{L''M''}(s\alpha)\delta_{l_\alpha l_{\nu'}} F^*_{LM}(\nu\alpha)-\begin{Bmatrix} l_\nu & l_\alpha & L'' \\ l_s & l_{\nu'} & L\end{Bmatrix} C^{\omega_n^*}_{L''M''}(\alpha\nu) F^*_{LM}(\alpha s)\right],$$

$$X^{\omega_n *}_{L''\lambda L}(\nu\nu' s,\ \kappa\kappa'\alpha) \equiv (3m-b+h) C^{\omega_n *}_{L''M''}(\kappa\nu') \begin{Bmatrix} L'' & l_{\nu'} & l_\kappa \\ l_\nu & \lambda & L \end{Bmatrix} (-)^{l_{\nu'}+l_\alpha}$$

$$\times \left[(-)^{L''+\lambda-L} \begin{Bmatrix} L'' & l_\alpha & l_s \\ l_{\kappa'} & \lambda & L \end{Bmatrix} C^{\omega_n *}_{L''M''}(\alpha s) F^*_{LM}(\alpha\kappa') - \begin{Bmatrix} L'' & l_\alpha & l_{\kappa'} \\ l_s & \lambda & L \end{Bmatrix} C^{\omega_n *}_{L''M''}(\kappa'\alpha) F^*_{LM}(s\alpha) \right],$$

$$Y^{\omega_n}_{L''\lambda L}(\nu\nu' s,\ \kappa\kappa'\alpha) \equiv (m+b+h)\delta_{L''\lambda}\delta_{\mu M''}(-)^{l_\kappa+l_{\kappa'}-l_\nu-l_s} C^{\omega_n}_{L''M''}(\kappa' s)$$

$$\times \left[(-)^{L-\lambda} \begin{Bmatrix} l_\kappa & l_\nu & \lambda \\ l_{\nu'} & l_\alpha & L \end{Bmatrix} C^{\omega_n}_{L''M''}(\alpha\nu') F_{LM}(\alpha\kappa) - [l_\nu]^{-1} C^{L}_{\omega'' M''}(\kappa\alpha)\delta_{l_\alpha l_\nu} F_{LM}(\nu'\alpha) \right].$$

Here $C^{\omega_n *}_{LM}(\alpha\alpha')$ and $F^*_{LM}(\alpha\alpha')$ stand for $C^{\omega_n *}_{LM,01}(\alpha\alpha')$ and $F^{01*}_{LM}(\alpha\alpha')$. All the other symbols are explained in the main text.

References

1) K. Sawada, Phys. Rev. **106** (1957) 372;
Sawada, Brueckner, Fukuda and Brout, Phys. Rev. **108** (1957) 507
2) H. Ehrenreich and M. H. Cohen, Phys. Rev. **115** (1959) 786;
P. A. M. Dirac, Proc. Cambridge Phil. Soc. **26** (1930) 376
3) J. Sawicki, Nuclear Physics **23** (1961) 285
4) K. Sawada and T. Soda, Phys. Rev. (1961), submitted for publication
5) M. Moshinsky and T. A. Brody, Tablas de Paréntesis de Transformación, Monografías del Instituto de Fisica, Mexico (1960);
V. V. Balashov and V. A. Eltekov, Nuclear Physics **16** (1960) 423;
B. J. Verhaar, Physica **26** (1960) 1045
6) R. J. Ord-Smith, Phys. Rev. **94** (1954) 1227
7) G. E. Brown, J. A. Evans and D. J. Thouless, preprint (1960)
8) D. J. Thouless, Nuclear Physics **22** (1961) 78
9) R. A. Ferrell and J. J. Quinn, Phys. Rev. **108** (1957) 570
10) S. Fallieros, Thesis, University of Maryland (1959)
11) K. Sawada, Phys. Rev. **119** (1960) 2005
12) G. E. Brown, L. Castillejo and J. A. Evans, Nuclear Physics **22** (1961) 1;
G. E. Brown and D. J. Thouless, Physica **26** (1960) S145;
G. E. Brown and M. Bolsterli, Phys. Rev. Letters **3** (1959) 472;
W. Brenig, Nuclear Physics **22** (1961) 14
13) J. P. Elliott and B. H. Flowers, Proc. Roy. Soc. **A242** (1957) 57
14) R. A. Ferrell and W. M. Visscher, Phys. Rev. **102** (1956) 450
15) D. J. Thouless, private communication

2.L

Nuclear Physics **28** (1961) 293—303; © *North-Holland Publishing Co., Amsterdam*

Not to be reproduced by photoprint or microfilm without written permission from the publisher

EXCITATION DU NIVEAU DE 15.1 MeV DE C^{12} PAR DIFFUSION INÉLASTIQUE DES PROTONS DE 150 MeV

X. DE BOUARD, H. LANGEVIN-JOLIOT, N. MARTY et B. TATISCHEFF

Laboratoire Joliot-Curie de Physique Nucléaire, Orsay (S. et O.)

Reçu le 19 Mai 1961

Abstract: The excitation of the 15.1 MeV level of C^{12} ($J^\pi = 1^+$, $T = 1$) by 150 MeV protons has been studied. The angular distribution of the scattered protons in coincidence with the de-excitation γ rays emitted in the recoil direction of the nucleus has been determined. The angular correlation between inelastically scattered protons and γ rays has been measured at a scattering angle of 8°.

1. Introduction

Plusieurs auteurs [1–5]) ont montré que des protons de 100 à 200 MeV excitent, par diffusion inélastique, des niveaux bien séparés des noyaux légers. Pour certains d'entre eux, en particulier pour le niveau de 4.4 MeV de C^{12}, les différents résultats expérimentaux sont en accord; les interprétations théoriques [6–10]) rendent bien compte de la forme de la distribution angulaire et même de la valeur absolue de la section efficace de diffusion inélastique des protons si l'on considère que les nucléons dans l'état excité à 4.4 MeV obéissent à un mode de couplage $\mathbf{L} \cdot \mathbf{S}$. Par contre ces mesures de corrélation angulaire entre protons diffusés inélastiquement p' et γ de désexcitation, pour des protons de l'ordre de 20 MeV [11]) semblent mieux s'interpréter dans le cas d'un couplage jj. La corrélation p'γ relative au niveau de 4.4 MeV a aussi été déterminée [12]) à 150 MeV.

Le cas du niveau de C^{12} au voisinage de 15 MeV a été moins étudié. Les seuls auteurs [3]) qui ont mis en évidence de façon nette l'excitation d'un tel niveau par diffusion inélastique de protons de 180 MeV l'ont assimilé au niveau de 15.1 MeV (1^+, $T = 1$) atteint dans un grand nombre de réactions [13,14]). Cette valeur du spin isobarique explique et entraîne le fait que la désexcitation de ce niveau a lieu presque totalement par émission d'un rayon γ au niveau fondamental de C^{12} alors qu'énergétiquement est possible l'émission d'une particule α donnant Be^8 à l'état fondamental ou au premier état excité.

La section efficace différentielle d'excitation par protons de ce niveau n'a pu être donnée qu'entre 3° et 9° d'angle de diffusion des protons en raison de sa forme présentant un maximum vers l'avant où les mesures sont rendues difficiles par la présence de protons diffusés élastiquement. Aux angles supérieurs

à 10°, la section efficace devient trop faible pour être mesurée directement. Il semble qu'un niveau d'énergie voisine de 15 MeV soit excité pour des angles de diffusion plus grands des protons [5]).

Nous avons pensé que, si le niveau mis en évidence par Tyrén et Maris était bien le niveau de 15.1 MeV de C^{12}, il serait intéressant, utilisant sa propriété de se désexciter par émission γ, d'étudier les protons diffusés inélastiquement en coïncidence avec les rayons γ de désexcitation, ce qui permet d'éliminer les protons diffusés élastiquement ou inélastiquement correspondant à d'autres niveaux.

2. Dispositif Expérimental

Nous avons légèrement modifié pour cette étude un dispositif expérimental utilisé précédemment [15]) (fig. 1).

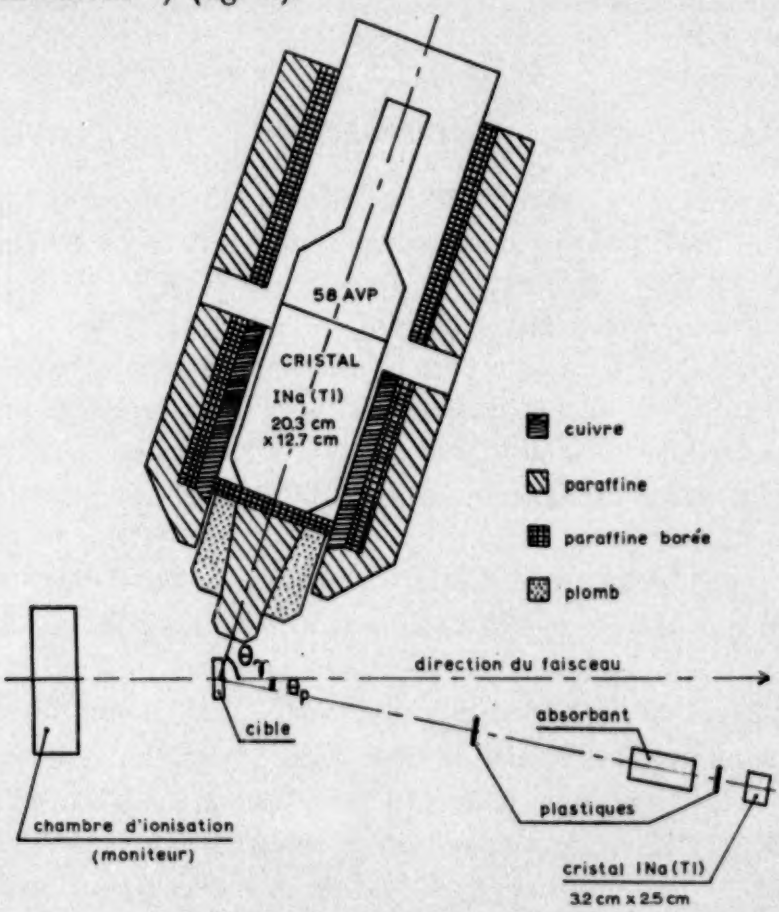

Fig. 1. Dispositif expérimental.

Le faisceau de protons de 157 MeV frappe une cible de carbone; les protons diffusés sont détectés par un télescope comprenant deux scintillateurs plastiques et un scintillateur NaI (Tl). Les photons sont étudiés à l'aide d'un spectromètre à scintillation comportant un cristal NaI (Tl) de grande dimension.

Le dispositif électronique associé (fig. 2) permet d'étudier le spectre des

photons en coïncidence avec les protons diffusés possédant l'énergie voulue.

Le faisceau de protons de 157 MeV du synchrocyclotron d'Orsay [16]), extrait par régénérateur et canal magnétique, est focalisé par un ensemble de deux lentilles quadrupolaires, et défléchi par un aimant déflecteur; ses dimensions à l'endroit de la cible étaient d'environ 4 cm de haut sur 2 cm de large. La structure en temps, modifiée par un programme auxiliaire haute-fréquence [17]) donnait un temps d'occupation d'environ 10 %. L'intensité du faisceau était monitorée à l'aide d'une chambre à ionisation.

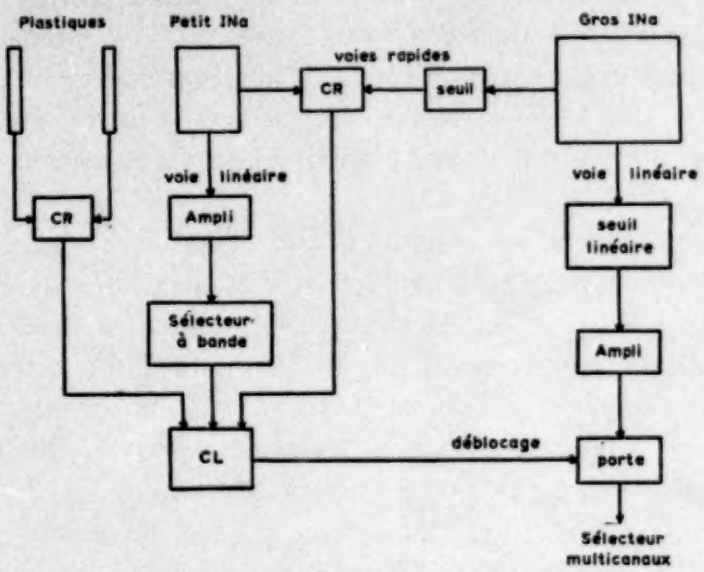

Fig. 2. Partie électronique.

La cible de graphite, de 4 cm de haut et de largeur 3 cm ou 2 cm suivant le cas, correspondait à une perte d'énergie de 7.5 MeV pour les protons. Compte tenu du ralentissement du faisceau dans différentes fenêtres, on peut adopter 151.5 MeV pour l'énergie moyenne des protons lors de la diffusion.

Le télescope à protons porté par un bras mobile autour de la cible, comporte 2 scintillateurs plastiques de 0.2 cm d'épaisseur, montés par l'intermédiaire de conduits de lumière sur des P. M. 55 A.V.P.; le premier avait 2.4 cm de large et 3.2 cm de haut, le second, circulaire, de 2.4 cm de diamètre, définissait l'ouverture angulaire du télescope; il était distant de la cible de 58 cm à la position proche, et de 110 cm à la position éloignée. Le scintillateur NaI (Tl) de 3.25 cm de diamètre et 2.5 cm d'épaisseur était monté sur un P. M. 53 A.V.P. qui comportait une sortie pour les coïncidences rapides, et une sortie linéaire pour l'analyse en énergie des impulsions. Un absorbant de graphite interposé entre les deux scintillateurs plastiques ne laissait parvenir au scintillateur NaI que les protons diffusés d'énergie supérieure à 120 MeV.

Le détecteur γ est un cristal de NaI (Tl) de 12.5 cm de diamètre, 20 cm d'épaisseur, tronc conique sur les cinq premiers centimètres, monté sur un

PM 58 A.V.P. La face avant se trouvait à 20 cm de l'axe de la cible; un canaliseur de Pb de 10 cm de long et d'ouverture 8 cm de diamètre à la face avant du cristal était interposé entre la cible et le scintillateur. Le cristal était protégé latéralement des neutrons par une enveloppe de 6 cm de paraffine à l'intérieur de laquelle était coulé un cylindre de 3 cm d'épaisseur de paraffine borée. Dans l'ouverture du canaliseur était disposé un cône de paraffine de 15 cm d'épaisseur terminé par une plaque de paraffine borée, de façon à absorber totalement les protons et au maximum les neutrons lents issus de la cible.

Le détecteur γ était monté sur un bras mobile autour de la cible; il pouvait balayer les angles de 45° à 135° avec la direction du faisceau incident sans que l'enveloppe de protection n'affleure le faisceau. Son ouverture angulaire était de $\pm$ 11°. Le facteur d'efficacité de détection ε_γ calculé pour des photons de 15.1 MeV compte tenu de l'ouverture angulaire de détection et de l'absorption dans la paraffine était de $8 \cdot 10^{-3}$.

Le circuit de détection des γ comporte lui aussi une sortie rapide et une sortie proportionnelle. Sur les deux sorties sont placés des seuils, rapide pour le premier et linéaire pour le deuxième, de manière à ne pas surcharger l' appareillage électronique par des impulsions non utiles à notre étude.

Les temps de résolution étaient de $2 \cdot 10^{-8}$ s pour les circuits de coïncidence rapide, de $6 \cdot 10^{-7}$ s pour le circuit de coïncidence lente. Les impulsions en coïncidence commandent une porte linéaire qui s'ouvre pendant $2 \cdot 10^{-6}$ s et ne laisse parvenir au sélecteur à 256 canaux que les impulsions en coïncidence avec les impulsions provenant du télescope à protons, d'énergie voulue. Nous avons réglé les différents circuits de coïncidence, retards et temps de résolution, à l'aide de coïncidences entre protons diffusés et protons de recul dans une diffusion sur une cible de $(CH_2)_n$.

3. Mesures Préliminaires

Nous avons tout d'abord, à l'aide du télescope à protons, étudié le spectre de protons diffusés à 10° par la cible de C^{12}, les impulsions de la voie linéaire du scintillateur NaI(Tl) étaient, après amplification, envoyées directement sur le sélecteur à 256 canaux. Après leur traversée de l'absorbant interposé entre les deux scintillateurs plastiques, les protons diffusés sont d'autant plus ralentis qu'ils étaient moins énergiques. Pour étalonner la hauteur des impulsions en fonction de l'energie des protons diffusés, nous avons utilisé les pics de protons diffusés à 25° correspondant à l'excitation de niveaux bien connus de C^{12} à 4.4 et 9.6 MeV, ainsi que des pics de protons diffusés élastiquement, ralentis par des absorbants pour lesquels la perte d'énergie des protons avait été calculée.

Le spectre des protons diffusés à 10° est représenté fig. 3. On y distingue à peine un pic attribuable à l'excitation du niveau de 15.1 MeV de C^{12}; en raison de la mauvaise résolution du détecteur NaI(Tl), il est masqué par le fond

d'impulsions provenant du pic élastique et correspondant à des protons qui, à la suite de réactions nucléaires, n'ont pas perdu toute leur énergie dans le cristal, et aussi par le groupe de protons correspondant à l'excitation de niveaux dans le domaine de la résonance géante.

Si l'on augmente l'intensité du faisceau (les mesures sont alors faites avec un sélecteur à un canal, le multicanaux n'analysant pas des impulsions très rapprochées), l'amplitude des impulsions augmente, le pic de diffusion élastique

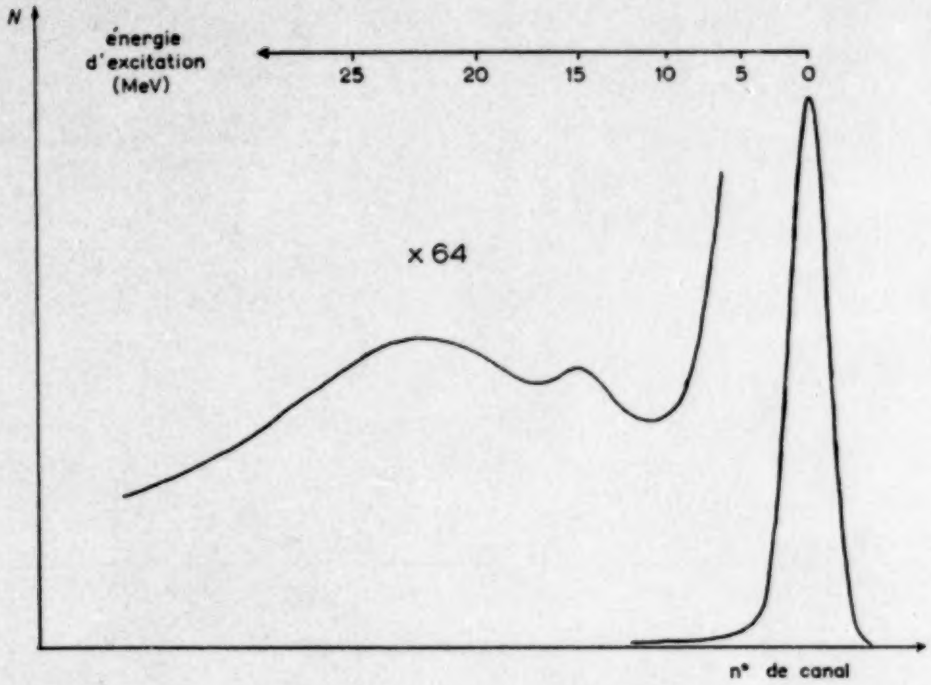

Fig. 3. Spectre des protons diffusés à 10°

s'élargit, présentant une „queue" vers les basses énergies; nous avons diminué cet effet pour une intensité de faisceau donnant 10 000 impulsions/s (équivalentes à 100 0000 impulsions/s réparties au hasard) en utilisant dans le montage des P.M. des chaînes de résistance qui permettent de travailler à gros débit.

On peut facilement par réglage de la tension des P.M. maintenir fixe la hauteur des impulsions correspondant au pic élastique, et en même temps celle provenant des autres pics.

Le spectre d'impulsion du spectromètre à scintillation pour la détection des γ est représenté fig. 4; la raie de 15.1 MeV provenant de la désexcitation du niveau par emission γ directe au fondamental, est à peine décelable; la hauteur des impulsions dépend ici aussi de leur nombre, mais de façon moins sensible en raison du débit plus faible du P.M. Nous avons en géneral réglé les seuils de façon à ne laisser passer que les impulsions d'énergie supérieure à 6 MeV.

Sur la même figure est représenté le spectre de photons à 10° du faisceau incident en coïncidence avec les protons diffusés inélastiquement au même

angle. Le spectre tracé est corrigé des coïncidences fortuites; on mesure le spectre de coïncidences fortuites par coïncidence entre les photons et l'ensemble des impulsions du télescope à protons (sans sélection en énergie) en intercalant sur la voie rapide γ un retard de $5 \cdot 10^{-8}$ s correspondant à l'intervalle fixé par la haute fréquence du synchrocyclotron. Par comparaison avec le nombre de coïncidences fortuites obtenues pour les énergies supérieures à celle de la

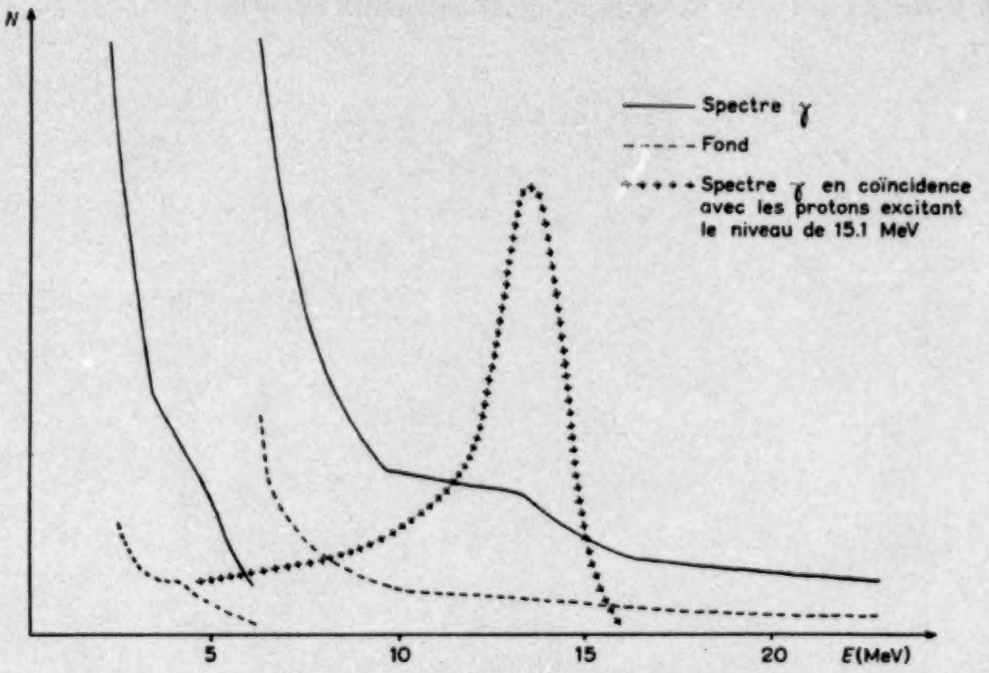

Fig. 4. Spectre γ émis par la cible ^{12}C.

raie de 15 MeV, on en déduit le nombre de coïncidences fortuites dans la région de la raie.

D'après l'intensité de cette raie γ de 15 MeV, on peut dire que le niveau excité à 15 MeV se désexcite presque totalement par γ au niveau fondamental de C^{12} et est bien de niveau 1^+, $T = 1$.

4. Distribution Angulaire des Protons Diffusés Inélastiquement

Nous avons étudié la distribution angulaire des protons diffusés en coïncidence avec les photons de 15.1 MeV émis à 70° du faisceau incident dans le plan de diffusion. Pour cela nous avons déterminé pour chaque angle de diffusion des protons, le nombre d'impulsions en coïncidence dans une bande d'énergie comprise entre 10.5 et 15.1 MeV. Nous avons choisi cette méthode, car on pouvait facilement ajuster la bande du sélecteur dans la voie linéaire de détection des protons à l'énergie voulue, par comparaison avec la position de la raie de protons diffusés élastiquement. L'angle de 70° pour la direction du détecteur γ reste très voisin de la direction du noyau de recul dans la diffu-

sion p $C^{12} \rightarrow p' C^{12*}$, direction dans laquelle on pouvait s'attendre à observer le maximum de rayonnements γ de désexcitation (voir § 5).

Une première série de mesures pour les angles de diffusion 8°, 10°, 15°, 20°, 25°, 40° a été effectuée avec le télescope en position proche et la cible de 3 cm de large; la deuxième série de mesures faites pour les angles 5°, 7°.5, 10° a été effectuée avec une cible de 2 cm de large et le télescope en position éloignée.

La fig. 5 représente le nombre de coïncidences entre protons et γ en fonction

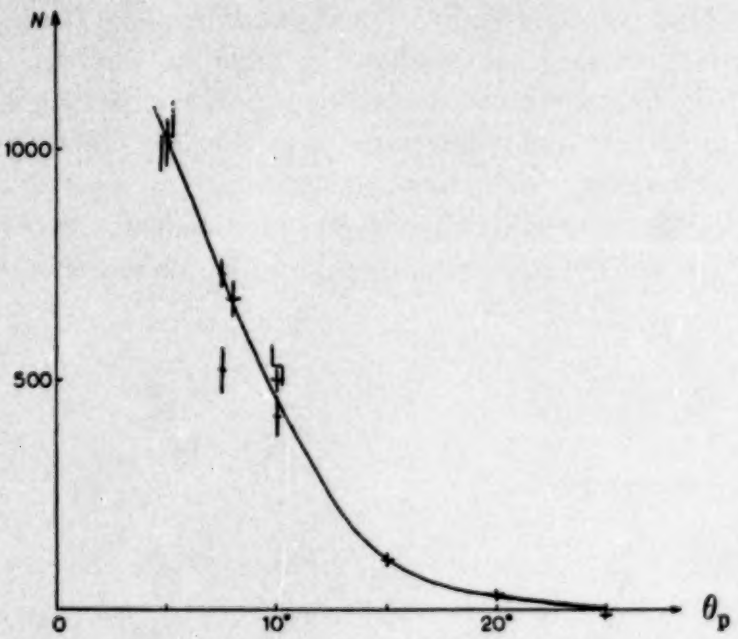

Fig. 5. Distribution angulaire des protons diffusés.

de l'angle de diffusion des protons par unité d'intensité du faisceau. Les mesures en position proche et éloignée ont été normalisées sur les valeurs obtenues à 7°.5 et 10° d'une part, 8° et 10° d'autre part. Au cours de ces mesures on a maintenu sensiblement constant le nombre de particules détectées par le télescope à protons.

Les erreurs indiquées sur la figure sont les erreurs statistiques standard; les corrections d'ouverture angulaire sont négligeables (<1 %) compte tenu de la forme de la courbe expérimentale, Une erreur systématique peut s'introduire si le faisceau de protons ne reste pas bien centré sur la cible, un déplacement de 2 mm-maximum possible étant données les vérifications de centrage faites au cours des mesures — entraine une erreur de 0°.35 en position proche, de 0°.2 en position éloignée.

La courbe tracée fig. 5 représente la distribution angulaire des protons diffusés inélastiquement au niveau de 15.1 MeV, si la distribution angulaire des γ de désexcitation est isotrope ou si elle conserve la même forme quel que

soit l'angle de diffusion des protons associés. Sinon une correction doit lui être apportée tenant compte de la forme de la corrélation angulaire entre protons diffusés inélastiquement et γ de désexcitation.

5. Corrélation Angulaire entre Protons Diffusés Inélastiquement et γ de Désexcitation

La même méthode et le même dispositif décrits précédemment ont été utilisés pour la mesure de la corrélation angulaire p'γ. Le télescope à protons est maintenu fixe, en position proche à un angle de 8° avec la direction du faisceau incident. Pour cet angle, la section efficace différentielle d'excitation du niveau est importante et les détecteurs sont assez éloignés du faisceau direct.

On fait alors varier la position du détecteur γ: les mesures ont été faites pour des angles θ avec la direction du faisceau incident de 135°, 130°, 120°, 105°, 90°, 75°, 60° et 50°. On dénombre dans chaque cas les impulsions γ en

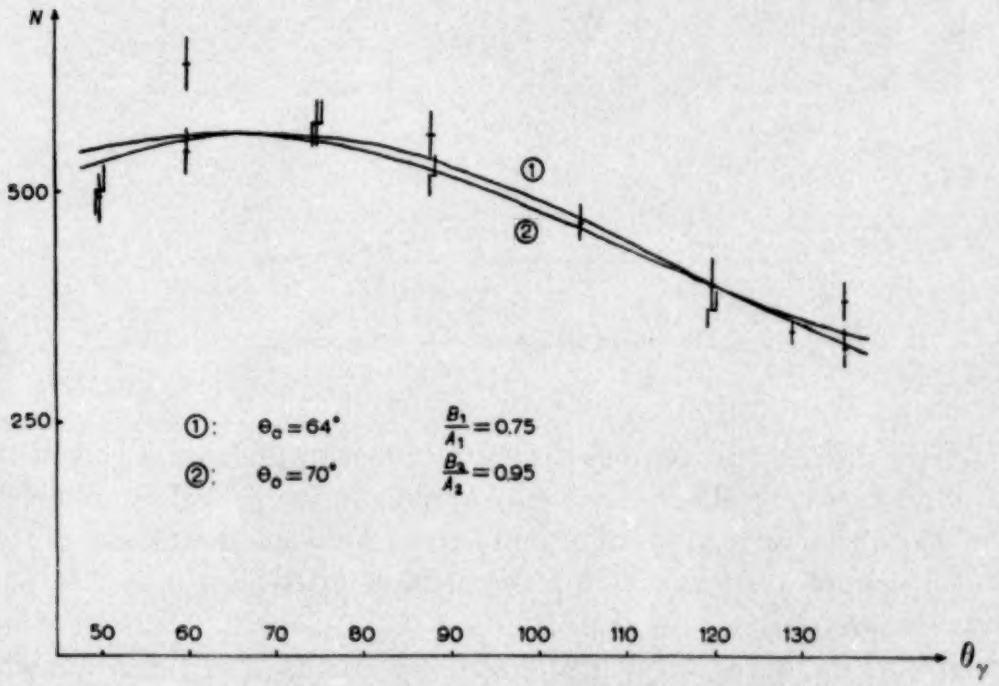

Fig 6. Corrélation angulaire p'—γ.

coïncidence dans une bande d'énergie comprise entre 10.5 et 15.1 MeV après soustraction des coïncidences fortuites; celles-ci étaient en géneral de l'ordre de 10 % des coïncidences vraies. La précision des mesures était supérieure à celle atteinte dans le cas du § 4, en raison du plus grand nombre de coïncidences par unité de temps ainsi que de la constance du nombre de particules détectées par le télescope à protons et le détecteur γ.

Sur la fig. 6 sont portés les points expérimentaux donnant le nombre de

coïncidences p'γ en fonction de l'angle de détection des γ, les erreurs portées sont les erreurs standard.

Le niveau de 15.1 MeV de C^{12} étant un niveau 1^+, $T = 1$ ne peut être excité par diffusion inélastique des protons à partir du fondamental 0^+ que par une interaction de spin et de spin isobarique avec des ondes de moment angulaire $l = 0$ et $l = 2$. Il se désexcite par émission d'un rayonnement γ dipolaire magnétique. La corrélation angulaire p'γ dans le plan de diffusion doit être de la forme $A+B\cos^2(\theta_\gamma - \theta_0)$ où B/A peut varier entre $+1$ et -1 suivant les peuplements de sous états $M = 1$, $M = 0$, $M = -1$. Si le traitement peut être fait en ondes planes, l'axe de symétrie de la courbe est la direction du noyau de recul dans la diffusion inélastique ($\theta_0 = \theta_R$) (ref. [11])). Ceci n'est plus vrai en cas de distorsion des ondes.

Par la méthode des moindres carrés nous avons déterminé la courbe 1 fig. 5 de la forme $A_1+B_1\cos^2(\theta_\gamma - \theta_R)$ qui donnait le meilleur accord avec la courbe expérimentale ($\theta_R = 65°$ pour l'angle de diffusion 8° de protons); la valeur correspondante B_1/A_1 est 0.75 ± 0.08.

Nous avons ensuite déterminé la courbe $A_2+B_2\cos^2(\theta_\gamma - \theta_0)$ où B_2/A_2 et θ_0 sont maintenant des paramètres ajustables. La courbe donnant le meilleur accord est représentée en 2; on a $\theta_0 = 70°\pm5$ ($\theta_0 - \theta_R = 5°\pm5$) et $B_2/A_2 = 0.95\pm0.18$.

En raison de l'ouverture angulaire du détecteur de protons et du détecteur γ l'anisotropie mesurée expérimentalement est atténuée. En utilisant les calculs de Rose [18]) pour corriger la courbe expérimentale nous obtenons dans le cas de la courbe 1 la valeur $B'_1/A'_1 = 0.80\pm0.08$ et pour la courbe 2, $B'_2/A'_2 = 1.01\pm0.2$.

6. Valeur de la Section Efficace Différentielle de Diffusion Inélastique

Pour l'angle de diffusion 8° pour lequel la forme de la corrélation angulaire p'γ a été mesurée, on peut obtenir la valeur de la section efficace d'excitation du niveau de 15.1 MeV, $d\sigma_1(\theta_p)/d\Omega$. Nous l'avons mesurée par comparaison avec la section efficace de diffusion élastique au même angle, ce qui évite d'avoir à tenir compte de la faible partie du faisceau qui ne tombe pas sur la cible et d'avoir à estimer la proportion des impulsions pour lesquelles les protons ne perdent pas toute leur énergie dans le cristal ou subissent des réactions dans l'absorbant.

Soient N_e le nombre de protons diffusés élastiquement à 8° et comptés au sélecteur à bande, N_1 le nombre de protons diffusés inélastiquement sur le niveau de 15.1 MeV au même angle, N_c le nombre de coïncidences entre protons diffusés inélastiquement et γ de désexcitation comptés entre 10.5 et 15.1 MeV.

On a

$$\frac{N_1}{N_e} = \frac{d\sigma_1(\theta_p = 8°)/d\Omega}{d\sigma_e(\theta_p = 8°)/d\Omega}, \qquad N_e = N_1 \varepsilon_\gamma \eta \rho \alpha R,$$

où $\varepsilon_\gamma = 8 \cdot 10^{-3}$ représente l'efficacité de détection des rayons γ de 15.1 MeV; η est pour un rayonnement γ de 15.1 MeV la proportion des cas où l'énergie effectivement absorbée dans le cristal est comprise entre 10.5 et 15.1 MeV, et a été pris égal à 0.7 par extrapolation du spectre γ obtenu en coïncidence (fig. 4) et par comparaison avec les courbes données par Kockum et Starfelt [19]); ρ est le facteur de perte de notre circuit, évalué à 0.9; α est le rapport de la largeur partielle de désexcitation du niveau de 15.1 MeV par émission γ directe au fondamental à la largeur totale de ce niveau, et a été pris égal à 0.80 ± 0.20 [20, 21]); $R = 1.4$ est la correction due à l'anisotropie de la corrélation angulaire.

On trouve

$$\frac{d\sigma_1(\theta_p = 8°)/d\Omega}{d\sigma_e(\theta_p = 8°)/d\Omega} = 2.4 \cdot 10^{-3}.$$

En adoptant $d\sigma_e(\theta_p = 8°)/d\Omega = 380$ mb/sr [5]) on obtient $d\sigma_1(\theta_p = 8°)/d\Omega = 0.9$ mb/sr. En raison des imprécisions sur les différents facteurs qui interviennent dans la détermination de cette section efficace, et en particulier sur α, celle-ci est donnée à environ 40 % près.

7. Discussion

La valeur obtenue à 8° pour la section efficace de diffusion inélastique des protons sur le niveau de 15.1 MeV, bien qu'inférieure d'un facteur 1.5 à la valeur donnée par Tyrén et Maris [3]), est compatible avec elle en raison des imprécisions de la mesure.

Etant donné l'importance de l'anisotropie de la corrélation p'γ à un angle de diffusion de 8°, pour tout angle de diffusion pour lequel l'anisotropie est plus faible, il faudra apporter à la courbe (fig. 5) une correction pour obtenir la distribution angulaire des protons ayant excité le niveau de 15.1 MeV. Cette correction est un facteur multiplicatif égal à 1.8 dans le cas d'une corrélation isotrope. Pour retrouver à 40° la section efficace de 0.5 mb indiquée par Garron *et al.* [5]) il faudrait appliquer un facteur de correction de 60, facteur qui ne pourrait même pas être atteint, étant donnée l'ouverture angulaire du détecteur γ, si la corrélation était en $1 - \cos^2\theta$. Il semble donc bien plus probable que le niveau excité à cet angle soit le niveau de 16.1 MeV (2^+, $T = 1$) qui a été excité par diffusion inélastique des électrons dans le cas d'un grand transfert d'impulsion [22]).

Avec ou sans correction, la courbe de section efficace différentielle présente

une décroissance très rapide en fonction de l'angle de diffusion, ce qui laisse prévoir l'importance d'une onde $l = 0$.

La corrélation p'γ présente une anisotropie voisine de l'anisotropie maximum et l'analyse théorique de ces résultats doit permettre d'apporter davantage de renseignements sur le mode d'excitation du niveau de 15.1 MeV de C^{12}.

Nous n'avons pu, en raison de la faible intensité du phénomène et du manque de temps disponible auprès du synchrocyclotron, étudier la corrélation p'γ pour d'autres angles de diffusion des protons.

Nous tenons à remercier ici M. Corbé, du service d'Electronique Physique du Laboratoire, qui a monté et mis au point l'appareillage électronique, ainsi que M. Bergamaschi et l'équipe de conduite du synchrocyclotron, pour les heures de fonctionnement de l'appareil qu'ils nous ont assurées.

Bibliographie

1) K. Strauch et F. Titus, Phys. Rev. **103** (1956) 200
2) G. Gerstein, J. Niederer et K. Strauch, Phys. Rev. **108** (1957) 427
3) H. Tyrén et Th. A. J. Maris, Nuclear Physics **3** (1957) 52, **4** (1957) 277, **6** (1958) 82, 446, **7** (1958) 24, 281
4) J. M. Dickson et D. C. Salter, Nuovo Cim. **6** (1957) 235
5) J. P. Garron, J. C. Jacmart, L. Massonnet, M. Riou et P. Ruhla, J. Phys. Rad. **21** (1960) 317
6) Th. A. J. Maris et H. Tyrén, Nuclear Physics **3** (1957) 35
7) P. Benoist, C. Marty et P. Meyer, C. R. Acad. Sc. **245** (1957) 1389
8) E. J. Squires, Nuclear Physics **6** (1958) 504
9) H. S. Kohler, Nuclear Physics **6** (1958) 161
10) G. P. Mc-Caulley, Proc. Phys. Soc. **73** (1959) 309
11) E. A. Levinson et M. K. Banerjee, Ann. of Physics, **2** (1957) 471, 499
12) A. B. Clegg, K. J. Foley, G. L. Salmon et R. E. Segel, Bull. Am. Phys. Soc. **4** (1959) 444
13) F. Ajzenberg-Selove et T. Lauritsen, Nuclear Physics **11** (1959) 117
14) E. Hayward et E. C. Fuller, Phys. Rev. **106** (1957) 991
15) H. Langevin-Joliot, N. Marty et X. de Bouard, J. Phys. Rad. **21** (1960) 320
16) C. Bergamaschi *et al.*, J. Phys. Rad. **21** (1960) 305
17) A. Cabrespine, J. Phys. et Rad. **21** (1960) 332
18) M. E. Rose, Phys. Rev. **91** (1953) 610
19) J. Kockum et N. Starfelt, Nucl. Inst. and Methods **4** (1959) 171
20) E. L. Garwin, Phys. Rev. **114** (1959) 143
21) F. Almquist, P. A. Bromley, A. J. Fergusson, H. E. Gove et A. E. Litherland, Phys. Rev. **114** (1959) 1040
22) R. E. Taylor, Journal de Phys. et Rad., à paraître

1.C

Nuclear Physics **28** (1961) 304—330; © *North-Holland Publishing Co., Amsterdam*

Not to be reproduced by photoprint or microfilm without written permission from the publisher

DIFFERENT MODES OF MOTION IN SPECIAL TRANSLATIONALLY INVARIANT MANY-BODY SYSTEMS

P. MÖBIUS

Physikalisches Institut, Technische Hochschule, Aachen

Received 24 June 1961

Abstract: The motion of a system of A particles with translationally invariant interaction is separated into the centre-of-mass motion and the internal motion. For special examples the wave function of the internal motion is split again into a product of two functions, one describing the "global" mode of motion and the other the "specific" mode of motion. The functions of the centre-of-mass motion and the global mode of motion depend only on totally symmetric combinations of the particle coordinates. The contribution of the global motion to the energy spectrum is independent of the number of particles. The function describing the specific mode of motion takes into account all conditions for the total wave function which are connected with the Pauli principle, the spin and the isobaric spin of the system. The corresponding eigenvalue spectrum depends on the number of particles. With the help of these considerations a suggestion is offered on the structure of the so-called nuclear "collective coordinates".

1. Introduction

If it is possible to split the wave function of a many-body system into a product of different functions, every one of which contains the coordinates of all particles, it may be that these functions characterize different modes of motion. For this interpretation it is essential that one or more of the functions depend only on special symmetric combinations of the particle coordinates. A very simple example is the centre-of-mass coordinate. It is a totally symmetric homogeneous function of first degree in the particle coordinates. Separating the centre-of-mass motion from the internal motion means extracting from the total wave function a part depending only on a homogeneous function of first degree, the centre-of-mass coordinate. An extension of this idea will be to extract again from the remaining function a part depending only on totally symmetric homogeneous functions of the second degree in the particle coordinates. In the case of a translationally invariant interaction these combinations must have the same invariance property. In order to realize this concept of different modes of motion the structure of a many-body wave function must be investigated. Considering a time-independent nuclear many-body system with translationally invariant interaction between the A nucleons one must look for a function $\Psi'(1 \ldots A)$ which has to obey the following equations [1,2]):

$$\mathscr{H}'(1 \ldots i \ldots A)\Psi'(1 \ldots i \ldots A) = E'\Psi'(1 \ldots i \ldots A), \qquad (1)$$

$$\sum_1^A \frac{\hbar}{i}\frac{\partial \Psi'}{\partial r_i'} = \boldsymbol{P}\Psi'(1 \ldots i \ldots A), \tag{2}$$

$$\mathrm{P}(i,k)\Psi'(1 \ldots i, k \ldots A) = -\Psi'(1 \ldots i, k \ldots A), \tag{3}$$

where $\mathscr{H}'(1 \ldots A)$ is the Hamilton operator of the system and $\boldsymbol{P}$ is its total linear momentum. The number i is an abbreviation for the space vector r_i', the spin variable σ_i and the isobaric spin variable τ_i of the i-th particle:

$$i = (r_i', \sigma_i, \tau_i).$$

Eq. (3) expresses the Pauli principle, $\mathrm{P}(i,k)$ designating the permutation of the particle variables i and k. To eqs. (1)–(3), which must always be fulfilled, there must be added conditions depending on the structure of the Hamilton operator $\mathscr{H}'$. Charge independence of the nuclear forces requires that Ψ' is also an eigenfunction of

$$\mathscr{T}^2\Psi'(1 \ldots A) = T(T+1)\Psi'(1 \ldots A), \tag{4}$$

$$\mathscr{T}_z\Psi'(1 \ldots A) = M_T\Psi'(1 \ldots A), \tag{5}$$

where $\mathscr{T}$ is the operator of the isobaric spin of the system and $\mathscr{T}_z$ is its z-component. If the interaction potential depends only on the particle coordinates, further conditions for Ψ' are

$$\mathscr{S}^2\Psi'(1 \ldots A) = \hbar^2 S(S+1)\Psi'(1 \ldots A), \tag{6}$$

$$\mathscr{S}_z\Psi'(1 \ldots A) = \hbar M_S\Psi'(1 \ldots A), \tag{7}$$

where $\mathscr{S}$ and $\mathscr{S}_z$ represent the operators of the intrinsic spin and its z-component. Two similar equations exist for the angular momentum [2]).

The separation in centre-of-mass motion and internal motion is made by a linear orthogonal coordinate transformation replacing the A particle vectors $(r_1' \ldots r_A')$ by $(A-1)$ vectors $(r_1 \ldots r_{A-1})$ describing the internal motion and a vector r_A representing the centre-of-mass [1,2]). If $\varepsilon(r_A)$ describes the centre-of-mass motion, one obtains for Ψ' the product

$$\Psi'(1 \ldots A) = \varepsilon(r_A)\Psi(r_1 \ldots r_{A-1}, \sigma_1 \ldots \sigma_A, \tau_1 \ldots \tau_A), \tag{8}$$

where Ψ characterizes the internal motion. The centre-of-mass motion contributes a continuous part to the energy spectrum

$$E' = \frac{\boldsymbol{P}^2}{2MA} + E, \tag{9}$$

represented by the first term of (9), M being the mass of a nucleon, while E represents the energy eigenvalue of the internal motion. Eqs. (1), (3)–(7) permit us to decompose Ψ into the following form:

$$\Psi(r_1 \ldots r_{A-1}, \sigma_1 \ldots \sigma_A, \tau_1 \ldots \tau_A) = \sum_{\kappa\lambda\nu} q_{\kappa\lambda\nu}\psi^{r\kappa}(r_1 \ldots r_{A-1})\chi^{s\lambda}(\sigma_1 \ldots \sigma_A)\zeta^{t\nu}(\tau_1 \ldots \tau_A), \tag{10}$$

the summation covering all "standard tableaux" belonging to one "standard frame" for κ, λ, ν [2,3] †. In eq. (10), $\chi^s(\sigma_1 \dots \sigma_A)$ and $\zeta^t(\tau_1 \dots \tau_A)$ are the spin and isobaric spin functions fulfilling eqs. (6)–(7) and (4)–(5). They can be obtained for a given number of particles A and spin S or isobaric spin T as the expansion coefficients of a function $F(x, y; S, A)$ which is easy to determine [2,4]):

$$F(x, y; S, A) = \sum_{M_S=-S}^{+S} \chi_{SM_S} x^{S+M_S} y^{S-M_S}. \tag{11}$$

For the special examples treated in this paper it is possible to spit the wave function for the internal motion Ψ, satisfying the conditions (1), (3)—(7) into the following two parts:

$$\Psi = G(\rho, \xi, \eta) Z(\mathbf{r}_1 \dots \mathbf{r}_{A-1}, \sigma_1 \dots \sigma_A, \tau_1 \dots \tau_A), \tag{12}$$

the first one describing the "global" mode of motion and the second one describing the "specific" mode of motion. The function G depends only on the 3 variables ρ, ξ, η which are totally symmetric expressions of the particle coordinates of the following form:

$$\rho = \left(1 - \frac{1}{A}\right) \sum_1^A (x_i'^2 + y_i'^2 + z_i'^2) - \frac{2}{A} \sum_{i>k=1}^A (x_i' x_k' + y_i' y_k' + z_i' z_k'), \tag{13a}$$

$$\xi = \frac{\left(1 - \frac{1}{A}\right) \sum_1^A x_i'^2 - \frac{2}{A} \sum_{i>k=1}^A x_i' x_k'}{\left(1 - \frac{1}{A}\right) \sum_1^A (x_i'^2 + y_i'^2) - \frac{2}{A} \sum_{i>k=1}^A (x_i' x_k' + y_i' y_k')}, \tag{13b}$$

$$\eta = \frac{\left(1 - \frac{1}{A}\right) \sum_1^A (x_i'^2 + y_i'^2) - \frac{2}{A} \sum_{i>k=1}^A (x_i' x_k' + y_i' y_k')}{\left(1 - \frac{1}{A}\right) \sum_1^A (x_i'^2 + y_i'^2 + z_i'^2) - \frac{2}{A} \sum_{i>k=1}^A (x_i' x_k' + y_i' y_k' + z_i' z_k')}. \tag{13c}$$

They contain the sum of the squares of the particle coordinates as well as the sum of the products of two different particles coordinates. The structure of G as a function of ρ, ξ, η and its contribution to the energy spectrum are independent of the number of particles.

The function Z characterizing the specific motion is an abbreviation of the following expression:

$$Z = \sum_{\kappa\lambda\nu} q_{\kappa\lambda\nu} \phi^{r\kappa}(\mathbf{r}_1 \dots \mathbf{r}_{A-1}) \chi^{s\lambda}(\sigma_1 \dots \sigma_A) \zeta^{t\nu}(\tau_1 \dots \tau_A), \tag{14}$$

the sum having the same meaning as in eq. (10). The functions $\phi(\mathbf{r}_1 \dots \mathbf{r}_{A-1})$ are special homogeneous solutions of the $(3A-3)$-dimensional Laplace equation satis-

† All further references are to be found in these papers.

fying the conditions

$$\sum_{1}^{A-1} \frac{\partial^2 \phi}{\partial \boldsymbol{r}_i^2} = 0, \tag{15}$$

$$\sum_{1}^{A-1} x_i \frac{\partial \phi}{\partial x_i} = K_1 \phi, \qquad \sum_{1}^{A-1} y_i \frac{\partial \phi}{\partial y_i} = K_2 \phi, \qquad \sum_{1}^{A-1} z_i \frac{\partial \phi}{\partial z_i} = K_3 \phi, \tag{16}$$

where (K_1, K_2, K_3) are positive integer constants called the "eigenvalues" of the specific motion. The functions ϕ can be found with the help of the "many-particle variables" introduced in a preceding paper [1]). These variables are homogeneous functions of the internal coordinates from degree 1 up to degree A.

The method outlined here is developed in this paper only for those special translationally invariant interaction potentials which fulfil the condition

$$\sum_{i>k=1}^{A} \mathscr{V}(|\boldsymbol{r}_i' - \boldsymbol{r}_k'|) \to V(\rho, \xi, \eta), \tag{17}$$

i.e. for which the sum (17) is a function depending only on the 3 variables (ρ, ξ, η). Two simple examples of this class of Hamilton operators are

$$\mathscr{H}' = \sum_{1}^{A} - \frac{\hbar^2}{2M} \frac{\partial^2}{\partial \boldsymbol{r}_i'^2} + \sum_{i>k=1}^{A} \tfrac{1}{2} c (\boldsymbol{r}_i' - \boldsymbol{r}_k')^2, \tag{18}$$

representing a system of harmonically coupled particles and

$$\mathscr{H}' = \sum_{1}^{A} - \frac{\hbar^2}{2M} \frac{\partial^2}{\partial \boldsymbol{r}_i'^2} + \sum_{i>k=1}^{A} c_2 (\boldsymbol{r}_i' - \boldsymbol{r}_k')^2 + \sum_{\substack{i>k=1 \\ j>l=1}}^{A} c_4 (\boldsymbol{r}_i' - \boldsymbol{r}_k')^2 (\boldsymbol{r}_j' - \boldsymbol{r}_l')^2, \tag{19}$$

representing a system which contains many-body forces. They will be used to demonstrate the method in detail.

2. Separation of Centre-of-Mass Motion and Internal Motion

This problem can be treated in different ways [1, 5]) †. Here it is solved by a linear orthogonal coordinate transformation, already discussed in ref. [1]). The A particle vectors $(\boldsymbol{r}_1' \ldots \boldsymbol{r}_A')$ are replaced by $(A-1)$ vectors describing the internal motion and by a vector $\boldsymbol{r}_A$ representing the centre-of-mass. The essential point of this transformation is that the Pauli principle can still be easily surveyed in the remaining $(A-1)$ internal vectors. It is given by [1])

$$\boldsymbol{r}_i = \boldsymbol{r}_i' - \frac{\sqrt{A}}{\sqrt{A}-1} \boldsymbol{R} + \frac{1}{\sqrt{A}-1} \boldsymbol{r}_A' \qquad (1 \leqq i \leqq A-1), \tag{20a}$$

$$\boldsymbol{r}_A = \sqrt{A}\, \boldsymbol{R}, \tag{20b}$$

† All other references to this section can be found in the first paper of ref. [5]).

where $\boldsymbol{R}$ is the centre-of-mass vector

$$\boldsymbol{R} = \frac{1}{A}\sum_{1}^{A} \boldsymbol{r}_i'.$$

For an infinite number of particles equation (20a) becomes the familiar relation $\boldsymbol{r}_i = \boldsymbol{r}_i' - \boldsymbol{R}$. Using (20) the differences of two particle vectors are transformed into

$$\boldsymbol{r}_i' - \boldsymbol{r}_k' = \boldsymbol{r}_i - \boldsymbol{r}_k \qquad (i, k < A), \tag{21a}$$

$$\boldsymbol{r}_i' - \boldsymbol{r}_A' = \frac{1}{\sqrt{A}-1}\,[(\sqrt{A}-1)\boldsymbol{r}_i - \boldsymbol{y}] \qquad (1 \leqq i < A), \tag{21b}$$

with

$$\boldsymbol{y} = \sum_{1}^{A-1} \boldsymbol{r}_i. \tag{22}$$

Starting from the Hamilton operator

$$\mathscr{H}' = \sum_{1}^{A} -\frac{\hbar^2}{2M}\frac{\partial^2}{\partial \boldsymbol{r}_i'^2} + \sum_{i>k=1}^{A} \mathscr{V}(|\boldsymbol{r}_i' - \boldsymbol{r}_k'|), \tag{23}$$

the transformation (20) provides for $\mathscr{H}'$ the relation

$$\mathscr{H}' = -\frac{\hbar^2}{2M}\frac{\partial^2}{\partial \boldsymbol{r}_A^2} + \mathscr{H}(\boldsymbol{r}_1 \ldots \boldsymbol{r}_{A-1}), \tag{24}$$

where the first term is the kinetic energy of the centre-of-mass motion and the second term represents the Hamilton operator of the internal motion given by

$$\mathscr{H} = \sum_{1}^{A-1}\left[-\frac{\hbar^2}{2M}\frac{\partial^2}{\partial \boldsymbol{r}_i^2} + \mathscr{V}\left(\frac{|(\sqrt{A}-1)\boldsymbol{r}_i - \boldsymbol{y}|}{\sqrt{A}-1}\right)\right] + \sum_{i>k=1}^{A-1} \mathscr{V}(|\boldsymbol{r}_i - \boldsymbol{r}_k|). \tag{25}$$

Eq. (24) permits us to split the wave function $\Psi'(1 \ldots A)$, defined by (1) into a product of two functions as is done in (8); Ψ is then an eigenfunction of

$$\mathscr{H}\Psi = E\Psi \tag{26}$$

and the connection between E and E' is given by (9). Now the problem is that Ψ has to obey the Pauli principle. Therefore the permutation of two particle coordinates has to be expressed in the internal coordinates. If $\mathrm{P}(\boldsymbol{r}_i', \boldsymbol{r}_k')$ is the operator permuting $\boldsymbol{r}_i'$ with $\boldsymbol{r}_k'$ then the following relations are valid for $i, k < A$:

$$\mathrm{P}(\boldsymbol{r}_i', \boldsymbol{r}_k')\boldsymbol{r}_i = \boldsymbol{r}_k, \qquad \mathrm{P}(\boldsymbol{r}_i', \boldsymbol{r}_k')\boldsymbol{r}_k = \boldsymbol{r}_i, \tag{27a}$$

$$\mathrm{P}(\boldsymbol{r}_i', \boldsymbol{r}_k')\boldsymbol{r}_l = \boldsymbol{r}_l \qquad \text{for } l \neq i, k. \tag{27b}$$

They simply mean that a permutation if $\boldsymbol{r}_i'$ with $\boldsymbol{r}_k'$ is equivalent to a permutation of $\boldsymbol{r}_i$ with $\boldsymbol{r}_k$ for $i, k < A$. If $\boldsymbol{r}_k'$ is permuted with $\boldsymbol{r}_A'$ there results

$$\mathrm{P}(\boldsymbol{r}_k', \boldsymbol{r}_A')\boldsymbol{r}_k = \frac{1}{(\sqrt{A}-1)}\boldsymbol{r}_k + \frac{\sqrt{A}-2}{(\sqrt{A}-1)^2}\boldsymbol{y} \tag{27c}$$

and for all other $(A-2)$ vectors $\boldsymbol{r}_l$

$$\mathrm{P}(\boldsymbol{r}_k', \boldsymbol{r}_A')\boldsymbol{r}_l = \boldsymbol{r}_l + \frac{1}{(\sqrt{A}-1)^2}[(\sqrt{A}-1)\boldsymbol{r}_k - \boldsymbol{y}] \quad (l \neq k), \tag{27d}$$

with $\boldsymbol{y}$ defined in (22). With the help of the relations (27a—d) it is in principle possible to construct functions of the internal coordinates having the desired properties with respect to the permutation of two particle coordinates.

3. Global Mode of Motion

In the range of a description emphasizing the different modes of motion of a system of particles the concept of one-particle functions is not very useful. On the contrary, it is preferable to eliminate completely the independent-particle picture and to look only for the properties of the total system. This idea can be realized by the introduction of adapted coordinates in the $3A$-dimensional space, already carried out in the two preceding papers [1,2]). Much favoured for the treatment of the internal motion are homogeneous functions of the internal coordinates. This is due to the Pauli principle, because the relations (27c—d) involve several internal coordinates. In the following treatment Ψ will be computed as a function of the "many-particle variables" (m.p.v.), introduced earlier [1]). The m.p.v. are homogeneous functions of the internal coordinates (and therefore also of the particle coordinates) which are invariant under the permutation of a definite number of particle coordinates and which obey certain partial differential equations. In the introduction it was indicated that the global motion is an extrapolation of the centre-of-mass motion in the sense that both modes are described by variables which are invariant under the permutation of all particles. As opposed to the centre-of-mass coordinate there does not exist a totally symmetric combination of first degree in the internal coordinates. The quantity

$$g = \sum_1^{A-1} x_i \tag{28}$$

is invariant under the permutations (27a—b) but not under (27c—d). Of the second degree there exist 6 totally symmetric m.p.v.:

$$u = \sum_1^{A-1} x_i^2, \qquad v = \sum_1^{A-1} y_i^2, \qquad w = \sum_1^{A-1} z_i^2, \tag{29}$$

$$g_{110} = \sum_1^{A-1} x_i y_i, \qquad g_{101} = \sum_1^{A-1} x_i z_i, \qquad g_{011} = \sum_1^{A-1} y_i z_i. \tag{30}$$

Therefore the global motion is described by totally symmetric m.p.v. of the second degree. How many of the 6 m.p.v. are involved depends on the interaction potential between the particles. Because it has to be translationally invariant and also totally symmetric in the particle-coordinates it must be possible to express it in terms of the m.p.v.. In the simplest case the interaction energy depends only on u, v, w. This is

already the case for the examples (18) and (19):

$$\sum_{i>k=1}^{A} \tfrac{1}{2}c(r_i'-r_k')^2 \to \tfrac{1}{2}cA(u+v+w), \tag{31}$$

$$\sum_{i>k=1}^{A} c_2(r_i'-r_k')^2+\sum_{\substack{i>k=1\\ j>l=1}}^{A} c_4(r_i'-r_k')^2(r_j'-r_l')^2 \to c_2A(u+v+w)+c_4A^2(u+v+w)^2. \tag{32}$$

Considering this class of interacting systems with

$$\sum_{i>k=1}^{A} \mathscr{V}(|r_i'-r_k'|) \to V(u, v, w), \tag{33}$$

one can try the following Ansatz [1]) for $\psi(r_1 \ldots r_{A-1})$:

$$\psi(r_1 \ldots r_{A-1}) = G(u, v, w)\phi(r_1 \ldots r_{A-1}), \tag{34}$$

where both functions contain all coordinates. Instead of one unknown function two functions have now been introduced. Putting (34) into (26) and applying (33) one obtains

$$\left[4\left(u\frac{\partial^2 G}{\partial u^2}+v\frac{\partial^2 G}{\partial v^2}+w\frac{\partial^2 G}{\partial w^2}\right)+2(A-1)\left(\frac{\partial G}{\partial u}+\frac{\partial G}{\partial v}+\frac{\partial G}{\partial w}\right)\right]\phi+G\sum_{1}^{A-1}\frac{\partial^2\phi}{\partial r_i^2}$$
$$+4\left[\frac{\partial G}{\partial u}\left(\sum_{1}^{A-1}x_i\frac{\partial\phi}{\partial x_i}\right)+\frac{\partial G}{\partial v}\left(\sum_{1}^{A-1}y_i\frac{\partial\phi}{\partial y_i}\right)+\frac{\partial G}{\partial w}\left(\sum_{1}^{A-1}z_i\frac{\partial\phi}{\partial z_i}\right)\right] \tag{35}$$
$$+\frac{2M}{\hbar^2}[E-V(u, v, w)]G\phi = 0.$$

From (35) one can get an equation for $G(u, v, w)$ only if one imposes upon ϕ the following conditions:

$$\sum_{1}^{A-1}\frac{\partial^2\phi}{\partial r_i^2} = 0, \tag{36a}$$

$$\sum_{1}^{A-1}x_i\frac{\partial\phi}{\partial x_i} = K_1\phi, \qquad \sum_{1}^{A-1}y_i\frac{\partial\phi}{\partial y_i} = K_2\phi, \qquad \sum_{1}^{A-1}z_i\frac{\partial\phi}{\partial z_i} = K_3\phi, \tag{36b}$$

where K_1, K_2, K_3, are positive integer constants. There remains for $G(u, v, w)$ the equation

$$2\left[u\frac{\partial^2 G}{\partial u^2}+v\frac{\partial^2 G}{\partial v^2}+w\frac{\partial^2 G}{\partial w^2}\right]+[2K_1+A-1]\frac{\partial G}{\partial u}+[2K_2+A-1]\frac{\partial G}{\partial v}$$
$$+[2K_3+A-1]\frac{\partial G}{\partial w}+\frac{M}{\hbar^2}[E-V(u, v, w)]G(u, v, w) = 0. \tag{37}$$

With respect to the angular momentum classification it is advantageous to introduce

new variables ρ, ξ, η given by [1])

$$\rho = u+v+w, \qquad \xi = \frac{u}{u+v}, \qquad \eta = \frac{u+v}{u+v+w}. \tag{38}$$

The transformation of (37) then provides the fundamental equation of the global motion:

$$\left[\rho^2 \frac{\partial^2 G}{\partial \rho^2} + \frac{\xi(1-\xi)}{\eta}\frac{\partial^2 G}{\partial \xi^2} + \eta(1-\eta)\frac{\partial^2 G}{\partial \eta^2}\right] + [K_1+K_2+K_3+\tfrac{3}{2}(A-1)]\rho\frac{\partial G}{\partial \rho}$$
$$+ \frac{1}{\eta}[K_1+\tfrac{1}{2}(A-1)-(K_1+K_2+A-1)\xi]\frac{\partial G}{\partial \xi}$$
$$+ [K_1+K_2+A-1-(K_1+K_2+K_3+\tfrac{3}{2}(A-1))\eta]\frac{\partial G}{\partial \eta}$$
$$+ \frac{M}{2\hbar^2}\rho[E-V(\rho,\xi,\eta)]G(\rho,\xi,\eta) = 0. \tag{39}$$

The equations (36a—b) and (39) deduced from the Schrödinger equation (26) represent the separation of the internal motion into the two different modes. The function $\phi(r_1 \ldots r_{A-1})$ is the space dependent part of the specific motion and is determined by eqs. (36a—b), which are independent of the special form of $V(\rho, \xi, \eta)$. The global motion is described by the function G containing only the 3 variables ρ, ξ, η. In eqs. (13a—c) they are expressed in the particle-coordinates. The essential properties of G with respect to ρ, ξ, η are independent of the number of particles. Further information on the global motion depends on the explicit form of $V(\rho, \xi, \eta)$. If it depends only on ρ, as is the case for the examples (31) and (32), then eq. (39) can be solved by standard methods. The result is

$$G_{n\lambda\mu}(\rho, \xi, \eta) = \rho^{(\lambda+\mu)} f_{n,\lambda\mu}(\rho)\eta^{\mu}\vartheta_{\lambda,\mu}(\eta)\gamma_{\mu}(\xi), \tag{40}$$

where $\gamma_{\mu}(\xi)$ and $\vartheta_{\lambda,\mu}(\eta)$ are Jacobi polynomials obeying the equations

$$\xi(\xi-1)\frac{d^2\gamma_{\mu}}{d\xi^2} + [(K_1+K_2+A-1)\xi-(K_1+\tfrac{1}{2}(A-1))]\frac{d\gamma_{\mu}}{d\xi}$$
$$-\mu(\mu+K_1+K_2+K_3+A-2)\gamma_{\mu}(\xi) = 0 \qquad (\mu = 0, 1, 2 \ldots), \tag{41}$$

$$\eta(\eta-1)\frac{d^2\vartheta_{\lambda,\mu}}{d\eta^2} + [(2\mu+K_1+K_2+K_3+\tfrac{3}{2}(A-1))\eta-(2\mu+K_1+K_2+A-1)]\frac{d\vartheta_{\lambda,\mu}}{d\eta}$$
$$-\lambda(\lambda+2\mu+K_1+K_2+K_3+\tfrac{3}{2}A-\tfrac{5}{2})\vartheta_{\lambda,\mu}(\eta) = 0 \qquad (\lambda = 0, 1, 2 \ldots), \tag{42}$$

and $f_{n,\lambda\mu}(\rho)$ must be an eigenfunction of

$$\rho\frac{d^2 f_{n,\lambda\mu}}{d\rho^2} + [2(\lambda+\mu)+K_1+K_2+K_3+\tfrac{3}{2}(A-1)]\frac{df_{n,\lambda\mu}}{d\rho} + \frac{M}{2\hbar^2}[E_n-V(\rho)]f_{n,\lambda\mu}(\rho) = 0. \tag{43}$$

Without going into further details one already gets from (43) the degeneracy of the energy eigenvalues, because E_n is only a function of the two quantities n and $K_1+K_2+K_3+2(\lambda+\mu)$:

$$E_n = E_n(n, K_1+K_2+K_3+2(\lambda+\mu)), \tag{44}$$

where the permitted values of K_1, K_2, K_3 are determined by the specific motion, and those of λ, μ are given by (41), (42) and those of n follow from the eigenfunctions $f_{n,\lambda\mu}(\rho)$ of (43).

As an example, the energy spectrum of A harmonically coupled particles described by (18) is given by

$$E = \hbar\omega[\tfrac{3}{2}(A-1)+2(n+\lambda+\mu)+K_1+K_2+K_3] \quad (n, \lambda, \mu = 0, 1, 2\ldots), \tag{45}$$

with

$$\omega = \sqrt{\frac{Ac}{M}}.$$

The permitted values of n, λ, μ determined by the global motion are independent of the number of particles, which is not the case for the values of K_1, K_2, K_3, as will be shown later.

4. General Statements about the Specific Motion

4.1. SYMMETRY PROPERTIES OF THE SPACE FUNCTIONS

The function of the specific motion is responsible for the fact that all conditions for the total wave function with respect to the Pauli principle (3), spin (6)—(7) and isobaric spin (4)—(5) must be fulfilled. A great help for the decomposition of Z into the form (14) is provided by the so-called "Young-tableaux" [2,3]). The symmetry properties of a function of A particles with respect to the permutation of two particles

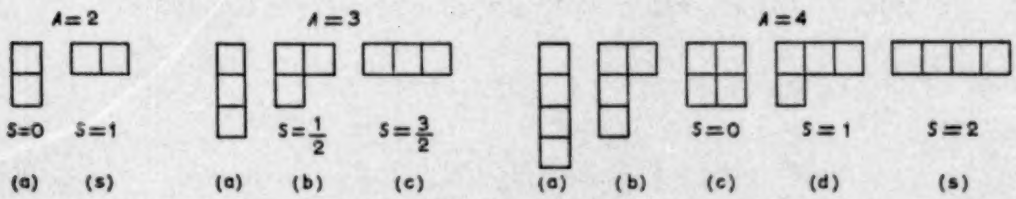

Fig. 1. Standard frames for 2, 3 and 4 particles.

can be characterized by the "standard frames" and the "standard tableaux". A standard frame is a scheme consisting of A squares placed in rows and columns in such a way that the number of squares in the rows does not increase downwards and the number of squares in the column does not increase from left to right. As examples the standard frames are given for $A = 2$, 3 and 4 particles in fig. 1. The standard tableaux are deduced from the standard frames by putting numbers in the squares in such a way that the numbers only increase if one goes from left to right or downwards.

For the above examples they are given in fig. 2. The symbols written in the brackets (r_ν) in fig. 2 indicating the frame and the tableau are added to the corresponding functions.

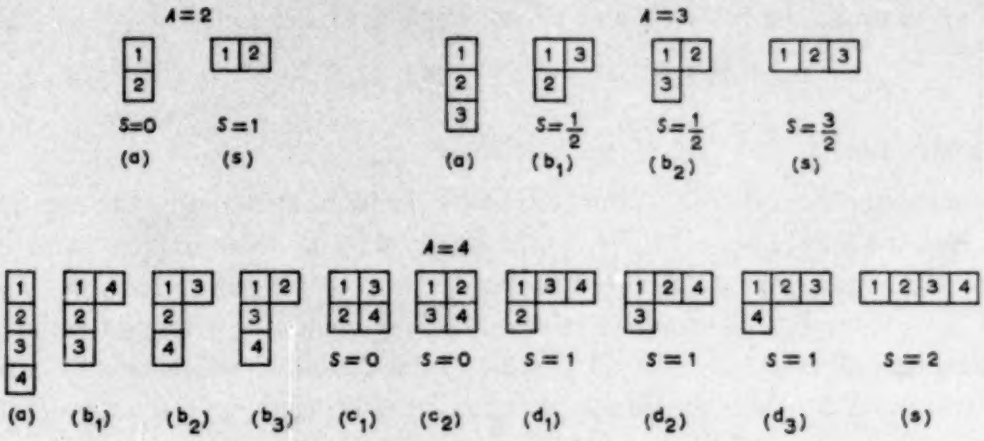

Fig. 2. Standard tableaux for 2, 3 and 4 particles.

About the Young tableaux and their application one can state the following rules [2,3])

I. If a standard frame (r) has z different standard tableaux (r_ν) with the corresponding functions $\phi^{r_1} \ldots \phi^{r_z}$, the application of the permutation operator $\mathrm{P}(i, k)$ on one of the functions provides a function which can be expressed as a linear combination of all the z functions ϕ^{r_ν}:

$$\mathrm{P}(i, k)\phi^{r_\nu} = \sum_{\rho=1}^{z} A_{\nu\rho}(i, k)\phi^{r_\rho}. \tag{46}$$

II. The determinant of the $A_{\nu\rho}(i, k)$ has the value -1:

$$\det |A_{\nu\rho}(i, k)| = -1. \tag{47}$$

III. The functions ϕ^{r_ν} are antisymmetric with respect to permutation of the numbers in each column:

$$\mathrm{P}(i, k)\phi^{r_\nu} = -\phi^{r_\nu}, \tag{48}$$

if i, k belong to the same column.

IV. The functions are symmetric with respect to the permutation of the numbers of those columns having only one square:

$$\mathrm{P}(i, k)\phi^{r_\nu} = \phi^{r_\nu}, \tag{49}$$

if i, k belong to columns with only one square.

V. The spin and isobaric spin functions are represented by Young tableaux having not more than two rows. If the number of the squares in the upper row is n_1 and that of the lower one is n_2, the spin quantum number of the corresponding function is

$$S = \tfrac{1}{2}(n_1 - n_2). \tag{50}$$

An analogous relation is valid for the isobaric spin quantum number T.

VI. Because of the Pauli principle only those functions ϕ^r of the specific motion (36a—b) are physically meaningful, which can be represented by Young tableaux having not more than 4 columns.

As an example the rules III and IV are applied to the function ϕ^{d_1} of fig. 2:

$$P(1,2)\phi^{d_1} = -\phi^{d_1}, \qquad P(3,4)\phi^{d_1} = \phi^{d_1}.$$

4.2. COMPUTATION OF THE SPIN FUNCTIONS

A simple application of the Young tableaux yields the spin and isobaric spin functions. Because they have only two rows the standard frame is determined by the spin S and by the number of particles A. The number of possible multiplets with spin S is equal to the number of standard tableaux belonging to this standard frame. The result is given in table 2 of ref. [2]). The $(2S+1)$ spin functions which exist for a multiplet with spin S can be obtained as the expansion coefficients of a function F of two variables x, y (refs. [2-4])):

$$F(x, y; S, A) = \sum_{M_S=-S}^{+S} \chi_{SM_S} x^{S+M_S} y^{S-M_S}. \tag{51}$$

The computation of F is easy. If a system of A particles has the spin S, then

$$g = \tfrac{1}{2}A - S \tag{52}$$

pairs exist in which the particles have opposite spin and

$$2S \tag{53}$$

particles have parallel spins. The corresponding standard tableau consists of g columns with two squares and $2S$ columns with only one square. If the spin function of the i-th particle with spin up is called α_i and that with spin down β_i, one must form for every column with two squares containing the number i and k the expression

$$\alpha_i\beta_k - \alpha_k\beta_i \tag{54}$$

and for every column with only one square containing the number j the expression

$$\alpha_j x + \beta_j y. \tag{55}$$

The function F is now obtained by multiplying the g factors (54) with the $2S$ factors (55):

$$F(x, y; S, A) = \prod_{i,k}^{g} (\alpha_i\beta_k - \alpha_k\beta_i) \prod_{j}^{2S} (\alpha_j x + \beta_j y). \tag{56}$$

The expansion coefficients of (56) are the spin functions χ_{SM_S} without normalisation factors. If a_i denotes that the i-th particle is in a proton state and b_i that it is in neutron state, the isobaric spin functions ζ_{TM_T} are obtained from the spin functions χ_{SM_S} by replacing α_i with a_i and β_i with b_i.

As an example, the function F is given for the tableau (d_1) of fig. 2:

$$F^{d_1}(x, y) = (\alpha_1\beta_2 - \alpha_2\beta_1)(\alpha_3 x + \beta_3 y)(\alpha_4 x + \beta_4 y). \tag{57}$$

4.3. COMBINATIONS OF SPACE, SPIN AND ISOBARIC SPIN FUNCTIONS

A function having to satisfy the conditions (1)—(7) can be written as a linear combination of products of space, spin and isobaric spin functions as shown by eq. (10). Because the global motion contains only totally symmetric expressions of the particle coordinates a similar decomposition is valid for the function Z of the specific motion (14). The conditions (4)—(7) are already satisfied by the single functions, therefore the next problem is to look for such linear combinations which fulfil the Pauli principle. A wave function with given values of S and T can contain only the corresponding spin and isobaric spin functions. The value of S determines the standard frame, so that a summation over all spin functions (with a fixed value of M_S) is equivalent to a summation over all standard tableaux belonging to this standard frame. In the case of the space functions a similar relation is valid. Only space functions of the same standard frame occur in the sum (14). There remain two problems:

A. To find the standard frame of the space functions which can provide an admitted combination with the given spin and isobaric spin functions.

B. Which functions belonging to the different standard tableaux have to be combined and what are the explicit values of the coefficients $q_{\kappa\lambda\nu}$ of eq. (14)?

For the knowledge of the energy eigenvalues of states with given values of S and T only problem (A) must be solved, while the explicit form of the function Z of (14) requires the solutions of the problems (A) and (B). The solutions can be found in different ways. A method presented in detail in ref. [2]) was there only applied to a system of 3 particles. But it can easily be extended to the case of an arbitrary number of particles.

To obtain the explicit form of the function Z with given values of S and T one starts with the Ansatz

$$Z = \sum_{\kappa,\lambda,\nu} q_{\kappa\lambda\nu}\phi^{r\kappa}\chi^{s\lambda}\zeta^{t\nu}, \tag{58}$$

where the $q_{\kappa\lambda\nu}$ are arbitrary coefficients and the sums over λ and ν run over all admitted spin and isobaric spin functions. The sum over κ runs over all tableaux belonging to a standard frame suitably assumed at the beginning. The function Z now has to obey the Pauli principle (3):

$$\mathrm{P}(i,k)Z + Z = 0. \tag{59}$$

Applying the permutation operator $\mathrm{P}(i,k)$ to the typical products on the right-hand side of (58) provides, with the help of rule I, the relation

$$\mathrm{P}(i,k)\phi^{r\kappa}\chi^{s\lambda}\zeta^{t\nu} = \sum_{\rho,\sigma,\tau} A_{\kappa\rho}A_{\lambda\sigma}A_{\nu\tau}(i,k)\phi^{r\rho}\chi^{s\sigma}\zeta^{t\tau}. \tag{60}$$

Putting the Ansatz (58) in eq. (59) and using (60) a linear homogeneous system of equations can be derived for the $q_{\kappa\lambda\nu}$ if one compares the coefficients of the same

combination of functions:

$$q_{\rho\sigma\tau} + \sum_{\kappa,\lambda,\nu} q_{\kappa\lambda\nu} A_{\kappa\rho} A_{\lambda\sigma} A_{\nu\tau}(i,k) = 0. \tag{61}$$

The investigation of the coefficient determinant provides in the case considered, with the help of the rules I—IV, certain relations between the $q_{\kappa\lambda\nu}$. If, for instance, the determinant does not vanish, all the $q_{\kappa\lambda\nu}$ must vanish. This would mean that one has combined the space functions of a wrong standard frame with the spin and isobaric spin functions. Usually the application of the rules I—IV causes some of the equations to become linearly dependent. Then not all the coefficients must vanish, and the remaining ones determine the function Z.

TABLE 1

Admitted combinations of space, spin and isobaric spin functions for 2, 3 and 4 particles

$A=2$			$A=3$		
	$S=1$	$S=0$		$S=\frac{3}{2}$	$S=\frac{1}{2}$
$T=1$	$\phi^a\chi^s\zeta^s$	$\phi^s\chi^a\zeta^s$	$T=\frac{3}{2}$	$\phi^a\chi^s\zeta^s$	$(\phi^{b_1}\chi^{b_2}-\phi^{b_2}\chi^{b_1})\zeta^s$
$T=0$	$\phi^s\chi^s\zeta^a$	$\phi^a\chi^a\zeta^a$	$T=\frac{1}{2}$	$(\phi^{b_1}\zeta^{b_2}-\phi^{b_2}\zeta^{b_1})\chi^s$	$\phi^s(\chi^{b_1}\zeta^{b_2}-\chi^{b_2}\zeta^{b_1})$

$A=4$			
	$S=2$	$S=1$	$S=0$
$T=2$	$\phi^a\chi^s\zeta^s$	$(\phi^{b_1}\chi^{d_2}-\phi^{b_2}\chi^{d_2}+\phi^{b_2}\chi^{d_1})\zeta^s$	$(\phi^{c_1}\chi^{c_2}-\phi^{c_2}\chi^{c_1})\zeta^s$
$T=1$	$(\phi^{b_1}\zeta^{d_2}-\phi^{b_2}\zeta^{d_2}+\phi^{b_2}\zeta^{d_1})\chi^s$	$\phi^{d_1}(\chi^{d_2}\zeta^{d_2}-\chi^{d_2}\zeta^{d_2})+$ $\phi^{d_2}(\chi^{d_2}\zeta^{d_1}-\chi^{d_1}\zeta^{d_2})+$ $\phi^{d_2}(\chi^{d_1}\zeta^{d_2}-\chi^{d_2}\zeta^{d_1})$	$(\phi^{d_1}\zeta^{d_2}+\phi^{d_2}\zeta^{d_1})(\chi^{c_1}-\chi^{c_2})$ $-(\phi^{d_2}\zeta^{d_2}+\phi^{d_2}\zeta^{d_2})\chi^{c_1}$ $+(\phi^{d_1}\zeta^{d_2}+\phi^{d_2}\zeta^{d_1})\chi^{c_2}$
$T=0$	$(\phi^{c_1}\zeta^{c_2}-\phi^{c_2}\zeta^{c_1})\chi^s$	$(\phi^{d_1}\chi^{d_2}+\phi^{d_2}\chi^{d_1})(\zeta^{c_1}-\zeta^{c_2})$ $-(\phi^{d_2}\chi^{d_2}+\phi^{d_2}\chi^{d_2})\zeta^{c_1}$ $+(\phi^{d_1}\chi^{d_2}+\phi^{d_2}\chi^{d_1})\zeta^{c_2}$	$\phi^s(\chi^{c_1}\zeta^{c_2}-\chi^{c_2}\zeta^{c_1})$

To become familiar with the possible combinations, they are given for the cases of 2, 3 and 4 particles in table 1.

5. Space Functions of the Specific Motion in the One-Dimensional Case

The space functions of the specific motion for a one-dimensional system of A particles are determined according to (36a—b) by the following "eigenvalue" problem

$$\sum_1^{A-1} \frac{\partial^2 \phi_k^{r_\nu}}{\partial x_i^2} = 0, \tag{62}$$

$$\sum_1^{A-1} x_i \frac{\partial \phi_k^{r_\nu}}{\partial x_i} = K\phi_k^{r_\nu}, \tag{63}$$

$$\phi_k^{r_\nu} \text{ belongs to the standard tableau } (r_\nu). \tag{64}$$

The values of K for which it is possible to find solutions of (62)—(64) are called the "eigenvalues" of the specific motion, though the problem does not coincide completely with a usual eigenvalue problem. In order to solve eqs. (62)—(64) one has to look for all homogeneous solutions of the $(A-1)$-dimensional Laplace equation having the symmetry properties of the corresponding tableau (r_ν). A great help for the computation of these functions is provided by the so-called m.p.v. already used for the description of the global motion.

The m.p.v. necessary for the computation of the functions $\phi_K^{r_\nu}$ are homogeneous functions of the internal coordinates which are symmetric with respect to the permutations of all particles a) belonging to one column, b) belonging to columns with only one square. Except u given by (29) they are designated by $g_l^{r_\nu}$, indicating the tableau (r_ν) and the degree l. The conditions (a) and (b) can then be written

$$P(x_i', x_k')g_l^{r_\nu}(x_1 \dots x_{A-1}) = g_l^{r_\nu}(x_1 \dots x_{A-1}) \tag{65}$$

for all i, k of the same column,

$$P(x_i', x_k')g_l^{r_\nu}(x_1 \dots x_{A-1}) = g_l^{r_\nu}(x_1 \dots x_{A-1}) \tag{66}$$

for all i, k of columns with only one square.
From the definitions (65) and (66) one can see that the m.p.v. can be equal for the different tableaux. To every tableau one has to construct $(A-1)$ independent m.p.v. of the lowest possible degree. This can always be achieved for the following values of l:

$$1 \leqq l \leqq A. \tag{67}$$

After having found the m.p.v. one has to look for the lowest admitted value of K, called k. The corresponding function, designated by $\phi_k^{r_\nu} \equiv \varphi_k^{r_\nu}$, plays an important role. It is now possible to write all the eigenfunctions of (62)—(64) in the form

$$\phi_K^{r_\nu}(x_1 \dots x_{A-1}) = \varphi_k^{r_\nu}(x_1 \dots x_{A-1})F_N^{r_\nu}(u, g_l^{r_\nu}), \tag{68}$$

with

$$K = k+N, \tag{69}$$

where the functions F are finite power series of the $(A-1)$ m.p.v.

To see how the method works, it is advantageous to begin the computations with the two extreme cases, where the corresponding tableaux have only one column or one row, i.e. with the totally antisymmetric and totally symmetric functions ϕ. The general case when ϕ has 4 columns can be deduced directly from these considerations.

The lowest eigenvalue of the totally antisymmetric function ϕ_K^a of a system of A particles is [1])

$$k^a = \tfrac{1}{2}A(A-1) \tag{70a}$$

and the corresponding function has the form

$$\varphi_k^a = \prod_{i>k=1}^{A-1}(x_i-x_k)\prod_{j=1}^{A-1}(g-(\sqrt{A}-1)x_j), \tag{71a}$$

where g is given by (28). The condition (65) requires that only totally symmetric m.p.v. can be used. There does not exist a m.p.v. of the first degree and for every degree between 2 and A there exists only one. Therefore the function F of (68) contains the $(A-1)$ m.p.v. from degree 2 up to degree A:

$$F^a = F^a(u, g_3^a \dots g_A^a). \tag{72a}$$

The conditions (65), (66) and the requirement of homogeneity does not determine completely the g_l^a. It is still possible to impose upon them the differential equation

$$\sum_1^{A-1} \frac{\partial^2}{\partial x_i^2}(\varphi^a g_l^a) = 0 \qquad \text{for} \quad l = 3, 4 \dots A. \tag{73a}$$

Putting the Ansatz (68) into (62) and using the simplification caused by (63),

$$2u \frac{\partial F_N}{\partial u} + \sum_{l=3}^{A} l g_l \frac{\partial F_N}{\partial g_l} = N F_N, \tag{74}$$

and that caused by (73), the following differential equation is obtained for $F_N(u, g_l)$:

$$(2N + A^2 - 5)\frac{\partial F_N}{\partial u} - 2u \frac{\partial^2 F_N}{\partial u^2} + \tfrac{1}{2}\sum_{l=3}^{A} \frac{\partial^2 F_N}{\partial g_l^2}\left[\sum_1^{A-1}\left(\frac{\partial g_l}{\partial x_i}\right)^2\right]$$
$$+ \sum_{n>l=3} \frac{\partial^2 F_N}{\partial g_n \partial g_l}\left[\sum_1^{A-1}\left(\frac{\partial g_n}{\partial x_i}\right)\left(\frac{\partial g_l}{\partial x_i}\right)\right] = 0, \tag{75}$$

where the sums

$$\sum_1^{A-1}\left(\frac{\partial g_n}{\partial x_i}\right)\left(\frac{\partial g_l}{\partial x_i}\right)$$

can always be expressed in term of the m.p.v. Because of the condition (63) the solutions of (75) are finite power series of the form

$$F_N^a(u, g_3 \dots g_A) = \sum_{\langle p_i \rangle} \alpha_{p_A p_{A-1} \dots p_3 p_2} g_A^{p_A} g_{A-1}^{p_{A-1}} \dots g_3^{p_3} u^{p_2}. \tag{76}$$

The symbol $\langle p_i \rangle$ means a summation running over all non-negative integral values of p_i obeying the subsidiary condition

$$N = A p_A + (A-1)p_{A-1} + \dots + 3p_3 + 2p_2. \tag{77}$$

The coefficients $\alpha_{p_A \dots p_2}$ are determined by the differential equation (75). To every expression of the form

$$g_A^{p_A} g_{A-1}^{p_{A-1}} \dots g_3^{p_3}, \tag{78}$$

there exists an independent solution. This degeneracy yields for the permitted values of N the relation

$$N = 3n_3 + 4n_4 + \dots + An_A, \tag{79}$$

where the numbers n_l can take on all non-negative integral values independently of

each other. Using (69) the eigenvalue spectrum of the specific motion of a standard frame with A squares in one column is thereby determined as

$$K^a = \tfrac{1}{2}A(A-1)+3n_3+4n_4+\ldots+An_A \qquad (n_i = 0, 1, 2\ldots). \tag{80a}$$

The totally symmetric function ϕ^s has the lowest eigenvalue

$$k = 0, \tag{70b}$$

demanding

$$\varphi = 1. \tag{71b}$$

The function F^s depends on the $(A-1)$ m.p.v.

$$F^s = F^s(u, g_3^s \ldots g_A^s), \tag{72b}$$

which fulfil the condition

$$\sum_1^{A-1} \frac{\partial^2 g_l^s}{\partial x_i^2} = 0 \qquad \text{for} \quad l = 3, 4 \ldots A. \tag{73b}$$

With the same method analogous expressions can be obtained for the differential equation of the function F^s and the corresponding solutions. The degeneracy is exactly the same. This yields according to (69) and (70b) for the eigenvalue spectrum of the specific motion of a standard frame with A squares in one row the relation

$$K^s = 3n_3+4n_4+\ldots+An_A \qquad (n_i = 0, 1, 2\ldots). \tag{80b}$$

Because of rule VI these functions are not needed for $A > 4$.

In the general case, when the tableau of ϕ has 4 columns, one has to construct for every column j the corresponding functions φ_{κ_j}. They are totally antisymmetric in all particles of the column j and their degree κ_j is the lowest possible one. The function $\varphi_k^{r_\nu}$ of (68) is now the product of the 4 functions φ_{κ_j}

$$\varphi_k^{r_\nu} = \prod_1^4 \varphi_{\kappa_j}, \tag{81}$$

with

$$k = \sum_1^4 \kappa_j. \tag{82}$$

Using conditions (65) and (66) the $(A-1)$ m.p.v. can be found and the Ansatz (68) provides a differential equation for F, which is similar to the equation (75). Further details of the solutions and their degeneracy depend on the special form of the tableau. It is always possible to give the eigenvalue spectrum a form analogous to (80). To become familiar with this procedure the case of a system of 4 particles will be studied in detail in one of the subsequent sections.

6. Space Functions of the Specific Motion in the Three-Dimensional Case

Considering the general case of a three-dimensional system of A particles the space functions of the specific motion are determined according to (36a—b) by the following

"eigenvalue" problem:

$$\sum_{1}^{A-1} \frac{\partial^2 \phi_K^{r_\nu}}{\partial r_i^2} = 0, \tag{83}$$

$$\sum_{1}^{A-1} x_i \frac{\partial \phi_K^{r_\nu}}{\partial x_i} = K_1 \phi_K^{r_\nu}, \qquad \sum_{1}^{A-1} y_i \frac{\partial \phi_K^{r_\nu}}{\partial y_i} = K_2 \phi_K^{r_\nu}, \qquad \sum_{1}^{A-1} z_i \frac{\partial \phi_K^{r_\nu}}{\partial z_i} = K_3 \phi_K^{r_\nu}; \tag{84}$$

$$\phi_K^{r_\nu} \text{ belongs to the standard tableau } (r_\nu). \tag{85}$$

The index K on the function $\phi_K^{r_\nu}$ is an abbreviation for the 3 indices K_1, K_2, K_3, which are called the "eigenvalues" of the specific motion. The problem is here to look for all solutions of the $(3A-3)$-dimensional Laplace equation which are homogeneous in the x_i as well as in the y_i and the z_i, having the symmetry properties of the corresponding tableau (r_ν). It is again advantageous to introduce the m.p.v. for the computation of these functions.

The m.p.v. for the tableau (r_ν) are designated by $g_{lnq}^{r_\nu}$ and are defined in the following way:

$$\sum_{1}^{A-1} x_i \frac{\partial g_{lnq}^{r_\nu}}{\partial x_i} = l g_{lnq}^{r_\nu}, \qquad \sum_{1}^{A-1} y_i \frac{\partial g_{lnq}^{r_\nu}}{\partial y_i} = n g_{lnq}^{r_\nu}, \qquad \sum_{1}^{A-1} z_i \frac{\partial g_{lnq}^{r_\nu}}{\partial z_i} = q g_{lnq}^{r_\nu}, \tag{86}$$

$$\mathrm{P}(r_i', r_k') g_{lnq}^{r_\nu}(r_1 \ldots r_{A-1}) = g_{lnq}^{r_\nu}(r_1 \ldots r_{A-1}) \tag{87}$$

for all i, k of the same column,

$$\mathrm{P}(r_i', r_k') g_{lnq}^{r_\nu}(r_1 \ldots r_{A-1}) = g_{lnq}^{r_\nu}(r_1 \ldots r_{A-1}) \tag{88}$$

for all i, k of columns with only one square.

The values of l, n, q are the lowest possible ones which are compatible with the conditions (87) and (88). They can be chosen such that their sum fulfils the relation

$$1 \leqq l+n+q \leqq A. \tag{89}$$

The m.p.v. satisfying the conditions (86)—(89) can be deduced from the m.p.v. of the one-dimensional case by cyclic permutation of x_i with y_i and z_i and by means of the "internal" orbital angular momentum operator [1,2]). The internal orbital angular momentum is obtained from the orbital angular momentum

$$\boldsymbol{L}' = \sum_{1}^{A-1} \boldsymbol{r}_i' \times \boldsymbol{p}_i', \tag{90}$$

by splitting off the angular momentum of the centre-of-mass about a fixed point in space. This is achieved by applying the transformation (20) on (90) giving for $\boldsymbol{L}'$ the expression

$$\boldsymbol{L}' = \boldsymbol{r}_A \times \boldsymbol{p}_A + \sum_{1}^{A-1} \boldsymbol{r}_i \times \boldsymbol{p}_i, \tag{91}$$

where the second term represents the internal orbital angular momentum:

$$\boldsymbol{L} = \sum_{1}^{A-1} \boldsymbol{r}_i \times \boldsymbol{p}_i . \tag{92}$$

The application of one of the components of the internal angular momentum operator $\mathscr{L}$, designated by $\mathscr{L}_x$, $\mathscr{L}_y$ and $\mathscr{L}_z$, on the m.p.v. $g_{l00}(x_1 \ldots x_{A-1})$ provide other m.p.v.:

$$\mathscr{L}_y g_{l00} \propto g_{(l-1)01}, \tag{93}$$

$$\mathscr{L}_z g_{l00} \propto g_{(l-1)10}. \tag{94}$$

The repeated applications of the operators $\mathscr{L}_x$, $\mathscr{L}_y$ or $\mathscr{L}_z$ provide either again a m.p.v. or a linear combination of them:

$$\mathscr{L}_y \mathscr{L}_z g_{l00} \propto g_{(l-2)11}, \tag{95}$$

$$\mathscr{L}_x \mathscr{L}_y \mathscr{L}_z g_{l00} \propto \alpha g_{(l-2)20} + \beta g_{(l-2)02}, \tag{96}$$

where α and β of eq. (96) are irrelevant coefficients. All the independent m.p.v. which can be deduced from the $(A-1)$ m.p.v. of the one-dimensional case have to be computed. Their number depends not only on A but also on the form of the standard frame.

As the next step one has to look for all "antisymmetric factors" $\varphi^{r_\nu}_{k_1k_2k_3}$. These are eigenfunctions of the equations (83)—(85) to the lowest possible values of $K_1+K_2+K_3$, and therefore they do not contain the m.p.v. As opposed to the one-dimensional case, in which only one factor exists for every tableau, given by (71a) and (81), there exist several such factors in the three-dimensional case. If the tableau has four columns, they are totally antisymmetric in all particles of the same column. Analogously to the one-dimensional case they can be written as products of four functions, every one of which is totally antisymmetric in the particles of the corresponding column:

$$\varphi_{k_1k_2k_3} = \prod_{1}^{4} \varphi_{\kappa_{1j}\kappa_{2j}\kappa_{3j}}, \tag{97}$$

with

$$k_1 = \sum_{1}^{4} \kappa_{1j}, \qquad k_2 = \sum_{1}^{4} \kappa_{2j}, \qquad k_3 = \sum_{1}^{4} \kappa_{3j}, \tag{98}$$

where κ_{1j}, κ_{2j} and κ_{3j} are the degrees of homogeneity in x, y and z of the column j. Unfortunately not all the functions $\varphi^{r_\nu}_{k_1k_2k_3}$ of the three-dimensional case can be derived from the corresponding ones of the one-dimensional case. But it is only necessary to look for one function with a given value of $K_1+K_2+K_3$, because all the other functions follow by cyclic permutation or by application of the components of the internal angular momentum operator on a given $\varphi^{r_\nu}_{k_1k_2k_3}$. The functions $\varphi_{\kappa_{1j}\kappa_{2j}\kappa_{3j}}$ can be found by means of determinants which provide directly totally antisymmetric functions. After having found all the needed quantities one can make for the general solution of (83)—(85) the Ansatz

$$\phi^{r_\nu}_K(\boldsymbol{r}_1 \ldots \boldsymbol{r}_{A-1}) = \sum_{\langle k_i \rangle} \varphi^{r_\nu}_{k_1k_2k_3}(\boldsymbol{r}_1 \ldots \boldsymbol{r}_{A-1}) F^{(k_1k_2k_3)}_{N_1N_2N_3}(u, v, w, g^{r_\nu}_{lnq}), \tag{99}$$

where the functions F are finite power series of the m.p.v. and the $\varphi^{r\nu}_{k_1k_2k_3}$ are the above considered antisymmetric factors. The symbol $\langle k_i \rangle$ signifies that one has to sum only over such values of k_i which fulfil the condition

$$k_1+N_1 = K_1, \quad k_2+N_2 = K_2, \quad k_3+N_3 = K_3. \tag{100}$$

The indices N_1, N_2, N_3 are the degrees of homogeneity in x, y and z of the function F, if the m.p.v. are expressed in the internal coordinates. In principle it is possible to put the Ansatz (99) in the equation (83) giving partial differential equations for the functions $F(u, v, w, g^{rn}_{inq})$ which are similar to eq. (75). If the sum (99) contains only a few terms, this method is useful [1]). Otherwise it is preferable to write down explicitly the power series of F with arbitrary coefficients which are compatible with the conditions (100) and to determine the coefficients by applying (83) and (85). In any case one has to take care that all conditions which are associated with the Young tableaux are satisfied. If e.g. the computations provide two equal functions for different tableaux,

$$\phi^{r_1}_K = \phi^{r_2}_K, \tag{101}$$

these functions belong neither to tableau (r_1) nor (r_2) but to a tableau where the conditions for (r_1) as well as for (r_2) have to be fulfilled.

So far the 3 quantities K_1, K_2, K_3 were considered as the eigenvalues of the specific motion. The "eigenvalue spectrum" is then determined by the permitted value of K_1, K_2, K_3, and by the degeneracy, i.e. the number of functions with given values of K_1, K_2, K_3. But being concerned with the energy spectrum (44) it is also meaningful to define the quantity K given by

$$K = K_1+K_2+K_3 \tag{102}$$

as the eigenvalue of the specific motion, though it does not occur explicitly in eqs. (83)—(85). The corresponding eigenvalue spectrum is then characterized by the values of K and their degeneracy. It is in general no longer so easy to give closed expressions for the eigenvalue spectrum of K for a given frame of the form

$$K^r = K^r(A, n_i) \qquad (n_i = 0, 1, 2 \ldots), \tag{103}$$

as it is in the one-dimensional case in the equations (80a—b). For the simple case such as the totally symmetric and the totally antisymmetric states for a system of 3 particles it is however possible. In the first case we find

$$K^s = 2(n_1+n_2+n_3)+3(m_1+m_2+\ldots+m_{10}) \qquad (n_i, m_i = 0, 1, 2 \ldots), \tag{104}$$

where the n_i, m_i can have all non-negative integral values independently of each other. The second case is described by

$$K^a = 2(n_1+n_2+n_3)+3(m_1+m_2+\ldots+m_{10}) \qquad (n_i, m_i = 0, 1, 2 \ldots), \tag{105a}$$

with the subsidiary condition

$$\sum_i (n_i+m_i) \neq 0, \tag{105b}$$

i.e. not all the numbers n_i, m_i should vanish at the same time; otherwise they are completely independent as above.

7. Application to a System of 4 Particles

7.1. GENERAL REMARKS

The above considerations will now be applied to a system of 4 particles. After the separation of the centre-of-mass motion (20a—b) the wave function of the internal motion is written as a product of two functions (12), where one function describes the global motion and the other the specific motion. The global motion has already been treated for an arbitrary number of particles, and we must therefore now look in detail for the specific motion. The corresponding function can be written as a linear combination of products of space, spin and isobaric spin functions (14). The special form of these linear combinations is given in table 1 for 4 particles. The spin and isobaric spin functions are given explicitly by (56) so that the main problem is to compute the space functions of the specific motion. The standard frames and the standard tableaux for this case are given in fig. 1 and fig. 2. Because the space functions belonging to the same frame but to different tableaux have the same structure, they are computed only for the tableaux designated by (b_1), (c_1), (d_1) in fig. 2. It will be shown that the knowledge of the corresponding m.p.v. already permits us to make general statements about the eigenvalue spectrum.

7.2. THE TOTALLY SYMMETRIC SPACE FUNCTIONS

In the one-dimensional case one has to construct from the 3 internal coordinates x_1, x_2, x_3 the 3 totally symmetric m.p.v. according to (65), (66) and (73b):

$$\begin{aligned} u &= x_1^2+x_2^2+x_3^2, \qquad g_3 = x_1x_2x_3, \\ g_4 &= (x_1^4+x_2^4+x_3^4)-3(x_1^2x_2^2+x_1^2x_3^2+x_2^2x_3^2). \end{aligned} \tag{106}$$

Putting the Ansatz (68), which with the help of (71b) assumes the form

$$\phi_K^s(x_1, x_2, x_3) = F_N(u, g_3, g_4), \tag{107}$$

in the equation (62) and using the relations (63), (73b) and (74) the following partial differential equation is obtained for F_N:

$$(2N-1)\frac{\partial F_N}{\partial u} - 2u\frac{\partial^2 F_N}{\partial u^2} + \tfrac{1}{10}(u^2-g_4)\frac{\partial^2 F_N}{\partial g_3^2} - 8g_3u\frac{\partial^2 F_N}{\partial g_3 \partial g_4} + 2(u^3+3g_4u+75g_3^2)\frac{\partial^2 F_N}{\partial g_4^2} = 0. \tag{108}$$

The solutions for the 4 lowest values of N are

$$F_0 = 1, \quad F_3 = g_3, \quad F_4 = g_4, \quad F_6 = 5g_3^2+\tfrac{1}{11}g_4u-\tfrac{1}{21}u^3. \tag{109}$$

The general solutions of (108) are finite power series of the form (76):

$$F_N = \sum_{\langle p_i \rangle} \alpha_{p_4p_3p_2} g_4^{p_4} g_3^{p_3} u^{p_2}, \tag{110}$$

where the symbol $\langle p_i \rangle$ means that one has to sum only over those integral values of p_i obeying the condition

$$N = 4p_4+3p_3+2p_2. \tag{111}$$

Because there exists for every expression of the form $g_4^{p_4} g_3^{p_3}$ an independent solution, the eigenvalue spectrum of K^s is given by

$$K^s = 3n_3+4n_4 \qquad (n_i = 0, 1, 2 \ldots), \tag{112}$$

where the n_i can take on all integral values independently of each other.

In the three-dimensional case one has to look for all m.p.v. which can be deduced from the m.p.v. of the one-dimensional case given by (106.) It is necessary to give only the following m.p.v., because all the other m.p.v. follow by cyclic permutation of x_i with y_i and z_i:

for $l+n+q = 2$:

$$u = \sum_1^3 x_i^2, \qquad g_{110} = \sum_1^3 x_i y_i; \tag{113}$$

for $l+n+q = 3$:

$$\begin{aligned} g_{300} &= x_1 x_2 x_3, \qquad g_{210} = x_1 x_2 y_3+x_1 y_2 x_3+y_1 x_2 x_3, \\ g_{111} &= x_1(y_2 z_3+z_2 y_3)+x_2(y_1 z_3+z_1 y_3)+x_3(y_1 z_2+z_1 y_2); \end{aligned} \tag{114}$$

for $l+n+q = 4$:

$$\begin{aligned} g_{400} &= (x_1^4+x_2^4+x_3^4)-3(x_1^2 x_2^2+x_1^2 x_3^2+x_2^2 x_3^2), \\ g_{310} &= 2(x_1^3 y_1+x_2^3 y_2+x_3^3 y_3)-3[x_1 y_1(x_2^2+x_3^2)+x_2 y_2(x_1^2+x_3^2)+x_3 y_3(x_1^2+x_2^2)], \\ g_{211} &= z_1[-2x_1^2 y_1+y_1(x_2^2+x_3^2)+2x_1(x_2 y_2+x_3 y_3)]+z_2[\ldots]+z_3[\ldots], \\ g_{220} &= y_1^2(-2x_1^2+x_2^2+x_3^2)+y_2^2(-2x_2^2+x_1^2+x_3^2) \\ &\quad +y_3^2(-2x_3^2+x_1^2+x_2^2)+4(x_1 y_1 x_2 y_2+x_1 y_1 x_3 y_3+x_2 y_2 x_3 y_3). \end{aligned} \tag{115}$$

The incomplete brackets in (115) are obtainable from the preceding ones by cyclic permutation of the indices of x, y and z.

Using $\varphi^s = 1$ the Ansatz (99) reduces to

$$\phi_K^s(r_1 \ldots r_{A-1}) = F^s_{N_1 N_2 N_3}(u, v, w, g^s_{inq}), \tag{116}$$

providing for $F^s_{N_1 N_2 N_3}$ the partial differential equation ($F^s_{N_1 N_2 N_3} \equiv F$)

$$[2N_1-1]\frac{\partial F}{\partial u}+[2N_2-1]\frac{\partial F}{\partial v}+[2N_3-1]\frac{\partial F}{\partial w}-2\left[u\frac{\partial^2 F}{\partial u^2}+v\frac{\partial^2 F}{\partial v^2}+w\frac{\partial^2 F}{\partial w^2}\right]$$

$$+\tfrac{1}{2}\sum_{g_{inq}}\sum_{g'_{inq}}\frac{\partial^2 F}{\partial g_{inq}\partial g'_{inq}}\left[\sum_{i=1}^3\frac{\partial g_{inq}}{\partial r_i}\frac{\partial g'_{inq}}{\partial r_i}\right] = 0, \tag{117}$$

where the last sum can also be expressed in terms of the m.p.v. [1]). The solutions for

the 4 lowest values of $N = N_1+N_2+N_3$ are

for $N = 0$: 1;
$N = 1$: no solution;
$N = 2$: g_{110}, g_{101}, g_{011};
$N = 3$: all the 10 functions g_{lnq} with $l+n+q = 3$;
$N = 4$: all the 15 functions g_{lnq} with $l+n+q = 4$ and

$$F_{220} = 3g_{110}^2-uv, \quad F_{022} = 3g_{011}^2-vw, \quad F_{202} = 3g_{101}^2-uw, \tag{118}$$
$$F_{211} = 3g_{110}g_{101}-ug_{011}, \quad F_{112} = 3g_{101}g_{011}-wg_{110}, \quad F_{121} = 3g_{110}g_{011}-vg_{101}.$$

Because there exists for every expression of the form

$$g_{110}^{q_1}g_{101}^{q_2}g_{011}^{q_3}g_{300}^{r_1}\cdots g_{111}^{r_{10}}g_{400}^{s_1}\cdots g_{211}^{s_{13}}g_{112}^{s_{14}}g_{121}^{s_{15}} \tag{119}$$

an independent solution, the eigenvalue spectrum of K^s can by means of (100) be given as

$$K^s = 2\left(\sum_1^3 n_i\right)+3\left(\sum_1^{10} m_i\right)+4\left(\sum_1^{15} p_i\right) \qquad (n_i, m_i, p_i = 0, 1, 2\ldots), \tag{120}$$

where the numbers n_i, m_i, p_i can take all non-negative integral values independently of each other. All further information about the totally symmetric functions ϕ_K^s can easily be derived from the given results.

7.3. THE SPACE FUNCTIONS OF THE REMAINING TABLEAUX

The space functions belonging to the remaining tableaux of fig. 2 will now be treated. Let us begin with the tableaux (d_1) and (c_1) of fig. 2, which have according to (65)—(66) the same m.p.v. In the one-dimensional case they are

$$g_1 = x_1+x_2, \quad g_1' = x_3, \quad u = x_1^2+x_2^2+x_3^2, \tag{121}$$

while the antisymmetric factors are

$$\varphi_1^{d_1} = x_1-x_2, \tag{122}$$
$$\varphi_2^{c_1} = \varphi_1^{d_1}g_1. \tag{123}$$

For both cases the Ansatz (68) can be used:

$$\phi_K^{d_1, c_1}(x_1, x_2, x_3) = \varphi_1^{d_1}F_N(g_1, g_1', u), \tag{124a}$$

with

$$K = 1+N, \tag{124b}$$

providing for F_N the differential equation

$$(2N+1)\frac{\partial F_N}{\partial u}-2u\frac{\partial^2 F_N}{\partial u^2}+\frac{\partial^2 F_N}{\partial g_1^2}+\tfrac{1}{2}\frac{\partial^2 F_N}{\partial g_1'^2} = 0. \tag{125}$$

If a solution contains g_1 as a factor, it belongs to tableau (c_1) because of (123) while

all the other solutions belong to tableau (d_1). The solutions for $N = 0, 1, 2$ which belong to (d_1) are

$$F_0 = 1, \quad F_1 = g_1', \quad F_2^{(1)} = 5g_1^2 - 2u, \quad F_2^{(2)} = 5g_1'^2 - u, \tag{126}$$

and those belonging to (c_1) are

$$F_1 = g_1, \quad F_2 = g_1 g_1'. \tag{127}$$

The general solutions of (125) have the form

$$F_N = \sum_{\langle p_i \rangle} \alpha_{p_1 p_1' p_2} g_1^{p_1} g_1'^{p_1'} u^{p_2}, \tag{128}$$

where $\langle p_i \rangle$ means that one has to sum over all integral values of p_i fulfilling the condition

$$N = p_1 + p_1' + 2p_2. \tag{129}$$

Because there exists for every expression of the form $g_1^{p_1} g'^{p_1'}$ an independent solution belonging either to tableau (d_1) or (c_1) the permitted values of N are

$$N = n_1 + n_1' \qquad (n_1, n_1' = 0, 1, 2 \ldots). \tag{130}$$

Using (124b) and (130) the eigenvalue spectrum of K^d and K^c can be found.

For the three-dimensional treatment it is sufficient to give the following m.p.v., because all other m.p.v. are obtained by cyclic permutation of x_i with y_i and z_i:

for $l+n+q = 1$: $\quad g_{100} = x_1 + x_2, \quad g_{100}' = x_3,$ (131)

$l+n+q = 2$: $\quad g_{110} = \sum_1^3 x_i y_i, \quad u = \sum_1^3 x_i^2.$ (132)

The antisymmetric factors for the tableau (d_1) are given by

$$\varphi_{100} = x_1 - x_2, \quad \varphi_{010} = y_1 - y_2, \quad \varphi_{001} = z_1 - z_2, \tag{133}$$

and for the tableau (c_1) they are the product of one of the functions φ of (133) with one of the m.p.v. $g_{100}, g_{010}, g_{001}$. Using the Ansatz (99) it is preferable to put immediately into the function F the corresponding power series with arbitrary coefficients and to determine them by applying (83)—(85). For the rest of this paper only the "essential" quantities will be given, i.e. that all quantities will be omitted which can be deduced from the given ones by cyclic permutation of x_i with y_i and z_i. The essential solutions for the values of $K = 1, 2$, for the tableaux (d_1) and (c_2) are easy to compute and will therefore be given. For tableau (d_1) they are

for $K = 1$: $\quad \phi_{100} = \varphi_{100},$ (134)

$K = 2$: $\quad \phi_{200} = \varphi_{100} g_{100}',$ (135)

$\phi_{110} = \varphi_{100} g_{010}' + \varphi_{010} g_{100}',$ (136)

and for tableau (c_1)

for $K = 2$: $\quad \phi_{200} = \varphi_{100} g_{100},$ (137)

$\phi_{110} = \varphi_{100} g_{010} + \varphi_{010} g_{100}.$ (138)

With this method it is however not so easy to obtain closed expressions for the eigenvalue of K^{d} and K^{c} as in the case of K^{a}.

Next, the tableau (b_1) of fig. 2 will be considered. For the one-dimensional treatment the following m.p.v. are needed:

$$\begin{aligned} g_1 &= x_1+x_2+x_3, \qquad u = x_1^2+x_2^2+x_3^2, \\ g_3 &= 2(x_1^3+x_2^3+x_3^3)-3[x_1^2(x_2+x_3)+x_2^2(x_1+x_3)+x_3^2(x_1+x_2)]+12x_1x_2x_3 \end{aligned} \tag{139}$$

and the corresponding antisymmetric factor is given by

$$\varphi_3^{b_1} = (x_1-x_2)(x_1-x_3)(x_2-x_3). \tag{140}$$

The m.p.v. of (139) are so chosen that they fulfil besides the conditions (65) and (66) an equation analogous to (73a):

$$\sum_1^3 \frac{\partial^2}{\partial x_i^2}(\varphi_3^{b_1} g_l^{b_1}) = 0 \qquad \text{for } l = 1, 3. \tag{141}$$

The Ansatz (68) having here the form

$$\phi_K^{b_1}(x_1, x_2, x_3) = \varphi_3^{b_1} F_N(g_1, u, g_3), \tag{142a}$$

with

$$K = 3+N, \tag{142b}$$

provides the following differential equation for F_N:

$$\begin{aligned} (5+2N)\frac{\partial F_N}{\partial u} - 2u\frac{\partial^2 F_N}{\partial u^2} + \tfrac{3}{2}\frac{\partial^2 F_N}{\partial g_1^2} + 6(u-g_1^2)\frac{\partial^2 F_N}{\partial g_1 \partial g_3} \\ + \tfrac{1}{16}(61g_1^4 - 198g_1^2u + 136g_1g_3 + 297u^2)\frac{\partial^2 F_N}{\partial g_3^2} = 0. \end{aligned} \tag{143}$$

The solutions for the 4 lowest values of N are

$$F_0 = 1, \quad F_1 = g_1, \quad F_2 = 3g_1^2-u, \quad F_3^{(1)} = g_3, \quad F_3^{(2)} = 11g_1^3-9g_1u, \tag{144}$$

and the general solutions have the form

$$F_N = \sum_{\langle p_i \rangle} \alpha_{p_1p_2p_3} g_1^{p_1} u^{p_2} g_3^{p_3}, \tag{145}$$

where again there exists for every expression of the form $g_1^{p_1}g_3^{p_3}$ an independent solution. The permitted values of N are therefore

$$N = n_1+3n_3 \qquad (n_i = 0, 1, 2\ldots), \tag{146}$$

and putting this into (142b) the eigenvalue spectrum of K^{b} can be found.

The three-dimensional treatment is analogous to that of ϕ_K^{d} and ϕ_K^{c}. The m.p.v. can easily deduced from the one-dimensional m.p.v. and the essential antisymmetric factors are

for $k_1+k_2+k_3 = 2$: $\varphi_{110} = (x_1-x_2)(y_1-y_3)-(y_1-y_2)(x_1-x_3)$, (147)

and for $k_1+k_2+k_3 = 3$:

$$\varphi_{300} = (x_1-x_2)(x_1-x_3)(x_2-x_3),$$

$$\varphi_{210} = (x_1-x_2)[(x_1-x_3)(y_2-y_3)+(y_1-y_3)(x_2-x_3)] + (y_1-y_2)(x_1-x_3)(x_2-x_3), \quad (148)$$

$$\varphi_{111} = (x_1-x_2)[(y_1-y_3)(z_2-z_3)+(z_1-z_3)(y_2-y_3)] + (x_1-x_2)[(y_1-y_2)(z_2-z_3)+(z_1-z_2)(y_2-y_3)] + (x_2-x_3)[(y_1-y_2)(z_1-z_3)+(z_1-z_2)(y_1-y_3)].$$

The functions ϕ_K^b can again be obtained with the help of the Ansatz (99).

The treatment of the totally antisymmetric space functions is omitted because it is already given in ref. [1]) for a one-dimensional system of A particles and in ref. [2]) for a three-dimensional system of 3 particles. The spectra of these two cases are given as examples in eqs. (80a) and (105a) of this paper. The extension of the above considerations to the case of totally antisymmetric space functions is straightforward.

8. Concluding Remarks

The considerations of this paper are governed by the aspect of the different modes of motion which can occur in a many-body system. This aspect is in opposition to the description by the independent-particle model. Therefore the concept of one-particle functions is dropped and the particle coordinates are replaced by suitable combinations in the $3A$-dimensional space. For the treatment of phenomena which do not vary essentially with the number of particles, totally symmetric combinations of the particle coordinates are favoured. The simplest totally symmetric combinations are homogeneous functions depending after the separation of the centre-of-mass motion only on the internal coordinates. If the Schrödinger equation of a many-body system can now be replaced by two independent eigenvalue problems, one of which having solutions which contain only totally symmetric homogeneous functions of the internal coordinates, then a rigorous separation into a global and a specific mode of motion is possible.

The considerations of this paper are concerned with the case when the function G of the global motion depends only on the 3 m.p.v. u, v, w. The next step will be the extension to the case where G depends on all the 6 m.p.v. of degree two:

$$G = G(u, v, w, g_{110}, g_{101}, g_{011}), \quad (149)$$

and the suggestion is now that this form of the global motion will describe the so-called nuclear "collective" phenomena. In this case the nuclear "collective coordinates" ought to be suitable combinations of the m.p.v. and the requirement with respect to the angular momentum favour the following choice:

$$\rho = u+v+w, \quad \eta_0 = 2w-(u+v), \quad (150)$$

$$\eta_1 = g_{101}+ig_{011}, \quad \eta_2 = u-v+2ig_{110},$$

$$\eta_{-1} = g_{101}-ig_{011}, \quad \eta_{-2} = u-v-2ig_{110}.$$

The suggestion is supported by the two following intuitive arguments:

I. The "collective coordinates" defined by (150) are the simplest totally symmetric combinations of the particle coordinates which are translationally invariant and at the same time eigenfunctions of the internal angular momentum operator and its z-component. With their help it is very easy to describe sequences of states which are similar to those of the collective model [6]) †, which becomes rather difficult with all other quantities having the same properties.

II. Though it is an entirely open question which correlation exists between the form of the interaction potential and the m.p.v. occurring in the function G of the global motion, there exists an interaction potential depending only on the 6 quantities of (150), where the corresponding eigenvalue spectrum exhibits sequences of states which are similar to the rotational bands of the collective model. This was introduced by Elliot [7]) and is stated in the translationally invariant formulation

$$\mathscr{V}(\boldsymbol{r}'_1 \dots \boldsymbol{r}'_A) \propto \sum_{i,k=1}^{A} \sum_{j,l=1}^{A} (\boldsymbol{r}'_i - \boldsymbol{r}'_k)^2 (\boldsymbol{r}'_j - \boldsymbol{r}'_l)^2 Y_2^0 \left(\frac{(\boldsymbol{r}'_i - \boldsymbol{r}'_k) \cdot (\boldsymbol{r}'_j - \boldsymbol{r}'_l)}{|\boldsymbol{r}'_i - \boldsymbol{r}'_k||\boldsymbol{r}'_j - \boldsymbol{r}'_l|} \right), \quad (151a)$$

or, after introduction of the internal coordinates,

$$\mathscr{V}(\boldsymbol{r}_1 \dots \boldsymbol{r}_{A-1}) \propto \sum_{i,j=1}^{A-1} r_i^2 r_j^2 Y_2^0 \left(\frac{\boldsymbol{r}_i \cdot \boldsymbol{r}_j}{|\boldsymbol{r}_i||\boldsymbol{r}_j|} \right), \quad (151b)$$

where Y_l^n are spherical harmonics. From (151b) one can see directly, that it is only a function of the quantities (150).

There is, however, the difficulty that the energy spectrum is a combination of the spectra of the global and of the specific motion. For the latter there seems to exist the general trend that a great number of states will be removed if more than 3 m.p.v. occur in the interaction potential and if one includes state-dependent potentials. Taking into account state dependent potentials the space functions of the specific motion are determined by a system of coupled partial differential equations [8]).

Using all the above considerations one may suggest that after the separation of the centre-of-mass motion the so-called nuclear "collective phenomena" are described by the following wave function

$$\Psi(\boldsymbol{r}_1 \dots \boldsymbol{r}_{A-1}, \sigma_1 \dots \sigma_A, \tau_1 \dots \tau_A) = G(\rho, \eta_0, \eta_1, \eta_{-1}, \eta_2, \eta_{-2}) \cdot \sum_{\kappa\lambda\nu} q_{\kappa\lambda\nu} \phi^{\Gamma\kappa}(\boldsymbol{r}_1 \dots \boldsymbol{r}_{A-1}) \chi^{S\lambda}(\sigma_1 \dots \sigma_A) \zeta^{T\nu}(\tau_1 \dots \tau_A), \quad (152)$$

where the function G is determined by an ordinary eigenvalue problem, while the function ϕ is a solution of a system of coupled partial differential equations having the symmetry properties of the corresponding Young tableaux.

† All other references to this model can be found in the second paper of ref. [6]).

References

1) P. Möbius, Nuclear Physics **16** (1960) 278
2) P. Möbius, Nuclear Physics **18** (1960) 224
3) H. Boerner, Darstellungen von Gruppen (Springer-Verlag, Berlin 1955);
A. Pais, Ann. of Phys. **9** (1960) 548;
M. Kretschmar, Z. f. Phys. **157** (1960) 433; **158** (1960) 284;
4) B. L. van der Waerden, Die gruppentheoretische Methode in der Quantenmechanik (Springer-Verlag, Berlin, 1932);
H. C. Brinkmann, Applications of spinor invariants in atomic physics (North-Holland Publishing Company, Amsterdam, 1956)
5) S. Gartenhaus and C. Schwarz, Phys. Rev. **108** (1957) 482;
H. J. Lipkin, Phys. Rev. **110** (1958) 1395
6) K. Alder, A. Bohr, T. Huus, V. Mottelson and A. Winther, Rev. Mod. Phys. **28** (1956) 432;
A. Bohr and B. R. Mottelson, Kongel. Norske Vid. Selsk. Forh. **31**, No. 12 (1958)
7) J. P. Elliot, Proc. Roy. Soc. A **245** (1958) 128, 562
8) P. Möbius, to be published

2.G

Nuclear Physics **28** (1961) 331—341; © *North-Holland Publishing Co., Amsterdam*

Not to be reproduced by photoprint or microfilm without written permission from the publisher

STRIPPING OF HEAVY PROJECTILES

M. EL NADI and H. SHERIF

Faculty of Science, Cairo University, U.A.R.

Received 13 March 1961

Abstract: The differential cross sections for the multiple stripping processes of heavy projectiles are given and discussed. Comparison with experimental data is given when the heavy projectiles are He^3, He^4 and Li^6 nuclei. Reasonable agreement between theoretical and experimental data is observed. In some cases an isotropic contribution from the compound nucleus mechanism is introduced to insure better agreement with experimental data.

In recent years, extensive studies of nuclear reactions produced by the collision of He^3 and He^4 particles with light nuclei were carried out [1]. In most of these reactions the differential cross-sections show a forward peaking, which is characteristic of the Butler deuteron stripping mechanism [2]. The theory of such processes was also studied and the resulting theoretical formulae show reasonable agreement with experimental data.

In this note an outline is given of the theoretical formulae [3]) for the stripping of heavy projectiles. The assumption that the stripping reaction occurs at the surface, introduced by Bhatia *et al.*[2]) is generalized to the case of stripping of heavy projectiles. A somewhat different formulation for the nuclear surface reaction condition is introduced here for the stripping of heavy particles, which is perhaps more convenient than that introduced before [3]). Finally, the derived formulae are applied to several nuclear reactions in which more than one nucleon were captured from He^3, He^4 and Li^6 projectiles.

We consider the case when an incident α-particle strikes a target nucleus i and is stripped of two of its nucleons, giving rise to a final nucleus f and an outgoing deuteron d. The Coulomb effects of the interacting particles are neglected; neither is the nuclear interaction between the outgoing particles and the residual nucleus taken into account. Hence our considerations are limited to the cases when the energies of the incident particles are above the Coulomb barrier.

The differential cross section for the i(α, d)f stripping reaction, according to the first Born approximation, may be written as

$$d\sigma = \frac{M_d^* M_\alpha^*}{4\pi^2\hbar^4} \frac{K_d}{K_\alpha} \langle |I|^2 \rangle, \qquad (1)$$

where

$$M_d^* = [M_d M_f/(M_d+M_f)], \qquad M_\alpha^* = [M_\alpha M_1/(M_\alpha+M_1)],$$
$$K_\alpha = (2M_\alpha^* E_\alpha)^{\frac{1}{2}}/\hbar, \qquad K_d = (2M_d^* E_d)^{\frac{1}{2}}/\hbar$$

and E_α, E_d are the energies of the incident and outgoing particles. The quantity $\langle|I|^2\rangle$ is formed from the matrix element [3])

$$I = \int d\mathbf{r}_p d\mathbf{r}_n d\mathbf{r}_d \varphi^*(r_d)\exp[-i\mathbf{K}_d\cdot\mathbf{r}'_d]\psi_f^*(\xi\mathbf{r}_p\mathbf{r}_n)(V_n+V_p)\exp[i\mathbf{K}_\alpha\cdot\mathbf{r}_\alpha]\varphi(r_\alpha)\psi_1(\xi)d\xi, \quad (2)$$

where

$$r'_d = \mathbf{r}_d - \frac{M_n+M_p}{M_f}\mathbf{R}, \qquad \mathbf{R} = \tfrac{1}{2}(\mathbf{r}_n+\mathbf{r}_p).$$

We now pick out first from (2) the integral over $d\xi$:

$$I' = \int \Psi_f^*(\xi\mathbf{r}_p\mathbf{r}_n)(V_n+V_p)\Psi_1(\xi)d\xi, \quad (3)$$

which is a function of $\mathbf{r}_p$ and $\mathbf{r}_n$. Assuming now that stripping occurs at the nuclear surface R_0, the integral (3) may be expanded in terms of the angular part of the centre-of-mass of the captured particles as

$$I' = \frac{\delta(R-R_0)}{R^2}\sum_{LM} A_L f_{l_n l_p}(R)Y_L^{*M}(\Omega), \quad (4)$$

where R is the radial coordinate of the centre-of-mass of the two captured particles. The function $f_{l_n l_p}(R_0)$ is the product of the radial functions of the two captured nucleons characterized with the orbital angular momentum quantum numbers l_n and l_p at the value $|\mathbf{r}_p| = |\mathbf{r}_n| = R_0$. Further,

$$Y_L^M(\Omega) = \sum_{m_n m_p}\begin{pmatrix} l_p & l_n & L \\ m_p & m_n & M\end{pmatrix} Y_{l_p}^{m_p}(\Omega_p)Y_{l_n}^{m_n}(\Omega_n), \quad (5)$$

where the first bracket on the right hand side denotes the Wigner vector addition coefficient and A_L is an expansion coefficient.

The internal wave function for the α-particle may be taken of the Gaussian form

$$\varphi(\alpha) = N_\alpha^{\frac{1}{2}}\exp[-\gamma_\alpha^2\sum_{i<j} r_{ij}^2] = N_\alpha^{\frac{1}{2}}\exp[-\gamma_\alpha^2(2u^2+2v^2+4\rho^2)], \quad (6)$$

where $N_\alpha^{\frac{1}{2}}$ is the normalization constant, $\mathbf{v}$ is the vector joining the two nucleons which form the outgoing deuteron, $\mathbf{u} = \mathbf{r}_p - \mathbf{r}_n$ and $\boldsymbol{\rho} = \mathbf{r}_d - \frac{1}{2}(\mathbf{r}_p+\mathbf{r}_n)$ is the vector representing the distance between the centre-of-mass of the two captured nucleons and the centre-of-mass of the outgoing deuteron.

The internal wave function of the deuteron may also be taken as

$$\varphi(\mathrm{d}) = N_d^{\frac{1}{2}}\exp[-\gamma_d^2 v^2],$$

where $N_d^{\frac{1}{2}}$ is the normalization constant.

If now the integration variables in (2) are changed from $\mathbf{r}_p$, $\mathbf{r}_n$ and $\mathbf{r}_d$ to $\mathbf{R}$, $\boldsymbol{\rho}$ and $\mathbf{u}$, one gets

$$I = N_\alpha^{\frac{1}{2}} N_d^{\frac{1}{2}} \sum_{LM} A_L \int \mathrm{d}\boldsymbol{\rho}\,\mathrm{d}\mathbf{u}\,\mathrm{d}\mathbf{v}\,\mathrm{d}\mathbf{R}\, f_{l_n l_p}(R)$$
$$\exp\left[i\mathbf{Q}\cdot\mathbf{R} - i\mathbf{K}\cdot\boldsymbol{\rho} - \gamma_d^2 v^2 - \gamma_\alpha^2(2u^2+2v^2+4\rho^2)\right]\delta(R-R_0)/R^2 \quad (7)$$
$$= T \exp\left[-K^2/16\gamma_\alpha^2\right] \sum_L A_L i^L (2L+1)^{\frac{1}{2}} j_L(QR_0),$$

where

$$\mathbf{Q} = \mathbf{K}_\alpha - \frac{M_1}{M_f}\mathbf{K}_d \quad \text{and} \quad \mathbf{K} = \mathbf{K}_d - \tfrac{1}{2}\mathbf{K}_\alpha.$$

The numerical factor T is given by

$$T = \frac{2\pi^2 \gamma_d^{\frac{3}{2}}}{\gamma_\alpha^{\frac{3}{2}}} \left(1 + \frac{\gamma_d^2}{2\gamma_\alpha^2}\right)^{-\frac{1}{2}} f_{l_n l_p}(R_0)$$

and $j_L(QR_0)$ is the spherical Bessel function.

Squaring (7) and taking the spin functions into account one gets [3]) for the differential cross-section

$$\mathrm{d}\sigma = \frac{M_d^* M_\alpha^*}{4\pi^2\hbar^4} \frac{K_d}{K_\alpha} \frac{(2J_f+1)T^2}{3(2J_1+1)} \exp\left[-K^2/8\gamma_\alpha^2\right] \sum_L A_L^2 j_L^2(QR_0), \quad (8)$$

and for the (He^3, p) reaction one gets the corresponding expression

$$\mathrm{d}\sigma = \frac{M_p^* M_h^*}{4\pi^2\hbar^4} \frac{K_p}{K_h} \frac{(2J_f+1)T^2}{2(2J_1+1)} \exp\left[-K^2/4\gamma_h^2\right] \sum_L A_L^2 j_L^2(QR_0), \quad (9)$$

where T in this case is given by

$$T = 2.49 \frac{\pi^2}{\gamma_h^3} f_{l_m l_p}(R_0), \qquad \mathbf{Q} = \mathbf{K}_h - \frac{M_1}{M_f}\mathbf{K}_p, \qquad \mathbf{K} = \mathbf{K}_p - \tfrac{1}{3}\mathbf{K}_h.$$

Similarly for the case when three nucleons are captured from a heavy projectile, such as the α-particle, the following expansion is introduced for the overlap integral (3):

$$I' = \int \Psi_f^*(\xi \mathbf{r}_{p_1} \mathbf{r}_{n_1} \mathbf{r}_{n_2})[V_{n_1} + V_{n_2} + V_{p_1}]\Psi_1(\xi)\mathrm{d}\xi$$
$$= [\delta(R-R_0)/R^2 \sum_{LM} A_L f_{l_{n_1} l_{n_2} l_{p_1}}(R) Y_L^{*M}(\Omega), \quad (10)$$

where R and Ω are the radial and angular coordinates of the centre-of-mass of the three captured particles, and R_0 is the nuclear radius at which the stripping process is assumed to take place. Consequently one gets for the differential cross-section for the process (α, p) the following expression:

$$\mathrm{d}\sigma = \frac{M_p^* M_\alpha^*}{4\pi^2\hbar^4} \frac{K_p}{K_\alpha} \frac{(2J_f+1)T^2}{2(2J_1+1)} \exp\left[-K^2/6\gamma_\alpha^2\right] \sum_L A_L^2 j_L^2(QR_0), \quad (11)$$

where

$$T = \frac{4\sqrt{2}\pi^{11/4}}{\gamma_\alpha^{\frac{3}{2}}} f_{l_{n_1} l_{n_2} l_{p_1}}(R_0), \qquad \mathbf{Q} = \mathbf{K}_\alpha - \frac{M_1}{M_f}\mathbf{K}_p, \qquad \mathbf{K} = \mathbf{K}_p - \tfrac{1}{4}\mathbf{K}_\alpha.$$

The selection rules associated with the two and three particle stripping run as follows:

$$\mathbf{J}_f = \mathbf{J}_1 + \mathbf{L} + \mathbf{s}_1 + \mathbf{s}_2, \tag{12}$$

$$\mathbf{J}_f = \mathbf{J}_1 + \mathbf{L} + \mathbf{s}_1 + \mathbf{s}_2 + \mathbf{s}_3, \tag{13}$$

where the $\mathbf{s}_i$ are the intrinsic spins of the particles. In both expressions $|L|$ is even or odd according as the parity of the final state is or is not different from that of the initial state.

Before proceeding to compare the theoretical formulae with the experimental data, an alternate derivation for the above formulae may be given [4]) with special reference to the two nucleon stripping process. The scattering amplitude for such process may be written as:

$$I = -\frac{1}{4\pi}\frac{2M_d}{\hbar^2}\int \mathrm{d}\mathbf{r}_d \mathrm{d}\mathbf{r}_p \mathrm{d}\mathbf{r}_n \mathrm{d}v \mathrm{d}\xi \exp\left[-i\mathbf{K}_d \cdot \mathbf{r}'_d\right]\varphi^*(\mathbf{r}_p \mathbf{r}_n \xi) \times \chi(\mathrm{d})(V_{nd}+V_{pd})\varphi(\xi)\chi(\alpha)\exp[i\mathbf{K}_\alpha \cdot \mathbf{r}_\alpha], \tag{14}$$

where the incident particle is an α-particle, consisting of a deuteron d, a proton p and a neutron n. The interaction potentials in (14) are those between the outgoing deuteron and the two captured nucleons. Taking the δ-function representation for V_{nd} and V_{pd} and assuming the surface stripping assumption, one gets for the differential cross-section

$$\mathrm{d}\sigma \approx \exp\left[-K^2/24\gamma_\alpha^2\right] \sum_L A_L^2 j_L^2(QR_0). \tag{15}$$

Eq. (15) is identical with the corresponding eq. (8), except for the form factor. The difference in the form factor is due to the special form of the interaction potential introduced in (14).

We now proceed to compare eq. (9) with the experimental data on the $Be^9(He^3, p)B^{11}$ reaction as given by Wolicki *et al.* [5]). The solid curves in figs. 1 and 2 show the theoretical formulae (9).

The solid curves are represented by

$$\mathrm{d}\sigma = 32 + 164 \exp\left[-K^2/4\gamma_h^2\right] j_0^2(QR_0) \tag{16}$$

for the ground state, and by

$$\mathrm{d}\sigma = \exp\left[-K^2/4\gamma_h^2\right]\{41 j_0^2(QR_0) + 545 j_2^2(QR_0)\} \tag{17}$$

for the first excited state.

The selection rule (12) implies that $L = 0$ or 2 for the ground state and $L = 0$ or 2 for the first excited state. If $\mathbf{l}_n$ and $\mathbf{j}_p$ are the orbital angular momenta of the captured nucleons,then $\mathbf{L} = \mathbf{l}_n + \mathbf{l}_p$ and hence the two captured nucleons are in the p-state, which is in agreement with the shell model.

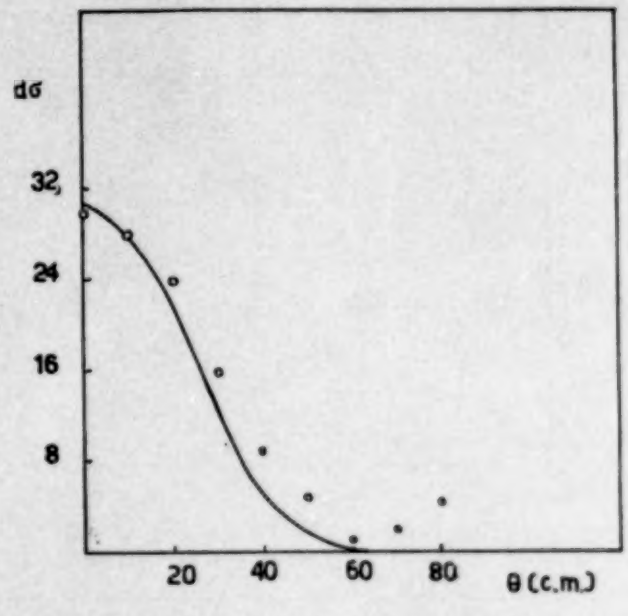

Fig. 1. The centre-of-mass differential cross section for the ground state proton groups from the reaction $Be^9(He^3, p)B^{11}$ as a function of centre-of-mass angle at 4.5 MeV incident He^3 energy. The experimental points are those of E. A. Wolicki *et al* [5]). The solid curve represents the theoretical formula (16) ($R_0 = 4.5$ fm).

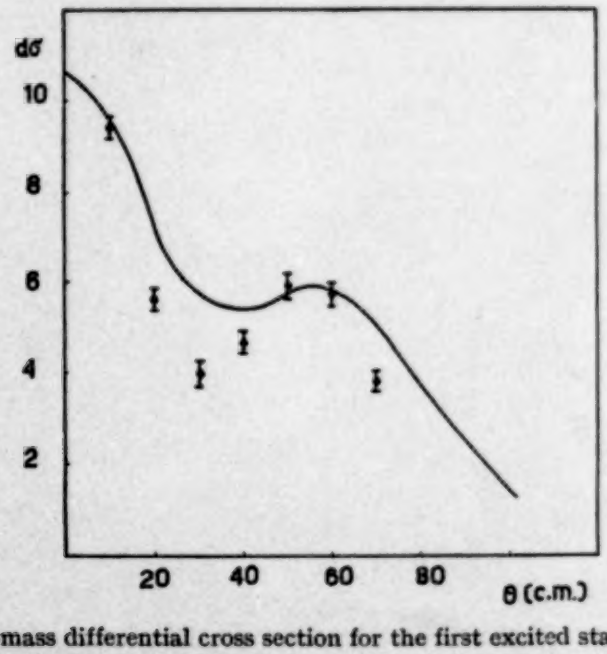

Fig. 2. The centre-of-mass differential cross section for the first excited state proton groups from the reaction $Be^9(He^3, p)B^{11}$ as a function of the centre-of-mass angle at 4.5 MeV incident He^3 energy. The experimental points are those of E. A. Wolicki *et al* [5]). The solid curve represents the theoretical formula (17) ($R_0 = 4.8$ fm).

Figs. 3 and 4 represent a comparison between the experimental data of B. G. Harvey and J. Cerny [6]) on the $C^{12}(\alpha, d)N^{14}$ and the theoretical formula

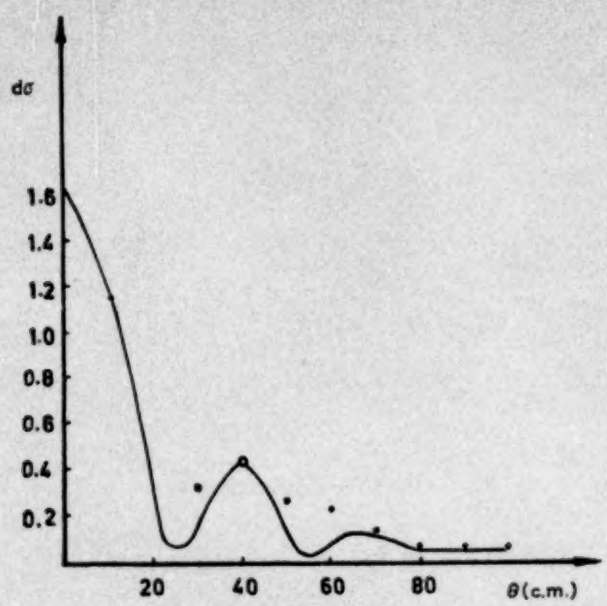

Fig. 3. The centre-of-mass differential cross section for the ground state deuteron groups from the reaction C^{12} $(\alpha, d)N^{14}$ as a function of centre-of-mass angle at 47.5 MeV incident α-particle energy. The experimental points are those of B. G. Harvey and J. Cerny [6]). The solid curve represents the theoretical formula (18) ($R_0 = 4.4$ fm).

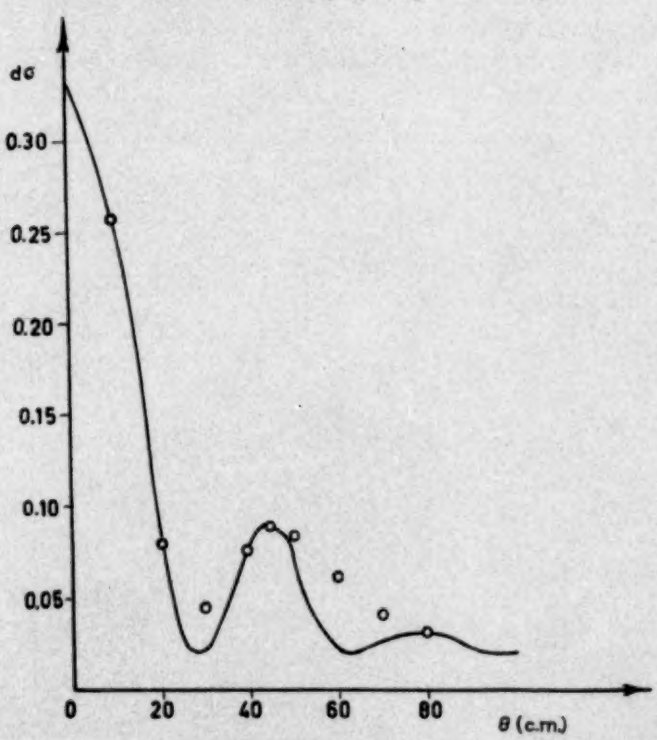

Fig. 4. The centre-of mass differential cross section for the second excited state deuteron groups from the reaction C^{12} $(\alpha, d)N^{14}$ as a function of centre-of-mass angle at 47.5 MeV incident α-particle energy. The experimental points are those of B. G. Harvey and J. Cerny [6]). The solid curve represents the theoretical formula (19). ($R_0 = 4.2$ fm).

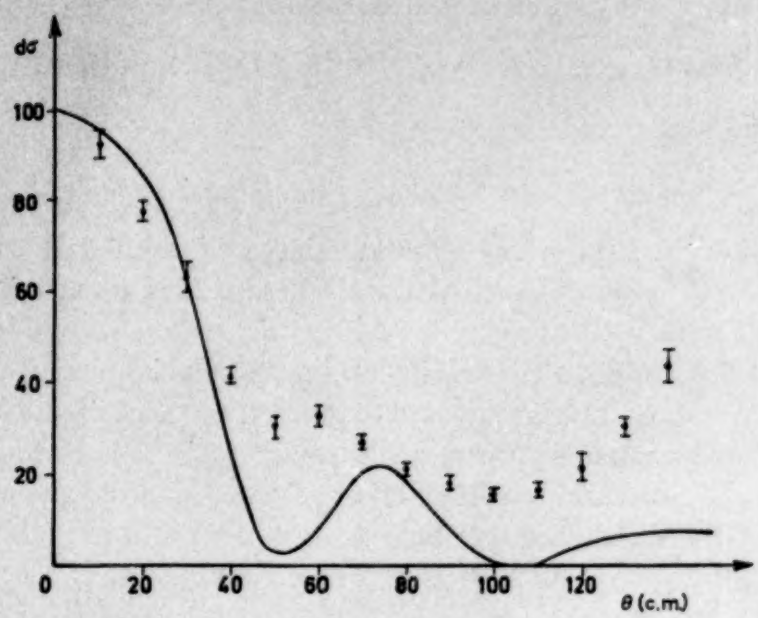

Fig. 5. The centre-of-mass differential cross section for the first excited state α-particle groups from the reaction $Be^9(Li^6, \alpha)B^{11}$ as a function of centre-of-mass angle at 3.00 MeV incident Li^6 energy. The experimental points are those of J. J. Leigh and J. M. Blair[7]). The solid curve represents the theoretical formula (20) ($R_0 = 6.5$ fm).

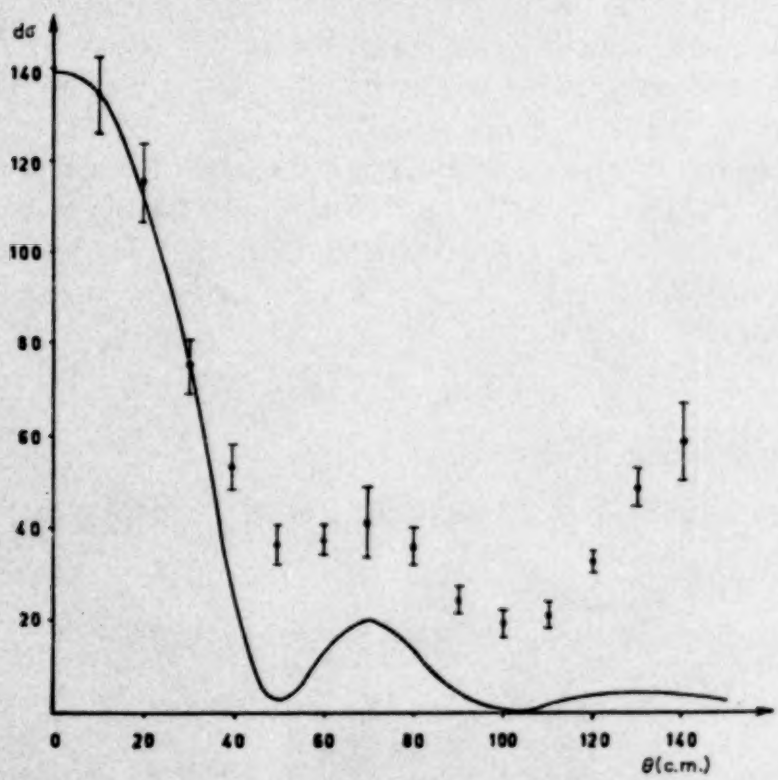

Fig. 6. The centre-of-mass differential cross section for the first excited state α-particle groups from the reaction $Be^9(Li^6, \alpha)B^{11}$ as a function of centre-of-mass angle at 3.25 MeV incident Li^6 energy. The experimental points are those of J. J. Leigh and J. M. Blair[7]). The solid curve represents the theoretical formula (21) ($R_0 = 6.6$ fm).

(15). The solid curves represent the equation

$$d\sigma = 0.058 + \exp[-K^2/24\gamma_\alpha^2]\{16.78 j_0^2(QR_0) + 29.1 j_2^2(QR_0)\} \quad (18)$$

for the ground state, and

$$d\sigma = 0.02 + \exp[-K^2/24\gamma_\alpha^2]\{7.73 j_0^2(QR_0) + 1.48 j_2^2(QR_0)\} \quad (19)$$

for the second excited state. The allowed values of L are 0 and 2 for both the ground state and the second excited state. These values are also in agreement with the shell model.

Figs. 5 and 6 represent the experimental data of Leigh and Blair [7]) on the $Be^9(Li^6, \alpha)B^{11}$. This reaction is supposed to proceed by the stripping mechanism, in which two nucleons are captured from the Li^6 projectiles to form low lying levels of B^{11}. The internal wave function of the Li^6 projectile was roughly taken to be of the same Gaussian form as that for the α-particle.

Curve (5) for $E_{Li} = 3.00$ MeV is represented by

$$d\sigma = \exp[-K^2/24\gamma_{Li}^2]\{1800 j_0^2(QR_0) + 2250 j_2^2(QR_0)\}. \quad (20)$$

Curve (6) for $E_{Li} = 3.25$ MeV is represented by

$$d\sigma = \exp[-K^2/24\gamma_{Li}^2]\{1528 j_0^2(QR_0) + 3480 j_2^2(QR_0)\}. \quad (21)$$

The allowed L-values for the first excited state concerned are $L = 0$ or 2. These values also correspond to values of $l_p = l_n = 1$, which are in agreement with predictions of the shell model.

To compare the theoretical formula (11) for the three-nucleon stripping, some experimental data on $Be^9(\alpha, n)C^{12}$ were chosen for the ground, first and second excited states by Ajzenberg-Selove and Stelson [8]). The results are shown in figs. 7, 8 and 9.

Curve 7 is represented by

$$d\sigma = \exp[-K^2/6\gamma_\alpha^2]\{380 j_1^2(QR_0)\}. \quad (22)$$

Curve (8) is represented by

$$d\sigma = 30 + \exp[-K^2/6\gamma_\alpha^2]\{442.5 j_1^2(QR_0) + 226 j_3^2(QR_0)\}. \quad (23)$$

Curve (9) is represented by

$$d\sigma = \exp[-K^2/6\gamma_\alpha^2]\{203 j_1^2(QR_0)\}. \quad (24)$$

The selection rules corresponding to these reactions allow the following L-values:

for the ground state $L = 1$;
for the first excited state $L = 1$ or 3;
for the second excited state $L = 1$.

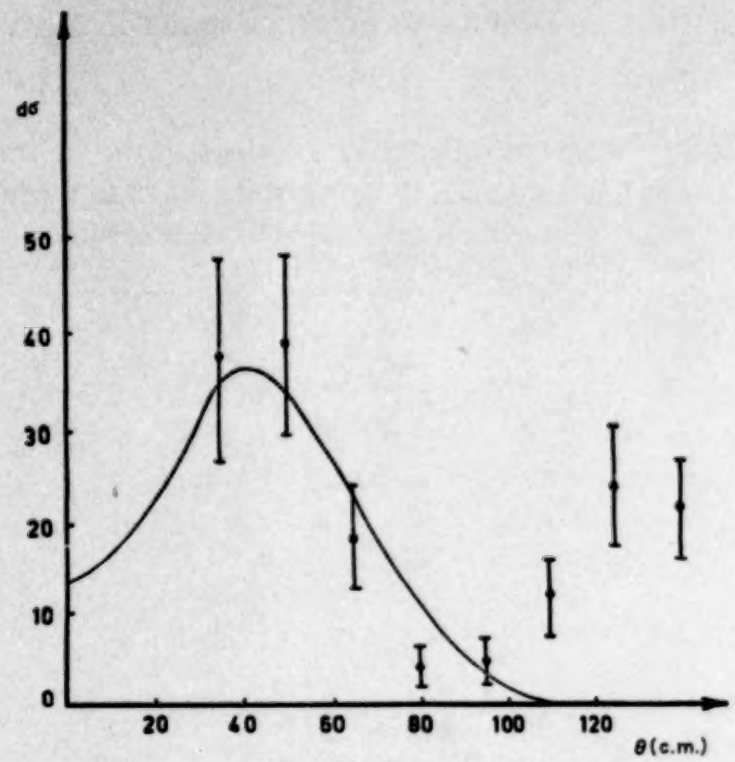

Fig. 7. The centre-of-mass differential cross section for the ground state neutron groups from the reaction $Be^9(\alpha, n)C^{12}$ as a function of centre-of-mass angle at 5.6 MeV incident α-particle energy. The experimental points are those of F. Ajzenberg-Selove and P. H. Stelson [8]). The solid curve represents the theoretical formula (22) ($R_0 = 4.0$ fm).

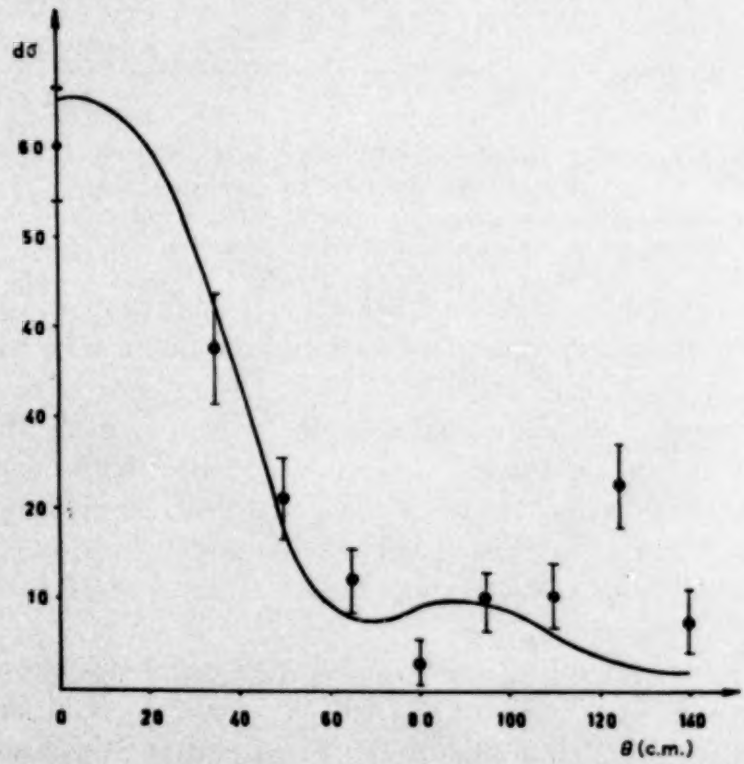

Fig. 8. The centre-of-mass differential cross section from the first excited state neutron groups from the reaction $Be^9(\alpha, n)C^{12}$ as a function of centre-of-mass angle at 5.6 MeV incident α-particle energy. The experimental points are those of F. Ajzenberg-Selove and P. H. Stelson [8]). The solid curve represents the theoretical formula (23) ($R_0 = 6.8$ fm).

In these reactions the resultant angular momentum L is given by

$$\mathbf{L} = \mathbf{l}_1 + \mathbf{l}_2 + \mathbf{l}_3,$$

where $\mathbf{l}_1$, $\mathbf{l}_2$ and $\mathbf{l}_3$ are the orbital angular momenta of the captured nucleons. The above values of L are satisfied if one assumes that the captured nucleons are captured in p-states in accordance with the shell model.

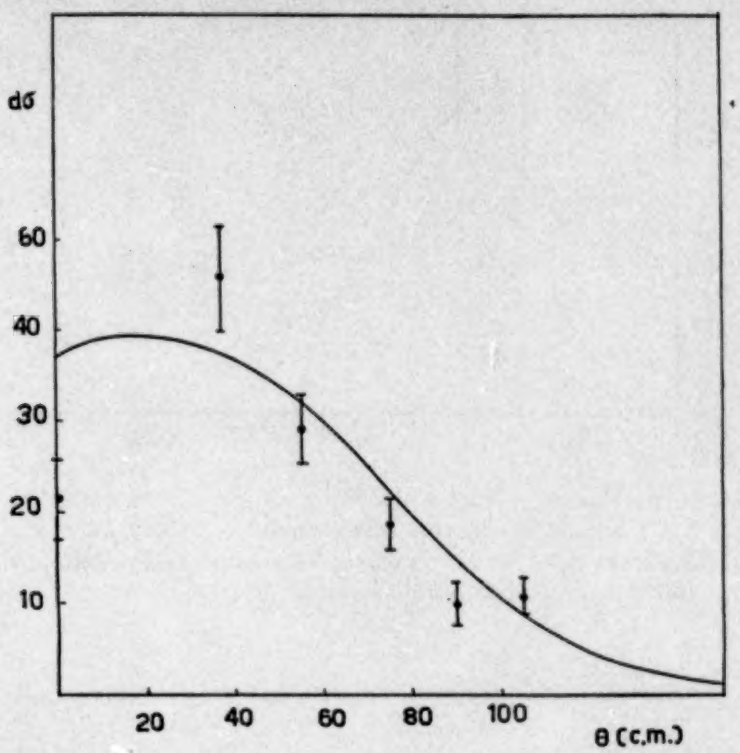

Fig. 9. The centre-of-mass differential cross section from the second excited state neutron groups from the reaction $Be^9(\alpha, n)C^{12}$ as a function of centre-of-mass angle at 5.6 MeV incident α-particle energy. The experimental points are those of F. Ajzenberg-Selove and P. H. Stelson [8]). The solid curve represents the theoretical formula (24) ($R_0 = 4.2$ fm).

The above comparison between theory and experiment shows clearly the validity of the stripping process for reactions in which two or more nucleons are captured by the target nucleus.

The justification of the introduction of the special form of the interaction potentials (4) and (10) may be seen from the agreement with the experimental data given above just as from the theoretical considerations given by Rodberg [9]), who has shown that the single particle wave function Ψ_t falls off rather sharply and symmetrically about the nuclear radius R_0.

The authors are grateful to Dr. W. Tobocman for preprint of his paper on two nucleon stripping process and to Dr. B. G. Harvey and Dr. J. Cerney, Dr. J. J. Leigh and Dr. J. M. Blair, Dr. F. Ajzenberg-Selove and Dr. P. H. Stelson for reprints of their papers.

References

1) H. D. Holmgren, E. H. Geer, R. L. Johnston and E. A. Wolicki, Phys. Rev. **106** (1957) 102;
R. J. Johnston, H. D. Holmgren, E. A. Wolicki and E. Geer Ilsley, Phys. Rev. **109** (1958) 884;
E. A. Wolicki, H. D. Holmgren, R. L. Johnston and E. Geer Illsley, Phys. Rev. **116** (1959) 1585;
S. Hinds and R. Middleton, Proc. Phys. Soc. **74** (1959) 196;
B. G. Harvey and J. Cerny, Phys. Rev. **120**, (1960) 2162;
F. Ajzenberg-Selove and P. H. Stelson, Phys. Rev. **120** (1960) 500;
J. J. Leigh and J. M. Blair, Phys. Rev. Let. **5** (1960) 455

2) S. T. Butler, Proc. Roy. Soc. **208** (1951) 559;
A. B. Bhatia, Kun Huang, R. Huby and H. C. Newns, Phil. Mag. **43** (1952) 485;
F. L. Friedman and W. Tobocman, Phys. Rev. **92** (1953) 93;
W. Tobocman, Phys. Rev. **94** (1954) 1655;
G. Breit, Handbuch der Physik (Springer-Verlag, Berlin, 1959), vol. **41**/1;
S. T. Butler and O. Hittmair, Nuclear stripping reactions (John Wiley and Sons, Inc. New York, 1957);
R. Huby, Progress in nuclear physics (Butterworths-Springer, London, 1953) vol. **3**, p. 177;
A. G. Sitenko, Uspekhi Fiz. Nauk **67** (1959) 377 (translation: Soviet Physics -Uspekhi **67** (2) (1959) 195;
W. Tobocman, Case Institute technical report no. 29, 1956 (unpublished)

3) M. El Nadi, Phys. Rev. **120** (1960) 1360

4) M. El Nadi, Phys. Rev. **119** (1960) 242, **120** (1960) 1368

5) E. A. Wolicke, H. D. Holmgren, R. L. Johnston and E. Geer Illsley, Phys. Rev. **116** (1959) 1585

6) B. G. Harvey and J. Cerny, Phys. Rev. **120** (1960) 2162

7) J. J. Leigh and J. M. Blair, Phys. Rev. Lett. **5** (1960) 455

8) F. Ajzenberg-Selove and P. H. Stelson, Phys. Rev. **120** (1960) 500

9) L. Rodberg, Nuclear Physics **21** (1960) 270

2.D

Nuclear Physics **28** (1961) 342—352; © *North-Holland Publsihing Co., Amsterdam*

Not to be reproduced by photoprint or microfilm without written permission from the publisher

ANGULAR CORRELATIONS IN STATISTICAL NUCLEAR REACTIONS

V. M. STRUTINSKI

I. V. Kurchatov Atomic Energy Institute, Academy of Sciences, Moscow

Received 20 February 1961

Abstract: The paper considers the angular correlation of particles emitted consecutively by a nucleus of high angular momentum. Simple analytical expressions are obtained for the angular correlation of two particles under the condition that the final nucleus remains in a state of low momentum. Consideration is also given to particle-fragment angular correlation.

1. Introduction

The dependence of nuclear level density on nuclear angular momentum leads to the anisotropy of the angular distribution of the particles emitted by a compound nucleus [1–3]). A similar effect leads to the anisotropy of nuclear fission. In the case of the consecutive emission of two particles or fission, we observe, after the escape of a particle, angular particle-particle or particle-fragment correlation. In contrast to the usual treatment given to the angular correlation of particles in nuclear physics when the transitions between strictly determined quantum states are dealt with, separate nuclear levels in the statistical nuclear reactions are unresolved but both angular correlation and angular distribution emerge as a result of averaging over a large number of nuclear states. The effects thus arising usually lend themselves to a simple classical interpretation (see refs. [1–3])). Against this background the application of semi-classical methods of calculation appears quite appropriate.

2. Angular Particle Correlation

Let us first consider a simple case, a cascade of two particles. The probability of a nucleus with angular momentum $\mathbf{j}_1$ emitting the first particle in the direction $\mathbf{n}_1$ and the second in the direction $\mathbf{n}_2$ is

$$W_{\mathbf{j}_1}(1,2)\,\mathrm{d}\Omega_1\mathrm{d}\Omega_2 = \iint \frac{\mathrm{d}\Gamma^{(1)}_{\mathrm{p}_1}(\mathbf{j}_1,\mathbf{j}_2;\mathbf{l}_1,\mathbf{n}_1)}{\Gamma^{(1)}_{\mathrm{t}}(\mathbf{j}_1)}\,\frac{\mathrm{d}\Gamma^{(2)}_{\mathrm{p}_2}(\mathbf{j}_2,\mathbf{j}_3;\mathbf{l}_2,\mathbf{n}_2)}{\Gamma^{(2)}_{\mathrm{t}}(\mathbf{j}_2)}, \qquad (1)$$

where $\mathrm{d}\Gamma^{(1)}_{\mathrm{p}_1}(\mathbf{j}_1,\mathbf{j}_2;\mathbf{l}_1,\mathbf{n}_1)$ is the partial width for the emission of a particle p_1 with orbital momentum $\mathbf{l}_1$ by a nucleus with momentum $\mathbf{j}_1$ in the direction $\mathbf{n}_1$, $\mathrm{d}\Gamma^{(2)}_{\mathrm{p}_2}$ is a similar width for the emission of the second particle, $\mathbf{j}_1$, $\mathbf{j}_2$ and $\mathbf{j}_3$

are the angular momenta of the initial, intermediate, and final nuclei respectively, $\Gamma_t^{(1)}$ and $\Gamma_t^{(2)}$ are the total widths of the decay of the initial and intermediate nuclei: $\Gamma_t^{(1)} = \Gamma_{p_1}^{(1)}(\mathbf{j}_1)+\Gamma_n^{(1)}(\mathbf{j}_1)+\ldots$ and similarly for $\Gamma_t^{(2)}$. The quantity $\Gamma_{p_1}^{(1)}(\mathbf{j}_1)$ is the total width for the emission by the initial nucleus of the particle p_1 and $\Gamma_{p_2}^{(2)}(\mathbf{j}_2)$ is a similar quantity for the emission of the particle p_2 by the intermediate nucleus; we have

$$\Gamma_{p_2}^{(2)}(\mathbf{j}_1) = \int d\Gamma_{p_1}^{(1)}(\mathbf{j}_1, \mathbf{j}_2; \mathbf{l}_1, \mathbf{n}_1). \tag{2}$$

For $d\Gamma_{p_1}^{(1)}$ we can use the semi-classical expressions [1-3])

$$d\Gamma_{p_1}^{(1)}(\mathbf{j}_1, \mathbf{j}_2; \mathbf{l}_1, \mathbf{n}) = C_1 \frac{\rho^{(2)}(\mathbf{j}_2)}{\rho^{(1)}(\mathbf{j}_1)} T_1(l_1)$$
$$\times \delta^3(\mathbf{j}_1-\mathbf{j}_2-\mathbf{l}_1)\delta(\mathbf{l}_1\cdot\mathbf{n}_1)d^3\mathbf{j}_2 d^3\mathbf{l}_1 d\Omega_1. \tag{3}$$

In eq. (3) and the similar expression for $d\Gamma_{p_2}^{(2)}$, $\delta^3(\mathbf{x})$ and $\delta(x)$ are three-dimensional and one-dimensional δ-functions, $T_1(l_1)$ and $T_2(l_2)$ are the barrier factors for the particles p_1 and p_2, and ρ_1, ρ_2 and ρ_3 are the level densities of the initial, intermediate and final nuclei. In the following we shall need no explicit form of the energy dependence of these factors or the coefficients C_1 and C_2. Using (3) we obtain for the total partial width

$$\Gamma_{p_2}^{(2)}(\mathbf{j}_2) = 4\pi C_2 \int \frac{T_2(l_2)}{l_2} \frac{\rho^{(3)}(|\mathbf{j}_2-\mathbf{l}_2|)}{\rho^{(2)}(\mathbf{j}_1)} d^3\mathbf{l}_2. \tag{4}$$

The quantity $\Gamma_{p_1}^{(1)}(\mathbf{j}_1)$ is expressed in a similar manner. After substituting (3) and (4) into (1) we can write $W_{\mathbf{j}_1}(1, 2)$ in the form

$$W_{\mathbf{j}_1}(1, 2) = C_1 C_2 \iint d^3l_1 d^3l_2 \frac{T_1(l_1)T_2(l_2)}{\Gamma_t^{(1)}(j_1)\Gamma_t^{(2)}(|\mathbf{j}_1-\mathbf{l}_1|)}$$
$$\times \frac{\rho^{(3)}(|\mathbf{j}_1-\mathbf{l}_1-\mathbf{l}_2|)}{\rho^{(1)}(j_1)} \delta(\mathbf{l}_1\cdot\mathbf{n}_1)\delta(\mathbf{l}_2\cdot\mathbf{n}_2). \tag{5}$$

The integration in (5) is performed over $\mathbf{j}_2$ and $\mathbf{j}_3$. In the following it will be more convenient to represent eq. (5) in the form

$$W_{\mathbf{j}}(1, 2) = \frac{1}{(2\pi)^2} \iint d^3l_1 d^3l_2 \gamma_{p_1}^{(1)}(j_1)\gamma_{p_2}^{(2)}(j_2)\rho^{(2)}(|\mathbf{j}_1-\mathbf{l}_1|)$$
$$\times \rho^{(3)}(|\mathbf{j}_1-\mathbf{l}_1-\mathbf{l}_2|) \frac{T_1(l_1)T_2(l_1)}{N_1(j_1)N_2(|j_1-l_2|)} \delta(\mathbf{l}_1\cdot\mathbf{n}_1)\delta\mathbf{l}_2\cdot\mathbf{n}_2), \tag{6}$$

where $\gamma_{p_1}^{(1)}(j_1)$ is the relative probability of the emission of the particle p_1 by a nucleus in a state with momentum j_1:

$$\gamma_{p_1}^{(1)}(j_1) = \Gamma_{p_1}^{(1)}(j_1)/\Gamma_t^{(1)}(j_1). \tag{7}$$

In (6) N_1 and N_2 are the norm factors; one has

$$N_1(j_1) = \frac{1}{(2\pi)}\iint \mathrm{d}^3k_1\,\mathrm{d}\Omega_1\,T(l_1)\rho^{(2)}(|\mathbf{j}_1-\mathbf{l}_1|)\delta(\mathbf{l}_1\cdot\mathbf{n}_1),$$

$$= \int \frac{\mathrm{d}^3l_1}{l_1}\,T_1(l_1)\rho^{(2)}(|\mathbf{j}_1-\mathbf{l}_1|), \qquad (8)$$

and $N_2(j_2)$ is expressed similarly. It is clear from (6) that

$$\iint W_{\mathbf{j}_1}(1,2)\mathrm{d}\Omega_1\,\mathrm{d}\Omega_2 = \gamma^{(1)}_{\mathrm{p}_1}(j_1)\int \frac{\mathrm{d}^3l_1}{l_1}\,\frac{T_1(l_1)\rho^{(2)}(|\mathbf{j}_1-\mathbf{l}_1|)}{N_1(j_1)}\,\gamma^{(2)}_{\mathrm{p}_2}(|\mathbf{j}_1-\mathbf{l}_1|) \qquad (9)$$

is the relative probability of emission of the pair of particles $\mathfrak{p}_1$ and $\mathfrak{p}_2$ by a nucleus with momentum j_1. Generally speaking, the dependence of the integrand (6) on the orientation of the momentum is determined if the momentum dependence of nuclear level densities is known. In the statistical theory of the nucleus

$$\rho(j) = \rho_0(u)\exp(-\alpha j^2), \qquad (10)$$

where $\alpha = \hbar^2/2\mathscr{I}T$ (here, $\mathscr{I} = \frac{2}{5}\mathrm{Am}\,R^2$ is the nuclear moment of inertia and T is the temperature of the nucleus). With $\rho(j)$ in this form the analytical integration over $\mathbf{l}_1$ and $\mathbf{l}_2$ in (6) is impossible. Let us consider an important particular case when the nucleus remains in a low-momentum state after the escape of the second particle. Putting in (6)

$$\rho^{(3)}(|\mathbf{j}_1-\mathbf{l}_1-\mathbf{l}_2|) = \rho_0\delta^3(\mathbf{j}_1-\mathbf{l}_1-\mathbf{l}_2), \qquad (11)$$

we obtain

$$W_{\mathbf{j}}(1,2) = \frac{1}{(2\pi)^2}\,\frac{\gamma^{(1)}_{\mathrm{p}}(j_1)}{N_1(j_1)}\int \mathrm{d}^3l_1 f(|\mathbf{j}_1-\mathbf{l}_1|)T_1(l_1)\delta(\mathbf{l}_1\cdot\mathbf{n}_1)\delta(\mathbf{j}_1\cdot\mathbf{n}_1-\mathbf{l}_1\cdot\mathbf{n}_2), \qquad (12)$$

where

$$f(|\mathbf{j}_1-\mathbf{l}_1|) = \gamma^{(2)}_{\mathrm{p}_2}(j_2)j_2\rho^{(2)}(j_2), \qquad j_2 = |\mathbf{j}_1-\mathbf{l}_1|.$$

Let us assume $j \gg l_1$ and expand the function $f(j_2)$ into a series

$$f(j_2) \approx f(j_1)(1+a_1x+a_2x^2+\ldots). \qquad (13)$$

The coefficients a_1 and a_2 are equal to

$$a_1 = 2\alpha_2 j_1^2 - 1 + q_1, \qquad a_2 = 2\alpha_2^2 j_1^4 - \tfrac{1}{2} - 2\alpha_2 j_1^2 + q_1q_2 + 2q_1\alpha_2 j_1^2, \qquad (14)$$

where q_1 and q_2 are determined by the equation

$$\gamma^{(2)}_{\mathrm{p}_2}(j_2) = \gamma^{(2)}_{\mathrm{p}_2}(j_1)(1+q_1x+q_2x^2+\ldots). \qquad (15)$$

Let us consider an important particular case when one of the counters is located at right angles to the beam and the seconds counter is either moved

in the plane of the beam or placed also in the normal plane. We shall designate θ_1, θ_2, ϕ_1 and ϕ_2, the angular coordinates of the directions of $\mathbf{n}_1$ and $\mathbf{n}_2$, through ϑ_1, φ_1, ϑ_j and φ_j, the angular coordinates of the vectors $\mathbf{l}_1$ and $\mathbf{j}_1$. It is obvious that $\vartheta_j = \frac{1}{2}\pi$. Let us consider the above cases separately.

2.1. BOTH COUNTERS LIE IN THE NORMAL PLANE ($\theta_1 = \theta_2 = \frac{1}{2}\pi$).

After integration in (6) over the orientation of the vector $\mathbf{l}_1$ we obtain

$$W_{j_1}(1,2) = \frac{2}{(2\pi)^2}\gamma^{(1)}\frac{f(j_1)}{N_1(j_1)}\int_0^\infty \frac{l_1 dl_1 T_1(l_1)(1+a_1\bar{x}+a_2\bar{x}^2)}{\sqrt{l_1^2\sin^2\omega-(\mathbf{j}_1\cdot\mathbf{n}_2)^2}}, \tag{16}$$

where

$$\bar{x} = \cos(\varphi_j-\omega)\sin\varphi_j/\sin\omega$$

and ω is the angle between the counters: $\omega = \phi_1-\phi_2$. Eq. (16) should be integrated over all values of the angle φ_j for which the redicand in (16) is positive. The result is expressed through elliptical integrals. In the limiting case of practical interest, $j \gg l$, we have

$$W_j = \frac{\gamma^{(1)}(j_1)\gamma^{(2)}(j_1)\rho^{(2)}(j_1)}{(2\pi)^2 N^{(1)}(j_1)}\int_0^\infty\left(1+\frac{a_1-a_2}{2}\frac{l^2\sin^2\omega}{j^2}\right)l_1 T(l_1)\,dl_1. \tag{17}$$

The discarded terms are at least as small as l^4/j^4. Without worsening the accuracy of eq. (17) we can put

$$N^{(1)}(j) \approx 4\pi\rho^{(2)}(j)\int_0^\infty l_1 T_1(l_1)\,dl_1, \tag{18}$$

which makes it possible to write (17) in the form

$$W_j = \frac{1}{16\pi^2}\gamma^{(1)}_{p_1}(j)\gamma^{(2)}_{p_2}(j)\left(1+\frac{a_1-a_2}{2}\frac{\overline{l^2}\sin^2\omega}{j^2}\right), \tag{19}$$

where

$$\overline{l^2} = \int_0^\infty l^3 T_1(l)dl \Big/ \int_0^\infty l T_1(l)dl.$$

Eq. (19) should now be integrated over j, taking account of the probability of the capture of an incident particle of moment j,

$$\overline{W} = \int_0^\infty jT_i(j)W_j dj \Big/ \int_0^\infty jT_j(j)dj, \tag{20}$$

where $T_1(j)$ is the absorption coefficient for the incident particle of momentum j. The coefficients a_1 and a_2 are calculated according to (14). If the emission of the second detectable particle is the sole or principal process, $\gamma^{(2)}_{p_2} \approx 1$ and $q_1 \approx q_2 \approx 0$. For $\overline{W}$ we obtain in this case

$$\overline{W}(1,2)) \approx 1+\tfrac{1}{2}\alpha_2\overline{l^2}[4-\tfrac{1}{2}(\alpha_2 j_0^2)^{-1}\ln(\overline{j_0^2}/\overline{l^2})-\alpha_2 j_0^2]\sin^2\omega, \tag{21}$$

where $T_1(j)$ was taken equal to

$$[T_1(j)]_{\text{cl}} = \begin{cases} 1 & \text{for } j \leqq j_0 \\ 0 & \text{for } j > j_0 \end{cases}. \tag{22}$$

For estimating the magnitude of the correlation effect we shall consider the specific reaction Cu(α, 2p) studied by Lasen and Sidorov [4]). With an energy of α-particles ≈ 20 MeV and that of the first proton from 6 to 9 MeV, only two modes of decay of the intermediate nucleus are possible; the emission of a subbarrier proton of energy 1 or 2 MeV or a γ-quantum. For $\alpha_2 = 0.05$, which corresponds to the rigid moment of inertia of the intermediate nucleus, $\overline{l^2} = 3$ to 4 and $\overline{j^2} = 50$, we obtain the value +0.1 for the coefficient of $\sin^2\omega$ in (21). The magnitude and sign of the coefficient strongly depend on the ralation between the parameters $\alpha_2\overline{l^2}$ and $\alpha_2\overline{j^2}$. For larger $\overline{j^2}$ at larger energy of the α-particle, for example, this coefficient goes to zero and then becomes negative. The measurement of the angular correlation of two protons in the normal plane in the reaction $Ni^{58}(\alpha, 2p)$ ($E_\alpha = 32$ MeV) was performed by Bodansky *et al.* [5]). Their results correspond to a value of the coefficient of $\sin^2\omega$ of about −0.15. This value agrees with (21). It is assumed here that the given reaction can be considered as a transition of the excited nucleus, produced by the capture of the α-particle, to the ground or close-to-ground state by emission of only two protons, which is not self-evident.

2.2. COUNTERS AND BEAM LOCATED IN THE SAME PLANE

Here we can distinguish two cases: a) $\theta_2 = \frac{1}{2}\pi$, $\varphi_1 = \phi_2 = 0$ and b) $\theta_1 = \frac{1}{2}\pi$, $\phi_1 = \phi_2 = 0$. Let us first consider the case a). Substituting (13) into the integral (12) we obtain, after integrating over **l** and orientation of the vector **j**, to the same approximation as in (21),

$$W_j(1, 2) = \frac{1}{16\pi^3}\gamma^{(1)}_{p_2}(j)\gamma^{(2)}_{p_2}(j)\left\{1 + \frac{\overline{l^2}}{2j^2}\left(\tfrac{1}{2} + a_1\right)\cos^2\theta_1\right\}. \tag{23}$$

Accurately to the order of l^4/j^4 the angular distribution od the first particle for a fixed direction of the second is determined in this case only by the coefficient a_1. Substituting eq. (14) for a_1 into (23) and putting $q_1 = q_2 = 0$ in (14), we obtain, after integrating over $|j|$,

$$\overline{W}(1, 2) \propto 1 + \left(\alpha_2\overline{l^2} - \frac{\overline{l^2}}{2j_0^2}\ln\frac{j_0}{l_0}\right)\cos^2\theta_1. \tag{24}$$

Just as in (21) the coefficient of $\cos^2\theta_1$ can change sign with the change of momentum of the compound nucleus. If the momentum is large, so that $\alpha_2 j^2 \gg 1$, the angular distribution of the first particle under the condition that the direction of the second is fixed at the angle $\theta_2 = \frac{1}{2}\pi$ does not depend on j,

unlike the usual angular particle distribution where the anisotropy equals $\frac{1}{2}\alpha_2^2\overline{l^2}\overline{j^2}$ (refs. [1,2])).

In case b) we have $\theta_1 = \frac{1}{2}\pi$, $\phi_1 = 0$, $\phi_2 = 0$ or π. After integrating over the orientations of the vectors **l** and **j** we obtain from (12)

$$W_j(1,2) = \frac{1}{4\pi^2}\frac{\gamma_{p_1}^{(1)}(j)f(j)}{jN(j)}\int_0^\infty W_{l,j}lT_1(l)\mathrm{d}l,$$
$$W_{j,l}(1,2) = \frac{1}{\sin\theta_2}\left[A(k)+\frac{a_2 l^2}{3j^2}B(k)\right], \tag{25}$$

where

$$A(k) = \frac{2}{\pi}\begin{cases} K(k) & \text{for } k = \dfrac{l\,\mathrm{tg}\,\theta_2}{j} \leqq 1, \\ \dfrac{1}{k}K(k^{-1}) & \text{for } k \geqq 1 \end{cases}$$

$$B(k) = \frac{2}{\pi}\begin{cases} K(k)+E(k)-k^{-2}[K(k)-E(k)] & \text{for } k \leqq 1 \\ k^{-1}\{K(k^{-1})+E(k^{-1})-k^2[K(k^{-1})-E(k^{-1})]\} & \text{for } k \geqq 1, \end{cases}$$

where $K(k)$ and $E(k)$ are the complete elliptical integrals of the first and second kind, respectively:

$$K(k) = \int_0^{\frac{1}{2}\pi}(1-k^2\sin^2\varphi)^{-\frac{1}{2}}\mathrm{d}\varphi, \qquad E(k) = \int_0^{\frac{1}{2}\pi}(1-k^2\sin^2\varphi)^{\frac{1}{2}}\mathrm{d}\varphi.$$

The function $W_{j,l}$ (1, 2) describes the angular correlation of particles for fixed j and l. The dependence $W_{l,j}$ on the angle θ_2 is determined mainly by the factor $1/\sin\theta_2$, which arises because at $l_1 \ll j$ the orbital momentum of the second particle is close to the direction of **j** and consequently lies in the plane normal to the beam. The deviations of $\mathbf{l}_2$ from this plane, attributable to the fact that the first particle has carried a portion of the momentum, lead to the angular distribution being different from $1/\sin\theta_2$. These deviations are described by the factor in brackets in the expression for $W_{l,j}$. The function $\theta_2 W_{l,j}$ sharply depends on the angle in the region of small angles $\theta_2 \lesssim l_1^2/j^2$. At large angles the deviations from $1/\sin\theta_2$ are as small as l_1^2/j^2:

$$\overline{W} \propto \frac{1}{\sin\theta_2}\{1+(\overline{l_1^2/4j^2})\,\mathrm{ctg}^2\theta_2+\ldots\}, \tag{26}$$

where the terms of the order $l_1^4\,\mathrm{ctg}^4\theta_2/j^4$ are discarded. It is natural to compare the angular distribution (25) of the second particle when the direction of the first particle is fixed, with the same when the first particle is not detected. Normalized to unity at $\theta_2 = \frac{1}{2}\pi$, the latter distribution is given by the expression

$$\arcsin(l/j\sin\theta_2)/\arcsin(l/j), \tag{27}$$

which can easily be obtained from (12). Comparing (27) and (26) we see that at $\theta_2 \gtrsim l/j$ the angular distribution of the second particle, with the counter detecting the first particle, changes by the amount

$$\frac{1}{12 \sin^3 \theta_2} \left(\frac{\overline{l^2}}{j^2}\right) \operatorname{ctg}^2 \theta_2. \tag{28}$$

It should be borne in mind that the distribution $1/\sin \theta_2$ is valid only within quasi-classical accuracy in the region $\theta \gtrsim l_1/j$ and is by no means valid for $\theta \lesssim l_1/j$. Therefore, in the present case the angular correlation effect could be established only if the angular distribution of the second particle with a fixed direction (close to $\theta_1 = \frac{1}{2}\pi$) of the first one is compared with the angular distribution in free emission. Herein lies the essential difference of this case from the two above-mentioned ones, in which the result of zero approximation (isotropy) is known accurately, and the inaccuracy of quasi-classical approximation will lead to an inessential error in the coefficients.

If $a_1 = a_2 = 0$ we obtain rhe following general expression for the function of the angular correlation $W_{l,j}$ (1, 2), valid for any orientation of the counters with respect to the beam and with respect to each other ($\rho^{(3)}(j_3) = \rho_0 \delta(j_3)$):

$$W_{l,j} = \frac{2}{\pi} \frac{1}{\sin \theta_2} \begin{cases} K(\kappa) & \text{for} \quad x = l \sin \gamma / j \sin \theta_2 \leqq 1, \\ \dfrac{1}{\kappa} K(\kappa) & \text{for} \quad \kappa \geqq 1, \end{cases} \tag{29}$$

where γ is the angle between the counters. If for the penetrability coefficient $T_1(l_1)$ we make use of a classical expression similar to (22) eq. (29) for $W_{l,j}$ can be integrated over l. As a result we obtain

$$(W_j(1, 2))_{\text{av } l} = \frac{1}{\sin \theta_2} \begin{cases} \kappa_0^{-1} E(\kappa_0^{-1}) & \text{for} \quad \kappa_0 = l_0 \sin \gamma / j \sin \theta_2 \leqq 1, \\ \kappa_0^{-2} \{E(\kappa_0) - (1 - \kappa_0^2) K(\kappa_0)\} & \text{for} \quad \kappa_0 > 1. \end{cases} \tag{30}$$

Alongside the above two-particle correlation when the final nucleus remains in a state with small angular momentum, other cases may be also of interest. In particular, using (12) it is not difficult to calculate the angular correlation of two particles when, for example, the level densities of the final nucleus just as those of the initial and intermediate nuclei weakly depend on the momentum. This can happen if the excitation energy of the final nucleus is comparatively large and the momentum of the initial nucleus is not too large. It is also easy to obtain a generalization of eq. (5) for the case of a large number of particles in the cascade. The probability of the detection of ν particles in the directions $\mathbf{n}_1, \mathbf{n}_2, \ldots$ and $\mathbf{n}_\nu$ is

$$W_{\mathbf{j}}(\mathbf{n}_1, \ldots, \mathbf{n}_\nu) = \frac{1}{(2\pi)^\nu} \int \mathrm{d}^3 l_1 \ldots \mathrm{d}^3 l_\nu \prod_{i=1}^{\nu} \gamma_{\mathrm{p}_i}^{(i)}(j_i) \rho^{(i+1)}\{|\mathbf{j} - \sum_{k=1}^{i} \mathbf{l}_k|\}$$
$$\times T_i(l_i) N_i^{-1}(j_i) \delta(\mathbf{l}_i \cdot \mathbf{n}_i). \tag{31}$$

If the direction of a particle is not detected in the experiment, eq. (31) should be integrated over the angular variables of the corresponding particle. The angular correlation in this case also depends on the parameters describing the emission of the undetected particle. This circumstance makes the experimental result of the angular correlation less definite. If, however, the unobserved particle is light while the detected ones are heavy, α-particles, for example, the correlation will approximately be the same as though the escape of only two particles took place. If identical particles are detected the expression for angular correlation must be duly symmetrized. There may be no need for it, however, if the energy of the particles is also registered in the experiment. Since the probability of the emission of a particle strongly depends on its energy and the energy of nuclear excitation, it is sometimes easy to establish which of the particles is the first and which the second. This refers in particular to the above-mentioned reaction Cu (α, 2p), in which the second proton is a subbarrier one and consequently the probability that the particle of such energy will be the first to escape the nucleus is negligibly small.

3. Angular Correlation of Particle and Fragments

Let us now consider the angular correlation of the emitted particle and fragments from the fission following the emission. Formally speaking, this case can be regarded as a particular case of the angular correlation of two particles. In eq. (6) the level density of the final nucleus ρ should be replaced by the product of the level densities of the fragments and the corresponding summation over the fragment spins be introduced. It is more convenient, however, to go over to the total distribution of the number of fragment states over the total spin of both fragments, $\rho(s)$, $\mathbf{s} = \mathbf{j}' + \mathbf{j}''$. This distribution formally coincides with (10), the constant being

$$\alpha \equiv \frac{1}{2K_0^2} = \frac{1}{T'}\left(\frac{1}{\mathscr{J}'} + \frac{1}{\mathscr{J}''}\right),$$

where $\mathscr{J}'$, $\mathscr{J}''$ and T' are the moments of inertia and the temperature of the fragments [6]). For calculating the particle-fragment angular correlation, therefore, use can be made directly of eq. (6) if $\rho^{(3)}(j_3)$ in it is replaced by the distribution function $\rho(s)$, $\mathbf{j}_3$ by the vector $\mathbf{s}$, and $\mathbf{l}_2$ by the orbital momentum of the fragments $\mathbf{l}'$. The factor of penetrability $T_2(l')$ can be put equal to unity since the mass of the fragments is large and the classical restriction imposed on the magnitude of the angular momentum is not essential even in the case when the nuclear energy does not much exceed the fission threshold. Integration over $\mathbf{l}'$ can be performed in general form. After the integration over $\mathbf{l}'$ we obtain

$$W_{\mathbf{j}_1}(\mathrm{p}, \mathrm{f}) = \frac{1}{(2\pi)^2}\frac{\gamma_{\mathrm{p}}^{(1)}(j_1)}{N_1(j_1)}\int \mathrm{d}^3 l_1 \gamma_{\mathrm{f}}^{(2)}(j_2)\rho^{(2)}(j_2)\delta(\mathbf{l}_1 \cdot \mathbf{n}_1)\mathscr{N}(\mathbf{j}_2 \cdot \mathbf{n}_{\mathrm{f}}), \qquad (32)$$

where $\mathbf{j}_2 = \mathbf{j}_1 - \mathbf{l}_1$, $\mathbf{n}_1$ and $\mathbf{n}_f$ are the directions of the emission of a particle and that of fragments, $\gamma_f^{(2)}$ is the relative probability of the fission of the intermediate nucleus, and the function

$$\mathcal{N}(\mathbf{j}_2 \cdot \mathbf{n}_f) = R(j^2/2K_0^2) \exp(-K^2/2K_0^2), \tag{33}$$

where $K = \mathbf{j}_2 \cdot \mathbf{n}_f$ is the projection of the momentum of the intermediate nucleus on the direction of the fission. In (33) we have

$$R(z) = \int_{-1}^{+1} e^{-zx^2}\, dx.$$

The function (33) gives the K-distribution of the number of fission events. The above expression for K_0^2 corresponds to the assmuption made in deriving (32) that the fission probability is determined by the statistical weight of the fragments. It can also be supposed that the fission probability for a given value of K is determined by the statistical distribution of K in the "transitional" nucleus with a deformation approximately corresponding to the saddle point. The distribution of K in this case corresponds to (33) but the constant K_0^2 is equal to $(T^*)^{-1}\ (\mathcal{J}_\parallel^{-1} - \mathcal{J}_\perp^{-1})^{-1}$ where $\mathcal{J}_\parallel$ and $\mathcal{J}_\perp$ are the moments of inertia of the "transitional" nucleus with respect to the axis of symmetry and the perpendicular direction, and T^* is the temperature of the "transitional" nucleus. The formal identity of these two assumptions was mentioned in ref. [6]). It should be borne in mind that strictly speaking the angular-fragment distribution is determined by the distribution of K at infinity [7]). Since the projection of the orbital momentum of the fragments on the direction of emission is equal to zero, the distribution of the projection K of the total momentum of the fissioning system $\mathbf{j} = \mathbf{l}' + \mathbf{s}$ on the direction of emission coincides with the distribution of the projection of the total spin of the fragments on this direction. The question thus reduces to whether the distribution of the projection of the vector $\mathbf{s}$ is determined by the level density of the fragments or coincides with the distribution of K in the "transitional" nucleus. On the strength of the data available at present it can be concluded that the second hypothesis is in agreement with reality at least for the fission close to the threshold and with low excitation of the initial nucleus. From the formal viewpoint the existence of these two different approaches is not essential since in both cases the K-distribution is given by the same expression (33).

If the angular momentum of the compound nucleus is sufficiently large, so that the inequality

$$j^2/2K_0^2 \gg 1 \tag{34}$$

is fulfilled, eq. (33) for $\mathcal{N}(K)$ truns into $j_2\delta(\mathbf{j}_2 \cdot \mathbf{n}_f)$ and (32) formally coincides with (12). Therefore, all expressions obtained above for particle-particle correlation describe the particle-fragment correlation when the nuclear momentum

is sufficiently large. The proximity of the angular-fragment distribution to $1/\sin\theta_f$ [8]) may serve as evidence that the condition (34) is fulfilled. This usually occurs in the case of fission in the capture of heavy ions. A large momentum of the compound nucleus in this case is also conducive to better nuclear fissibility and consequently increases the probability of the nucleus splitting immediately after the emission of the detected particle.

Using eq. (32) the particle-fragment angular correlation can also be found when the condition (34) is not fulfilled. Let us consider a case when

$$lj/2K_0^2 \ll 1. \tag{35}$$

The parameter $j^2/2K_0^2$ can be of any magnitude, but not too large, so that the inequality (35) be not violated. Introducing the same approximations as in the derivation of (18) we write W_j (p, f) in the form

$$W_f(\mathrm{p,f}) \approx \frac{1}{(2\pi)^3}\gamma_p^{(1)}(j)\gamma_f^{(2)}(j)\mathcal{N}(|\mathbf{j}-\mathbf{n}_f|)\left((4\pi\int_0^\infty l\,\mathrm{d}l\,T(l)\right)^{-1}$$

$$\times\int \mathrm{d}^3l\,T(l)\delta(\mathbf{l}\cdot\mathbf{n}_1)(1+r(\mathbf{l}\cdot\mathbf{j})+\ldots)\exp\left[(\mathbf{l}\cdot\mathbf{n}_f)[2(\mathbf{j}\cdot\mathbf{n}_f)-\mathbf{l}\cdot\mathbf{n}_f]/2K_0^2\right], \tag{36}$$

where $\mathbf{j}=\mathbf{j}_1$, $\mathbf{l}=\mathbf{l}_1$ and

$$1+r(\mathbf{l}\cdot\mathbf{j})+\ldots = G(|\mathbf{j}-\mathbf{l}|)/G(j), \tag{37}$$

with

$$G(j) = \gamma_f^{(2)}(j)\rho^{(2)}(j)R^{-1}(j^2/2K_0^2). \tag{38}$$

Let us consider the case when the particle and fragment directions both lie in the plane normal to the beam. Let us expand the exponential factor in the integrand of eq. (36) into a series and perform integration over $\mathbf{j}$. After averaging over the orientation of the vector $\mathbf{j}$ we obtain

$$W_j(\mathrm{p,f}) = \frac{1}{(2\pi)^3}\gamma_p^{(1)}(j)\gamma_f^{(2)}(j)\exp\left(-\frac{z}{2}\right)I_0\left(\frac{z}{2}\right) \tag{39}$$

$$\times\left\{1-(\overline{l^2}/4K_0^2)\sin^2\omega_t+(\overline{l^2}j^2/8K_0^4)(1+2K_0^2r)\left(1-I_1\left(\frac{z}{2}\right)\Big/I_0\left(\frac{z}{2}\right)\right)\sin^2\omega_t\right\},$$

where $z = j^2/2K_0^2$ and I_0, I_1 are Bessel functions of imaginary argument. Eq. (39) has also to be averaged over the magnitude $|j|$ with the weight $jT(j)$.

The coefficient r in (39) depends, generally speaking, on l. For determining r we can use explicit expressions of the form (10) $\rho^{(2)}(j^2)$, $R(z)$ and $\gamma_f^{(2)}(j^2)$. For $\gamma_f^{(2)}$ we can take the statistical expression

$$\gamma_f^{(2)}(j_2) = (1+\gamma_r^{(2)}(j_2)/\gamma_f^{(2)}(j_2))^{-1}, \tag{40}$$

where

$$\gamma_r^{(2)}(j_2)/\gamma_f^{(2)}(j_2) = \frac{\Gamma_r(0)}{\Gamma_f(0)}\exp\left[(\alpha_3-\alpha_\perp)j_2^2\right]R^{-1}(j_2^2/2K_0^2)$$

Writing

$$\rho^{(2)}(j_2) \approx \rho^{(2)}(j)(1+2\alpha_2(\mathbf{l}\cdot\mathbf{j})+\ldots),$$
$$R(j_2^2/2K_0^2) \approx R(j^2/2K_0^2)(1-s(\mathbf{l}\cdot\mathbf{j})+\ldots),$$
$$\gamma_l^{(2)}(j^2) \approx \gamma_l^{(2)}(j)(l-t(\mathbf{l}\cdot\mathbf{j})+\ldots),$$

we obtain

$$\gamma = 2\alpha_2+s-t.$$

The coefficient γ is a quantity of the same ofder of smallness as $1/2K_0^2$. The parameter $\overline{j^2}/2K_0^2$ can be determined independently by the anisotropy of the fragment angular distribution [8]). The measurement of the particle-fragment angular correlation makes it possible to obtain additional data on the orbital momentum of the particle and the dependence of the probability of nuclear fission on the angular momentum. It will be noted that in eq. (39) the angular dependence does not vanish even when $j = 0$. This is attributable to the fact that a correlation is known to exist between the directions of two particles in a state of total momentum $j = 0$. The probability of the angle ω is proportional to the square of the Legendre polynomial

$$P_l^2(\omega) \propto 1/\sin\omega \qquad (41)$$

if $l \gg 1$. This expression coincides with (16) if we put $j = 0$ in the latter. The term which does not depend on j in eq. (39) is a trace of the correlation (41) and turns into the latter at $l^2/2K_0^2 \gg 1$.

The author expresses his gratitude to Dr. V. Sidorov for stimulating discussions.

References

1) V. M. Strutinski, Proc. All-Union Conf. on Nuclear Reactions, Moscow, 1957, published in: Nuclear Reactions at Low Energies (Moscow, 1958) [in Russian]
2) T. Erikson and V. Strutinski, Nuclear Physics **8** (1958) 284
3) T. Erikson, Nuclear Physics **17** (1960) 250
4) N. O. Lassen and V. Sidorov, Nuclear Physics **19** (1960) 579
5) D. Bodanski *et al.*, Cycl. Res. Univ. Wash., Ann. Rep. 1960
6) V. M. Strutinski, Atomnaya Energia **2** (1957) 558
7) V. M. Strutinski, JETP **30** (1956) 606
8) I. Halpern and V. Strutinski, Second Geneva Conf. Geneva, 1958, paper p/1513

NORTH-HOLLAND BOOKS

Elements of Hamiltonian Mechanics

by D. TER HAAR
University Reader in Theoretical Physics and Fellow of Magdalen College, Oxford

CONTENTS:

1. Newtonian mechanics
2. The Lagrangian equations of motion
3. Small vibrations
4. Dynamics of rigid bodies
5. The canonical equations of motion
6. Hamilton-Jacobi theory
7. Perturbation theory
8. Continuous systems

Bibliography - Problems

This book is based upon a course of lectures given to final year undergraduates and first year graduate students at Oxford University. The emphasis and the selection of subject matter differs in a number of points from those in existing modern text-books. The main differences are in the way constraints are introduced by freezing in of degrees of freedom, and in the discussion of classical perturbation theory.

6 x 9" 196 pp. Gld. 20.— (40s.)

NORTH-HOLLAND PUBLISHING COMPANY
P. O. BOX 103 - AMSTERDAM

Distributor for U.S.A.: Interscience Publishers, Inc. — New York

NORTH-HOLLAND BOOKS

QUANTUM MECHANICS

VOL. I

by ALBERT MESSIAH (Centre d'Etudes Nucléaires de Saclay)

translated from the French by G. M. Temmer (Florida State University, Tallahassee)

6×9" 520 pp. Gld. 50.- (100s.)

CONTENTS VOL. I. *The formalism and its interpretation.* Origins of the Quantum Theory. Matter waves and the Schrödinger equation. One dimensional quantum systems. Statistical interpretation of the wave-corpuscle duality and uncertainty relations. The development of the formalism of Wave Mechanics and its interpretation. Classical approximation and WKB method. The general formalism of Quantum Theory: A) Mathematical framework. B) Description of physical phenomena. — *Simple systems.* Solution of the Schrödinger equation by separation of variables. Central force field. Scattering problems. Central force field and the method of phase shifts. Coulomb interaction. Harmonic oscillator. — *Appendices:* «δ function» and distributions. Special functions and related formulae.

". . . . the reviewer would like to recommend the book to students taking a beginner's course in quantum mechanics, to teachers for broadening the scope of such courses, and also to research workers in understanding the principles and methods of quantum mechanics and for acquiring the necessary knowledge for an understanding of the advanced parts of the field."

(PHYSICS TODAY on the original French Edition)

VOLUME II
in preparation

Ask your bookseller or

NORTH-HOLLAND PUBLISHING COMPANY

P.O. BOX 103—AMSTERDAM

Distributor for U.S.A.: Interscience Publishers, Inc. — New York